KINETIC AND THERMODYNAMIC STUDIES OF METAL COMPLEXES FORMED BY LIX 65N AND RELATED HYDROXYOXIME LIGANDS.

A thesis submitted in partial fulfilment of the requirements for the degree of Doctor of Philosophy from the University of Warwick, Department of Chemistry and Molecular Sciences.

William Q. Gilmour

March 1980.

ABSTRACT.

An investigation of some divalent transition metal complexes of the commercial liquid-liquid extractant LIX 65N (H_2L) has been carried out and the results from these studies have been compared to observations found for a series of model compounds of these types of extractant. In the course of this work an improved method for obtaining pure forms of the two isomers of LIX 65N has been developed. A ^{13}C n.m.r. investigation has been made of LIX 65N and the model ligands and the trends observed have been compared to the results found from infra-red and electronic spectral studies. The nickel(II) and copper(II) bis-complexes of LIX 65N exist in a square-planar trans-configuration in non-donor and weakly donating solvents. The extremely oxygen sensitive cobalt(II) bis-complex of LIX 65N has been isolated. The kinetics of bis-complex formation have been investigated for these complexes of LIX 65N in methanol solutions by stopped-flow spectrophotometric methods. For nickel(II) and cobalt(II) these reactions appear to proceed with the normal I_d mechanism. The corresponding reaction with copper(II) was found to be too fast to be measured with the techniques available. By comparing the complex formation rates determined for the nickel(II) complex of LIX 65N with similar rates for a series of nickel(II) complexes of aromatic hydroxyoxime ligands it has been found that the long alkyl chains associated with the commercial extractants have a small retarding effect on the rate of complexation. Variation of the oximino carbon substituent in these ligands by replacing hydrogen with both methyl and phenyl groups enhances the complexation rates to approximately the same extent. It is found that the outer-sphere complex formed initially in these reactions is that involving the neutral forms of the ligands. The rate determining step is believed to be formation of the first metal-to-oximino nitrogen atom bond.

An investigation of the metal exchange reaction involving $Ni(HL)_2$ and Cu(II) by the technique of rapid scanning spectrometry (RSS) reveals that this reaction proceeds through three distinct stages. Two transient intermediate species are observed and the mechanisms involved have been investigated by single wavelength stopped-flow methods taking advantage of isosbestic points established for each stage by RSS. The overall mechanism is believed to involve dinuclear bridged intermediate species. The nickel(II) complex of the non-alkylated model compound for LIX 65N has been found to form octahedral bis-adducts with two alkylamine ligands. These species have been isolated and investigations of the alkylamine exchange processes have been established using ^{13}C line broadening methods. An equilibrium is found to exist between the square-planar bis-complex and the pseudo-octahedral bis-adduct, and this phenomenon has been investigated by variable temperature U.V.-visible spectrophotometry. As a continuation of previous studies from these laboratories two other systems have been investigated. The equilibrium between the trans-III isomer of $[Ni(TMC)]^{2+}$ (TMC = 1,4,8,11-tetramethyl-1,4,8,11-tetra-azacyclotetradecane) and its octahedral bis-adduct with DMF has been investigated by variable temperature ^1H n.m.r. methods. It has been found that this adduct exists in both the cis- and trans-isomeric forms. The equilibrium processes associated with both isomers have been investigated. An investigation of the co-ordination number and rate of exchange of methanol on $[Zn(MeOH)_6]^{2+}$ ion has also been studied by ^1H n.m.r. methods. It has been found that the tetrafluoroborate anion has a weaker co-ordinating ability to zinc(II) than the perchlorate anion and the activation parameters have been determined for this dynamic process using the tetrafluoroborate salt.

TABLE OF CONTENTS.

TABLE OF CONTENTS (cont'd.)

TABLE OF CONTENTS (cont'd.)

TABLE OF CONTENTS (cont'd.)

LIST OF TABLES.

LIST OF TABLES (cont'd)

LIST OF FIGURES.

LIST OF FIGURES (cont'd.)

LIST OF FIGURES (cont'd.)

LIST OF FIGURES (cont'd.)

ACKNOWLEDGEMENTS.

I am indebted to my supervisor Dr. P. Moore for his constant encouragement and invaluable discussion throughout the course of this work. I would also like to thank Dr. C. Brown of Borax Consolidated Ltd. for useful discussion.

I also include a special 'thank you' to my wife, Julie, for typing the manuscript.

Finally, I thank the Science Research Council and Borax Consolidated Ltd. for the financial support, through a CASE award, that made this thesis possible.

TO MY PARENTS

LIST OF ABBREVIATIONS.

ACETOX	2-hydroxyacetophenone oxime
AKUFVE	apparatus for continuous measurement of distribution factors in solvent extraction
BENZOX	2-hydroxybenzophenone oxime
β	overall stability constant
$BuNH_2$	n-butylamine
CC	Curie constant
CDTA	trans-1,2-diaminocyclohexane-N,N,N',N'-tetraacetic acid
ClACETOX	2-hydroxy-5-chloroacetophenone oxime
ClBENZOX	2-hydroxy-5-chlorobenzophenone oxime
cyclam	1,4,8,11-tetra-azacyclotetradecane
ΔG°	free energy associated with adduct formation
ΔH^*	activation enthalpy
ΔH°	enthalpy change associated with adduct formation
ΔS^*	activation entropy
ΔS°	entropy change associated with adduct formation
DMF	N,N-dimethylformamide
DMSO	dimethylsulphoxide
EDDA	ethylenediaminediacetic acid
EDTA	ethylenediaminetetraacetic acid
ϵ_m	molar extinction coefficient
g.l.c.	gas-liquid chromatography
HPLC	high performance liquid chromatography
I.R.	infra-red
k_{ex}^I	exchange rate for one solvent molecule
MeACETOX	2-hydroxy-5-methylacetophenone oxime
MeOH	methanol

LIST OF ABBREVIATIONS (cont'd.)

MeOSALO	5-methoxysalicylaldoxime
n.m.r.	nuclear magnetic resonance
NOBENZOX	2-hydroxy-5-nitrobenzophenone oxime
NOE	Nuclear Overhauser Effect
phen	1,10-phenanthroline
p.p.m.	parts per million
$PrNH_2$	n-propylamine
py	pyridine
RSS	rapid scanning spectrometry
SALO	salicylaldoxime
τ	time spent by one solvent molecule at a particular exchange site
t.l.c.	thin layer chromatography
TMC	1,4,8,11-tetramethyl-1,4,8,11-tetra-azacyclotetradecane
TMS	tetramethylsilane
U.V.	ultra-violet
v/v	volume for volume

CHAPTER 1.

INTRODUCTION.

1.1. Liquid-Liquid Extraction - General [1,2]

The process of liquid-liquid extraction dates from the early 1930's when it was first employed for the removal of aromatic hydrocarbons from kerosene. Since then it has been employed ever more frequently in fields ranging from copper production to the manufacture of antibiotics.

The principle of a liquid-liquid extraction process is that a solvent is added to a solution of a solute in a second solvent. This second solvent is either immiscible or partly miscible with the added solvent. An equilibrium is established where the solute is distributed between the two phases and the position of this equilibrium will depend on the relative affinities of the two solvents for the solute. The added solvent is referred to as the "solvent", the resulting solute extracted into the "solvent" is referred to as the "extract", and the remaining solute in the initial phase is known as the "raffinate".

At equilibrium the distribution of the solute between the two phases is defined by the distribution coefficient, D. Thus:

$$D_A = y_A / x_A$$

where y_A is the concentration of A in the extract and x_A is the concentration of A in the raffinate. If the value of D exceeds unity, this indicates a preference of the solute for the added solvent. This preference can be the result of either a physical interaction, such as polarity or hydrogen bonding,

or a chemical interaction.

If two solutes are present then a selectivity of one over the other is desirable and this selectivity is defined by the separation factor, α.

Thus:

$$\alpha_{AB} = D_A / D_B$$

When the extraction interaction is of a chemical nature, the solvent is a solution of a chemically active reagent. In this case the reagent is referred to as the "extractant" and the solvent as the "diluent". If the extractant-solute complex is not totally soluble in the diluent, a third agent is introduced into the solvent and this is referred to as the "modifier".

It is usual to employ a system involving a multi-stage extraction procedure, with the aim of maximising solute recovery from the raffinate and also maximising extract concentration. The most succesful method for achieving this is known as multi-stage countercurrent contacting. This process is demonstrated below.

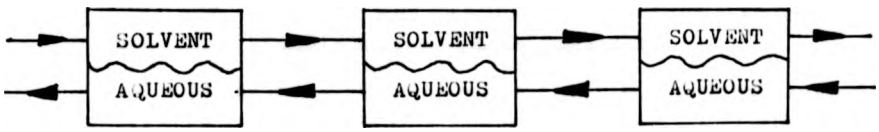

Figure 1.1. The Multi-stage Countercurrent Contacting Procedure.

Few liquid-liquid extractants are fully selective and

so impurities can also be extracted into the solvent. This problem is overcome, in industry, by the use of the technique of "scrubbing". This process involves the use of another liquid phase which frequently utilises the same solvent as the initial feed solution. Conditions are such that the desired solute is retained in the extract whereas the undesirable impurities are removed.

The final task in a liquid-liquid extraction process is recovery of the solute. In the case where the extraction interaction is of a physical nature the most common course of recovery is distillation. In the alternative case where a chemical extraction reaction occurs, a chemical method of recovery has to be employed.

In the extraction of copper, the metal is recovered by use of a relatively strong acid. This procedure is known as "stripping" and is essentially the reversal of the extraction process. Thus, as in extraction, multi-stage countercurrent contacting is most successfully employed. A schematic diagram of a liquid-liquid extraction plant for the recovery of copper is given in Figure 1.2. .

1.2. Copper Selective Liquid-Liquid Extractants.

Currently 10 - 15 commercial liquid-liquid extraction plants are employed for the recovery of copper [3]. This hydrometallurgical approach, which functions alongside traditional methods of copper recovery, is utilised to extract copper from low grade ores, scraps and tailings.

Figure 1.2. The Multistage Countercurrent Contacting Process

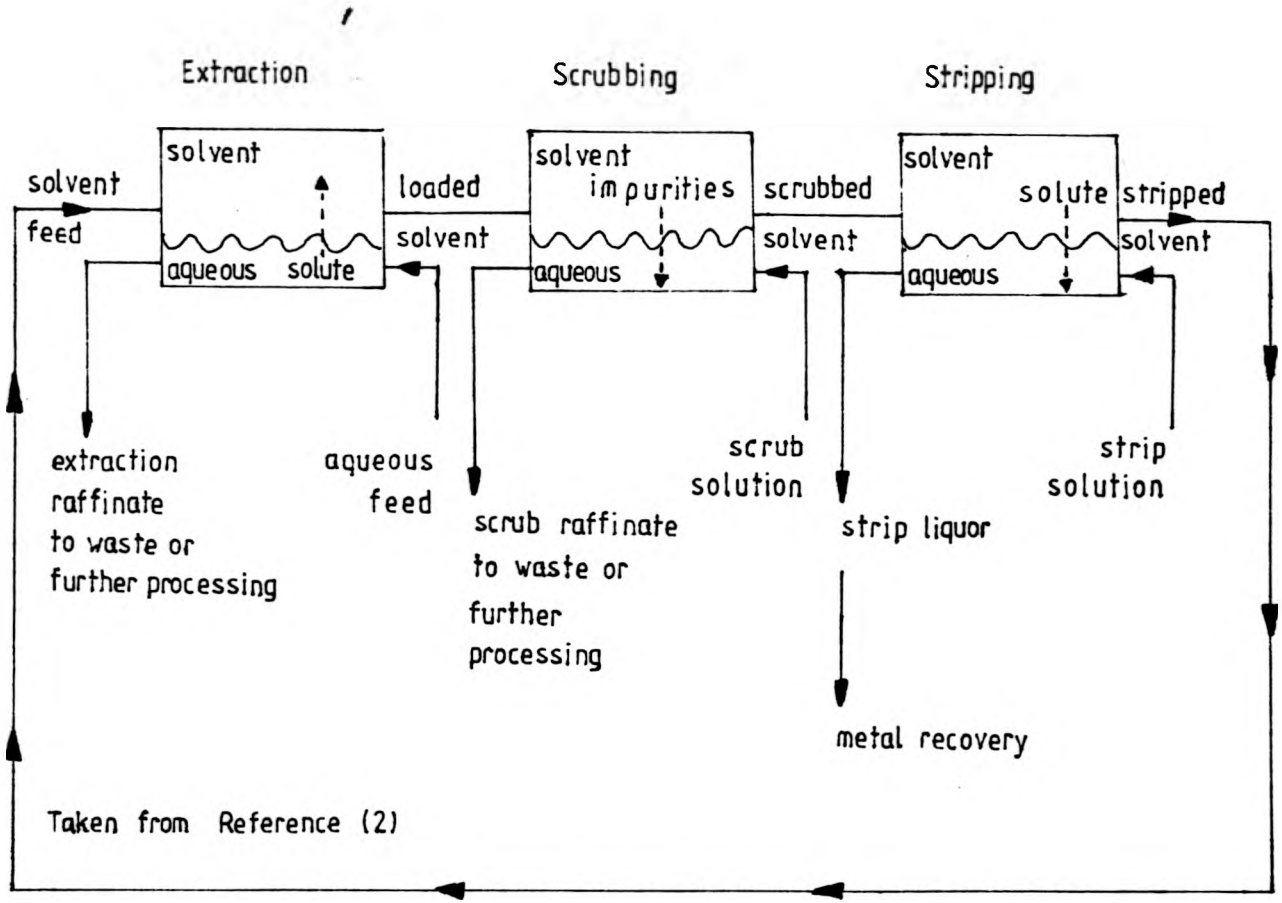

Metal selectivity is one of the prime objectives in developing a commercial liquid-liquid extractant for copper. Considerable progress has been made in recent years towards this achievement by the use of chelating agents. These reagents have been developed over the last fifteen years or so. Those that have been proposed or are in actual use are listed and their chemical structures given in Table 1.1. .

The most commonly used copper selective extractants are the LIX* series manufactured by General Mills. Their reagent LIX 63, which became available in 1964 [4], was the first commercially produced chelating reagent designed for copper recovery from dump leach liquors. LIX 63, however, does not satisfactorily discriminate copper(II) over iron(III) and possesses inadequate loading characteristics at the pH normally used for dump leach liquors. The properties of LIX 63 are such that despite these problems, its development provided enough interest to stimulate investigation of other hydroxyoxime systems for the selective extraction of copper.

Further research resulted in the production of LIX 64 in 1965 [5]. This reagent, a 2-hydroxybenzophenone oxime, alkylated in the 5-position is a significant improvement over LIX 63, both in copper selectivity and pH functionality. However, it does display slow extraction kinetics.

Further developments gave rise to another LIX reagent, LIX 64N [6], which demonstrates much improved extraction kinetic

* LIX is a registered trademark of the General Mills Chemical Company Ltd. .

Table 1.1. The Commercial Liquid-Liquid Extractants

NAME	YEAR OF INTRODUCTION	PRODUCER	ACTIVE INGREDIENT
LIX 63	1963	General Mills	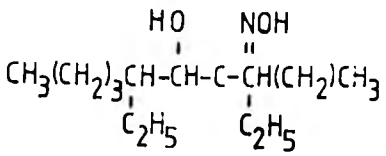
LIX 64	1965	General Mills	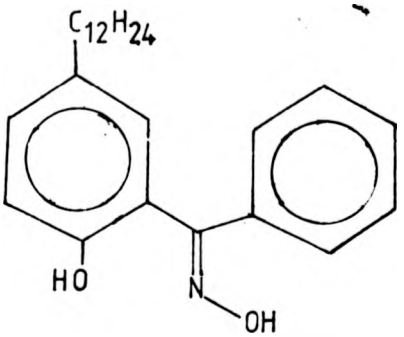
Kelex 100	1968	Ashland Chemicals	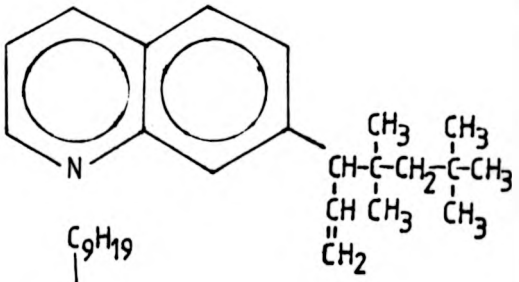
Kelex 120*			
SME 529	1969	Shell Ltd.	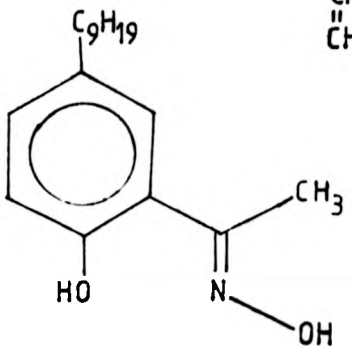

*Kelex 120 = Kelex 100 in p-nonylphenol

Table 1.1.(cont'd)

NAME	YEAR OF INTRODUCTION	PRODUCER	ACTIVE INGREDIENT
LIX 65N	1971	General Mills	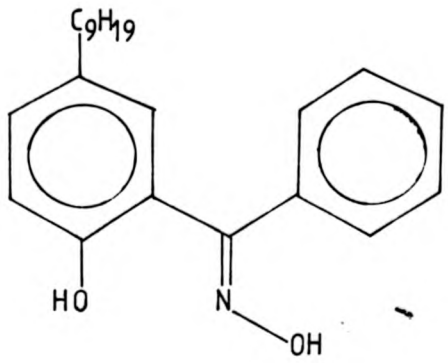
LIX 64N	1970	General Mills	LIX 65N + LIX 63 44:1
LIX 70	1970	General Mills	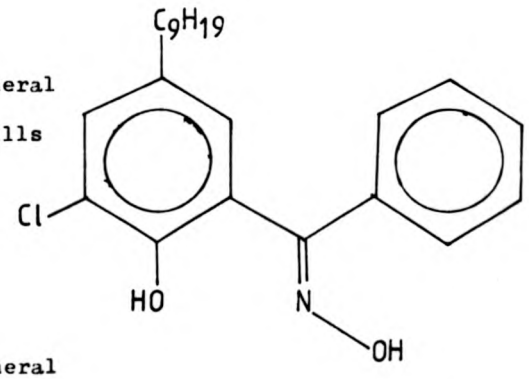
LIX 71	1971	General Mills	LIX 70 + LIX 65N
LIX 73	1971	General Mills	LIX 71 + LIX 63

Table 1.1.(cont'd)

NAME	YEAR OF INTRODUCTION	PRODUCER	ACTIVE INGREDIENT
P17	——	Acorga Ltd.	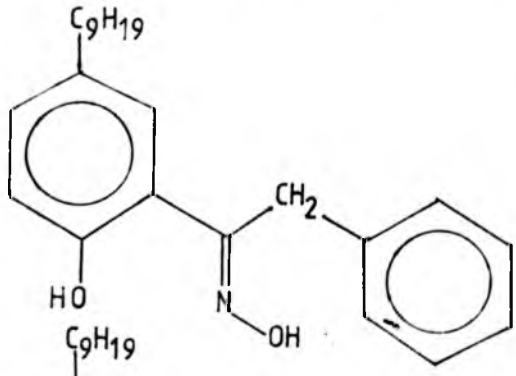
P50	——	Acorga Ltd.	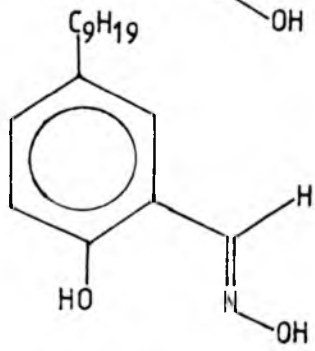
——	——	General Mills (USSR)	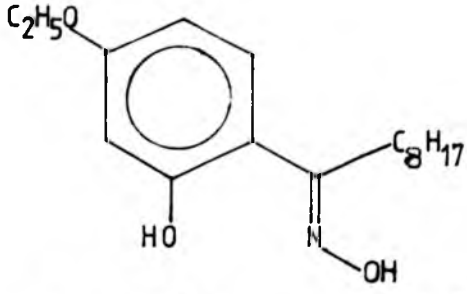 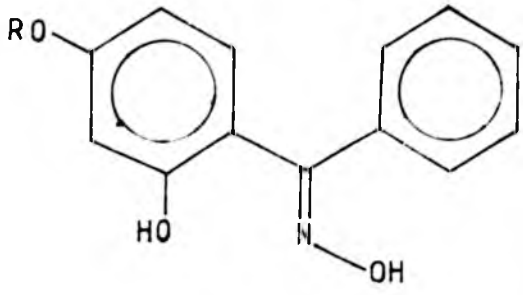

behaviour over LIX 64. This reagent is, in fact, still used more frequently in industry than any other copper selective commercial liquid-liquid extractant.

The early 1970's saw the introduction of more LIX reagents designed for use with different types of leach liquors. LIX 70 [7], a 3-chloro substituted derivative of an alkylated 2-hydroxybenzophenone oxime, is designed for use with highly acidic leach liquors. Further reagents [8,9] have been developed primarily for use at low pH and elevated temperatures.

Apart from the LIX reagents, numerous other chelating liquid-liquid extractants have been developed by various industrial concerns. Other hydroxyoxime type extractants based on salicylaldehyde and 2-hydroxyacetophenone have been developed, namely the Acorga Ltd. produced P50 and the Shell produced SME 529. These reagents display extraction behaviour similar to the 2-hydroxybenzophenone oxime derivatives, but their increased solubility in water and resultant loss during the extraction process has been a major drawback [3].

An alternative design of copper selective extractants based on 8-hydroxyquinoline has been produced. These constitute the two members of the Kelex* series, produced by the Ashland Chemical Company. The two reagents, namely Kelex 100 and Kelex 120, have the same active ingredient but Kelex 120 contains p-nonylphenol. Kelex 100 is intended for use with concentrated solutions of copper and Kelex 120 for use with dilute solutions of copper.

* Kelex is a registered trademark of the Ashland Chemical Company Ltd. .

Both reagents are employed to extract from acidic aqueous solutions.

It is the LIX series which has been most widely incorporated by industry and it is these reagents and their derivatives upon which this thesis will concentrate.

Oximes of 2-hydroxybenzophenone show a high selectivity in acidic solutions. At pH = 2 only Cu(II) is well extracted. Fe(III) is only slightly complexed and Mo(VI) and V(IV) are extracted to an even smaller degree. Zn(II), Sn(II), Ca(II), Mg(II), As(III), Al(III), Fe(II), Co(II) and Ni(II) do not form complexes at all under these conditions [10]. This has also been shown to be true for salicylaldoxime [11] and its derivatives [12]. Nickel(II) only begins to be appreciably extracted above pH = 4. It has been found, however, that with α-dioximes in molar solutions of ammonium nitrate that Ni(II) is extracted preferentially over Cu(II) and that under these conditions it would be quite difficult to separate Cu(II) from Co(II) [13].

2-Hydroxybenzophenone oxime derivatives are also capable of complex formation in ammoniacal solutions. This ability is taken advantage of in the separation of copper from nickel. Copper is extracted from acidic solutions and nickel is removed after neutralisation with ammonia.

LIX 64, LIX 64N and LIX 65 do not extract copper efficiently from strongly acidic solutions. Under these conditions LIX 70, LIX 71 and LIX 73 are more successfully employed. LIX 70 and LIX 73 display reasonable extraction and reextraction kinetics and can be applied at room temperature, whereas LIX 71 is designed to operate at elevated temperatures. The higher stability

of the copper complexes of these reagents requires the use of more strongly acidic solutions than is usual to strip copper from the solvent. In fact, in the case of LIX 70, such a high concentration of acid would be required to strip the copper that technological alterations would have to be made to the usual conditions of electrolyser operation. As a direct result of this LIX 70 does not find industrial application. However LIX 71 and LIX 73, which are both mixtures of LIX 70 and LIX 65N show reextraction behaviour intermediary to the separate constituent reagents of the mixtures and thus overcome the problem discovered with LIX 70.

1.3. Structural and Isomeric Properties of Hydroxyoxime Liquid-Liquid Extractants.

Hydroxyoximes can exist in two possible isomeric forms, namely the 'syn' and 'anti' configurations. As a result of this observation the active constituents of commercial liquid-liquid extractants based on hydroxyoximes could be expected to demonstrate this behaviour. This isomerisation phenomenon has only been observed with benzophenone derivatives and not with other aromatic hydroxyoximes. So the LIX reagents can exist in the following isomeric forms:-

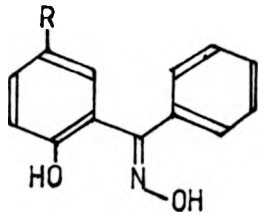

'anti'

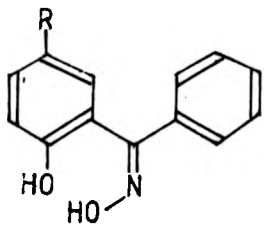

'syn'

These two structural isomers can be differentiated by a number of techniques. Ultra-violet spectrophotometry [14] has been used for this purpose and 'syn' isomers have been identified as absorbing at higher energy (shorter wavelength) than the 'anti' isomers. This observation has been explained on the grounds of steric interactions. Infra-red spectroscopy [15] makes use of the differences in hydrogen bonding existing between the two isomeric forms to distinguish them.

Ashbrook [16] has investigated the structural behaviour of the hydroxyoximes which constitute the LIX series. He has shown that there are four different molecules which either as sole constituents or as mixtures make up this series.

These four distinct species are LIX 63, LIX 64, LIX 65N and LIX 70. The latter three reagents, which are based on 2-hydroxybenzophenone, were originally believed to occur only in the 'anti' form [17]. Ashbrook [16] has shown that the three oximes do in fact exist in both 'syn' and 'anti' forms. Both isomeric forms of the three reagents have been isolated and a full spectroscopic study undertaken. Their spectral properties have been compared with the parent 2-hydroxybenzophenone oxime (BENZOX). They have been characterised by infra-red, ultra-violet and proton magnetic resonance spectroscopy [18], thin layer chromatography (t.l.c.) and microanalysis [16], gas-liquid chromatography (g.l.c.) and high performance liquid chromatography (HPLC) [19]. The infra-red and ultra-violet spectral data for these oximes are given in Tables 1.2. and 1.3. .

Ultra-violet spectrophotometry shows that the two isomeric forms of these reagents can be readily distinguished by

Table 1.2. Electronic Spectral Data* for LIX Reagents [18].

ISOMER	λ_{max} / nm ; (logϵ)	
SYN		
LIX 64	285 sh (3.50)	249 sh (3.98)
LIX 65N	290 sh (3.48)	250 sh (4.02)
LIX 70	290 sh (3.52)	249 sh (4.13)
BENZOX	280 sh (3.67)	250 sh (4.08)
ANTI		
LIX 64	314 (3.51)	260 (3.95)
LIX 65N	314 (3.49)	260 (3.92)
LIX 70	319 (3.53)	264 (4.01)
BENZOX	308 (3.88)	259 (4.19)
LIX 63	310 sh	265 sh

*Recorded in ethanol solution.

Table 1.3. Infra-red Spectral Data for LIX Reagents [18].

ISOMER	ASSIGNMENT					
	ν_{OH} free /cm^{-1}	ν_{OH} assoc. /cm^{-1}	$\nu_{C=N}$ /cm^{-1}	ν_{OH} /cm^{-1}	ν_{N-O} /cm^{-1}	$\Delta\nu_{OH}$ /cm^{-1}
SYN						
LIX 64	3580	3260	1620	1285	918	320
LIX 65N	3580	3240	1620	1280	915	340
LIX 70	3580	3270	1620	1278	930	310
	3345				918	275
BENZOX	3590	3260	1620	1280	915	330
ANTI						
LIX 64	3592	3400	1622	1292	965	192
LIX 65N	3580	3395	1620	1292	965	185
LIX 70	3575	3410	1620	1280	880	165
BENZOX	3590	3410	1620	1292	965	180
LIX 63	3590	3330	1650	1270	945	260

study of the lowest electronic energy band. This band is attributed to a $\pi^* \leftarrow n$ transition involving unpaired electrons of the phenolic hydroxyl function.

Infra-red spectroscopic studies demonstrate major differences in hydrogen bonding between the two isomers. Dilution experiments show that the 'syn' isomers possess an intramolecularly hydrogen bonded system whereas the major hydrogen bonding phenomenon in the 'anti' isomers is of an intermolecular nature.

In the solution phase two hydroxyl stretching frequencies are observed for both isomeric forms. The higher energy band, ca. 3600 cm^{-1}, is sharp and characteristic of a non-associated hydroxyl group, whereas the intense broad band ca. 3200 - 3400 cm^{-1} is indicative of associated hydroxyl functions. This phenomenon has been observed with salicylaldoxime [20-22] and the higher energy band is assigned to the stretch of the oximino hydroxyl function and the lower energy band to the stretch of the phenolic hydroxyl function.

Salicylaldoxime is only found in the 'anti' form, so the assignments can be considered as correct for the 'anti' forms of the LIX reagents.

The evidence for existence of a strong intramolecular hydrogen bonded system with the 'syn' isomers is further supported by pK_a data [16]. The 'syn' isomers are observed to act as stronger acids than the 'anti' isomers. This has been suggested as being a result of the strong intramolecular hydrogen bond being able to stabilise the anionic form of the oxime.

The nature of the intermolecular association observed

for the 'anti' forms of these reagents has been a matter of discussion for several years. Neelameggham [23] concludes from slope analysis studies on the extraction of Cu(II) and Fe(III) by LIX 64N that the reagent exists in dimeric form. Ashbrook [18] has also suggested, from infra-red evidence ($\Delta\nu$(OH) values), that the 'anti' isomers possess a dimeric structure. However, it would appear that the degree of polymerisation in these systems is very solvent dependent. For example, molecular weight determinations on P50 in freezing cyclohexane indicate at least a trimeric structure [24]. SME 529 displays higher association in aromatic solvents than in aliphatic solvents [24,25]. Several solvent dependent associations ranging from monomeric to polymeric structures have been reported [17,25-28].

Price and Tumulty [29] have deduced that a P50 dimer at an aqueous/organic interface would adsorb with such orientation that preferential hydrogen bonding between phenolic oxygen lone pair electrons and water would occur. Flett [30], however, suggests that hydrogen bonding with water would compete with molecular associative forces and render interfacial dimer adsorption unlikely. Dalton et al [31] have calculated the interfacial area that would be occupied by a P50 dimer as 125 Å^2, and that of a P50 monomer as 17 Å^2. This compares with an experimentally determined value of 60-70 Å^2, indicating that the 'anti' isomers are associated to a certain extent at the interface.

So in solution the structures of the 'syn' and 'anti' isomers of the aromatic LIX reagents can be represented thus:-

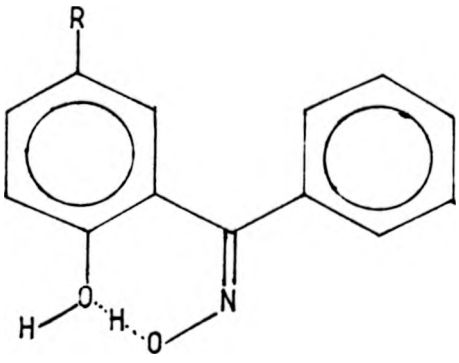

Intramolecular hydrogen bond

SYN ISOMERS

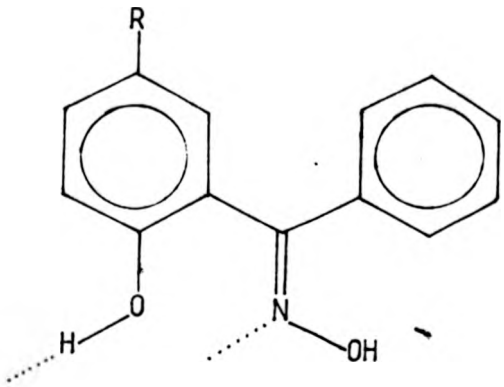

Intermolecular hydrogen bonds

ANTI ISOMERS

It is well known that these benzophenone derivatives will only form metal complexes in the 'anti' form [32]. In fact this information is usually employed to rapidly distinguish between the two forms [33,34].

An equilibrium between the 'syn' and 'anti' isomers is known to exist with related compounds [35,36] and has been shown to exist with the LIX reagents [16]. It has been observed that isomerically pure samples of the 'anti' form of the LIX reagents which have been left standing for several months contain a quantity of the 'syn' isomer. The mechanism for this conversion has been suggested as occurring through the formation of a nitrone intermediate. This mechanism (see below) has, however, not been verified.

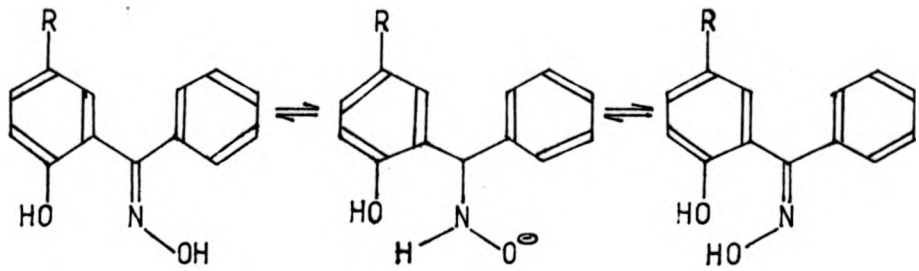

This equilibrium is known to be very pH dependent. As pH increases the 'syn' isomers are observed to be more capable of complexing copper(II). This observation is explained by consideration of a 'syn' to 'anti' conversion at high pH, immediately after which complexation can occur. Thus it can be expected that at high pH the loading characteristics of the LIX reagents will improve as any 'syn' isomer present can be converted fairly readily to the 'anti' form which can then complex with copper(II).

Determined pK_a values of hydroxyoxime commercial liquid-liquid extractants and some related compounds are listed in Table 1.4. .

Examination of this data reveals that LIX 70 in both 'syn' and 'anti' forms has an increased acid strength over the other LIX reagents. This is also demonstrated in its ability to extract copper at lower pH than the other reagents. These observations are a direct consequence of chlorine substitution

Table 1.4. pK_a's of the LIX Reagents and Some Related Ligands.

OXIME	pK_a (a,b)	pK_a (c,d)	OXIME	pK_a
SYN				
LIX 65N	10.56	12.25	P50	14.48 [c,d]
LIX 64	10.72		P17	14.58 [c,d]
LIX 70	9.58		SME 529	14.78 [c,d]
BENZOX	10.30			
			SALO	12.08 (pK_a^1) [e,f]
ANTI				11.72 (pK_a^2) [e,f]
LIX 65N	12.33	14.82	ACETOX	11.95 [e,g]
LIX 64	12.34		MeACETOX	11.89 [e,g]
LIX 70	11.46		ClACETOX	11.24 [e,g]
BENZOX	11.89		ClBENZOX [h]	11.42 [e,g]
LIX 63	13.50	17.0		

a) 0.33 mole fraction dioxane

b) Reference 18

c) 10% aqueous acetone

d) Reference 37

e) 75% aqueous dioxane

f) Reference 38

g) Reference 39

h) The authors do not report as to which isomer this value relates

in the 3-position. This substitution causes withdrawal of electron density from the phenolic oxygen and hence increases the acidity of the phenolic proton.

It is also noticed that only one value of pK_a is recorded for each oxime apart from salicylaldoxime (SALO). Each compound possesses two ionisable protons and so two values of pK_a would be expected for every oxime listed in Table 1.4. .

Ashbrook [18] assigns the values of pK_a reported for the LIX reagents to deprotonation of the phenolic group. Attempts to obtain values of pK_a for the oximino proton were unsuccessful and it is concluded that either the oximino proton is only weakly acidic or that its dissociation overlaps that of the phenolic proton. Patel and Patel [39] find with 2-hydroxy-5-chlorobenzophenone oxime (ClBENZOX), 2-hydroxy-5-methylacetophenone oxime (MeACETOX) and 2-hydroxy-5-chloroacetophenone oxime (ClACETOX) that apparently only one proton, which is assigned as the phenolic proton, dissociates.

With salicylaldoxime, Japalpurwala et al [38] report an indirectly calculated value of pK_a for the oximino proton and this is very close to the value of the pK_a of the phenolic proton. This, however, is the only reported value of this stability constant.

It is also reported [38] that for a series of oximes studied, the value of pK_a is lowest when no intramolecular hydrogen bonding occurs in the molecule. In this series salicylnitrile exhibits no internal hydrogen bonding and has the lowest pK_a. Once again the importance of hydrogen bonding with these hydroxyoximes is demonstrated.

1.4. Kinetics and Mechanisms in the Liquid-Liquid Extraction of Copper.

Mechanisms of metal extraction from an aqueous phase to an organic phase have been studied frequently over the last ten years or so. Two possible mechanisms have been postulated for this type of interaction. One involves the formation of a metal-extractant species in the aqueous phase which is subsequently transferred to the organic phase i.e. a homogeneous process. The second suggested mechanism involves metal-extractant complex formation at the interface of the aqueous and organic phases followed by transfer to the organic phase i.e. a heterogeneous process. These two types of mechanism should be readily distinguishable by their different extraction kinetics characteristics as the heterogeneous type mechanism should display a large dependence on interfacial area and other physical properties of the extraction system.

Early studies on several liquid-liquid extraction processes produced a series of inconclusive results [40-44]. Since 1974, however, a number of studies on the kinetics of extraction of copper by commercial extractants, particularly LIX 64N, have lead to a much greater understanding of the mechanisms involved with these molecules.

These studies of extraction kinetics of the hydroxyoxime extractants have been performed almost exclusively with two separate techniques. The one makes use of an AKUFVE, which is a Swedish abbreviation for "apparatus for continuous measurement of distribution factors in solvent extraction". This apparatus has been described and developed by Rydberg and coworkers [45-48]. A

schematic diagram of this apparatus is given in Figure 1.3.. The principle of this technique involves initial introduction of the two phases into the mixing chamber. These are then stirred together at a predetermined rate which is high enough so that the kinetics of extraction are independent of mixer speed. Then there follows the injection of either the active constituent of the organic or the aqueous phase. The mixture is carried down to a continuous flow centrifuge where absolute phase separation is induced. The two separated phases can then flow through appropriate measuring devices and then either leave the system or return to the mixer in a continuous loop system.

With this apparatus the parameters that are usually continuously monitored are pH, temperature and the distribution factor, D. There are several disadvantages in employing this technique to measure extraction kinetics. These are the inability to alter interfacial area and the large amounts of solution that are required.

The second most frequently used method of monitoring two phase extraction kinetics is the single drop technique. The apparatus used was originally developed by Nitsch [49] and has been employed in studies of the extraction behaviour of uranium(VI) and plutonium(IV) with tributyl phosphate [50]. It was first adapted for study of the extraction of copper by Whewell et al [51] where extraction by LIX 64N was studied. The apparatus used by Whewell et al is shown in Figure 1.4..

The principle of the technique is that a droplet of either the organic or aqueous solution is allowed to enter the apparatus and either rise or drop through the bulk aqueous or

schematic diagram of this apparatus is given in Figure 1.3.. The principle of this technique involves initial introduction of the two phases into the mixing chamber. These are then stirred together at a predetermined rate which is high enough so that the kinetics of extraction are independent of mixer speed. Then there follows the injection of either the active constituent of the organic or the aqueous phase. The mixture is carried down to a continuous flow centrifuge where absolute phase separation is induced. The two separated phases can then flow through appropriate measuring devices and then either leave the system or return to the mixer in a continuous loop system.

With this apparatus the parameters that are usually continuously monitored are pH, temperature and the distribution factor, D. There are several disadvantages in employing this technique to measure extraction kinetics. These are the inability to alter interfacial area and the large amounts of solution that are required.

The second most frequently used method of monitoring two phase extraction kinetics is the single drop technique. The apparatus used was originally developed by Nitsch [49] and has been employed in studies of the extraction behaviour of uranium(VI) and plutonium(IV) with tributyl phosphate [50]. It was first adapted for study of the extraction of copper by Whewell et al [51] where extraction by LIX 64N was studied. The apparatus used by Whewell et al is shown in Figure 1.4..

The principle of the technique is that a droplet of either the organic or aqueous solution is allowed to enter the apparatus and either rise or drop through the bulk aqueous or

Figure 1.3. Schematic Diagram of AKUFVE apparatus (Ref. 45)

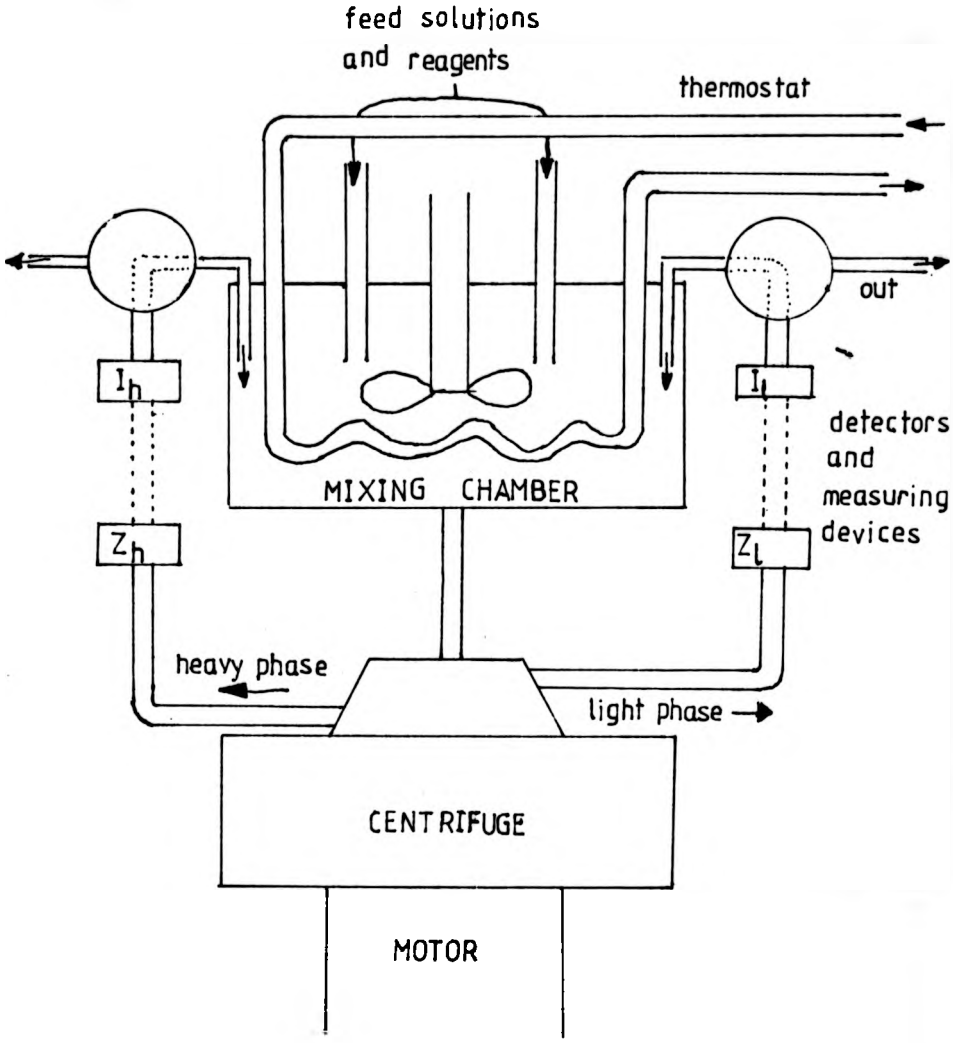

Figure 1.4. Single Drop Apparatus (Ref. 51)

[arranged as for rising drop experiment]

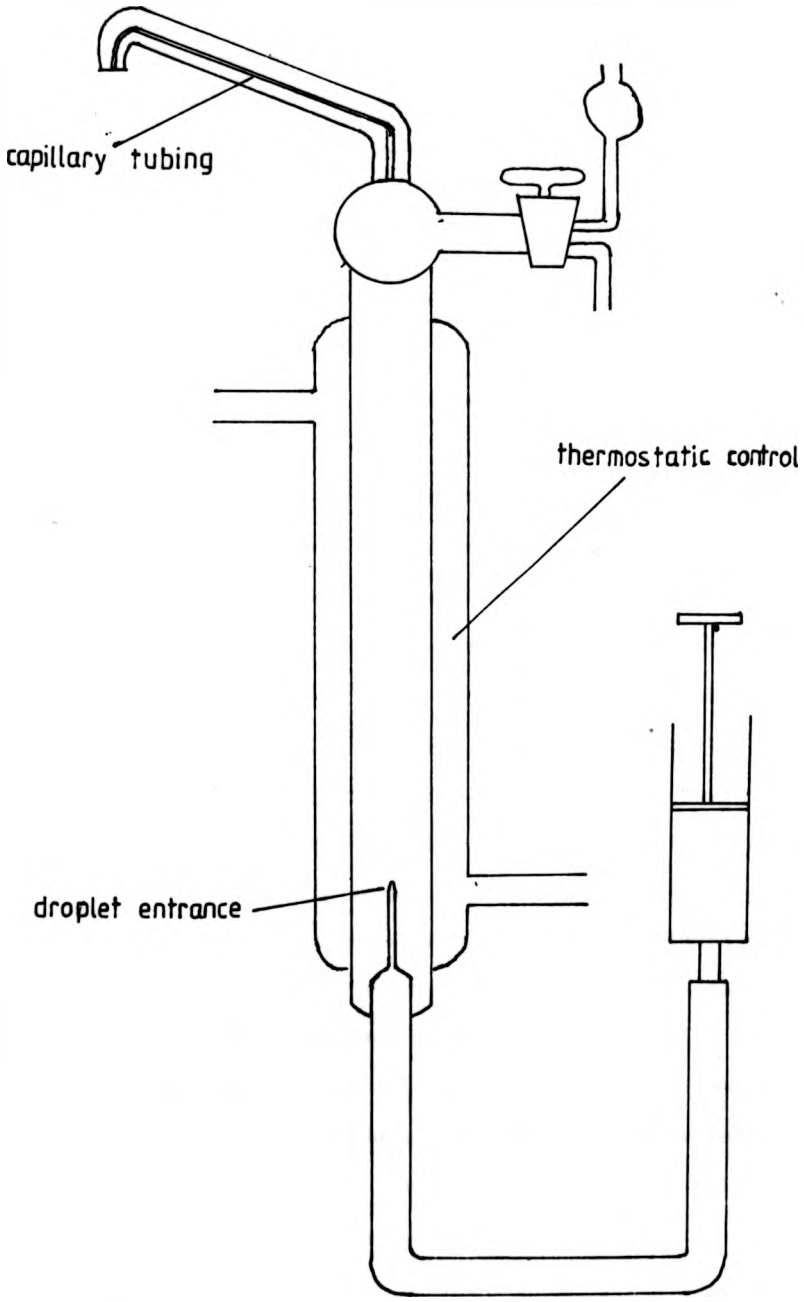

organic solution contained in the main part of the system. This single drop is collected, after travelling the length of the tube, in a length of constant diameter capillary tubing and as more drops are received by the capillary they exit the apparatus into a collection vessel.

The great advantage with this apparatus over the AKUFVE is that droplet size can be varied and hence interfacial area is varied. It is thus possible by use of this technique to investigate the dependence of the rate of extraction on this parameter. However, two major problems arise with the single drop technique. The hydrodynamics of droplet systems are only moderately characterised and also the time of contact of the two phases is limited as only a moderate size tube is practical.

An alternative technique to the two systems described above has been described and has been shown to be applicable to this type of kinetic determination by Kirchner and Ferdinando [52]. This method involves a rapidly stirred mixture of the two solution phases and monitoring of the rate of copper extraction by use of a copper(II) ion selective electrode alongside a double junction reference electrode. The method described appears to yield reliable results and the only drawback is eventual buildup of the organic phase components in the outer compartment of the double junction reference electrode. This compartment can be easily washed out and reconstituted. No mechanistic studies have been reported in which this method has been employed but the usefulness of the technique seems clear as it does produce reliable results and it is reported that an experimentally reproducible interfacial area is possible with the apparatus.

The first mechanistic studies on the extraction of copper(II) by commercial liquid-liquid extractants were performed by Neelameggham [23] who concluded that the extracted species is formed in the aqueous phase and is then reextracted into the organic phase in a homogeneous process. The mechanism proposed is described by the following reaction scheme in which a bar denotes the organic phase:

$$\underset{\text{dimer}}{\overline{R_2H_2}} \rightleftharpoons \overline{2RH} \qquad (1)$$

$$\overline{2RH} \rightleftharpoons 2RH \qquad (2)$$

$$2RH \rightleftharpoons 2R^- + 2H^+ \qquad (3)$$

$$Cu(OH_2)_6^{2+} + R^- \rightleftharpoons Cu(OH_2)_4R^+ + 2H_2O \qquad (4)$$

$$Cu(OH_2)_4R^+ \rightleftharpoons Cu(OH_2)_2R^+ + 2H_2O \qquad (5)$$

$$Cu(OH_2)_2R^+ + R^- \rightleftharpoons CuR_2 + 2H_2O \qquad (6)$$

$$CuR_2 \rightleftharpoons \overline{CuR_2} \qquad (7)$$

The apparent rate law determined by Neelameggham is as follows:

$$-\frac{d[Cu]}{dt} = k_{obs}[Cu][RH]^{\frac{1}{2}} / [H^+] \qquad (8)$$

Several objections have been made to this proposed mechanism, the main one being that the solubility in the aqueous phase of LIX 65N and LIX 63 which are the active constituents of

LIX 64N has been shown [53] to be less than 10^{-5} M and determined pK_a values of these two hydroxyoximes [18] show that at the pH studied there would be a maximum concentration of ionised extractant of less than 10^{-10} M [54]. Also no consideration of the fact that LIX 64N is a mixture of LIX 65N and LIX 63 is taken into account.

Flett et al [55] using the AKUFVE, and being aware of the constitution of LIX 64N have performed studies using LIX 65N alone and have studied the effect of addition of LIX 63. Equilibrium studies show that in the absence of LIX 63, only one type of copper(II)-LIX 65N complex is present in the organic phase and this is of the stoichiometry CuR_2, where R is the monodeprotonated form of LIX 65N.

Addition of LIX 63 is shown to enhance the kinetics of extraction although it does not affect the equilibrium position. It is deduced, therefore, to behave in a catalytic role during the extraction process. These studies showed that the rate of extraction had a first-order dependence on copper concentration, an inverse first-order dependence on hydrogen ion concentration, first or slightly larger order dependence on LIX 65N concentration and a slightly less than half-order dependence on LIX 63 concentration. This non-integer order dependence on LIX 63 concentration is concluded to be evidence for a heterogeneous rate determining step i.e. an interfacial reaction. The fact that the respective orders with respect to concentrations of LIX 63 and LIX 65N do not add up to that of the order of the hydrogen ion dependence is concluded to indicate that one of these components is reacting in an unionised form. Determinations of the relative pK_a values of LIX 65N and LIX 63 [18,37] indicate that LIX 63 deprotonates at a

much higher pH than LIX 65N and indeed it has been shown that this α-hydroxyoxime is readily protonated at low pH [37,56,57]. The assumption that is made by Flett et al [55] that it would be LIX 63 which reacts in an unprotonated form would thus seem to be valid.

These authors recognise the low solubility of these reagents in water and postulate that the extraction reaction occurs with unionised oxime molecules. Thus the pH dependency indicates a rate controlling step inwhich an intermediate species is formed whose formation constant includes the value of the pH of the aqueous phase.

The following reaction scheme was proposed where RH signifies LIX 65N and BH signifies LIX 63. Subscripts "o" and "int" indicate the organic phase and the interface respectively.

$$(RH)_o \rightleftharpoons (RH)_{int} \quad (9)$$

$$Cu^{2+} + (RH)_{int} \rightleftharpoons CuR^+ + H^+ \quad (10)$$

$$CuR^+ + (BH)_{int} \rightleftharpoons (CuRB)_{int} + H^+ \quad (11)$$

$$(CuRB)_{int} \rightleftharpoons (CuRB)_o \quad (12)$$

$$(CuRB)_o + (RH)_o \rightleftharpoons (CuR_2)_o + (BH)_o \quad (13)$$

Equation (11) is believed to be the rate controlling step.

It is suggested that the pH dependency of equation (10)

can be removed by the following scheme.

$$CuR^+ + (BH)_{int} \rightleftharpoons (CuRBH^+)_{int} \quad (14)$$

$$(CuRBH^+)_{int} \rightleftharpoons (CuRBH^+)_o \quad (15)$$

$$(CuRBH^+)_o + (RH)_o \rightleftharpoons (CuR_2)_o + (BH)_o + H^+ \quad (16)$$

Atwood and Miller [58] have criticised the rate law which was derived from the above mechanism and is given by Flett et al as

$$k_{obs} = [Cu^{2+}][LIX\ 65N]_o[LIX\ 63]_o^{0.5} / [H^+] \quad (17)$$

They deduced from first principles that k_{obs} was in fact k_f, the rate constant for the forward complexation reaction. The fact that no back reaction mechanism had been considered in the rate law determination was also criticised. Atwood and Miller postulated that the formation rate did not in fact display an inverse first order dependence on hydrogen ion concentration, but the back reaction was first order in respect to hydrogen ion concentration. The following rate law was thus put forward:

$$-\frac{d[Cu^{2+}]}{dt} = k_f[LIX\ 65N]_o[LIX\ 63]_o^{0.5}[Cu^{2+}] - k_r[CuR_2]_o[H^+] \quad (18)$$

Flett et al [59] in a reply to this criticism agreed that k_{obs} should be replaced by k_f, a fact they had already realised. However, they did not agree with the derived rate law of Atwood

and Miller on the grounds that it indicates that the back reaction occurs through a different mechanism to the forward reaction. Considering the expression for both the forward reaction and the equilibrium constant the following amended rate law was postulated.

$$-\frac{d[Cu^{2+}]}{dt} = k_f[\text{LIX 65N}]_o[\text{LIX 63}]_o^{0.5}[Cu^{2+}] / [H^+] - k_r[\text{LIX 63}]_o^{0.5}[H^+][Cu(\text{LIX 65N})_2]_o / [\text{LIX 65N}]_o$$

This rate law was applied to experimental results determined by use of the single drop apparatus by Atwood et al [60]. This application improved the linearity of the kinetic plot quite significantly indicating this final rate law to be the more correct version.

The catalytic role of LIX 63 in LIX 64N liquid-liquid extraction of copper and nickel has been a point of interest for several years. As stated previously, Flett et al deduce that a mixed Cu(LIX 65N)(LIX 63) complex is formed and this somehow catalyses the extraction. Ashbrook [54] shows no objections to this scheme but points out that there is no reason why a species of the sort $Cu(\text{LIX 63})^+$ should not form prior to any interaction of copper(II) with LIX 65N. Indeed, it is suggested by Ashbrook, on the grounds that copper(II) is known to form 1:1 complexes with α-acyloinoximes, that this may be the most likely mechanism. Thus the following alteration was proposed:

$$Cu^{2+} + (BH)_{int} \rightleftharpoons (CuB^+)_{int} + H^+ \qquad (20)$$

$$(CuB^+)_{int} + (RH)_{int} \rightleftharpoons (CuBR)_{int} + H^+ \quad (21)$$

$$(CuBR)_{int} + (RH)_{int} \rightleftharpoons (CuR_2)_{int} + (BH)_o \quad (22)$$

$$(CuR_2)_{int} \rightleftharpoons (CuR_2)_o \quad (23)$$

Preston [61] has reported that LIX 63 can form 1:1 complexes with copper, but these are of the form CuL where LIX 63 = H_2L i.e. the oxime is in the doubly deprotonated form and forms a neutral complex with copper. The complex has been found to be polymeric in the solid state in units of 9 - 10 molecules. It does not seem likely that this complex would be formed in the extraction reaction.

An alternative explanation of the catalytic role of LIX 63 was first suggested by Atwood and Miller [58]. It was proposed that LIX 63 could protonate more readily than LIX 65N and this ability assisted the deprotonation of LIX 65N. Hence as this hydroxyoxime would be in an anionic form an increase in the rate of extraction would be expected. Since this idea was first postulated other workers have in fact demonstrated the ease of protonation of LIX 63 [56,57,62,65].

Whewell et al [62], postulate that if LIX 63 was indeed a true interfacially active component an addition of a small amount of this hydroxyoxime would have a marked effect on the kinetics of extraction. This phenomenon was not observed. Interfacial tension measurements [59] have demonstrated that at the concentrations of LIX 63 in the commercial extractant (~2%) no measurable difference in interfacial tension is observed on this

addition to LIX 65N. This indicates that in fact LIX 63 is not present at the interface to any great degree in LIX 64N extraction reactions. It is possible [64] to observe a decrease in interfacial tension but at relatively high concentrations of LIX 63. This piece of evidence shows that LIX 63 may in fact get to the interface but is not present in significantly large enough quantities to be likely to catalyse the extraction reaction by complex formation. The observation that extraction by LIX 63 alone seems remarkably slower than with LIX 64N [62] also supports this hypothesis. So the protonation theory of Atwood and Miller does seem more likely than the previous metal-LIX 63 complexation theory but this is certainly not proven.

The dependence of the rate of copper extraction on other factors in the system has also been investigated. p-Nonylphenol, which is known to be present in the aromatic LIX reagent preparation [62] at quite high levels, has been demonstrated to have a deleterious effect on extraction kinetics [65]. Single drop studies have shown that a marked retardation in extraction rate occurs with increasing p-nonylphenol concentration. No great decrease is observed on addition of a small amount of p-nonylphenol and from this piece of evidence it is concluded that the phenol is not a highly interfacially active agent. Interfacial tension measurements confirm this observation and it has been postulated that the retardation in reaction rate is the result of preferential solvation of the aromatic hydroxyoximes by the p-nonylphenol.

The effect of a change of diluent on the rate of extraction has also been investigated. It has been shown [64] that copper is extracted by LIX 65N more rapidly when the oxime is in

a hexane solution than when it is in a toluene solution. It has also been observed that LIX 65N [66] can form a complex with copper(II) at a lower pH in kerosene than it can in both toluene and xylene, though it is more difficult to strip the copper from a kerosene solution. It has been demonstrated with LIX 65N, SME 529 and Kelex 100 [29,31,67] that the use of an aliphatic solvent lowers the interfacial area per molecule, thus increasing the interfacial extractant concentration and thus improving the extraction kinetics.

Hughes et al [68] have performed diffusion studies with LIX 64N and found that the extractant exhibits a higher diffusivity in heptane than it does in toluene and postulate that viscosity of the diluent may be the important factor which alters the rate of extraction.

The presence of the 'syn' isomers of these hydroxyoximes has been neglected in consideration of any reaction mechanism in previous studies. Some interfacial tension measurements [56] have shown that the 'syn' isomer of LIX 65N is more interfacially active than the 'anti' isomer. This would mean that if relatively high concentrations of the 'syn' isomer were present the interface would essentially be blocked.

So in conclusion it seems that there are many difficulties encountered in studies of kinetics of these extractants. All previous studies have employed either the commercial reagent as received or less than 100% pure samples of these hydroxyoximes and this situation results in many factors which can determine the reaction kinetics and cause irreproducibility of any rate constants derived from sample to sample.

As a result of these observations the work that will be discussed in Chapter 3 of this thesis was initiated. These investigations concern the complex formation reactions of these types of ligand which have been performed in a single phase situation to avoid the problems induced by the presence of an interface in two phase kinetics.

Only the pure 'anti' isomers of these ligands have been used in these studies and thus by simplifying the reaction conditions for metal complexation it was hoped that an understanding of the mechanisms involved would be more readily attained.

1.5. The Structural Chemistry of Some Transition Metal Complexes of Hydroxyoximes and Related Ligands.

A. Structural behaviour in the solid state and in non-donor solvents.

The structural chemistry of transition metal complexes of hydroxyoxime ligands has been reviewed by Chakravorty [69]. Of the ligands which are most closely related to the commercial hydroxyoxime liquid-liquid extractants, salicylaldoxime (SALO) is by far the most comprehensively studied and a good deal is known about the structural chemistry of its metal complexes. This ligand, which is the parent molecule of the Acorga Ltd. produced P50, has been shown to form complexes of the type ML_2 (SALO = LH) with divalent transition metals [70] as do all the hydroxyoximes. Crystal structures of the Cu(II) complexes of SALO [71] and its 5-chloro substituted analogue have been determined [72]. Both complexes display a square-planar trans-configuration around the metal atom and exhibit a degree of molecular association. This association is in the form of an axial type interaction with oxygen atoms of neighbouring molecules. In the case of the SALO complex the oxygen atoms involved are of the oximino type and in the case of the 5-chlorosalicylaldoximate it is the phenolic oxygens which participate in this association. The respective interatomic distances (Cu·····O) are 2.66 Å and 3.01 Å. Two observations of note with these two structures are the existence of hydrogen bonding between the two ligand molecules and the 'stepped' arrangement of the ligands. These are demonstrated in Figure 1.5..

The molecular structures of the Ni(II) [73,74], Pd(II) [75] and Be(II) [76] complexes of SALO have also been determined by

Figure 1.5. Representations of the Molecular Structure of bis(5-chlorosalicylaldoximato)copper(II)

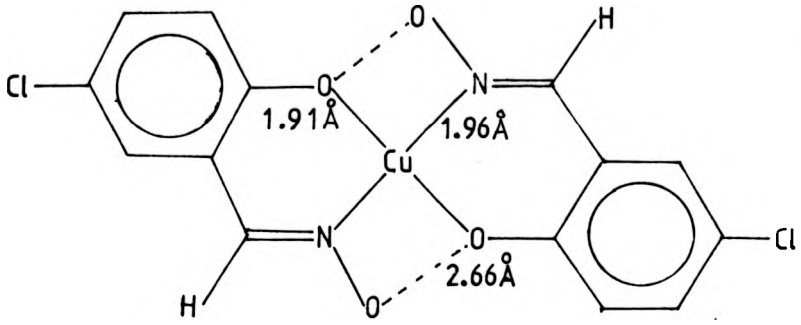

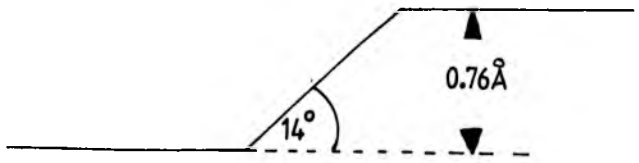

crystallographic methods. No molecular association is observed but both the Ni(II) and Pd(II) complexes exhibit hydrogen bonding between the ligand molecules, the 'stepped' structure and a square-planar trans-geometry.

Salicylaldoxime is one of a series of ligands based on salicylideneimine, whose structure is shown below.

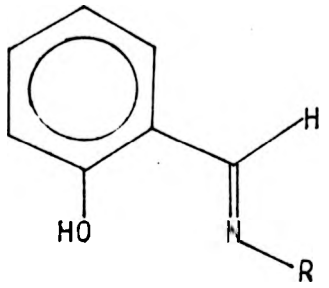

By alteration of the imine nitrogen substituent (R) a large series of different ligands can be produced. Extensive studies have been performed with these ligands and their metal complexes as it has been found that R can be readily varied and the nature of this group can directly determine the co-ordination geometry of the complexes. The structural behaviour of these complexes has been well reviewed [77-81].

The following discussion will concentrate on the complexes of Co(II), Ni(II) and Cu(II) as this thesis is concerned mainly with these three divalent metal ions. Salicylideneimine complexes where R does not equal hydroxyl will be discussed and compared with the respective SALO complexes.

As stated above a 'stepped' structure has been observed with several complexes of SALO and indeed this structure is frequently observed in Cu(II) [82-86], Ni(II) [87,88] and Pd(II) [89,90]

complexes of other salicylideneimine type ligands. Maslen and Waters [81] have suggested an explanation for this phenomenon. They postulate that when complexes exhibit a 'step' distance of less than 0.4 Å this is merely a result of the bonding requirements of the chelate ring. In complexes where this 'step' distance is greater than 0.4 Å it is suggested that the phenolic oxygen atoms have undergone a hybridisation change. The evidence for this is in the observation that as the imine substituent is altered and becomes more electron donating 'step' distances are found to increase. Determination of metal-phenolic oxygen-carbon bond angles in these complexes indicate that as the 'step' distance increases, these bond angles tend towards a tetrahedral value. Thus it is postulated by Maslen and Waters that as electron density is pushed into the chelate ring the hybridisation of the phenolic oxygen orbitals increases in p character and there follows a loss of ligand co-planarity.

A very large number of studies have been performed on Ni(II) complexes of these salicylideneimine ligands. The reason for this interest in these complexes is the observation that equilibria of the type

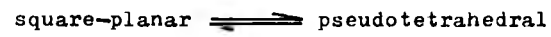

are very common in non-donor solvents. Many examples of this type of equilibrium have been investigated and thermodynamic parameters for the process evaluated (A comprehensive list of ΔH°, ΔS° and ΔG° values can be found in References 79 and 91). This type of equilibrium has been monitored primarily by two

techniques. The first, proton magnetic resonance, has proven very useful for this purpose mainly as a result of the differing magnetic properties of the two species. Nickel(II) has a d^8 electronic configuration and,as a result of this, square-planar complexes are diamagnetic. Any deviations from this planarity, towards a tetrahedral configuration result in paramagnetic properties. Paramagnetic species display large contact shifts in their nuclear magnetic resonance (n.m.r.) spectra, whereas diamagnetic species do not. This difference in behaviour between the two configurational isomers can be employed to establish thermodynamic parameters for the equilibrium process. The experimental observations and subsequent evaluation of results has been reviewed by Holm [92], and paramagnetic n.m.r. will be discussed more fully in Chapter 4.

The second method of study which has been extensively employed in these studies is that of electronic spectrophotometry. The differing geometries of Ni(II) complexes can be readily distinguished by this technique and indeed, is virtually diagnostic of their co-ordination geometry [93]. Thus the dependence of the electronic spectra of these complexes on change in temperature can be employed to ascertain the thermodynamic parameters associated with the equilibrium process.

It has been found that as the nature of R is varied in these salicylideneimine complexes the preference for a tetrahedral configuration around the metal centre generally increases in the following manner:

t-butyl>α-branched alkyl $\gg$ aryl $\sim$ n-alkyl $\sim$ Me $\sim$ H

techniques. The first, proton magnetic resonance, has proven very useful for this purpose mainly as a result of the differing magnetic properties of the two species. Nickel(II) has a d^8 electronic configuration and,as a result of this, square-planar complexes are diamagnetic. Any deviations from this planarity, towards a tetrahedral configuration result in paramagnetic properties. Paramagnetic species display large contact shifts in their nuclear magnetic resonance (n.m.r.) spectra, whereas diamagnetic species do not. This difference in behaviour between the two configurational isomers can be employed to establish thermodynamic parameters for the equilibrium process. The experimental observations and subsequent evaluation of results has been reviewed by Holm [92], and paramagnetic n.m.r. will be discussed more fully in Chapter 4.

The second method of study which has been extensively employed in these studies is that of electronic spectrophotometry. The differing geometries of Ni(II) complexes can be readily distinguished by this technique and indeed, is virtually diagnostic of their co-ordination geometry [93]. Thus the dependence of the electronic spectra of these complexes on change in temperature can be employed to ascertain the thermodynamic parameters associated with the equilibrium process.

It has been found that as the nature of R is varied in these salicylideneimine complexes the preference for a tetrahedral configuration around the metal centre generally increases in the following manner:

t-butyl>α-branched alkyl $\gg$ aryl $\sim$ n-alkyl $\sim$ Me $\sim$ H

The factors which determine this trend are mainly steric [77-80] although to rationalise the configurations of certain complexes electronic considerations must be taken into account [81].

Bis(salicylaldoximato)nickel(II) would then be expected to exhibit a square-planar geometry and indeed, as indicated previously, this is the case. There is no evidence for tetrahedral species in the solid phase or in non-donor solvents [94]. However, magnetic studies have provided evidence which indicates a degree of intermolecular association in chloroform solution [95]. This type of solution association has been observed with other salicylideneimine complexes and, as would be expected, demonstrates a concentration dependence [96,97].

A large number of cobalt(II) complexes of these ligands have also been isolated and characterised. When R = CH_3 or C_2H_5 the complexes are found to be extremely oxygen sensitive [98]. Indeed cobalt(II) complexes of this type are well known reversible or irreversible oxygen carriers and have been recognised as such since as early as 1947 [99]. This subject has been recently reviewed [100] and will be discussed in greater detail in Chapters 2 and 3.

Most cobalt(II)-salicylideneimine complexes exhibit a high-spin tetrahedral configuration both in the solid state and in non-donor solvents. Complexes of the type shown below

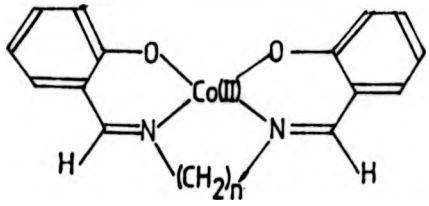

are found to display square planar or tetrahedral configurations depending on the number of methylene groups in the bridging alkyl chain. When the number is small the molecule is necessarily constrained in a square-planar configuration. As the number of methylene groups in the bridging chain is increased a gradual loss of planarity is observed and the complexes tend towards a tetra hedral geometry [101,102]. In contrast, nickel(II) complexes of these ligands retain their square-planar geometries even when four methylene groups are present in the chain [103] (although recently it has been shown that when bulky substituents are introduced into the bridging chain the nickel(II) complexes do deviate from a planar configuration [104]). This demonstrates the preference for cobalt(II) complexes to adopt a tetrahedral configuration, and it is therefore somewhat surprising to find that the cobalt(II) complexes of salicylideneimine itself and SALO exist as low-spin square planar complexes in inert solvents [20,105]. This deviation from the preferred tetrahedral configuration is found to be the result of strong internal hydrogen bonding in the complexes. This once again demonstrates the importance of this phenomenon in these hydroxyoxime systems.

Copper(II) complexes of salicylideneimines exhibit both square-planar and tetrahedral configurations and the trends in geometry generally follow that of the corresponding nickel(II) complexes. The square-planar trans-complexes of copper(II) tend to retain their configurations in non-donor solvents, as magnetic moments and electronic spectra remain unchanged [106]. Bis(salicylaldoximato)copper(II) behaves as such [20], but there are exceptions to this generalisation [79,107]. The pseudotetrahedral

complexes also seem to retain their configuration in non-donor solvents [108,109] and no investigations of square-planar/pseudo-tetrahedral equilibria have been performed.

In conclusion, the nickel(II), cobalt(II) and copper(II) complexes of SALO all exhibit square planar configurations. This is as would be expected for nickel(II) and copper(II),but the cobalt(II) complex demonstrates that the strength of the intra-molecular hydrogen bonding is sufficient to cause a deviation from the preferred geometry for this metal ion.

B. Adduct formation in donor solvents.

Four co-ordinate complexes of salicylideneimines are potentially six co-ordinate and indeed the formation of both penta- and hexaco-ordinate adducts have been frequently studied and reviewed [78,110]. The majority of these studies have been with nickel(II) complexes and their pyridine adducts using electronic spectral and magnetic data as the means of study.

Two main factors determine the ability of these complexes to form adducts, namely steric and electronic factors. The role of steric constraint can be demonstrated by the study of nickel(II) salicylideneimine complexes [78]. When R = H, OH, n-alkyl or phenyl it is found that bis pyridine adducts are readily formed. However, when R = iso-propyl or t-butyl the complexes retain their pseudotetrahedral configurations in pyridine solutions. This observation is a direct result of the presence of the bulky imine substituents. To increase co-ordination number around the nickel(II) centre the two ligands

would have to adopt a more coplanar geometry and this would produce unfavourable interactions between the imine substituents. Thus no adduct formation occurs.

Certain metal complexes of this type retain their square-planar configurations in the absence of any obvious steric factors. This phenomenon has been explained on the grounds of differences in ligand field strengths. It has been suggested [110] that a strong ligand field would favour a square planar environment over penta- or hexaco-ordination. The nature of the metal-ligand bond can also affect the ability of these complexes to form adducts as if extensive π-bonding exists in this bond then the retention of four co-ordinate geometry would be preferred.

The different behaviour of cobalt(II), nickel(II) and copper(II) toward adduct formation can be demonstrated by reference to the complexes of the salicylideneimine where R = 2,6-dimethyl phenyl. This bulky substituent would be expected to hinder adduct formation on steric grounds, and indeed the nickel(II) complex of this ligand retains its four co-ordinate geometry in pyridine solutions [111]. The copper(II) [111] and cobalt(II) [112] complexes, however, bind only one pyridine molecule and thus assume a pentaco-ordinate geometry. These observations are explained for cobalt(II) on steric grounds and for copper(II) on the grounds of the Jahn-Teller effect. The electronic configuration of copper(II) is d^9 and thus it exhibits Jahn-Teller distortions. An elongation of the axial bonds between the metal ion and pyridine occurs and steric interference is reduced. Nickel(II), which has a d^8 electronic configuration, is not

susceptible to this type of distortion and its complexes are generally of a regular geometry. Thus steric problems can not be alleviated and no adduct formation occurs.

The nickel(II)-salicylaldoxime complex has been shown to form trans-octahedral bis-adducts with pyridine [94,95,113,114] and related nitrogen bases [113-115]. These will be discussed in Chapter 4, as will other adducts of this complex.

Nickel(II) [116-120], cobalt(II) [121,122] and copper(II) [122,123] complexes of salicylideneimine type ligands have been shown to exhibit an equilibrium between tetraco-ordinate and hexaco-ordinate geometry in several donor solvents. These equilibrium processes have been investigated mainly by spectrophotometric methods and thermodynamic parameters have been evaluated. These will also be discussed in Chapter 4.

The bis-adduct formation process is reported to be stepwise in nature i.e. the reaction proceeds via a pentaco-ordinate mono-adduct. Thus:-

$$NiL_2 + B \overset{K_1}{\rightleftharpoons} NiL_2B$$

$$NiL_2B + B \overset{K_2}{\rightleftharpoons} NiL_2B_2$$

Mono-adduct species have indeed been detected with these types of complex by calorimetry [119], spectrophotometry [120,124] and n.m.r. spectroscopy [125].

Dakternieks et al [120] in a study with three different hydroxyimine complexes report electronic spectra that show the presence of weak absorptions around 1400 - 1500 nm which are

susceptible to this type of distortion and its complexes are generally of a regular geometry. Thus steric problems can not be alleviated and no adduct formation occurs.

The nickel(II)-salicylaldoxime complex has been shown to form trans-octahedral bis-adducts with pyridine [94,95,113,114] and related nitrogen bases [113-115]. These will be discussed in Chapter 4, as will other adducts of this complex.

Nickel(II) [116-120], cobalt(II) [121,122] and copper(II) [122,123] complexes of salicylideneimine type ligands have been shown to exhibit an equilibrium between tetraco-ordinate and hexaco-ordinate geometry in several donor solvents. These equilibrium processes have been investigated mainly by spectrophotometric methods and thermodynamic parameters have been evaluated. These will also be discussed in Chapter 4.

The bis-adduct formation process is reported to be stepwise in nature i.e. the reaction proceeds via a pentaco-ordinate mono-adduct. Thus:-

$$NiL_2 + B \overset{K_1}{\rightleftharpoons} NiL_2B$$

$$NiL_2B + B \overset{K_2}{\rightleftharpoons} NiL_2B_2$$

Mono-adduct species have indeed been detected with these types of complex by calorimetry [119], spectrophotometry [120,124] and n.m.r. spectroscopy [125].

Dakternieks et al [120] in a study with three different hydroxyimine complexes report electronic spectra that show the pres ence of weak absorptions around 1400 - 1500 nm which are

typical of a high-spin pentaco-ordinate nickel(II) complex. From these spectra they have been able to obtain values for K_1 and K_2 and have shown that K_2 is significantly greater (between 20 and 50 times) than K_1. This is as expected as only small amounts of these five co-ordinate species have been detected. ΔH° and ΔS° values have also been calculated for the overall bis-adduct formation and typical values are -60 $KJmole^{-1}$ and -150 $JK^{-1}mole^{-1}$ respectively. Calorimetric studies linked with magnetic studies [119] have shown that for the complex bis(N-butylsalicylideneiminato)-nickel(II) at a concentration of 7.5×10^{-3} mole l^{-1} in benzene and pyridine, ΔH_o^1 (enthalpy term for addition of first mole of pyridine) has a value of approximately -10 $KJmole^{-1}$ indicating that it is the addition of the second molecule of pyridine which is the major contribution to the enthalpy term.

Studies of nickel(II)-salicylideneimine complexes in 2-methylpyridine solutions have shown that this heterocyclic base will only form mono adducts and even in neat 2-methyl-pyridine solutions 100% formation is not achieved [120,126]. Equilibrium studies by Lindoy and Mockler [126] reveal low adduct formation constants demonstrating the preference for tetra-co-ordination. It is suggested that steric factors influence the ability to form bis-adducts in solution of this nitrogen base. As described previously, complexes of this type are not perfectly coplanar and it is postulated that the methyl substituent on the 2-methylpyridine forces a structural change on the complex which is such as to prevent co-ordination of a second 2-methylpyridine molecule. Thus:-

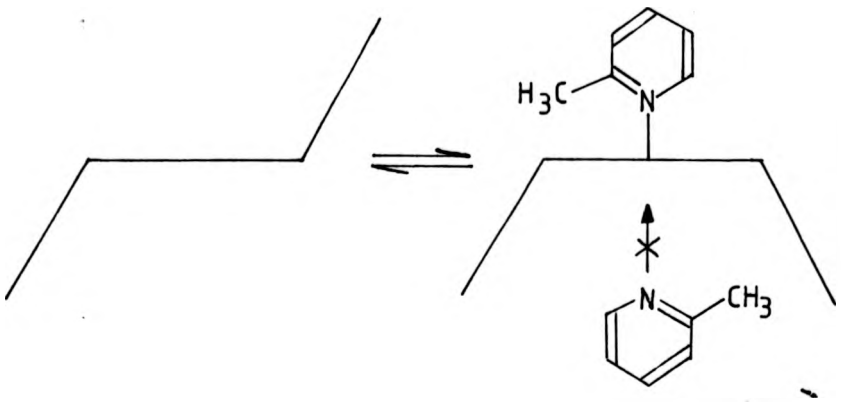

The study of the exchange of these nitrogen bases on salicylideneimine complexes has been neglected, although studies have been performed on related quadridentate ligands. There is no reason why metal complexes of hydroxyoxime commercial solvent extractants should not form adducts and as these reagents can be employed to extract from ammoniacal solutions, an investigation of adduct formation with these complexes has been performed and will be discussed in Chapter 4.

CHAPTER 2.

SPECTROSCOPIC STUDY OF LIX 65N AND SOME RELATED HYDROXYOXIME LIGANDS AND THEIR METAL COMPLEXES.

2.1. Introduction.

The complexes formed on reaction of divalent transition metal ions with commercial hydroxyoxime liquid-liquid extractants have not been studied to any great extent. Hosking and Rice [24] have, however, reported the isolation of the Ni(II) and Cu(II) complexes of some of these reagents, namely LIX 65N, P50 and SME 529. All of the complexes studied by these authors exhibit metal-ligand stoichiometries of 1:2 in the solution phase, and an electronic spectral study indicated that only one distinct metal-ligand species is present in solution.

Comparisons have often been made between these commercial liquid-liquid extractants and salicylaldoxime [12,24,54]; their molecular structures are closely related, and indeed u.v.-visible studies in solution of the Ni(II) and Cu(II) complexes of these commercial extractants [24] show that they have very similar extinction coefficients and absorption maxima to those of the corresponding metal complexes formed by salicylaldoxime. Therefore, in the investigation of these metal complexes, salicylaldoximates can be used as models on account of the relatively large amount of knowledge accumulated about them.

As described in the introductory chapter, the complexes of Ni(II), Cu(II) and Co(II) with salicylaldoxime have been isolated. Many other metal-salicylaldoxime complexes have been prepared and display various stoichiometries. Complexes where the metal-ligand ratio is 1:1 have been found for U(VI) [127], Mn(II) [128,129], Fe(III) [130], Ti(IV) [131], Zr(IV) [131], Hf(IV) [131], Rh(I) [132] and several of the rare earth elements [133]. Complexes with metal-ligand ratios of 1:2 have been found for Fe(II) [20],

Mn(II) [20,134], Zn(II) [20], Pd(II) [75,135,136], Ce(IV) [133], Ti(IV) [131] and V(V) [137]. Pd(II) has also been found to display a stoichiometry of 1:3 resulting in a complex of the type $PdL_2(HL)$ where HL = SALO [135].

The complexes of 1:2 stoichiometry are the main concern of this work as this is the stoichiometry found with the Ni(II) and Cu(II) complexes of the commercial extractants [23,24]. The salicylaldoximate complexes, where the donor atom set is $[N_2O_2]$, are all thought to exist with a square planar arrangement of the ligand molecules around the metal centre. There are two possible ways of arranging this $[N_2O_2]$ donor atom set around the metal to form a square-planar complex, namely in the cis- or trans-configuration:

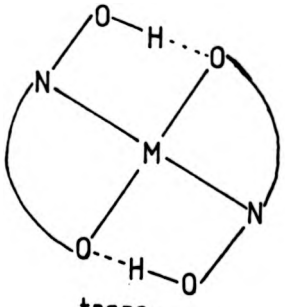

trans-

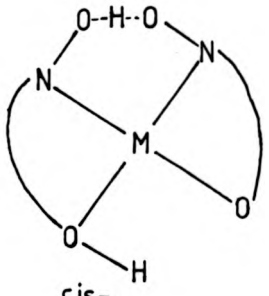

cis-

The crystal structures of the Ni(II) [73], Cu(II) [71] and Pd(II) [75] complexes of salicylaldoxime reveal a trans-configuration around the metals in each case. No crystallographic studies on complexes formed with other divalent transition metal ions have been reported, and the question as to which configuration is adopted is uncertain. Burger et al [20] have suggested, from infra-red and electronic spectral evidence, that the Mn(II), Fe(II), Co(II) and Zn(II) complexes adopt the cis-configuration.

Their analysis figures indicate the presence of a sodium atom in these complexes and the structure shown below is suggested:

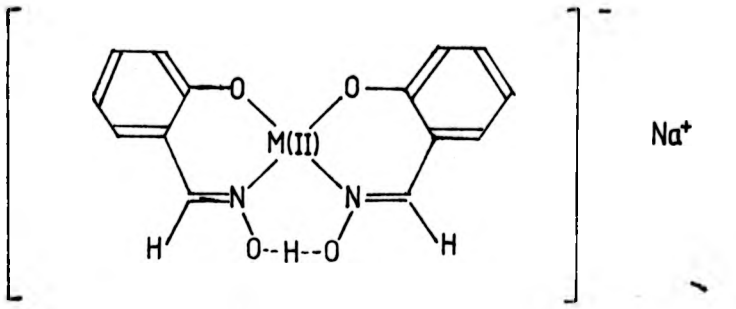

Burger and Buvari [138] have reported that the complex $[Ni(SALO)_2]$ can exhibit both cis- and trans-configurations as two species are observed in an X-ray photoelectron spectroscopic study. Recently, Nakamura et al [139,140] have postulated that a related complex, namely bis(α-D-camphorquinone dioxime)cobalt(II), exists in the cis-configuration. This is deduced from the observation that the complex exists as a dimer in benzene solution, and the association is believed to be a result of hydrogen bonding. The authors suggest that only the cis-configuration can accommodate such intermolecular association.

Conversely, the trans-configuration has been suggested for the Co(II) and Mn(II) complexes of salicylaldoxime. Biradar et al [134] have reported that the Mn(II)-salicylaldoxime is a non-electrolyte and has the formulation ML_2 where HL = SALO. The hydroxyl stretching frequency reported for this complex differs by 80 cm^{-1} from that of the corresponding complex reported by Burger et al [20]. Nishikawa and Yamada [105] have shown, from a u.v.-visible study, that the configuration of the

Co(II)-salicylaldoxime complex is indeed square-planar, and analysis figures suggest the formulation $[CoL_2]$. In view of the evidence that Co(II) would prefer a tetrahedral configuration in complexes with these types of ligands (See Chapter 1), it is suggested that strong intramolecular hydrogen bonding constrains this complex into a square-planar geometry, and the trans-configuration which allows two such bonds (the cis-configuration only allows one) is the more likely.

In view of the evidence reported above it would appear that these complexes may, in fact, be capable of existing in either of the two isomeric forms, and the configuration adopted may well depend on the method of preparation. Only a crystallographic study could leviate this uncertainty in configuration.

In this study some hydroxyoxime ligands and their metal complexes have been isolated, and a spectroscopic investigation of these compounds undertaken.

2.2. Hydroxyoxime Ligands.

The hydroxyoxime ligands which have been studied in this work are listed in Table 2.1.. This particular series of molecules was chosen because these ligands are all very closely related to the hydroxyoxime commercial liquid-liquid extractants.

The synthesis of hydroxyoxime molecules is usually achieved by reaction of the corresponding hydroxyketone with hydroxylamine. This method has been used for synthesis of hydroxyoxime ligands throughout this work unless the required molecules were commercially available. (Individual syntheses

Table 2.1. Hydroxyoxime Ligands

Name	Abbreviation	Corresponding commercial extractant	Chemical Structure	Relative molecular mass
salicylaldoxime	SALO	P50	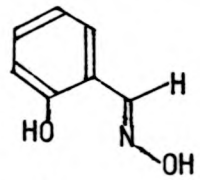	137.14
2-hydroxyacetophenone oxime	ACETOX	SME 529	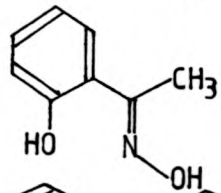	151.17
2-hydroxybenzophenone oxime	BENZOX	LIX 65N LIX 64	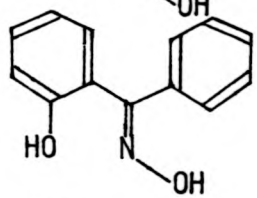	213.24
2-hydroxy-5-nonylbenzophenone oxime	LIX 65N	———	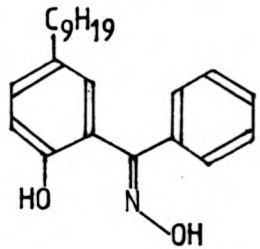	339.5 (average)

are described in Section 2.5.). LIX 65N was obtained from the commercial solvent LIX 64N and the active ingredients were removed from the diluent by published methods [16]. The purification and separation of both 'syn' and 'anti' isomers of LIX 65N is described below.

2.2.1. Isomer separation for LIX 65N.

Following the removal of kerosene from the reagent as received using the method of Ashbrook [16], a brown solution of the active constituents in hexane remained. This mixture was subjected to analysis by thin layer chromatography on silica, using toluene/ethyl acetate (96:4 v/v) as the mobile phase, and the resulting chromatograms were developed by exposure to an ammoniacal copper(II) sulphate solution. Three distinct species were observed (Chromatogram No.1.; Table 2.2.(a).). Two of these were identified as brown spots and the third as a green spot. The first two species correspond to the 'syn' and 'anti' isomers of LIX 65N and the third spot has not been identified. As can be seen from Table 2.2.(b) the R_f values found agree well with those reported by Ashbrook [18].

Slow evaporation of the hexane solution of this mixture resulted in the crystallisation of only a small quantity of white material (in contrast to the total crystallisation of the solution reported by Ashbrook). Isolation of this substance, and subsequent analysis by t.l.c., revealed that it consists of mostly the 'syn' isomer, although a small quantity of the 'anti' isomer and the unidentified impurity was present (Chromatogram No.2.; Table 2.2.(a).). Recrystallisation of this material from

chloroform resulted in a material which showed only one spot on subjection to t.l.c.. All samples of the 'syn' isomer were obtained in this manner.

The residual brown oil was shown by t.l.c. to be virtually identical to the original sample (Chromatogram No.3.; Table 2.2.(a).). Preparative t.l.c. was used to try to isolate the pure 'anti' isomer of LIX 65N. The resulting separation is shown in Chromatogram No.4.;Table 2.2.(a). When the resultant plates were examined with 254 nm radiation four distinct species were observed. These species were removed form the plates and extracted from the silica with ethanol. Subsequent thin layer chromatographic analysis of the bands corresponding to the 'syn' and 'anti' isomers of LIX 65N revealed that a degree of isomerisation had occurred between the time of running the chromatograms and isolation of the isomers. It was also noticed that, if the plates were allowed to stand exposed to light for any length of time, the three bands above the origin developed a brown colouration which presumably is a result of a photo-decomposition process. These factors and the discovery [37,65] that p-nonylphenol, which is a major constituent of the commercial solvent mixtures, has a very similar R_f value to that of the 'anti' isomer of LIX 65N in this chromatographic system led to the development of a different technique for isomer separation. This is outlined below.

The kerosene-free hexane solution of the mixture was brought into contact with an ammoniacal copper(II) sulphate solution. This resulted in the formation of the copper(II)-LIX 65N complex in the organic phase. Only the 'anti' isomer

Table 2.2 (a) Thin Layer Chromatography

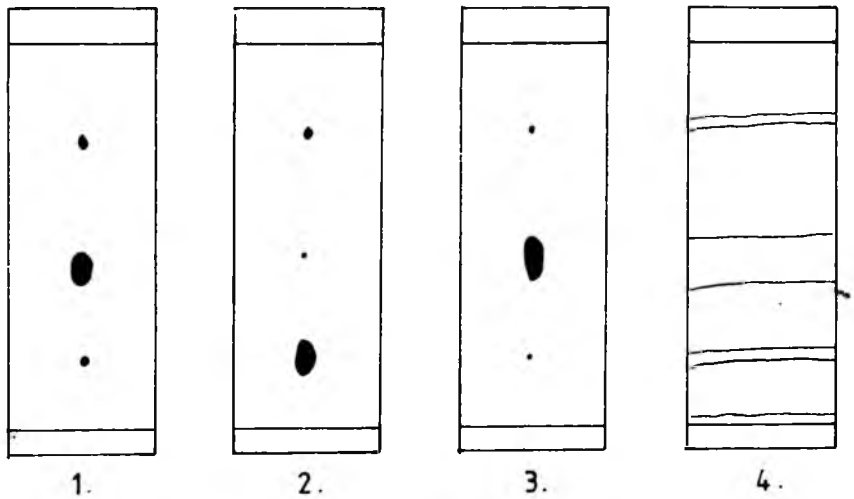

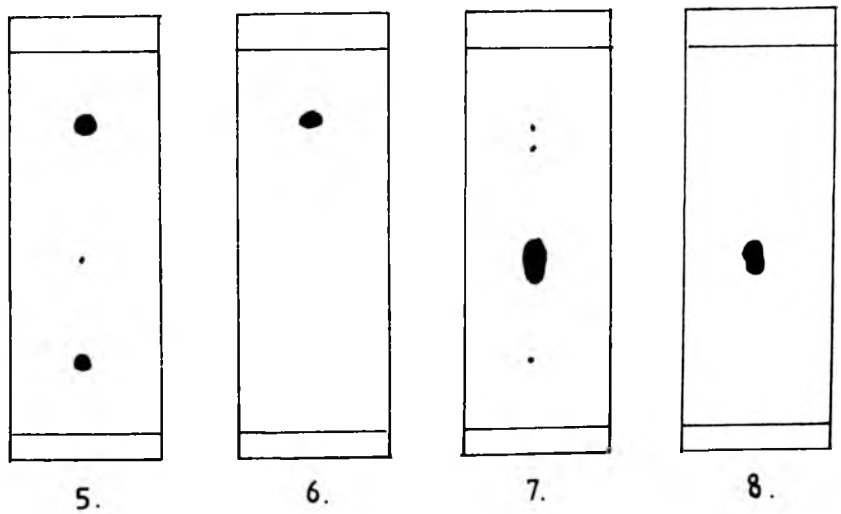

Table 2.2 (a) Thin Layer Chromatography

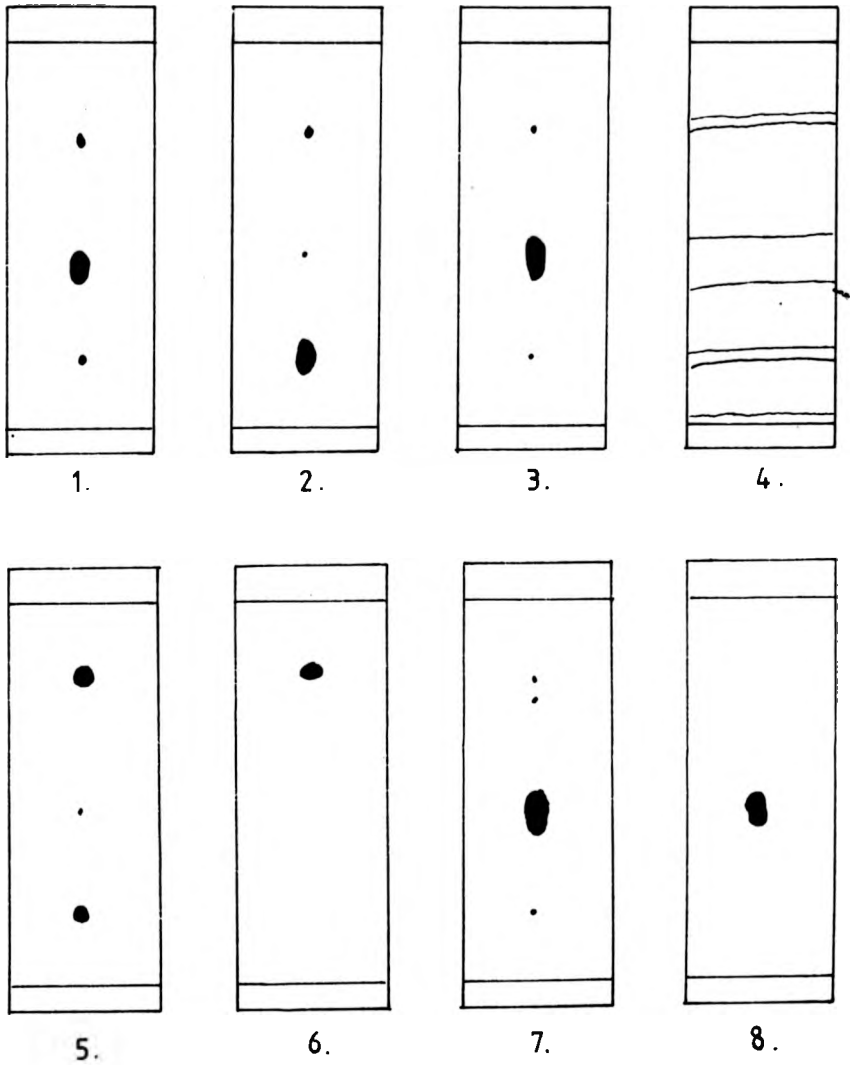

Table 2.2.(b). R_f values for chromatograms 1-8.

Chromatogram Number	R_f value	Assignment
1-3	0.18	'syn' isomer
	0.42	'anti' isomer
	0.75	unknown
4	0.00	unknown
	0.18	'syn' isomer
	0.42	'anti' isomer
	0.75	unknown
5	0.18	'syn' isomer
	0.42	'anti' isomer
	0.80	Cu(II)-LIX 65N complex
6	0.80	Cu(II)-LIX 65N complex
7	0.18	'syn' isomer
	0.42	'anti' isomer
	0.73	unknown
	0.78	unknown
8	0.42	'anti' isomer

Reported values:-

'syn' isomer [16]	R_f 0.20
'anti' isomer [16]	R_f 0.43

of these hydroxyoximes can form complexes, and it was thought that isolation of this metal complex, and subsequent removal of the metal ion, might result in the isolation of the pure 'anti' isomer. Thus the organic solution of the complex was allowed to slowly evaporate and the dark green copper(II) complex was deposited. Analysis by t.l.c. revealed that this green solid also contained quantities of free ligand (Chromatogram No.5.; Table 2.2.(a).), so further purification was necessary. This mixture was purified by use of column chromatography, again using toluene/ethyl acetate (96:4 v/v) as eluent, as this system gives a good separation of the complex from the free ligand. Beforehand, the copper(II) complex was washed thoroughly with ethanol, in which it is only slightly soluble, to remove as much of the organic impurities as possible. Subsequent t.l.c. experiments revealed only one spot corresponding to the copper(II) complex (Chromatogram No.6.;Table 2.2.(a).).

The usual method employed to liberate the hydroxyoxime ligand from the metal is to wash the complex with cold dilute sulphuric acid [16,37]. When this operation was performed, analysis by t.l.c. revealed that a small quantity of 'syn' isomer had been produced along with two unidentified species (Chromatogram No.7.;Table 2.2.(a).). It was concluded that this method is not totally successful for obtaining isomerically pure samples, and thus an alternative method of separating the ligand from the copper(II) complex was employed.

The method finally adopted involves the use of a complexing reagent, namely trans-1,2,-diaminocyclohexane-N,N,N',N',-tetraacetic acid (CDTA). This compound was used in preference

to ethylenediaminetetraacetic acid (EDTA) as a consequence of its greater solubility in methanol over this reagent. CDTA was added to a well stirred methanolic solution of the copper(II)-LIX 65N complex. Fairly rapidly the green colouration due to the complex was lost and the blue colour of the $[CuL]^{2-}$ ion (H_4L = CDTA) formed, indicating the liberation of LIX 65N. The free ligand was extracted into hexane, after removal of methanol, and t.l.c. of the resultant solution showed only one spot with an R_f value correspnding to that of the 'anti' isomer. Isomeric purity was confirmed by ^{13}C n.m.r. spectroscopy (Section 2.2.2.). All samples of the pure 'anti' isomer were wrapped in aluminium foil and stored at $0^{o}C$ to prevent thermal or photocatalysed isomerisation or decomposition.

2.2.2. Electronic spectral investigation of the ligands.

The variation of λ_{max} and the extinction coefficient of the lowest energy band in the electronic spectra of these ligands is shown in Table 2.3.. The largest change in λ_{max} is observed between BENZOX and LIX 65N. The shift to longer wavelengths ("red shift") is a direct result of the substitution of the alkyl group in a para-position to the phenolic hydroxyl function in LIX 65N [141]. This substitution induces a perturbation of the phenolic benzene ring by way of an inductive effect and lowers the ionisation energy of the ring producing the observed red shift. This effect can be further demonstrated by consideration of the electronic spectrum of SME 529. This extractant [24] displays a corresponding absorption band at 317 nm, which can be compared with the value of 305 nm for the non-alkylated parent molecule

Table 2.3. U.V. data for the ligands *.

Molecule	λ_{max}/nm	ϵ/dm^3 mol^{-1} cm^{-1}
SALO	304	3680
ACETOX	303	3500
'anti'-BENZOX	307	3690
'anti'-LIX 65N	315	3100

*Recorded in methanol solution

Table 2.4. I.R. data for the ligands *.

Molecule	Stretching frequency/cm^{-1}			
	$\nu_{C=N}$	$\nu_{C=C,C=N}$	ν_{C-O}	$\nu_{O-H(ass.)}$
SALO	1618	1582	1292	3360
ACETOX	1612	1587	1285	3330
'anti'-BENZOX	1608	1603	1292	3360
'anti'-LIX 65N **	1615	1580	1283	3395

*Recorded as nujol mulls

**Recorded in chloroform solution

ACETOX, i.e. a red shift of 15 nm.

The smaller red shift induced by substitution of a phenyl group for a methyl group in changing from ACETOX to BENZOX may be attributed to an increase in conjugation in the molecule. However, it must be realised that interpretations of the small shifts observed in these spectra are difficult as hydrogen bonding, which has been demonstrated to be present in these ligands, has been shown to play an important role in determining λ_{max} and the extinction coefficient in related systems [142], and may therefore influence the values of these two parameters in the electronic spectra of these hydroxyoximes.

2.2.3. Infra-red spectral investigation of ligands.

The four most important infra-red bands of these ligands are listed in Table 2.4.. The assignments of these bands are based on previous work and the observation of large shifts in these bands on complexation (See Section 2.3.). Neither of the stretching frequencies resulting from the C=N function can be used to correlate trends from ligand to ligand, as both are subject to some degree of conjugation in the system and are not pure stretching modes [143,144]. If spectra are recorded under the same conditions, the associated hydroxyl stretching mode can give an indication of the strength of the intermolecular hydrogen bonding in these systems [144]. Thus as the spectra of SALO, ACETOX and BENZOX were all recorded in the solid phase, as nujol mulls, some interpretations of the trends observed with this stretching frequency can be suggested. ACETOX displays a lower energy absorbance for this stretching mode than does SALO, indicating

a stronger intermolecular hydrogen bond exists for this molecule. This stronger bond can be interpreted as a result of the inductive effect of the substituted methyl group on the oximino carbon atom, pushing more electron density onto the oximino nitrogen atom and thus inducing a stronger intermolecular hydrogen bond. BENZOX, however, exhibits a higher energy associated with its hydroxyl stretching mode than does ACETOX. This observation is not as would be expected as substitution of a phenyl ring would be expected to increase the conjugation in the molecule resulting in a stronger intermolecular hydrogen bond. This weakening of the hydrogen bond may be a result of non-coplanarity of the two benzene rings, which has been suggested by Ashbrook [18] on the grounds that ortho-hydrogen atom interactions would not permit coplanarity, and this would lower the amount of conjugation possible and weaken the intermolecular hydrogen bond. These trends are also mirrored by the C-O stretching mode. As the 'anti' isomer of LIX 65N exists as an oil and not a solid the infra-red spectrum of this molecule cannot be considered in this context.

2.2.4. ^{13}C n.m.r. investigation of ligands.

For an investigation of these ligands ^{13}C n.m.r. spectroscopy has advantages over ^{1}H n.m.r. spectroscopy. As a result of ^{1}H-^{1}H coupling the aromatic region of the ^{1}H n.m.r. spectra of these ligands appears very complex. However, in the corresponding ^{13}C n.m.r. spectra the employment of broad-band proton decoupling removes all ^{13}C-^{1}H coupling and due to the low isotopic abundance of the ^{13}C nucleus ^{13}C-^{13}C coupling is not

observed in these spectra. Thus only one distinct resonance per carbon atom is observed for each ligand, greatly simplifying the spectra. Full ^{13}C n.m.r. spectra of the 'anti' isomers of the four hydroxyoxime molecules studied are shown in Figures 2.1. - 2.4. and from these, partial spectral assignments can be made.

It is known [145,146] that both phenolic and oximino carbon atoms resonate to low field of aromatic carbon atoms and thus the two resonances furthest downfield in the spectrum of SALO (Figure 2.1.) can be assigned to these resonances. The oximino carbon can be differentiated from the phenolic carbon as it is a protonated carbon atom and will thus exhibit Nuclear Overhauser Enhancement (NOE) whereas the phenolic carbon will not. Thus resonance (1) in Figure 2.1. is assigned as the phenolic carbon and resonance (2) as the oximino carbon. These assignments are further substantiated by the fact that phenol has been shown to have a chemical shift of 155.6 p.p.m. [147] and that the 'anti' isomer of benzaldehyde oxime is reported [145] to display a chemical shift of 149.6 p.p.m. i.e. phenolic carbon atoms resonate to lower field of oximino carbon atoms. Assignments for the remaining resonances in Figure 2.1. can be made by consideration of SALO as a substituted phenol. The ^{13}C n.m.r. spectrum of phenol [147] shows that the resonance frequencies of the ortho-, meta- and para-carbon atoms are shifted by -12.6, +1.8 and -7.9 p.p.m. respectively from benzene (128.7 p.p.m.). Using this information, and by consideration of the substitution of the oxime function, the assignments shown in Figure 2.1. can be made.

The ^{13}C n.m.r. spectrum of ACETOX (Figure 2.2.) differs

Figure 2.1. ^{13}C n.m.r. spectrum of salicylaldoxime

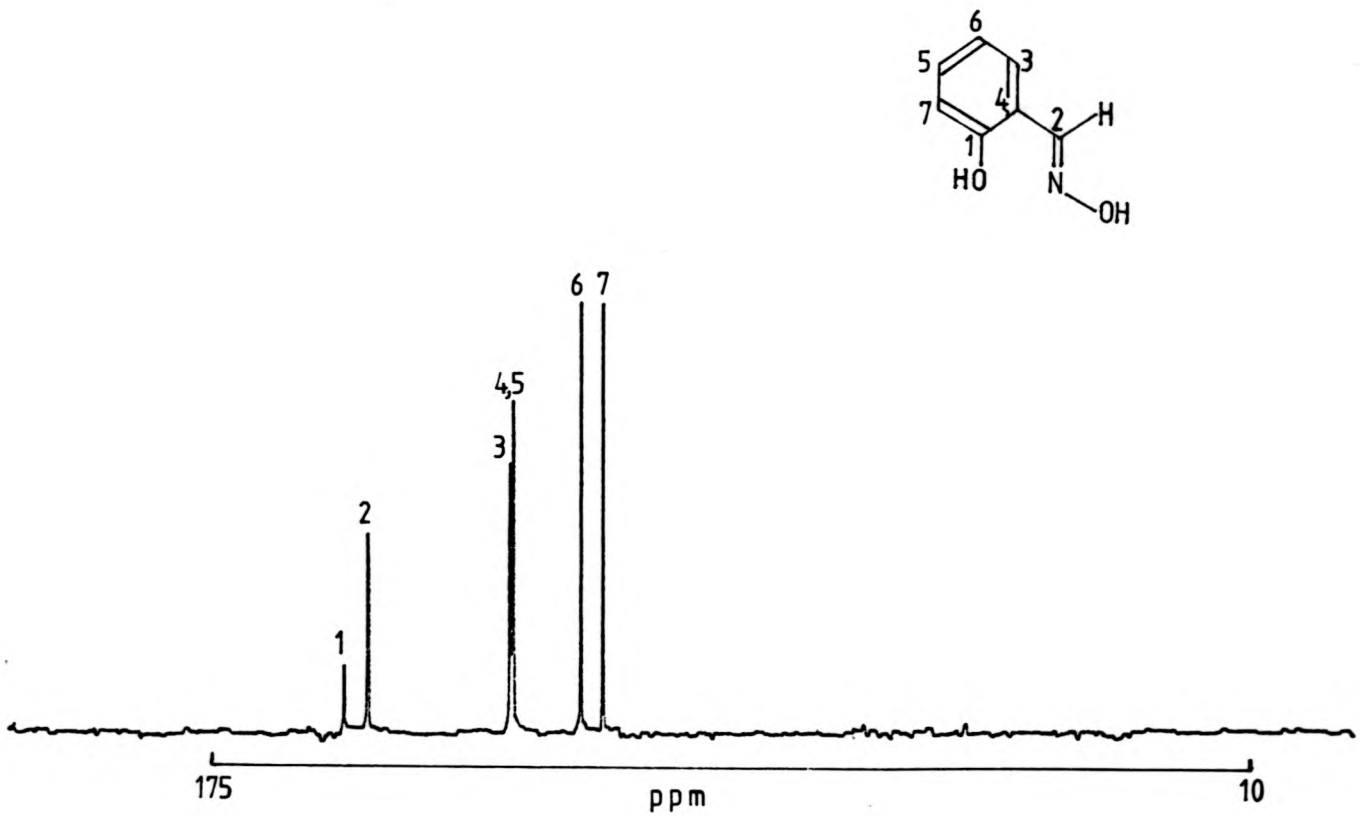

Figure 2.2. ^{13}C n.m.r. spectrum of 2-hydroxyacetophenone oxime

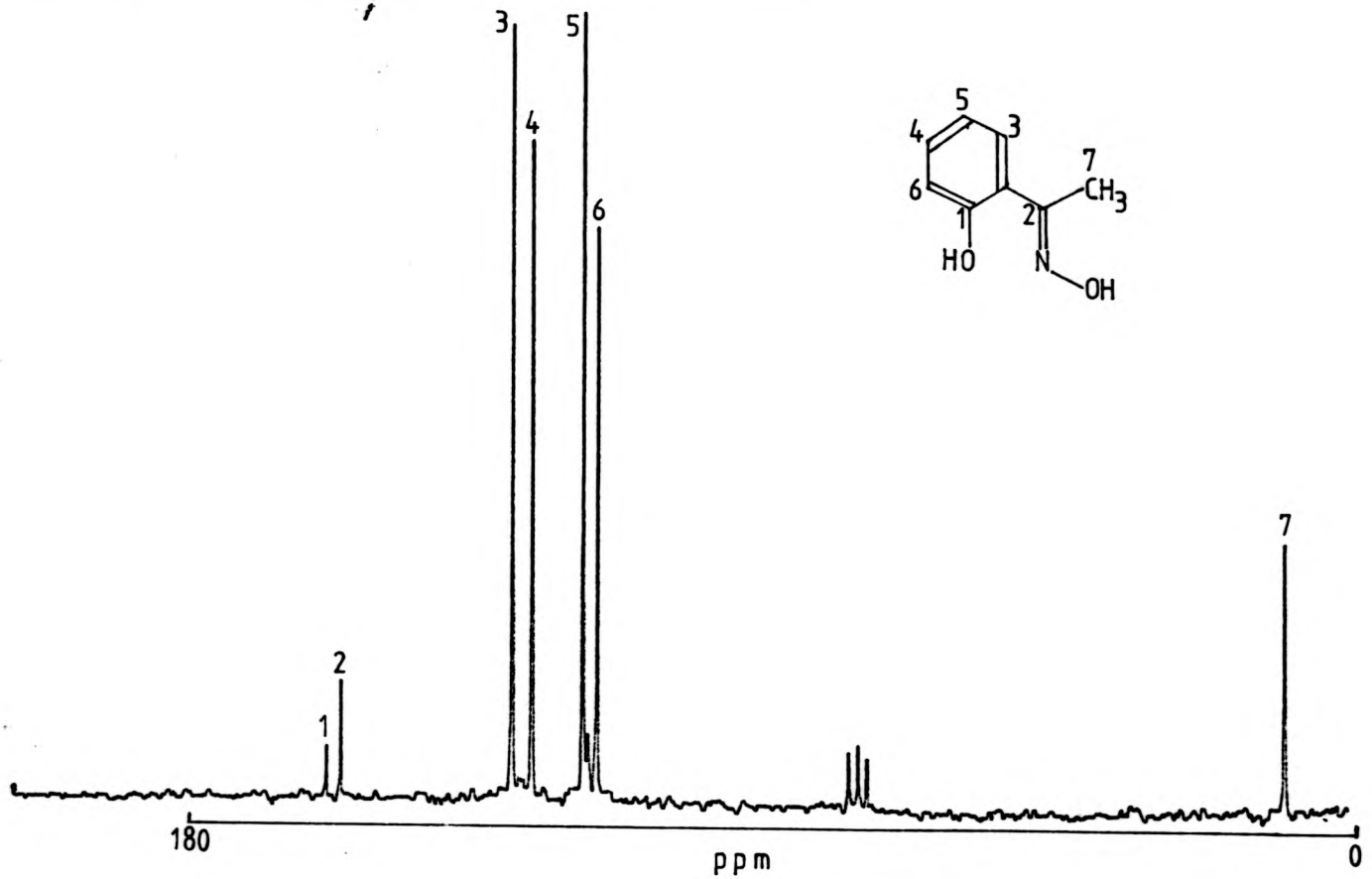

Figure 2.3. ^{13}C n.m.r. spectrum of 2-hydroxybenzophenone oxime

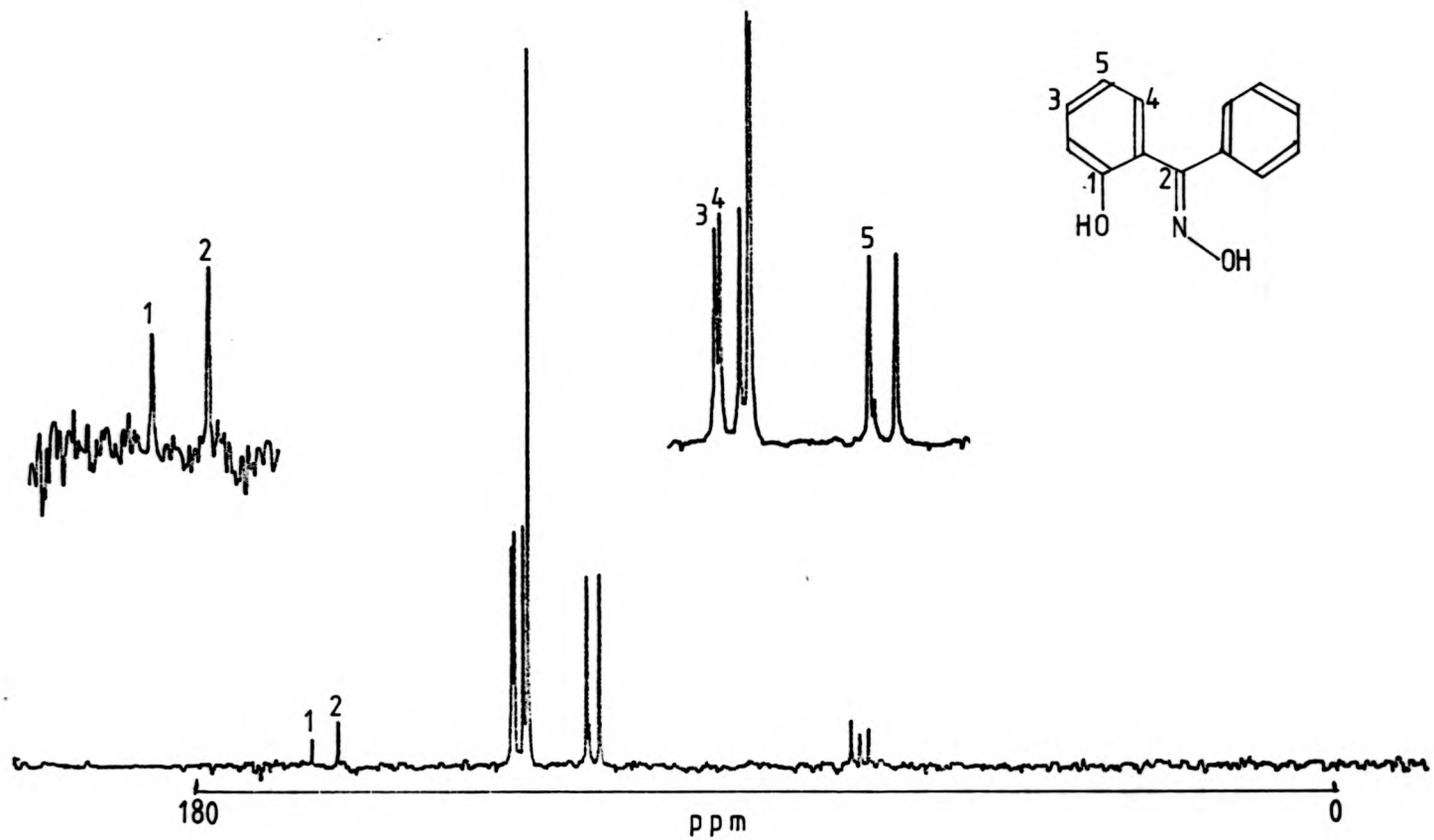

Figure 2.4. ^{13}C n.m.r. spectrum of LIX 65N

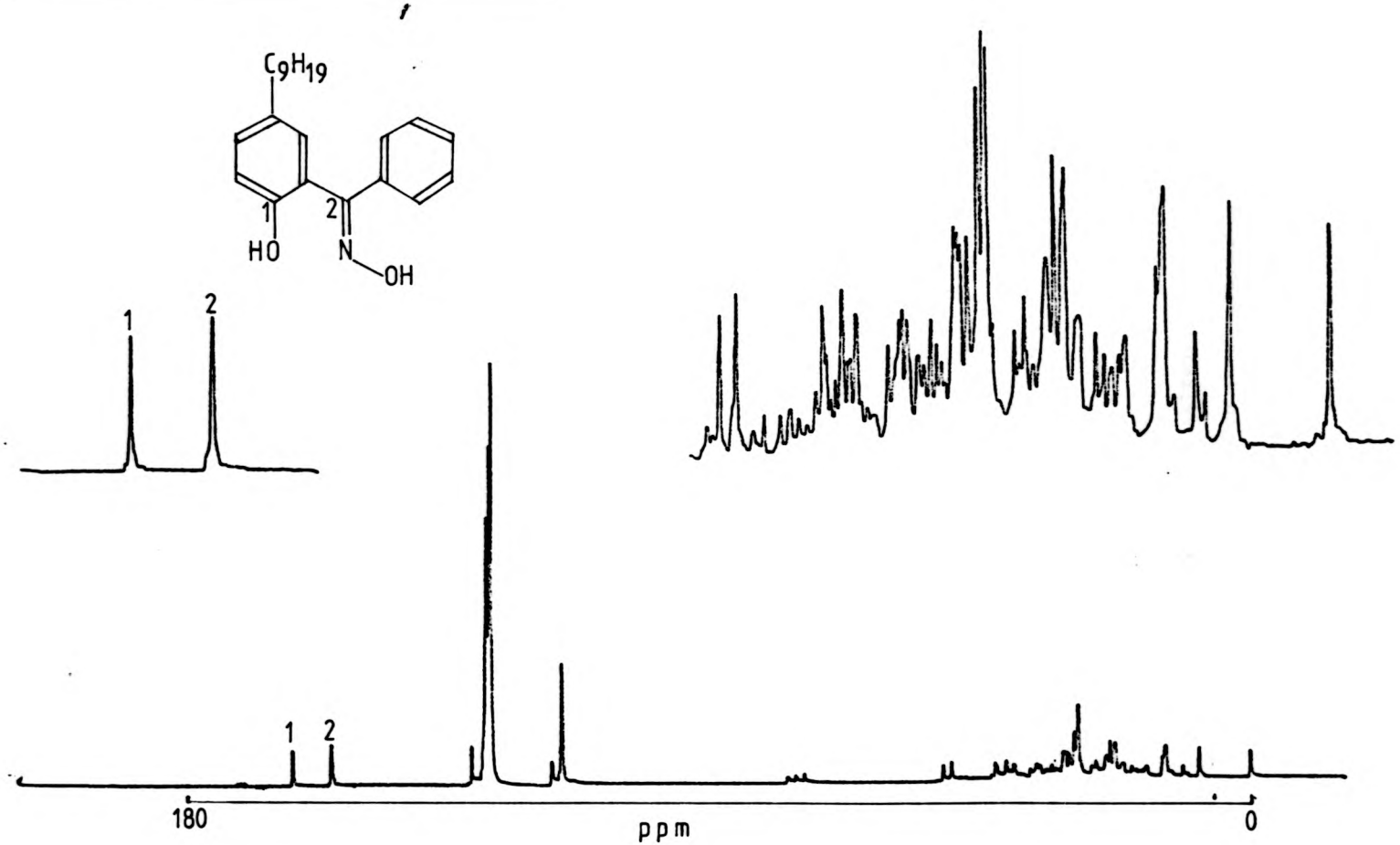

from that of SALO in two main features. These are the loss of NOE on the oximino carbon resonance, which is further evidence for the correct assignment of this carbon atom, and the presence of a resonance in the aliphatic region of the spectrum. Both of these observations are a direct result of methyl substitution at the oximino carbon. Small differences in the chemical shifts of the aromatic resonances are also observed.

Considering the aromatic and lower field regions of the ^{13}C n.m.r. spectra of both BENZOX and LIX 65N (Figures 2.3. and 2.4.) it can be seen that, in both cases, there are only two resonances downfield of the main aromatic resonances, which demonstrates the isomeric purity of these two compounds. The aromatic region, itself, is rather complicated and no definite assignments have been made, although the two most low field resonances in this group most probably correspond to the meta-carbon atoms of the phenolic ring. In the ^{13}C n.m.r. spectrum of BENZOX there are three resonances upfield of the main aromatic group, whereas in the spectrum of LIX 65N only two such resonances are found. As the only difference between the two molecules is the substitution of an alkyl group in a para-position to the phenolic hydroxyl function, the resonance which is present only in the spectrum of BENZOX can thus be assigned as being produced by the carbon atom in a para-position to the phenolic group in this molecule.

The aliphatic region of the ^{13}C n.m.r. spectrum of LIX 65N is observed to be extremely complicated. This is a result of the method by which these alkylated hydroxyoximes are synthesised. As selective n-alkylation in the 4-position of

phenol is extremely difficult and thus expensive, a method is used in industry which produces an alkylated phenol whose alkyl chain is a mixture of many different isomers. This is, in fact, an advantage when the resultant hydroxyoximes are used in liquid-liquid extraction as the many different isomers present help to prevent crystallisation of the metal complexes from solution.

As far as metal complex formation is concerned, which is the main subject of this work, the two most important resonances in the ^{13}C n.m.r. spectra of these molecules are those corresponding to the phenolic carbon and the oximino carbon as these two carbon atoms are closest to the oxygen and nitrogen atoms which are involved in co-ordination. As a result of their proximity to the co-ordination sites these two carbon atoms will be the most sensitive to any change in character of the co-ordinative atoms induced by the different substitutions in the hydroxyoxime ligands considered here.

The chemical shifts of these resonances for the four hydroxyoxime ligands are listed in Table 2.5..Comparing the chemical shifts of the phenolic and oximino carbon atoms of SALO and ACETOX it is observed that for ACETOX the two resonances are found to lower field than the corresponding resonances of SALO. Again this is most probably a result of the inductive effect of the oximino substituted methyl group in ACETOX pushing electron density onto the phenolic oxygen and oximino nitrogen atoms, thus shifting the two resonances downfield. This is in agreement with the observations of the infra-red spectra of these two molecules and also with pK_a data [38,39] (See Table 1.4.) which shows ACETOX to have a higher pK_a than SALO. The corresponding

Table 2.5. ^{13}C n.m.r. chemical shift data for the ligands *.

Molecule	Chemical shifts of carbon atoms/ p.p.m. on δ scale	
	oximino	phenolic
SALO	152.75	156.39
ACETOX	156.91	159.12
'anti'-BENZOX	157.69	161.78
'anti'-LIX 65N	155.14	161.90
'syn'-LIX 65N	153.46	158.53

*Recorded in $CDCl_3$ solution; shifts are given relative to TMS (TMS = 0.00 p.p.m.)

resonances in the ^{13}C n.m.r. spectrum of BENZOX are again shifted to lower field of the corresponding resonances of both ACETOX and SALO which is also probably a result of increased conjugation in this molecule. Considering the chemical shifts of these two resonances for BENZOX and 'anti'-LIX 65N it can be seen that the phenolic carbon atoms resonate at virtually identical chemical snifts and that the oximino carbon atom of 'anti'-LIX 65N resonates to higher field than the corresponding resonance of BENZOX. When an alkyl group is substituted in the 4-position of phenol, an upfield shift of -2 p.p.m. is induced by this substitution [146]. Very little chemical shift difference is observed on substitution in this case, so presumably the inductive of the alkyl group causes negation of this upfield shift. This would be in agreement with the previously discussed pK_a data as 'anti'-LIX 65N has a higher pK_a than BENZOX. The upfield shift of the oximino carbon in 'anti'-LIX 65N suggests a possible lowering of the conjugation throughout the molecule as the alkyl substitution is too remote to account for this shift. This may indicate even less coplanarity of the phenyl rings in LIX 65N than in the case of BENZOX, although there is no obvious explanation as to why this should be so.

Both resonances for the 'syn' isomer of LIX 65N are to higher field than those of the 'anti' isomer. This again agrees with the pK_a data of Ashbrook [18], indicating that the 'syn' isomer is a stronger acid than the 'anti' isomer, and is a direct result of the differences in hydrogen bonding between the two systems as discussed previously.

resonances in the ^{13}C n.m.r. spectrum of BENZOX are again shifted to lower field of the corresponding resonances of both ACETOX and SALO which is also probably a result of increased conjugation in this molecule. Considering the chemical shifts of these two resonances for BENZOX and 'anti'-LIX 65N it can be seen that the phenolic carbon atoms resonate at virtually identical chemical snifts and that the oximino carbon atom of 'anti'-LIX 65N resonates to higher field than the corresponding resonance of BENZOX. When an alkyl group is substituted in the 4-position of phenol, an upfield shift of -2 p.p.m. is induced by this substitution [146]. Very little chemical shift difference is observed on substitution in this case, so presumably the inductive of the alkyl group causes negation of this upfield shift. This would be in agreement with the previously discussed pK_a data as 'anti'-LIX 65N has a higher pK_a than BENZOX. The upfield shift of the oximino carbon in 'anti'-LIX 65N suggests a possible lowering of the conjugation throughout the molecule as the alkyl substitution is too remote to account for this shift. This may indicate even less coplanarity of the phenyl rings in LIX 65N than in the case of BENZOX, although there is no obvious explanation as to why this should be so.

Both resonances for the 'syn' isomer of LIX 65N are to higher field than those of the 'anti' isomer. This again agrees with the pK_a data of Ashbrook [18], indicating that the 'syn' isomer is a stronger acid than the 'anti' isomer, and is a direct result of the differences in hydrogen bonding between the two systems as discussed previously.

2.3. Metal Complexes.

The following section describes a spectroscopic investigation of the Ni(II) complexes of the hydroxyoxime ligands listed in Table 2.1. and the Co(II) and Cu(II) complexes of LIX 65N. The bulk of these studies have been performed on the Ni(II) complexes as they are generally more soluble than the corresponding Cu(II) complexes, and hence are better suited for an electronic spectral investigation. As discussed previously, Co(II) complexes of SALO and its related ligands are known to be very oxygen sensitive and for this reason are more difficult to investigate than the Ni(II) complexes. Also, the electronic spectra of Ni(II) complexes are more characteristic of co-ordination geometry than the electronic spectra of Co(II) and Cu(II) complexes, so co-ordination geometry can be more conclusively assigned.

2.3.1. Nickel(II) complexes.

All Ni(II) complexes discussed here were prepared by the general method of Cox et al [148] and isolated as green crystalline or semi-crystalline solids. All complexes analysed as having the general formula NiL_2, where HL = ligand, were subjected to a solid state infra-red spectral and a solution phase electronic spectral investigation.

The infra-red spectral properties of these and related complexes have been frequently investigated and indeed are still being studied [149,150]. A list of the important infra-red absorbances for the Ni(II) complexes of the four hydroxyoxime ligands considered here is given in Table 2.6.. Contradictory

assignments have previously been made [20-22] for the bands observed in the infra-red spectra of SALO complexes. Thus the assignments made in Table 2.6. are based on previous ^{15}N substitution experiments in complexes of N-aryl salicylaldimines [151,152] and on the work of Gluvchinsky et al [153] who make use of these assignments and have also used ^{62}Ni substitution to identify metal-oxygen and metal-nitrogen stretches in the low infra-red spectra of some complexes of 5-chloro-2-hydroxybenzophenone Schiff bases. Similar experiments would have to be performed to ascertain these low infra-red stretches for the complexes considered here as these give rise to very weak absorbances which are found amongst a series of ligand bonds.

As can be seen by comparing Table 2.4. and Table 2.6., in the Ni(II) complexes the C=N stretching modes are both shifted to lower energy than in the spectra of the free ligands. This observation indicates a lowering of bond order of the C=N moiety on complexation. This is as expected, as on complexation electron density is lost from this bond on formation of the metal-nitrogen bond. It is also observed that on complexation the C-O stretching mode shifts to higher energy. This phenomenon has been noted previously, again with complexes of N-aryl salicylaldimines [154] and has been postulated as being a result of a loss of hydrogen bonding on complexation. This would seem a valid hypothesis as no associated hydroxyl stretch is observed in the spectra of these complexes, indicating the loss of the proton involved in this association on complexation.

Again not many conclusions can be drawn from these spectra as both the C=N stretching frequencies are not pure

Table 2.6. I.R. data for Ni(II) complexes.

Complex	Stretching frequency/cm^{-1}			
	$\Delta(\nu_{C-O})$	$\nu_{C=N}$	$\nu_{C=C,C=N}$	ν_{C-O}
$Ni(SALO)_2$	+50	1603	1553	1342
$Ni(ACETOX)_2$	+45	1602	1557	1330
$Ni(BENZOX)_2$	+60	1598	1553	1352
$Ni(LIX\ 65N)_2$	+37	1610	1540	1320

Table 2.7. Electronic spectral data for Ni(II) complexes.

Complex	λ_{max}/nm ($\log \epsilon$/$dm^3\ mol^{-1}\ cm^{-1}$)		
	$^1A_g \leftarrow {}^1A_u$	$^1A_g \leftarrow {}^1B_{1g}$	
	Methanol	Methanol	Toluene
$Ni(SALO)_2$	360(3.58)	615(2.00)	610(1.93)
$Ni(ACETOX)_2$	360(3.56)	615(1.96)	610(1.96)
$Ni(BENZOX)_2$	380(3.58)	a	615(1.94)
$Ni(LIX\ 65N)_2$	380(3.61)	615(2.08)	610(2.16)

a) Insufficient solubility

stretches. If the quantity $\Delta(\nu_{C-O})$ is considered (See Table 2.6.) it can be seen that the value of this increases in the order ACETOX < SALO < BENZOX, indicating a greater loss of hydrogen bonding on complexation for BENZOX than for ACETOX and SALO, and may be an indication of the relative strengths of intramolecular hydrogen bonding in the complexes.

Electronic spectral data for these nickel(II) complexes obtained in methanolic and toluene solutions are listed in Table 2.7.. Bis(salicylaldoximato)nickel(II) is well known to exist in a square-planar geometry in non-co-ordinating solvents [94] and the spectral data reported for the other complexes are consistent with a square-planar geometry in both solution phases. The assignments of these transitions are based on the work of Kato and Sakamoto [155]. These authors have suggested that the electronic spectra of bis(N-methylsalicylaldiminato)nickel(II) in methanolic solution reported by Bosnich [156] indicate that an equilibrium of the type octahedral $\rightleftharpoons$ square-planar exists. If this were the case with the complexes considered here, a band at around 1000 nm with an extinction coefficient of approximately 10 $dm^3 mole^{-1} cm^{-1}$ would be observed, but no such band was noted in the electronic spectra of any of the nickel(II) complexes in either solution phase. Even at 333K no evidence for any six co-ordinate species was found for a methanolic solution of the Ni(II)-LIX 65N complex. Thus it is concluded that in both methanol and toluene solutions these complexes exist in four co-ordinate square-planar configurations. Bis(salicyl-aldoximato)nickel(II) exhibits the trans-configuration in the solid state [75] and in inert solvent [94] and it can be thus

concluded that all four of the complexes studied here also exist in the trans-square-planar configuration.

2.3.2. Cu(LIX 65N)$_2$.

This complex was prepared as described in Section 2.5. and isolated as waxy green needles. Infra-red spectral data for this complex are reported in Table 2.8. and it can be seen that values observed for the wavenumbers of the C=N and C-O stretching modes are very similar to those for the corresponding nickel(II) complex, indicating that the two complexes are structurally very similar. Analysis figures (Section 2.5.) also indicate a metal-ligand ratio of 1:2 as with the nickel(II) complex. Hosking and Rice [24] report that the Cu(II)-LIX 65N complex exists as a mixture of 1:1 and 1:2 stoichiometry in the solid state, but no evidence has been found for this hypothesis in this study. The complex was not sufficiently soluble in methanol to allow a conclusive determination of its co-ordination geometry by electronic spectral techniques but the ultra-violet region of this spectrum in methanol is virtually identical to that observed in toluene solution suggesting the retention of square-planar geometry in methanol solution. These electronic spectra are also virtually identical to the spectra of bis(salicylaldoximato)-copper(II) [20] which is known to exist in the trans-configuration [71], thus it can be deduced that this configuration is exhibited by the Cu(II)-LIX 65N complex.

2.3.3. Co(LIX 65N)$_2$.

The cobalt(II) complex of LIX 65N was prepared as

Table 2.8. I.R. spectral data for M(II) complexes of LIX 65N.

Complex	Stretching frequency/cm^{-1}		
	$\nu_{C=N}$	$\nu_{C=C,C=N}$	ν_{C-O}
$Co(LIX\ 65N)_2$	1600	a	1298
$Ni(LIX\ 65N)_2$	1610	1540	1320
$Cu(LIX\ 65N)_2$	1612	1549	1320

a) Not observed

described in Section 2.5. under stringent anaerobic conditions and isolated as a brown solid. Elemental analysis suggests that the compound exhibits a 1:2 metal-ligand stoichiometry. It was found extremely difficult to obtain good infra-red spectra of this complex as a nujol mull, but nevertheless the wavenumbers of the C-O and C=N stretches could be ascertained and are reported in Table 2.8.. As can be seen these two stretches for this complex both fall at lower energy than the corresponding Ni(II) and Cu(II) complexes which would indicate a weaker metal complex (little shift in C=N stretch) but a stronger intra-molecular hydrogen bond (little shift in C-O stretch). This has been observed previously in the cobalt(II) complex of salicyl-aldoxime by Burger et al [20]. These authors suggest that this is evidence for the adoption of the cis-configuration by this complex which would allow a stronger hydrogen bond to form. Indeed a fairly recent single crystal ESR and ENDOR study of both the Cu(II) and Ni(II) complexes of salicylaldoxime [159] indicate that the O-H-O hydrogen bonds in these trans-complexes are non-linear and the OHO angle is between 150° and 140°. Adoption of the cis-configuration by the cobalt(II)-LIX 65N complex may therefore produce a more linear and thus stronger hydrogen bond.

Electronic solution spectra of this complex show no distinct absorption bands over the total spectral range studied (200-1500 nm) and are typical of the spectra previously observed with $Co(SALO)_2$ when this complex has been exposed to oxygen [160]. The electronic spectrum of bis(salicylaldoximato)cobalt(II) reported by Nishikawa and Yamada [105] shows a narrow absorption

band at around 1200 nm which is characteristic of low-spin square-planar cobalt(II) species. The spectra of $Co(LIX\ 65N)_2$ show no such band and thus it is concluded that the complex is very susceptible to oxidation in solution. All attempts to exclude oxygen from the samples used was to no avail.

2.4. Summary and Conclusions.

An improved method for separating the 'syn' and 'anti' isomers of LIX 65N has been described which results in a very high isomeric purity of this reagent as proven by t.l.c. and ^{13}C n.m.r. spectroscopy. A spectroscopic study of LIX 65N and three ligands which are very closely related in molecular structure to the three most commonly used types of hydroxyoxime liquid-liquid extractants has been performed. This investigation has indicated the pres ence of a more strongly associated hydrogen bonded system in the compound ACETOX than in either BENZOX or SALO. Infra-red evidence supports a previous hypothesis that in the cases of both BENZOX and LIX 65N the two phenyl rings are non-coplanar. A ^{13}C n.m.r. spectroscopic investigation has allowed partial assignment of the spectra of these ligands and observed chemical shifts are consistent with previous pK_a and infra-red data.

A spectroscopic study of the Ni(II) complexes of these ligands has revealed that all exist in the trans-square-planar geometry in methanolic and toluene solutions with no evidence of six-co-ordinate species being found. The copper(II) and cobalt(II) complexes have been isolated and found to exist as of the general formula ML_2 where HL = LIX 65N in the solid state.

In methanol solution $Cu(LIX\ 65N)_2$ is found to exist also in the trans-square-planar geometry whereas the complex $[Co(LIX\ 65N)_2]$, which is found to be very oxygen sensitive, from infra-red evidence may adopt the cis-square-planar geometry.

2.5. Experimental.

Instrumentation.

Infra-red spectra.

All infra-red spectra were recorded with either a Perkin-Elmer 621 or a Perkin-Elmer 580B infra-red scanning spectrophotometer as nujol mulls or in a chloroform solution using 1 mm liquid cells with CsI windows.

Electronic spectra.

All electronic spectra were recorded with either a Pye-Unicam SP800 or a Carey 14 scanning spectrophotometer using 1 cm quartz cells.

^{13}C n.m.r. spectra.

All ^{13}C n.m.r. spectra were recorded in 10 mm diameter tubes at 22.628 MHz with a Bruker WH90 pulse Fourier transform n.m.r. spectrometer as saturated solutions in $[^2H]$-chloroform. All chemical shifts are quoted with respect to tetramethylsilane (TMS) using the δ scale in p.p.m. (TMS, δ = 0 p.p.m.).

Microanalysis.

All elemental analyses were performed by C.H.N. (ligands)

or B.M.A.C. Ltd. (metal complexes).

Chemicals and Solvents.

All solvents and chemicals purchased were reagent grade and used without further purification unless otherwise stated. Nujol for infra-red spectral determinations was dried over sodium wire. For electronic spectroscopy Analar grade methanol was purified by reflux and distillation from magnesium turnings under a nitrogen atmosphere using the method of Lund and Bjerrum [157]. Analar grade toluene was used as received.

Chromatography.

All chromatographic experiments were performed with toluene/ethyl acetate (96:4 v/v) as the mobile phase and silica as the stationary phase. Column chromatography was performed using silica (Fisons) 60-90 mesh and t.l.c. with prepared aluminium backed plates of 0.2 mm thickness silica (Merck).

Synthesis of Ligands.

Salicylaldoxime.

Salicylaldoxime was purchased from BDH Chemicals Ltd. and recrystallised from Analar grade diethyl ether, dried and stored over P_2O_5 in a vacuum desiccator. Purity was checked by ^{13}C n.m.r. spectroscopy and t.l.c..

2-Hydroxyacetophenone oxime.

This ligand was synthesised by reaction of 2-hydroxy-acetophenone (Aldrich) and hydroxylamine hydrochloride (BDH).

To 2-hydroxyacetophenone (30 g) was added sodium hydroxide (7.9 g) as a 40% solution in distilled water. On addition a yellow solid, the sodium salt of 2-hydroxyacetophenone, was immediately precipitated from solution. To this mixture was added distilled water (50 cm^3) containing hydroxylamine hydrochloride (13.7 g). The yellow solid soon dissolved and was left stirring for 1 hour. At this stage dilute hydrochloric acid was added dropwise, while the solution was stirring, until all the yellow colouration was removed from the solution. The solution was then evaporated with a Buchi rotary evaporator until 25-30 cm^3 of solution remained. This solution was stored at 0^oC overnight which resulted in the formation of white crystalline plates of the required hydroxyoxime. These crystals were isolated by filtration, dried and stored over P_2O_5 in a vacuum desiccator. The ligand was found to be pure by ^{13}C n.m.r. spectroscopy, t.l.c. and microanalysis.

Analysis (C.H.N.) Calculated: C: 63.56%; H: 6.00%; N: 9.27%.

Found: C: 63.66%; H: 5.96%; N: 9.22%.

2-Hydroxybenzophenone oxime.

This ligand was synthesised by reaction of 2-hydroxybenzophenone (Aldrich) with hydroxylamine hydrochloride (BDH) following published methods [158]. To 2-hydroxybenzophenone (6.44 g) was added hydroxylamine hydrochloride (3.51 g) dissolved in a 75% aqueous ethanol solution (15 cm^3). As this mixture was stirred sodium hydroxide (6.46 g), as a 40% aqueous solution, was slowly added. This resulted in the formation of a yellow solution followed by precipitation of a yellow solid which

eventually dissolved. This resulting yellow solution was left stirring overnight and then a dilute solution of hydrochloric acid was added in a dropwise fashion until all trace of colour was removed from the solution. This solution was then allowed to stand at $0^{o}C$ for several hours which resulted in crystallisation of white plates of the required product. These crystals were isolated by filtration, dried and stored over P_2O_5 in a vacuum desiccator. Thin layer chromatography showed only the prescence of the 'anti' isomer of the hydroxyoxime. The isomeric purity was verified by ^{13}C n.m.r. spectroscopy (See Section 2.2.). The purity of the compound was confirmed by elemental analysis.

Analysis (C.H.N.) Calculated: C: 73.22%; H: 5.20%; N: 6.57%.

Found: C: 73.19%; H: 5.23%; N: 6.67%.

LIX 65N.

LIX 64N was received as a gift from General Mills Incorporated as the commercial solvent mix, and LIX 65N was obtained from this as a hexane solution following the method of purification described by Ashbrook [16]. The dark brown, viscous LIX 64N solvent (50 cm^3) was reacted with a 10M sodium hydroxide solution until precipitation of the yellow sodium salt of LIX 65N was complete. This salt was then washed with 200 cm^3 aliquots of hexane to extract the commercial diluent, LIX 63 and any other organic impurities. This process was repeated until the hexane layer was essentially colourless. The sodium salt of LIX 65N was then collected by filtration and at this stage given a final washing with hexane. To this yellow solid hexane was added (200 cm^3) and the suspension was brought

into contact with a 25% sulphuric acid solution, liberating the hydroxyoxime ligand which dissolved into the hexane as a brown solution. This process was repeated until all of the sodium salt had been reacted. The hexane solution of LIX 65N was then washed repeatedly with water to remove any remaining acid and the separated hexane solution was dried with anhydrous sodium sulphate. Further purification and the separation of the 'syn' and 'anti' isomers of LIX 65N has been described in Section 2.2.1..

Synthesis of Metal Complexes.

Bis(salicylaldoximato)nickel(II).

This complex was prepared by the method of Cox et al [148]. Hydrated nickel(II) chloride (2 g) was dissolved in distilled water (250 cm^3) and to this was added a solution of salicylaldoxime (2.5 g) in distilled water (200 cm^3). While this mixture was stirring sodium acetate (4 g) was added resulting in the formation of a pale green precipitate of the required complex. This solid was isolated by filtration, washed with water and dried by suction. The complex was dissolved in hot chloroform and on cooling of this solution to 0^oC dark green needle shaped crystals of bis(salicylaldoximato)nickel(II) were formed. These were stored over P_2O_5 in a vacuum desiccator. U.V.-visible spectrophotometry (See Table 2.7.) of this compound compares favourably with previously published data [94].

Bis(2-hydroxyacetophenone oximato)nickel(II).

This complex was prepared in a similar manner to the salicylaldoximate described above. Hydrated nickel(II) tetra-

fluoroborate (2 g) was dissolved in distilled water (20 cm^3) and added to a solution of 2-hydroxyacetophenone oxime (1.76 g) in methanol (50 cm^3). As the mixture was stirring sodium acetate (1.6 g) was added resulting in the precipitation of a pale green powder. The complex was isolated by filtration, washed with water and recrystallised, as lustrous green plates, from chloroform. These crystals were dried and stored over P_2O_5 in a vacuum desiccator.

Analysis (B.M.A.C.).Calculated for ($C_{16}H_{16}N_2NiO_4$): C: 53.53%; H: 4.49%; N: 7.80%.

Found: C: 53.42%; H: 4.39%; N: 7.91%.

Bis(2-hydroxybenzophenone oximato)nickel(II).

Again, this compound was synthesised by the general method of Cox et al [148]. Hydrated nickel(II) tetrafluoroborate (2 g) was dissolved in distilled water (20 cm^3). To this was added a solution of 2-hydroxybenzophenone oxime (2.5 g) in methanol (50 cm^3). While stirring this mixture sodium acetate (1.6 g) was added resulting in the precipitation of a pale green powder. The complex was isolated by filtration, washed with water, dried by suction evaporation and recrystallised from chloroform as dark green needles. These were stored over P_2O_5 in a vacuum desiccator.

Analysis (B.M.A.C.). Calculated for ($C_{26}H_{20}N_2NiO_4$): C: 64.63%; H: 4.17%; N: 5.79%.

Found: C: 64.62%; H: 4.24%: N: 5.84%.

Ni(LIX 65N)$_2$.

This complex was prepared by use of a two phase process. LIX 65N (2 g) was dissolved in hexane and brought into contact with an ammoniacal solution of nickel(II) tetrafluoroborate in excess. The two phases were vigourously stirred together for several minutes and then allowed to separate by standing. The hexane phase was separated from the aqueous phase and allowed to evaporate very slowly. This allowed precipitation of a green waxy solid which was separated and recrystallised from chloroform. Only a slow evaporation of solvents allows solidification of the complex probably as a result of the isomerised alkyl chain of the molecule. Any attempts at rapid removal of solvents result in the formation of an oil. The waxy solid was dried and stored over P_2O_5 in a vacuum desiccator.

Analysis (B.M.A.C.). Calculated for ($C_{44}H_{56}N_2NiO_4$): C: 71.84%; H: 7.67%; N: 3.81%.

Found: C: 71.73%; H: 7.65%; N: 3.76%.

Cu(LIX 65N)$_2$.

This complex was prepared by the direct reaction of a methanolic solution of hydrated copper(II) tetrafluoroborate (2 g) and a methanolic solution of LIX 65N (3.9 g). On mixing, an immediate formation and precipitation of a green powder occurred. This complex was separated by filtration, dried and recrystallised from a methanol/chloroform solution by the slow evaporation technique. This resulted in the formation of green waxy needles of the desired complex which were dried and stored over P_2O_5 in a vacuum desiccator.

Analysis (B.M.A.C.). Calculated for ($C_{44}H_{56}CuN_2O_4$): C: 71.37%;
H: 7.62%; N: 3.78%.
Found: C: 71.22%; H: 7.78%; N: 3.88%.

Co(LIX 65N)$_2$.

This complex is extremely oxygen sensitive and thus the precipitate technique involves the use of anaerobic conditions. The complex was synthesised in the following manner. A solution of LIX 65N (1.86 g) in methanol (50 cm^3) was deoxygenated by bubbling dry nitrogen through the solution for a period of 15 to 20 minutes. An excess of cobalt(II) nitrate (1.15 g) was dissolved with sodium acetate (0.77 g) in dry methanol (50 cm^3) and this solution was deoxygenated in the same manner. The solution containing the ligand was placed in a three necked 250 cm^3 round bottomed flask and dry nitrogen passed continually through this solution as the solution of the metal salt was added slowly by way of a pressure equalising dropping funnel. On addition of this solution the mixture became an intense brown/red colour as the complex formed. The addition was completed in one hour. On completion the methanol was removed on a vacuum line and the complex extracted from the excess cobalt(II) nitrate with freshly deoxygenated dichloromethane. This solution was then slowly evaporated by means of bubbling dry nitrogen through the solution and the brown solid formed was pumped dry on the vacuum line. The complex was stored in sealed bottles in a nitrogen glove bag.
Analysis (B.M.A.C.). Calculated for ($C_{44}H_{56}CoN_2O_4$): C: 71.71%;
H: 7.66%; N: 3.80%; Co: 7.99%.
Found: C: 72.31%; H: 8.15%; N: 3.77%;
Co: 8.0%.

Analysis (B.M.A.C.). Calculated for ($C_{44}H_{56}CuN_2O_4$): C: 71.37%;
H: 7.62%; N: 3.78%.
Found: C: 71.22%; H: 7.78%; N: 3.88%.

Co(LIX 65N)$_2$.

This complex is extremely oxygen sensitive and thus the precipitate technique involves the use of anaerobic conditions. The complex was synthesised in the following manner. A solution of LIX 65N (1.86 *g*) in methanol (50 cm^3) was deoxygenated by bubbling dry nitrogen through the solution for a period of 15 to 20 minutes. An excess of cobalt(II) nitrate (1.15 *g*) was dissolved with sodium acetate (0.77 *g*) in dry methanol (50 cm^3) and this solution was deoxygenated in the same manner. The solution containing the ligand was placed in a three necked 250 cm^3 round bottomed flask and dry nitrogen passed continually through this solution as the solution of the metal salt was added slowly by way of a pressure equalising dropping funnel. On addition of this solution the mixture became an intense brown/red colour as the complex formed. The addition was completed in one hour. On completion the methanol was removed on a vacuum line and the complex extracted from the excess cobalt(II) nitrate with freshly deoxygenated dichloromethane. This solution was then slowly evaporated by means of bubbling dry nitrogen through the solution and the brown solid formed was pumped dry on the vacuum line. The complex was stored in sealed bottles in a nitrogen glove bag.
Analysis (B.M.A.C.). Calculated for ($C_{44}H_{56}CoN_2O_4$): C: 71.71%;
H: 7.66%; N: 3.80%; Co: 7.99%.
Found: C: 72.31%; H: 8.15%; N: 3.77%;
Co: 8.0%.

CHAPTER 3.

KINETICS STUDIES INVOLVING THE FORMATION OF BIS-COMPLEXES OF NICKEL(II) WITH SOME COMMERCIAL SOLVENT EXTRACTANTS, AND THE METAL EXCHANGE REACTION BETWEEN $[Ni(LIX\ 65N)_2]$ AND COPPER(II) ION IN METHANOL SOLUTION.

3.1. Introduction.

The study of the formation of metal complexes of the commercial hydroxyoxime liquid-liquid extractants, especially those of Cu(II), have been of great interest for several years (Chapter 1.). Many two phase extraction studies have been performed and these have most commonly utilised the commercial solvent mixes. No single phase reactions have been studied which is somewhat surprising. Although this situation is slightly removed from the extraction conditions in commercial plants, it does relieve the problems primarily induced by the pres ence of an interface in the two phase systems. The use of the purified forms of the liquid-liquid extractant chelating agents is also advantageous for studies of metal-ligand complex formation, as the complications produced by contaminants, such as p-nonyl phenol, and industrially introduced catalysts, such as LIX 63 in LIX 64N, are also removed. Thus introduction of these two alterations from the industrial process can allow an investigation of the fundamental metal-extractant complex formation reaction. For these reasons the work described in this Chapter was initiated.

The investigations of metal complex formation reactions described here have been studies of the overall reaction

$$MS_n^{2+} + 2HL \longrightarrow ML_2 + nS + 2H^+ \qquad (3.1)$$

where S is a solvent molecule, M a metal ion of co-ordination number n and HL is the hydroxyoxime ligand involved in the reaction. In this type of substitution reaction where solvent molecules are replaced by ligand molecules it is of importance to have

knowledge of the number of solvent molecules in the inner co-ordination sphere of the metal ion (the co-ordination number, n) and the rate at which these solvent molecules exchange with the bulk solvent (the solvent exchange rate, k_{ex}) as these parameters often play a rate-determining role in the formation reactions. The technique of n.m.r. spectroscopy is most widely used to determine n and k_{ex} as described in a number of reviews [161-163]. This topic will be discussed more fully in Chapter 4.

The bulk of the investigations reported here are concerned with the formation of complexes of nickel(II) in methanolic solutions. This metal ion has been chosen for study in preference to either Co(II) or Cu(II) for practical reasons. Nickel(II) usually forms complexes at rates which are readily monitored by U.V.-visible stopped-flow spectrophotometric methods [164,165] which have been employed exclusively throughout this work to evaluate the metal complex formation rates. The copper(II) ion is one of the most labile transition metal ions and, as a result of this, the use of relaxation methods is often necessary to monitor its substitution processes. As stated previously, the Co(II) complexes of these hydroxyoxime ligands are very oxygen sensitive, and are thus rendered less practical for study than the corresponding Ni(II) complexes. Methanol was chosen as the solvent as the metal salt, the ligand and the resulting metal complex are all soluble and methanol is also non-co-ordinating with respect to the metal complexes formed (See Chapter 2.).

In the case of the nickel(II) ion, investigations of the co-ordination number and the solvent exchange rate have been

performed in such solvents as water [166-170], ethanol [171], dimethylsulphoxide [172-177] and acetonitrile [178-182] as well as in methanol [183-187]. These studies have revealed that in all cases the solvation number has the value of six, and solvent exchange rates and activation parameters for these processes have been evaluated.

A lot of evidence [164,165,188] suggests that ligand substitution processes of labile metal ions in aqueous solution proceed by way of the dissociative interchange, I_d, mechanism. Pearson and Ellgen [189] have demonstrated that this mechanism is generally retained for the substitution reactions of nickel(II) in methanolic solutions. The reactions studied in this work can thus be expected to follow this mechanism. The principles of the I_d mechanism for complex formation are, that initially an outer-sphere complex between the ligand and the solvated metal ion is formed in a diffusion controlled first step. The rate determining step is then subsequent loss of a solvent molecule from the metal ion and formation of the first metal-ligand bond. In the case of multidentate ligands the subsequent ring closure is usually rapid and is not rate determining.

In general, steady-state concentrations of the outer-sphere complex and other intermediates in this reaction are present and under these conditions the following rate law is derived

$$\text{rate} = \frac{d[ML]}{dt} = k_f[M][L] \qquad (3.2)$$

This is obtained from the mechanism:

$$MS_6 + L \overset{K_o}{\rightleftharpoons} [MS_6,L] \qquad (3.3)$$

$$[MS_6,L] \xrightarrow{k_1} MS_5L + S \qquad (3.4)$$

where $$k_f = \underline{f}K_o k_1 \qquad (3.5)$$

In this scheme k_f is the observed second order rate constant, K_o is the outer sphere complex formation constant and k_1 is the first order rate constant for the formation of the metal-ligand bond. The factor, $\underline{f}$, is statistical and describes the probability that the ligand in the outer-sphere complex replaces a solvent molecule and is normally considered as close to unity (a value of $\frac{3}{4}$ is sometimes used). The rate constant k_1 is usually assumed to be the same as the solvent exchange rate ($k_1 = 6k^I_{ex}$ where k^I_{ex} is the rate constant for the exchange of a single solvent molecule. k^I_{ex} is the rate constant which is usually obtained by n.m.r. methods.).

The following chapter describes an investigation of the complex formation reactions of a variety of hydroxyoxime ligands and the mechanisms involved in these reactions. Also, a study has been made of the dissociation of one of these complexes and the mechanism involved in this reaction elucidated.

3.2. Formation of Ni(II) Complexes.

In this study the reactions of the metal solvate complex $[Ni(MeOH)_6](BF_4)_2$ with a variety of hydroxyoxime ligands, including two of the commercial hydroxyoxime liquid-liquid

extractants, have been examined. The tetrafluoroborate anion was chosen for this work as it is non-co-ordinating and has the advantage over the perchlorate anion, which is often used when a non-co-ordinating anion is required, in that its complexes of organic ligands are non-explosive. In fact the fluoroborate anion has been found to be less co-ordinating to the complex ion $[Zn(MeOH)_6]^{2+}$ than the perchlorate anion (See Chapter 4). The above nickel(II) solvate was prepared by the method of Van Ingen Schenau et al [190] and shown to have a solvation number of six as determined by the method of complexiometric titration [191]. The electronic spectrum of this species was also found to be typical of a six co-ordinate octahedral nickel(II) species [93]. The complex was stored as an anhydrous methanol solution and analysed for Ni(II) content by complexiometric titration before kinetic runs were performed.

3.2.1. Complex formation with LIX 65N.

Exploratory studies were performed with the nickel(II) solvate and the purified form of the 'anti' isomer of the commercial liquid-liquid extractant LIX 65N. These studies were necessary to evaluate the stoichiometry of the complexation reaction in methanol solution. Initial mixing experiments, monitored by U.V.-visible spectrophotometry, showed that the spectrum of the complex formed was identical to that observed when the complex of stoichiometry ML_2, (where HL = LIX 65N), was dissolved in methanol solution i.e. a trans-square-planar bis-complex. Thus the stoichiometry of the overall reaction is described by equation (3.1). Therefore, in the course of this

reaction there is a co-ordination number change from six to four at the nickel(II) centre.

Further experiments showed that even when excess nickel(II) was present the only species formed was that of formulation NiL_2. No evidence for a 1:1 complex was found. This fact indicates the situation exists in this reaction where the overall stability constant, β, for bis-complex formation is very much larger than that for mono-complex formation i.e. $\beta_2 \gg \beta_1$. This in fact has been observed for Ni(II) and salicylaldoxime [199] and has been explained on the grounds of hydrogen bonding stabilising the bis-complex.

As can be seen from reaction scheme 3.1 the overall reaction involves the loss of two protons, which are known to be the phenolic protons, one from each ligand molecule. Thus in the course of the complex formation reaction a decrease in pH will occur as a result of this proton liberation. It was decided to attempt to follow the formation reaction between the mono-sodium salt of the hydroxyoxime ligand and the nickel(II) solvate, to avoid this complication. Attempts to prepare this salt were made by the reaction of sodium hydroxide with the protonated ligand, and a yellow solid was isolated. Electronic spectra of this species, recorded in methanol solution, show that the lowest energy band occurs at 333 nm i.e. at a lower energy than the corresponding band arising from the protonated form of the ligand (See Chapter 2). On addition of a methanolic solution of the nickel(II) solvate only a slight spectral change was observed with a slight shift in the position of the lowest energy absorption band (Figure 3.1.). There is, however, no evidence

Figure 3.1. Reaction of the sodium salt of LIX 65N with Ni^{2+}

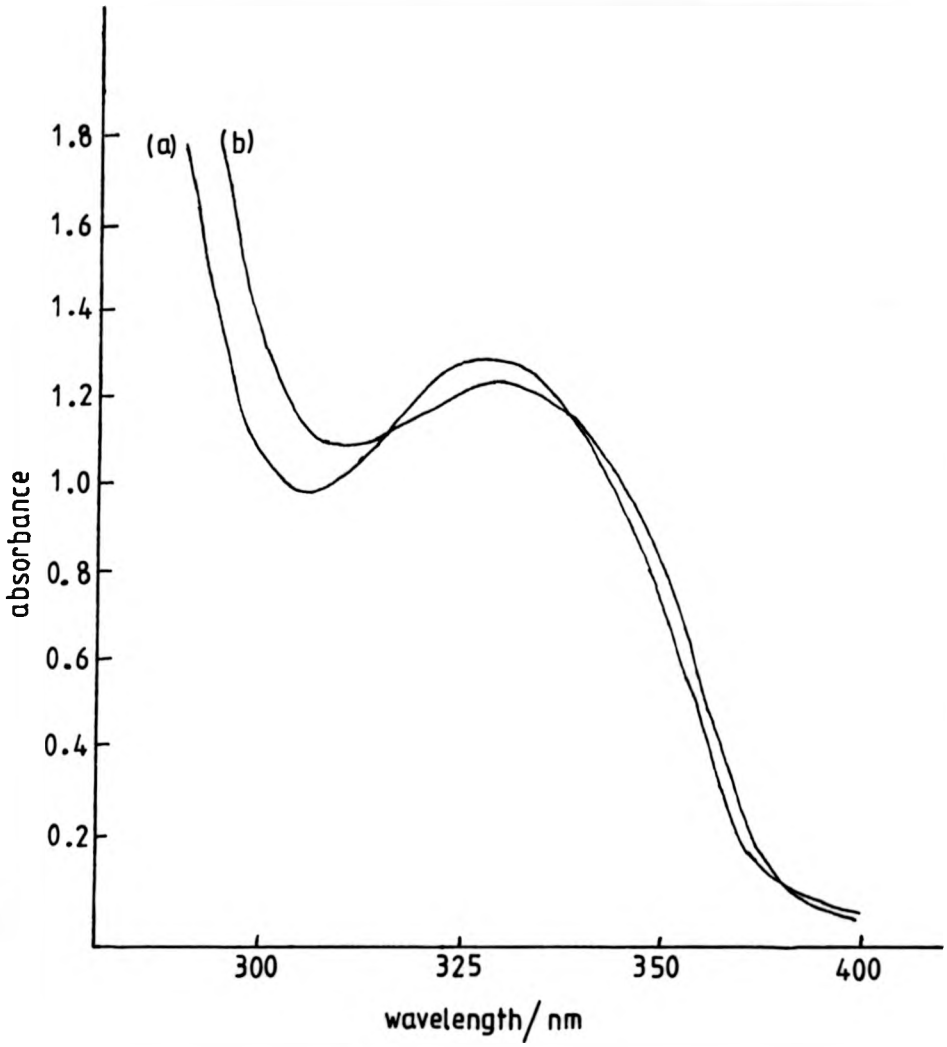

a) 5×10^{-4} mol dm^{-3} methanol solution of Na salt of LIX 65N

b) solution a) + 5×10^{-5} mol dm^{-3} Ni^{2+}

for the pres ence of the charge transfer band observed at ~380 nm in the electronic spectrum of the reaction product of Ni(II) with the neutral ligand. This would seem to indicate that different species are being formed in these two reactions. When a few drops of dilute hydrochloric acid were added to the solution of the sodium salt of LIX 65N and the Ni(II) solvate, spectral changes were observed to occur and these were found to correspond to the formation of the desired trans-square-planar complex as in Figure 3.2.. This observation seems to indicate that the reaction involved with the sodium salt was not that which was expected, but was the formation reaction involving the disodium salt of LIX 65N. Thus the reaction that was occurring is that described below, where H_2L is LIX 65N:

$$Ni^{2+} + 2Na_2L \longrightarrow Na_2[Ni(L)_2] + 2Na^+ \qquad (3.5)$$

On addition of acid solution the expected complex was formed. Thus:

$$[Ni(L)_2]^{2-} \xrightarrow{2H^+} [Ni(HL)_2] \qquad (3.6)$$

All further attempts to obtain the pure monosodium salt of this hydroxyoxime resulted in the formation of the compound described above, as determined by U.V.-visible spectrophotometry.

In view of the observations described above an alternative reaction system was explored. This system involves the use of 2,6-lutidine as a buffering agent to absorb all released protons from the reaction. In this way no pH change

Figure 3.2. Reaction of LIX 65N with Ni^{2+} in the presence of 2,6-lutidine buffer

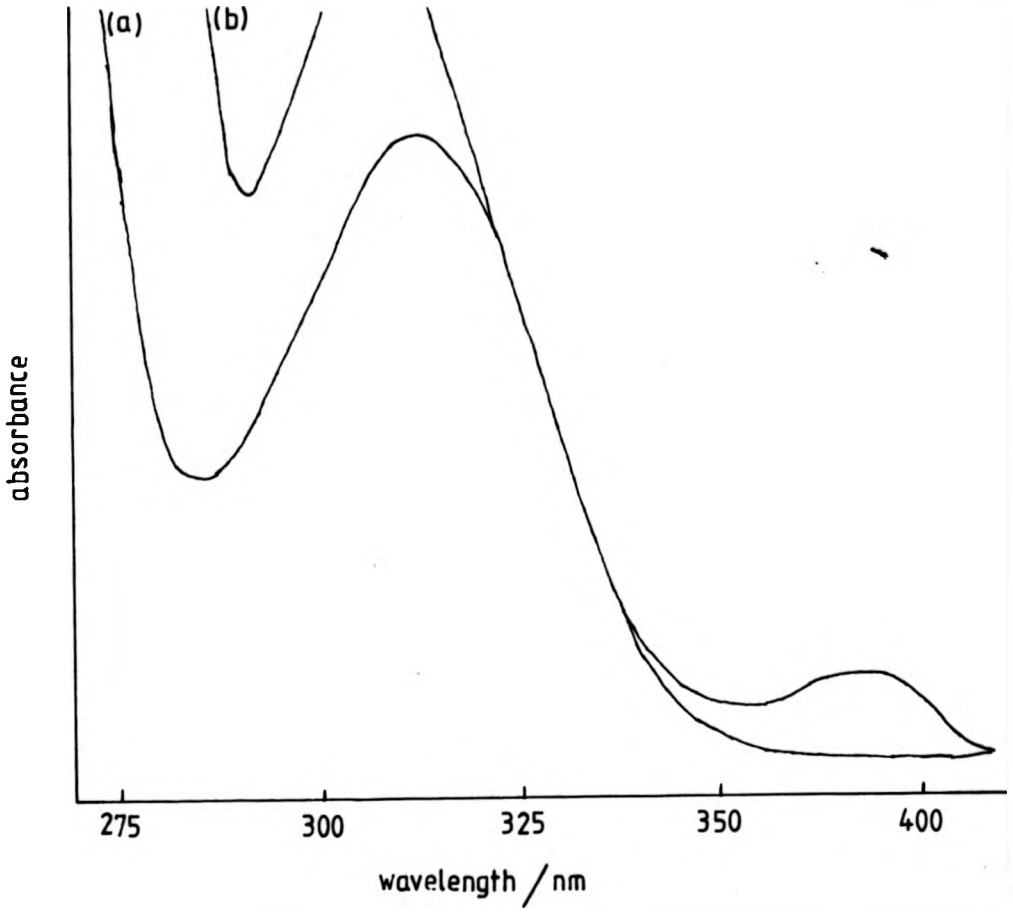

a) 5×10^{-4} mol dm^{-3} LIX 65N + 2×10^{-2} mol dm^{-3} 2,6-lutidine in methanol

b) solution (a) + 5×10^{-5} mol dm^{-3} Ni^{2+}

occurs during the course of the reaction. This nucleophilic buffer was chosen because the methyl groups in the 2- and 6-positions sterically hinder co-ordination to nickel(II). This molecule would not, therefore, interfere in the reaction mechanism by way of co-ordination. Also the compound has a reported pK_a value [164] of 6.7 and should not cause any deprotonation of the ligand at the concentrations used. The lack of interference by 2,6-lutidine was established by experiments involving the addition of the buffer to methanolic solutions of both the Ni(II) salt and the corresponding complex of LIX 65N. These experiments were again monitored by U.V.-visible spectrophotometry and on both occasions no change was observed in the spectra. It was therefore deduced that the buffer does not co-ordinate to either complex and could be assumed, therefore, not to participate in the complexation reaction by way of co-ordination.

On complexation the two most obvious changes in the electronic spectra resulting from the reaction are the appearance of two new absorbance bands at 380 nm and 610 nm. Solubility problems do not allow stopped-flow studies to be made by monitoring the gain in absorbance of the band found at 610 nm as a result of its relatively low extinction coefficient ($\epsilon_m \sim 10^2$ $dm^3 mol^{-1} cm^{-1}$. See Table 2.7.). Therefore the reaction was monitored by observing spectral changes at 380 nm. To obtain reasonable transmittance changes during the complex formation reaction a concentration of 5×10^{-5} mol dm^{-3} $[Ni(MeOH)_6](BF_4)_2$ was used with a tenfold excess of ligand (i.e. 5×10^{-4}mol dm^{-3} LIX 65N) to produce pseudo-first-order conditions. In the reaction 1×10^{-4} moles of protons are released assuming the reaction goes to completion. At least

one hundred fold excess buffer concentration is required, and to determine the optimum concentration to use in the kinetic experiments the effect of increase in buffer concentration on the extent of reaction was monitored by U.V.-visible spectrophotometry. It was found that as the concentration of 2,6-lutidine was increased from $1x10^{-2}$ mol dm^{-3} to $2x10^{-2}$ mol dm^{-3} a corresponding increase in the degree of complex formation from 85-100% was observed. This was determined from the known extinction coefficient of the complex (See Table 2.7.). As the concentration of 2,6-lutidine was further increased to 0.1 mol dm^{-3} a decrease in absorbance resulting from the electronic spectral band at 380 nm was observed. This would seem to indicate that deprotonation of the complex was occurring at higher concentrations of 2,6-lutidine. The two most acidic protons in this complex are those which participate in hydrogen bonding between the phenolic and oximino oxygen atoms. It was not known whether one or both of these protons are removed from the complex by 2,6-lutidine. In view of the fact that it has been previously observed [20] in the Mn(II), Fe(II), Co(II) and Zn(II) complexes of SALO that one sodium atom is present it seems most likely that only one of these protons is removed by 2,6-lutidine.

It was found that only in the narrow concentration range of $1.5x10^{-2}$ - $3.5x10^{-2}$ mol dm^{-3} buffer concentration could complete formation of $[Ni(LIX\ 65N)_2]$ be assured at the concentrations of metal ion and ligand used. It was therefore decided to monitor the reaction using a concentration of $2x10^{-2}$ mol dm^{-3} 2,6-lutidine as 100% complexation and no complex deprotonation was observed at this concentration.

Initial U.V.-visible stopped flow spectrophotometric studies were performed to monitor the reaction occurring when a $1x10^{-4}$ mol dm^{-3} solution of Ni^{2+} in methanol was mixed in equal proportion with a methanolic solution containing a $1x10^{-3}$ mol dm^{-3} concentration of LIX 65N. Both solutions contained a $2x10^{-2}$ mol dm^{-3} concentration of 2,6-lutidine. Thus the resulting mixture contained the required concentrations of all species.

When the two solutions were mixed the first observation was that the reaction proceeded in two distinct stages. The first stage was observed to have a half life ($t_{\frac{1}{2}}$) of around 5-6 seconds and the second stage a $t_{\frac{1}{2}}$ of around ten minutes. The first possible explanation of these observations is that the two stages are the result of a relatively rapid formation of the 1:1 metal-ligand complex followed by the slower formation of the 1:2 complex. This explanation was regarded as unlikely as no observation of a 1:1 complex had been made when excess metal ion was added to a solution of the ligand. Also on complexation of the first ligand it would be expected that labilisation of the remaining solvent molecules would occur and thus the formation of the bis-complex would be rapid. A second possible explanation is that there may be a small amount of the 'syn' isomer present if the process used for isomeric purification of the ligand was not totally successful and this isomer may be slowly converting to the 'anti' isomeric form and subsequently complexing nickel(II). This hypothesis was tested by repeating the stopped-flow experiment described above replacing the 'anti' isomer of LIX 65N with the 'syn' isomer. On mixing of the two solutions no reaction was observed over a period of thirty minutes or so. An electronic

spectrum of the same solution recorded after 24 hours of standing exposed to normal light showed no absorbance change; thus no isomer conversion was occurring as no complexation was observed. The third possible explanation considered was that a decomposition of either the ligand or the metal complex was occurring. It has been noticed previously [16] and in this work (See Chapter 2.) that when exposed to ordinary laboratory light a gradual darkening in colouration of the ligands occurs. To investigate the possibility of decomposition a methanolic solution of the 'anti' isomer of the ligand was left exposed to laboratory light for 24 hours and an electronic spectrum of the resulting solution recorded. This showed that no noticeable change had occurred over this 24 hour period. However when a similar solution was injected into the stopped flow apparatus it was observed that a gradual increase in absorbance occurred when the sample was exposed to 380 nm radiation. Resultant analysis of the recorder trace obtained from this experiment indicated a very similar rate constant to that observed for the second stage observed in the complexation reaction. An identical experiment was performed with the Ni(II) complex of LIX 65N and again a gradual increase in absorbance was observed with a very similar rate constant (Table 3.1.).

Molecule	Observed first order rate constant / s^{-1}
LIX 65N	$(2.40 \pm 0.05) \times 10^{-3}$
$Ni(LIX\ 65N)_2$	$(2.18 \pm 0.02) \times 10^{-3}$

Table 3.1. Kinetic data for decomposition processes.

Both decomposition processes gave excellent first order kinetic

plots. It would thus appear that the second stage observed in the complex formation reaction is indeed a photocatalysed decomposition of the ligand which is unaffected by complexation to Ni(II). The nature of the decomposition product has not been determined.

Analysis of the recorder traces resulting from the first stage of the formation reaction again revealed excellent first-order plots. The bis-complex formation reaction was thus monitored and stopped-flow experiments were performed to observe the effect of ligand concentration on this rate of complexation. All recorder traces from these experiments were used only if a reproducibility of at least three successive kinetic runs could be established. Resultant analysis of this data provided a set of rate constants which showed a first order dependence. When these rate constants were plotted graphically against concentration of ligand a linear relationship between the two parameters was revealed. These observed pseudo-first-order rate constants and the resultant second order plot are shown in Figure 3.3. (For values of the pseudo-first-order rate constants see Appendix B.).

As can be seen from Figure 3.3. a good linear relationship is found over a tenfold increase in ligand concentration. The data reported is in good agreement with the expected I_d mechanism of complex formation which indicates the overall reaction mechanism.

$$Ni(MeOH)_6^{2+} + HL \overset{K_o}{\rightleftharpoons} [Ni(MeOH)_6^{2+}, HL] \qquad (3.7)$$

$$[Ni(MeOH)_6^{2+}, HL] \underset{k_{-1}}{\overset{k_1}{\rightleftharpoons}} Ni(MeOH)_4L^+ + 2MeOH + H^+ \qquad (3.8)$$

plots. It would thus appear that the second stage observed in the complex formation reaction is indeed a photocatalysed decomposition of the ligand which is unaffected by complexation to Ni(II). The nature of the decomposition product has not been determined.

Analysis of the recorder traces resulting from the first stage of the formation reaction again revealed excellent first-order plots. The bis-complex formation reaction was thus monitored and stopped-flow experiments were performed to observe the effect of ligand concentration on this rate of complexation. All recorder traces from these experiments were used only if a reproducibility of at least three successive kinetic runs could be established. Resultant analysis of this data provided a set of rate constants which showed a first order dependence. When these rate constants were plotted graphically against concentration of ligand a linear relationship between the two parameters was revealed. These observed pseudo-first-order rate constants and the resultant second order plot are shown in Figure 3.3. (For values of the pseudo-first-order rate constants see Appendix B.).

As can be seen from Figure 3.3. a good linear relationship is found over a tenfold increase in ligand concentration. The data reported is in good agreement with the expected I_d mechanism of complex formation which indicates the overall reaction mechanism.

$$Ni(MeOH)_6^{2+} + HL \overset{K_o}{\rightleftharpoons} [Ni(MeOH)_6^{2+}, HL] \qquad (3.7)$$

$$[Ni(MeOH)_6^{2+}, HL] \underset{k_{-1}}{\overset{k_1}{\rightleftharpoons}} Ni(MeOH)_4L^+ + 2MeOH + H^+ \qquad (3.8)$$

Figure 3.3 Plot of pseudo-first-order rate constants(k_{obs}) against excess [LIX 65N] in 2,6-lutidine buffer (2×10^{-2} mol dm^{-3})

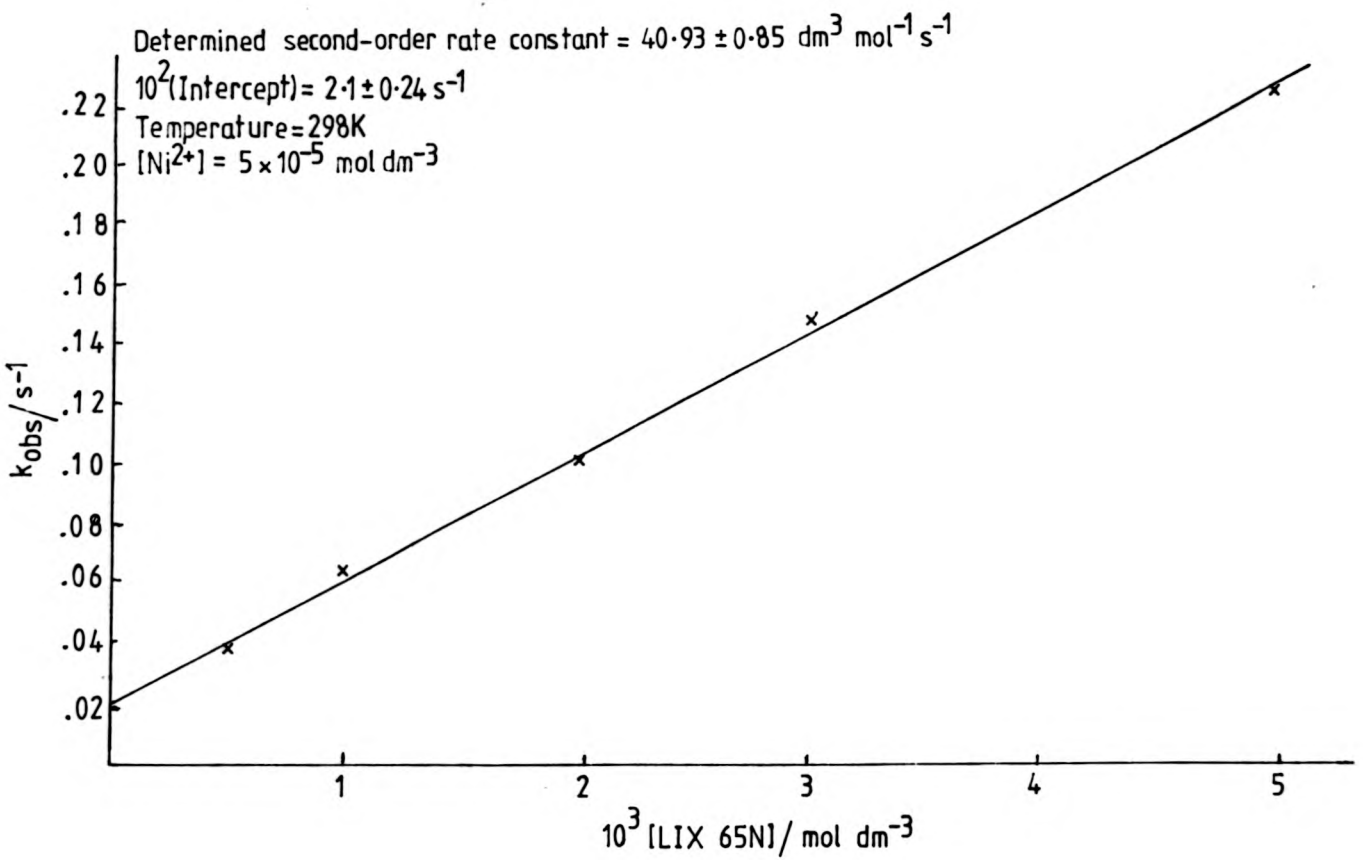

Figure 3.3 Plot of pseudo-first-order rate constants(k_{obs}) against excess [LIX 65N] in 2,6-lutidine buffer (2×10^{-2} mol dm^{-3})

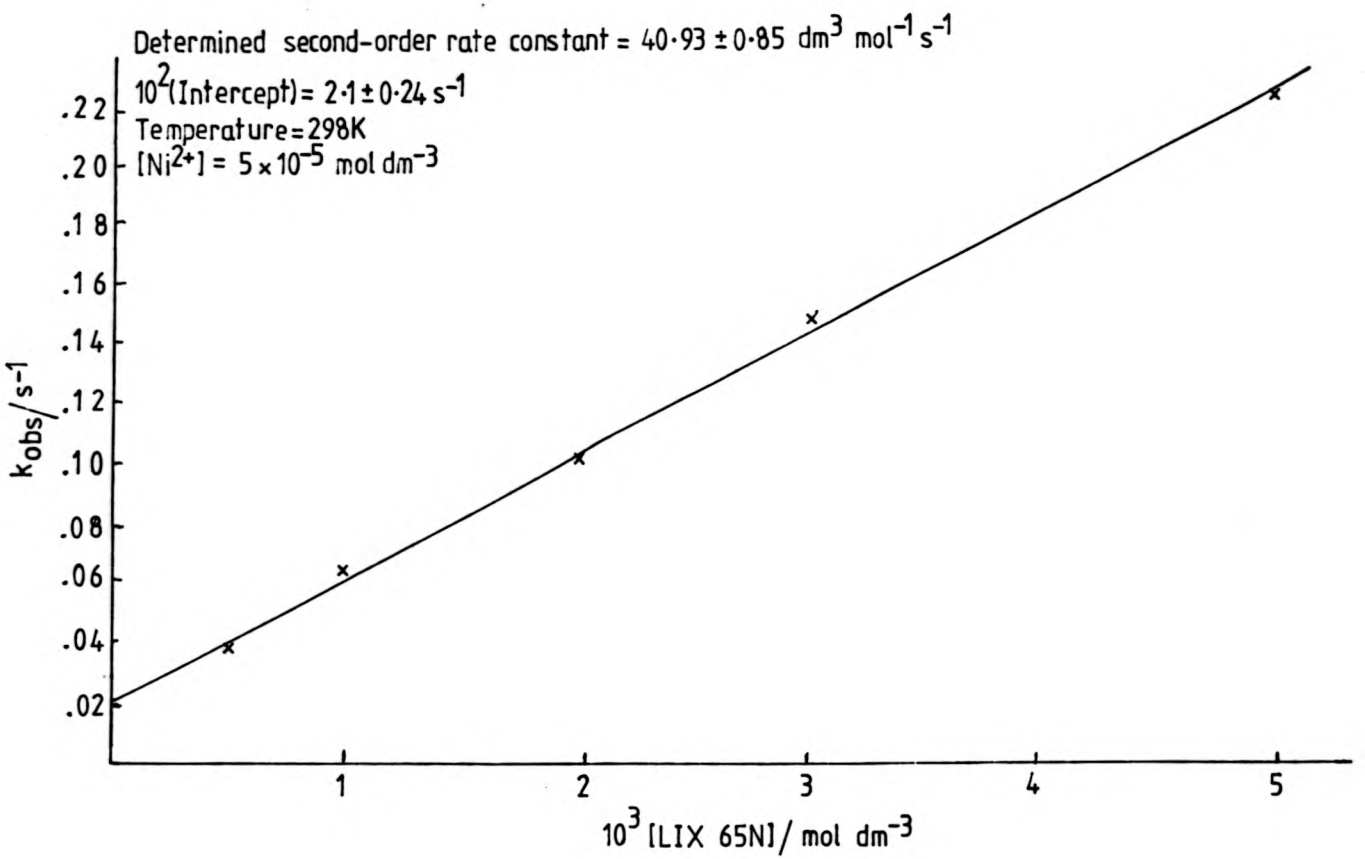

$$Ni(MeOH)_4L^+ + HL \underset{k_{-2}}{\overset{k_2}{\rightleftharpoons}} NiL_2 + 4MeOH + H^+ \qquad (3.9)$$

where $k_2 \gg k_1$ and $k_1K_o \simeq k_f$ (see 3.3).

As a consequence of the bidentate nature of the hydroxy-oxime ligand, reactions (3.8) and (3.9) are in fact two stage processes, but ring-closure is assumed to be rapid. The ligand which is a [N,O] donor is non-symmetric and either the phenolic oxygen atom or the oximino nitrogen atom can participate in the first metal-ligand bond co-ordination in either the mono- or bis-complex formation. Only reaction (3.8) is considered here as reaction (3.9) was not observed.

Two possible reaction mechanisms, therefore, exist for reaction (3.8) and these can be described by the following two reaction schemes:

Scheme 1.*

$$[Ni(MeOH)_6]^{2+} + HO\text{-}N \overset{K_o}{\rightleftharpoons} [Ni(MeOH)_6^{2+}, HO\text{-}N] \qquad (3.10)$$

$$[Ni(MeOH)_6^{2+}, HO\text{-}N] \underset{k_{-1}}{\overset{k_1}{\rightleftharpoons}} [(MeOH)_5Ni\langle O(H)\text{-}N]^{2+} + MeOH \qquad (3.11)$$

$$[(MeOH)_5Ni\langle O(H)\text{-}N]^{2+} \underset{k_{-2}}{\overset{k_2}{\rightleftharpoons}} [(MeOH)_5Ni\langle O\text{-}N]^{+} + H^+ \qquad (3.12)$$

$$[(MeOH)_5Ni\langle O\text{-}N]^{+} \xrightarrow{k_3} [(MeOH)_4Ni\langle O\text{-}N]^{+} + MeOH \qquad (3.13)$$

Scheme 2.*

$$[Ni(MeOH)_6]^{2+} + HO\text{-}N \overset{K_o}{\rightleftharpoons} [Ni(MeOH)_6^{2+}, HO\text{-}N] \qquad (3.14)$$

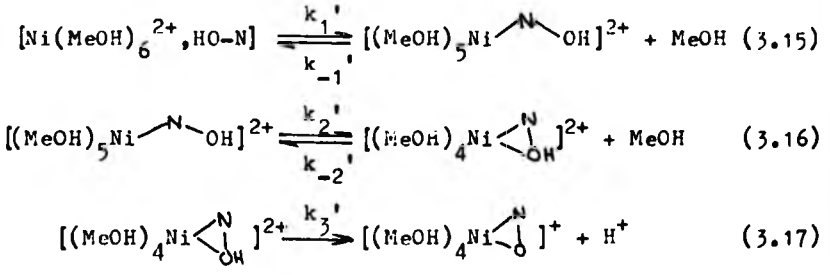

$$[Ni(MeOH)_6^{2+}, HO\text{-}N] \underset{k_{-1}'}{\overset{k_1'}{\rightleftharpoons}} [(MeOH)_5Ni(N,OH)]^{2+} + MeOH \quad (3.15)$$

$$[(MeOH)_5Ni(N,OH)]^{2+} \underset{k_{-2}'}{\overset{k_2'}{\rightleftharpoons}} [(MeOH)_4Ni(N,O)]^{2+} + MeOH \quad (3.16)$$

$$[(MeOH)_4Ni(N,O)]^{2+} \xrightarrow{k_3'} [(MeOH)_4Ni(N,O)]^{+} + H^{+} \quad (3.17)$$

* HO-N is the hydroxyoxime ligand.

The possibility of deprotonation of the ligand before formation of the outer-sphere complex is discounted on the grounds that the observed second order rate constant for the formation of the bis-complex is of the order previously reported [189] for reactions of this type with neutral bidentate ligands and the $[Ni(MeOH)_6]^{2+}$ solvated cation i.e. of the order of 10^2 dm^3 $mol^{-1}s^{-1}$ rather than of the order of 10^3 dm^3 mol^{-1} s^{-1} found for bidentate ligands possessing a single negative charge.

In reaction scheme 1 the first metal-ligand bond formation is that involving the phenolic oxygen of LIX 65N. This reaction step, whose rate is controlled by k_1, is expected to be fast and comparable to the solvent exchange rate, if the I_d mechanism is operative. However, as a consequence of the relative weakness of this bond to a protonated oxygen atom the reverse reaction, controlled by k_{-1}, is also expected to be rapid. The following deprotonation reaction step (rate constant k_2) can be expected to be comparable to this exchange reaction (rate constant k_{-1}) and indeed may well be the rate determining step. The ring-closure reaction (3.13) will be fast as a result of the close proximity of the oximino nitrogen atom to the co-ordination sites of tne nickel(II) centre.

In the second reaction scheme again the first complexation reaction, controlled by k_1', is expected to be comparable to the solvent exchange rate. As a result of the increased strength of the metal-nitrogen bond compared with the metal-hydroxyl bond the back reaction can be expected to be slow compared to the corresponding reaction in Scheme 1. The ring-closure reaction stage is again expected to be fast. The remaining step, whose rate is controlled by k_3' is that of deprotonation of the now fully co-ordinated ligand. As the hydroxyoxime ligand is now fully chelated it is unlikely that any back reaction will occur and if it does it will be slow. Thus it is expected that reaction (3.17) will occur relatively rapidly as the proton concerned will be somewhat labilised by the chelation of the ligand. Indeed this process is usually assumed to be rapid [192]. In comparing these two schemes it is considered that Scheme 2 is the most likely mechanism for formation of these complexes. This is in contrast to the case of zwitterions such as amino acids, where formation of the nickel-carboxylate bond is believed to be rate determining [193].

The value of 41 $dm^3\ mol^{-1}\ s^{-1}$ obtained for the second-order rate constant for the above reaction can be compared to the value of 350 $dm^3\ mol^{-1}\ s^{-1}$ obtained for the formation of the 1:1 complex of Ni(II) with 1,10-phenanthroline (phen) in methanol. This ligand although possessing a $[N_2]$ donor atom set and forming five-membered chelate rings can be considered structurally similar to LIX 65N in the sense that both molecules have a large aromatic character and in both cases the donor atoms are necessarily constrained in the manner of chelation. Taking into account the statistical factor of 2 for phen (this is necessary as phen has

two donor nitrogen atoms whereas LIX 65N has only one) it can be seen that the two second-order rate constants are quite similar. This suggests a similar mechanism of formation i.e. this is further evidence for the first metal-ligand bond formation to be that involving the oximino nitrogen atom of LIX 65N.

There are several factors which can possibly explain the small difference in the value of the second-order rate constants for these two reactions. To account for the observed low values of the second-order complex formation rate constants in the reactions of nickel(II) with salicylaldehyde [194], copper(II) with 2-hydroxyacetophenone [195] and both nickel(II) and copper(II) with 1-(2-pyridylazo)-2-naphthol [196] it has been suggested that deprotonation of the phenolic oxygen atom is in fact a slow process. In the cases above the pres ence of an intramolecular hydrogen bond between the phenolic hydroxyl proton and an adjacent donor atom is believed to cause this retardation of the rate of deprotonation. This possibility is discounted for the reaction with LIX 65N as it has been shown that the major hydrogen bonding phenomenon pertaining to the 'anti' isomer of this ligand is of an intermolecular nature (See Chapter 1.).

The second possible explanation which can account for this small difference stems from the structural differences between the two ligands. The hydroxyoxime ligand LIX 65N is believed to be non-planar as the result of interactions between meta-hydrogen atoms of the two benzene rings of this molecule (See Chapter 1.) whereas phen is a strictly planar ligand. This difference between the two molecules, as well as the difference in the two donor atom sets, will give rise to different properties of solution

two donor nitrogen atoms whereas LIX 65N has only one) it can be seen that the two second-order rate constants are quite similar. This suggests a similar mechanism of formation i.e. this is further evidence for the first metal-ligand bond formation to be that involving the oximino nitrogen atom of LIX 65N.

There are several factors which can possibly explain the small difference in the value of the second-order rate constants for these two reactions. To account for the observed low values of the second-order complex formation rate constants in the reactions of nickel(II) with salicylaldehyde [194], copper(II) with 2-hydroxyacetophenone [195] and both nickel(II) and copper(II) with 1-(2-pyridylazo)-2-naphthol [196] it has been suggested that deprotonation of the phenolic oxygen atom is in fact a slow process. In the cases above the pres ence of an intramolecular hydrogen bond between the phenolic hydroxyl proton and an adjacent donor atom is believed to cause this retardation of the rate of deprotonation. This possibility is discounted for the reaction with LIX 65N as it has been shown that the major hydrogen bonding phenomenon pertaining to the 'anti' isomer of this ligand is of an intermolecular nature (See Chapter 1.).

The second possible explanation which can account for this small difference stems from the structural differences between the two ligands. The hydroxyoxime ligand LIX 65N is believed to be non-planar as the result of interactions between meta-hydrogen atoms of the two benzene rings of this molecule (See Chapter 1.) whereas phen is a strictly planar ligand. This difference between the two molecules, as well as the difference in the two donor atom sets, will give rise to different properties of solution

and will thus affect the value of the outer-sphere equilibrium constant K_o.

Considering Figure 3.3. again it is observed that a positive intercept at zero ligand concentration occurs indicating some secondary reaction. The nature of this intercept will be discussed in section 3.2.3. in reference to observations made on complexation reactions with other hydroxyoxime ligands.

3.2.2. Complex formation with other hydroxyoxime ligands.

To gain further insight into the reactions described in section 3.2.1. further studies were initiated with some other hydroxyoxime ligands. All the investigations were performed in a similar manner to that described for the reaction with LIX 65N. The formation of all the Ni(II) complexes was monitored at around 380 nm using the U.V.-visible stopped-flow spectrophotometric technique. Solutions containing 1×10^{-4} mol dm^{-3} Ni(II) were mixed with solutions of the appropriate ligand in the concentration range of $1 \times 10^{-3} - 1 \times 10^{-2}$ mol dm^{-3}. In all cases a concentration of 2×10^{-2} mol dm^{-3} 2,6-lutidine as buffer was used. Under these conditions all reactions were found to proceed to completion as determined by U.V.-visible spectrophotometry. The reactions were characterised by the increase in absorbance of the charge-transfer band resulting from formation of the metal bis-complex. Resultant spectra indicated that the bis-complexes which formed were of a trans-square-planar geometry. Excellent pseudo-first-order rate plots were obtained in all cases. In obtaining second-order rate constants good linear relationships, analogous to that shown in Figure 3.3. were obtained. As in the case of the reaction involving

LIX 65N all kinetic determinations were made at 298K as controlled by the thermostat bath attached to the stopped-flow apparatus.

Before discussing individual complexation reactions it is of interest to note that only the liquid-liquid extractant LIX 70 showed the decomposition reaction observed previously with LIX 65N. This implies that it is only the alkylated hydroxyoximes of benzophenone which decompose. Why the alkylation of these oximes should cause the ligands to be susceptible to decomposition is unknown and no further investigations of this phenomenon were undertaken. Thus all complexation reactions involving non-alkylated hydroxyoximes were observed as discrete single stage reactions.

The reactions of the hydroxyoxime ligands discussed in Chapter 2 will be considered first so that the complexation kinetics of the three main types of liquid-liquid extractant which are commercially available can be compared. The kinetic data for these reactions are given in Table 3.2. (values of individual pseudo-first-order rate constants are collected in Appendix B). It is noticed that all second-order rate constants are of the same order of magnitude as that found for the complexation reaction involving LIX 65N. This indicates that a similar mechanism operates in all cases.

Comparing the second-order rate constants for SALO and ACETOX it is observed that the bis-complex of ACETOX forms at a faster rate than the corresponding complex of SALO. This observation can be ascribed to the pres ence of the methyl substituent at the oximino carbon atom of ACETOX. As demonstrated by a comparison of the chemical shifts of both the oximino carbon and the phenolic carbon atoms in the ^{13}C n.m.r. spectra of the two ligands

Table 3.2. Kinetic data for complexation reactions of nickel(II).

Ligand abbreviation	Second-order rate constant for complexation / $dm^3\ mol^{-1}\ s^{-1}$	10^3(Observed intercept / s^{-1}
SALO	47 ± 3	10.0 ± 5.5
ACETOX	67 ± 5	8 ± 9
BENZOX	63.6 ± 1.4	16 ± 2.5
LIX 65N	41 ± 1	21 ± 2.4
LIX 70	32.5 ± 2.1	23 ± 4
MeOSALO	49.5 ± 0.7	7.7 ± 1.7

this substitution, by way of an inductive effect, causes more electron density to be present on the donor atoms of ACETOX than on the corresponding nitrogen and oxygen atoms of SALO (See Table 2.8.). The enhancement of the rate of complexation of ACETOX is thus explained as a direct result of increased electron density on these donor atoms causing an increase in the value of the equilibrium constant for the outer-sphere complexation (reaction (3.15) in Scheme 2). This type of behaviour has been often observed previously in substitution reactions of octahedral Ni(II) [197,198].

The calculated second-order rate constant for the formation of $[Ni(BENZOX)_2]$ is observed to be very similar to that found for the formation of the corresponding complex of ACETOX. This can be attributed to the increased conjugation in this molecule compared to SALO. Again ^{13}C chemical shift data show that more electron density is present on the donor atoms of this molecule than in the case of SALO and thus the argument used above to explain the observed enhancement of the complexation rate for ACETOX over that for SALO can be used.

Comparing now the second-order rate constants for metal complex formation with Ni(II) of BENZOX and LIX 65N in methanol solution it is observed that the reaction of LIX 65N proceeds more slowly than that of BENZOX. Previously determined pK_a data [16] indicate that the two ligands have very similar pK_a's and if anything LIX 65N binds its phenolic proton more strongly than BENZOX. This indicates the presence of more electron density on the phenolic oxygen of LIX 65N than on BENZOX. From this evidence, if the arguments above are again employed, the complexation reaction of LIX 65N would be expected to proceed at a faster rate

than the corresponding reaction of BENZOX. The ^{13}C n.m.r. data for the two ligands show that the oximino carbon atoms have different chemical shifts and indicates that there is more electron density on the oximino nitrogen atom of LIX 65N than on that of BENZOX. Thus the value of the equilibrium constant resulting from reaction (3.15) should be greater for the reaction with LIX 65N than for that for BENZOX. Therefore, as electronic effects cannot explain these observations a consideration of steric factors must be made. The difference in the values of the complex formation rate constants for the two ligands must be attributed to the pres ence of the alkyl group substitution in the para-position to the phenolic oxygen atom in LIX 65N as this is the only structural difference between the two molecules. This long alkyl chain must cause a difference in the solvation of the outer-sphere complex formed which is unfavourable in the sense that the value of K_o for the reaction involving LIX 65N is decreased with respect to the reaction involving BENZOX. Also this alkyl chain by virtue of its length and ability to rotate in a relatively unhindered fashion occupies a rather large spatial volume. This phenomenon as well as causing solvation differences may also hinder the approach of the ligand molecule to the metal centre as the chain can fold back on itself.

A study of the complexation reaction involving the 'anti' isomer of LIX 70, purified in the same manner as was used to obtain LIX 65N, has also been performed. The kinetic data obtained are summarised in Table 3.2.. U.V.-visible spectral changes again indicate the formation of a trans-square-planar configuration of the bis-complex. The determined second-order rate constant is

found to be smaller than that obtained for the same reaction with LIX 65N. The decrease in magnitude of this rate constant for LIX 70 must be attributed to the substitution of a chlorine atom in the 3-position of the molecule. Previously determined pK_a values [16] show that the phenolic proton of LIX 70 has a markedly lower pK_a than the corresponding proton of LIX 65N. This indicates that there is less electron density on the phenolic oxygen atom of LIX 70 which is as expected since the substituent chlorine atom is electron withdrawing. The decrease in electron density causes a lowering of the interaction of the outer-sphere complex, thus lowering the value of k_1' in reaction scheme 2 and lowering the value of the observed pseudo-first-order complexation rate constant.

In the complexation reaction of Ni(II) with 2-hydroxy-5-methoxysalicylaldoxime (MeOSALO) in methanol solution unusually good separation of the absorbance bands corresponding to free ligand and the metal bis-complex in the electronic spectrum is found. This is shown in Figure 3.4. as a series of spectra recorded during a complexation reaction under the usual conditions. The pres ence of three isosbestic points shows the 'clean' nature of these reactions indicating that only one discrete species is formed. The U.V.-visible spectrum of the complex formed is typical of that observed for all of the reactions studied previously indicating that once again the trans-square-planar bis-complex is formed. Resultant kinetic data, from a stopped-flow study, are shown in Appendix B. The determined second-order rate constant (Table 3.3.) is observed to be very similar to that found for the corresponding reaction with SALO. This is somewhat surprising as the electron donating methoxy substituent would be expected to

Figure 3.4. Reaction of MeOSALO(2.5×10^{-4} mol dm^{-3}) with Ni^{2+}(2.5×10^{-5} mol dm^{-3}) in methanol [2,6-lutidine(10^{-2} mol dm^{-3})].

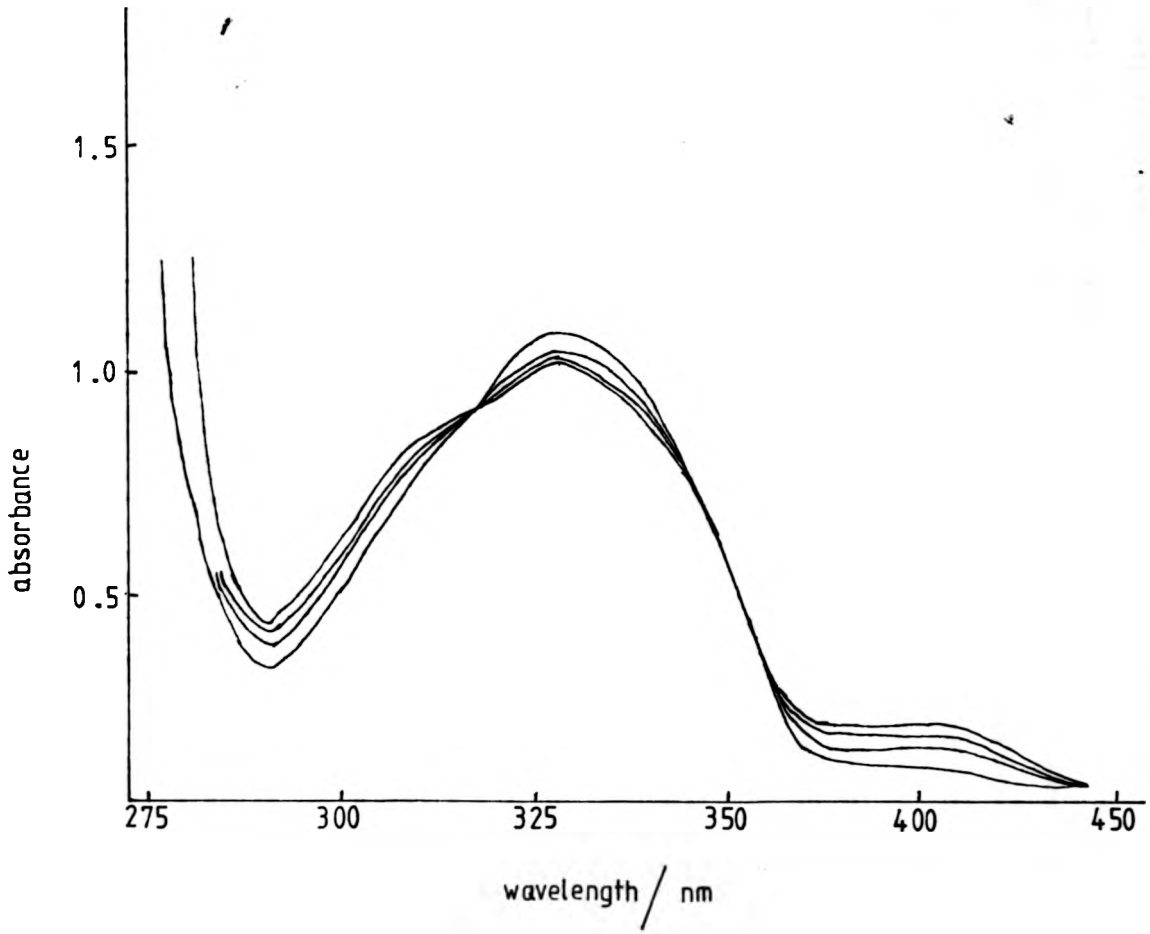

Figure 3.4. Reaction of MeOSALO(2.5×10^{-4} mol dm^{-3}) with Ni^{2+}(2.5×10^{-5} mol dm^{-3}) in methanol [2,6-lutidine(10^{-2} mol dm^{-3})]

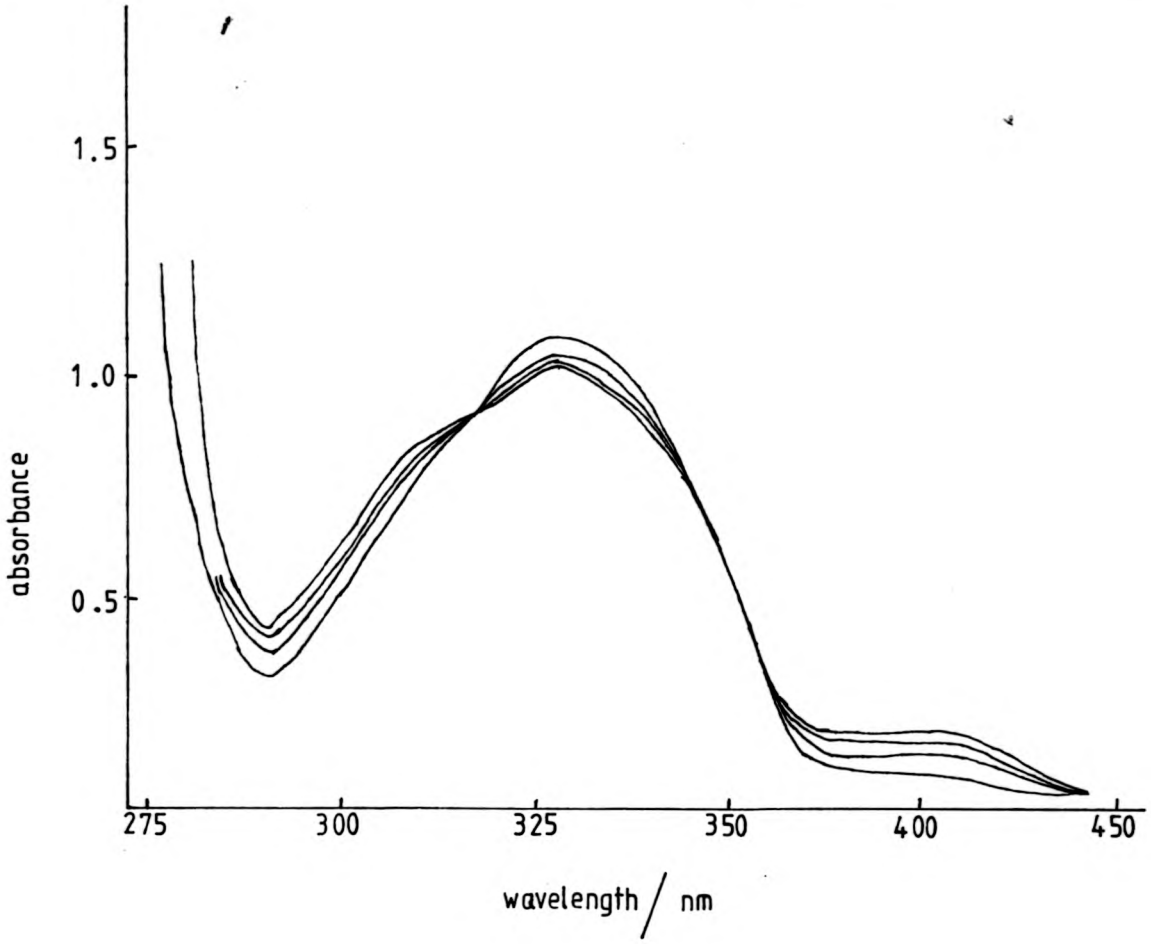

enhance the rate of complex formation by virtue of an increase in electron density on the phenolic oxygen atom. Solvation effects may well be important in the sense that the methoxy group substituted in the 5-position will cause differences in solvation, with respect to SALO, to arise and thus the value of K_o will be affected by this substitution.

The final ligand that was studied in this series of investigations was 2-hydroxy-5-nitrobenzophenone oxime (NOBENZOX). This study was performed to try to evaluate the effect on the rate of complexation of Ni(II) induced by substitution of an electron withdrawing group in the 5-position of one of the ligands already investigated. However, it was found that on addition of the required concentration (2×10^{-2} mol dm^{-3}) of the 2,6-lutidine buffer to a solution of the ligand an immediate deep yellow colouration occurred. A U.V.-visible spectrophotometric investigation of this phenomenon revealed that on addition of 2,6-lutidine to the ligand solution a new absorption band appeared with a λ_{max} of 380-390 nm as shown in Figure 3.5.. This is understandable by considering the effect that substitution of this nitro group has on the value of the pK_a of the phenolic proton. This electron withdrawing function will lower the value of this pK_a and thus the phenolic proton will be less strongly bound. This is substantiated by the observations of Burger and Egyed [199] who report that when a nitro-substituent is added to SALO there is a lowering of the pK_a value by three units. It was thus presumed that the deep yellow colouration observed on addition of 2,6-lutidine to the ligand solution was a result of deprotonation of the ligand. This hypothesis was tested by reacting NOBENZOX with

Figure 3.5. Effect of addition of 2,6-lutidine to a methanolic solution of NOBENZOX

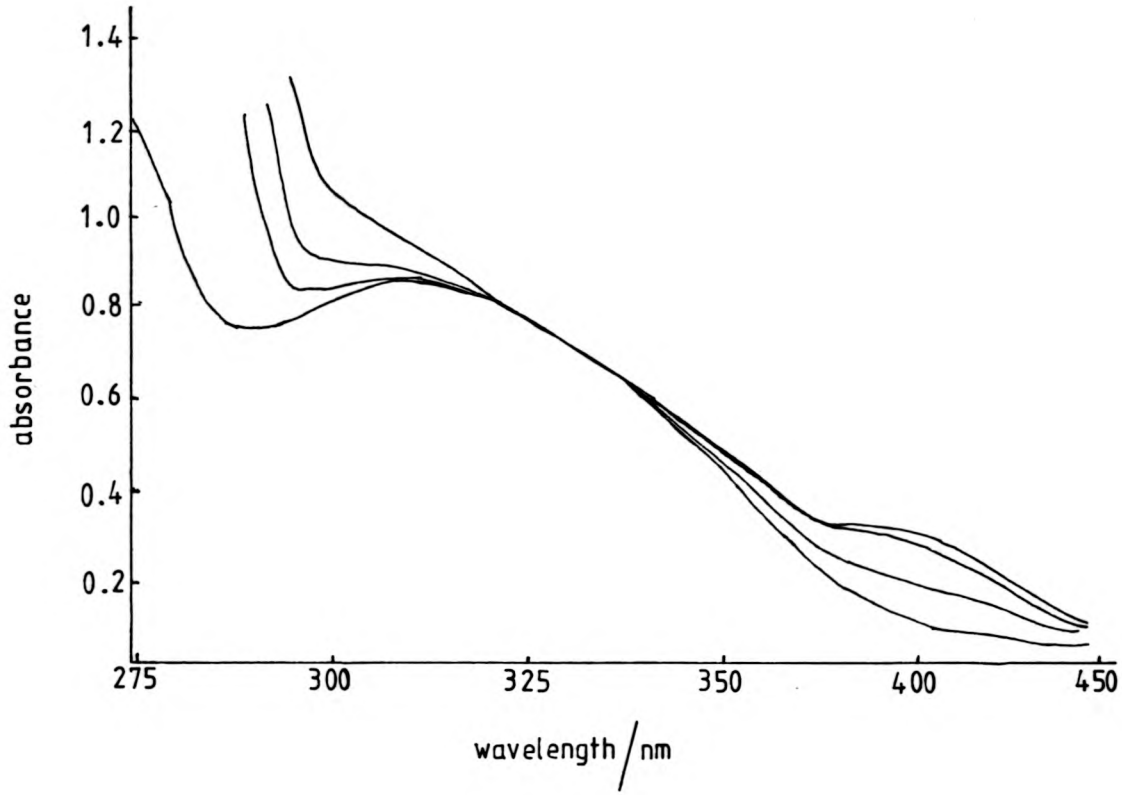

sodium hydroxide and then recording the resultant electronic spectrum. This showed that deprotonation was occurring as the spectrum of the sodium salt of the ligand was identical to that observed on addition of 2,6-lutidine to the neutral ligand.

Attempts were made to find an alternative buffer system but in all cases either deprotonation occurred or the solubility of the buffers in methanol was not sufficiently great. Thus no complexation studies could be performed.

3.2.3. The nature of the intercept in the second-order rate plots.

As described in section 3.2.1. a positive intercept occurs in the second-order complex formation rate plot for LIX 65N. This phenomenon is also observed in the corresponding rate plots resulting from the complexation reactions of all the ligands which were investigated in section 3.2.2.. The values are shown in Table 3.2..

One possible explanation of these small intercepts is that they are not very meaningful and are caused by experimental error in determination of the pseudo-first-order rate constants and/or the concentrations of the ligand solutions used. This possibility was discounted since a comparison of the values of these intercepts reveals consistencies which would be unlikely if experimental error was the cause. Considering the three hydroxy-oxime ligands studied that possess two benzene rings, namely BENZOX, LIX 65N and LIX 70, it is found that in the second-order complexation rate plots determined for these ligands the value of the intercepts are all close to 2×10^{-2} s^{-1}. Indeed the values

of the intercept for LIX 65N and LIX 70 are virtually identical within experimental error. The remaining three ligands whose complexation reactions with Ni(II) were studied give rise to values of this intercept close to 1 x 10^{-2} s^{-1}. These consistencies indicate that these intercepts do in fact have some physical meaning.

These observations also rule out the possibility that the observed intercepts arise from contamination of the methanol solvent by water. Addition of water has been shown to give rise to this type of intercept in the complexation reactions of other ligands with Ni(II) in methanol solution [189]. The complexation reactions of Ni(II) with the above hydroxyoxime ligands were investigated over a period of several months and different batches of purified and dried methanol were used for each study. So it would seem unlikely that the consistencies observed for the values of the intercepts could occur in this way.

Another possible explanation for these observations is that the intercept indicates the rate at which the reverse reaction to complexation occurs i.e. decomposition of either the mono- or bis-complex.

To try to resolve the problem as to which dissociation process the intercept is related to consideration of reactions (3.8) and (3.9) is useful. The overall stability constant for bis-complex formation, β_2, is defined as

$$\beta_2 = \frac{k_1 k_2}{k_{-1} k_{-2}} \qquad (3.19)$$

Considering now the example of the complex $[Ni(SALO)_2]$ the value

of β_2 has been reported [199] and the value of k_1 has been determined in the course of this work. Thus equation (3.19) can be rewritten as such;

$$10^{14.3} = \frac{47 \times k_2}{k_{-1}k_{-2}} \qquad (3.20)$$

During the formation of a bis-complex it is often found [193] that dissociation of the initially formed mono-complex occurs at a rate approximately a factor of ten times slower than the corresponding dissociation of the bis-complex. The observed value of the intercept found for the complex $[Ni(SALO)_2]$ is 1×10^{-2} s^{-1}. Thus if the observed intercepts in the second-order rate plots are equated to either k_{-1} or k_{-2} the following two possible approximate equations can be written for the case of $[Ni(SALO)_2]$ for when the observed intercept corresponds to k_{-1} or k_{-2} respectively.

$$10^{14.3} = \frac{47 \times k_2}{0.01 \times 0.1} \qquad 10^{14.3} = \frac{47 \times k_2}{0.001 \times 0.01} \qquad (3.21)$$

The solution of these two very approximate equations results in values of k_2 of roughly 2×10^8 s^{-1} and 2×10^{10} s^{-1} respectively. As the values of k_1 and k_2 are both formation rate constants associated with the co-ordination of a neutral ligand the value of 2×10^{10} s^{-1} for k_2 is very large and would indicate a diffusion controlled reaction. It would be expected [177,193] that on co-ordination of the first ligand molecule the solvent exchange

rate should increase by approximately a factor of 10^2 i.e. the methanol exchange rate, which determines k_2, would now be of the order of 10^5 s^{-1}. Thus the value of 2×10^8 s^{-1} for k_2 would also seem rather large. However, if it is considered that on co-ordination of the second hydroxyoxime ligand molecule, four solvent molecules are believed to be displaced from the nickel(II) centre, the large entropy change associated with this solvent liberation may well cause this increase in the value of k_2 from that which is expected. It would therefore seem that the observed intercepts are more likely to be associated with k_{-2} than with k_{-1}.

As can be seen from Table 3.2. the intercepts increase in value with ligand in the manner:

ACETOX < SALO ~ MeOSALO < BENZOX < LIX 65N ~ LIX 70

It is observed that the ligands which possess two benzene rings have intercepts which are larger than for the corresponding complexes of the other ligands. The reason for this can be attributed to the much greater bulkiness of these benzophenone derivatives which would increase the dissociation rates. Of the three other hydroxyoximes which are comparable as far as steric considerations are concerned, the nickel(II) complex of ACETOX exhibits the lowest value of the observed intercepts which is presumably a result of the inductive effect of the methyl substituent on this ligand producing a more stable nickel(II) complex.

3.3. Formation of the Cobalt(II) Complex of LIX 65N.

The following section describes an investigation of the complexation of the Co^{2+} ion by the 'anti' isomer of LIX 65N. In this study the tetrafluoroborate anion was again chosen as a suitable non-co-ordinating anion. The methanol solvate of $[Co(BF_4)_2]$ was prepared in a similar manner to that described for the corresponding nickel(II) solvate [190]. Complexiometric titration [200] showed that this cobalt(II) complex had a solvation number of six and solution U.V.-visible spectrophotometric analysis revealed a spectrum typical of an octahedral high-spin cobalt(II) species [93].

The nitrogen base 2,6-lutidine was again chosen as a buffer. An electronic spectral investigation revealed that this buffer did not co-ordinate to the metal solvate as on addition of this compound no obvious spectral changes were observed. As reported previously the cobalt(II) complex of LIX 65N is very oxygen sensitive especially when in the solution phase and all attempts to prevent oxygenation and/or oxidation of this species in solution were unsuccessful. Thus the extinction coefficients for the complex could not be ascertained accurately. It was not possible, therefore, to ascertain whether 100% complexation occurred on reaction of the metal solvate with the ligand although there seems no reason to suspect otherwise. The complexation reaction was studied using solutions with exactly the same concentrations of reactants and buffer as in the study of the complexation reactions of nickel(II) where 100% complex formation was shown to occur. It was, however, possible to investigate whether or not 2,6-lutidine co-ordinates to the cobalt(II) complex, and since no electronic spectral changes were observed on addition

of the buffer it was concluded that 2,6-lutidine did not co-ordinate. This was confirmed by observation of the effect of addition of pyridine to a solution of the complex. In this case distinct electronic spectral changes were observed indicating that co-ordination of pyridine was occurring.

Stopped-flow spectrophotometric studies were initiated, ensuring pseudo-first-order conditions, by use of at least a ten fold excess of ligand concentration. The complexation reaction was monitored at 350 nm where the most favourable transmittance changes were found to occur. Before each kinetic run the two reactant solutions were flushed with dry nitrogen for a period of approximately twenty minutes to reduce the concentration of dissolved oxygen and thus help to prevent the oxidation process.

On mixing of the two reactant solutions and monitoring of the reaction in the usual way it was observed that a two stage reaction was involved. The second stage of the reaction was found to occur at a faster rate than the previously observed photo-decomposition process, and indeed the observed rate for this stage was comparable to that found for the complexation reactions of Ni(II). To determine the nature of these two reaction stages the technique of rapid scanning spectrometry was employed (See Appendix A). This study reveals that the first stage of the reaction produces an increase in absorbance at low wavelengths in the rapid scanning spectrum (Figure 3.6.) which indicated that this stage of the reaction corresponds to the complexation reaction. In the rapid scanning spectrum of the second stage (Figure 3.6.) an increase in absorbance was observed throughout the spectral range resulting in a spectrum of the oxidised complex. Thus the second

Figure 3.6. Rapid scanning spectra of the reaction of Co^{2+} with excess LIX 65N in the presence of 2,6-lutidine

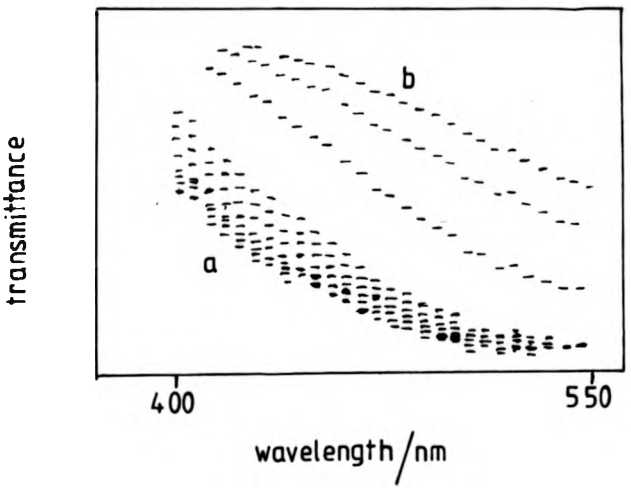

a). 1st stage: 10 scans; 2 ms delays. [COMPLEXATION]

b). 2nd stage: 5 scans; 50ms delays. [OXIDATION]

stage of the reaction corresponds to the oxidation process.

The dependence of the rates of both reaction stages on concentration of ligand was investigated. It was found that both stages give rise to good first-order kinetic plots. As shown in Figure 3.7. the dependence of the rate of the first reaction stage on ligand concentration is linear and thus confirms the assignment of this reaction to formation of the bis-complex. The determined second-order rate constant for this process is observed to be much larger than that for the corresponding reaction of Ni(II). The value of this rate constant can be compared to the solvent exchange rate for the $[Co(MeOH)_6]^{2+}$ complex ion (Figure 3.7.) and the values for the two processes are very similar which would suggest that the I_d mechanism operates for this complexation reaction with the value of the outer-sphere complex equilibrium constant, K_o, being close to unity.

The second stage of the reaction is much slower than the initial complexation reaction and seems virtually independent of ligand concentration (Figure 3.7.). This observation would be expected for an oxidation/oxygenation process. The small differences in the values of the first-order rate constants for this process can be attributed to varying concentrations of dissolved oxygen in the reactant solutions. The nature of the product from this reaction is not, however, known. As reported in the Introductory Chapter cobalt(II) complexes of the type investigated here are well known reversible or irreversible dioxygen carriers. The two most common types of oxygenated complex of this sort are where the dioxygen molecule either acts as a 'μ-peroxo' bridge or only binds to one complex molecule in an 'end-on' fashion [100]. The

Figure 3.7. Plots of k_{obs} versus [LIX 65N] for both stages in the reaction of $[Co(MeOH)_6]^{2+}$ ion (5×10^{-5} mol dm^{-3}) with LIX 65N at 298K

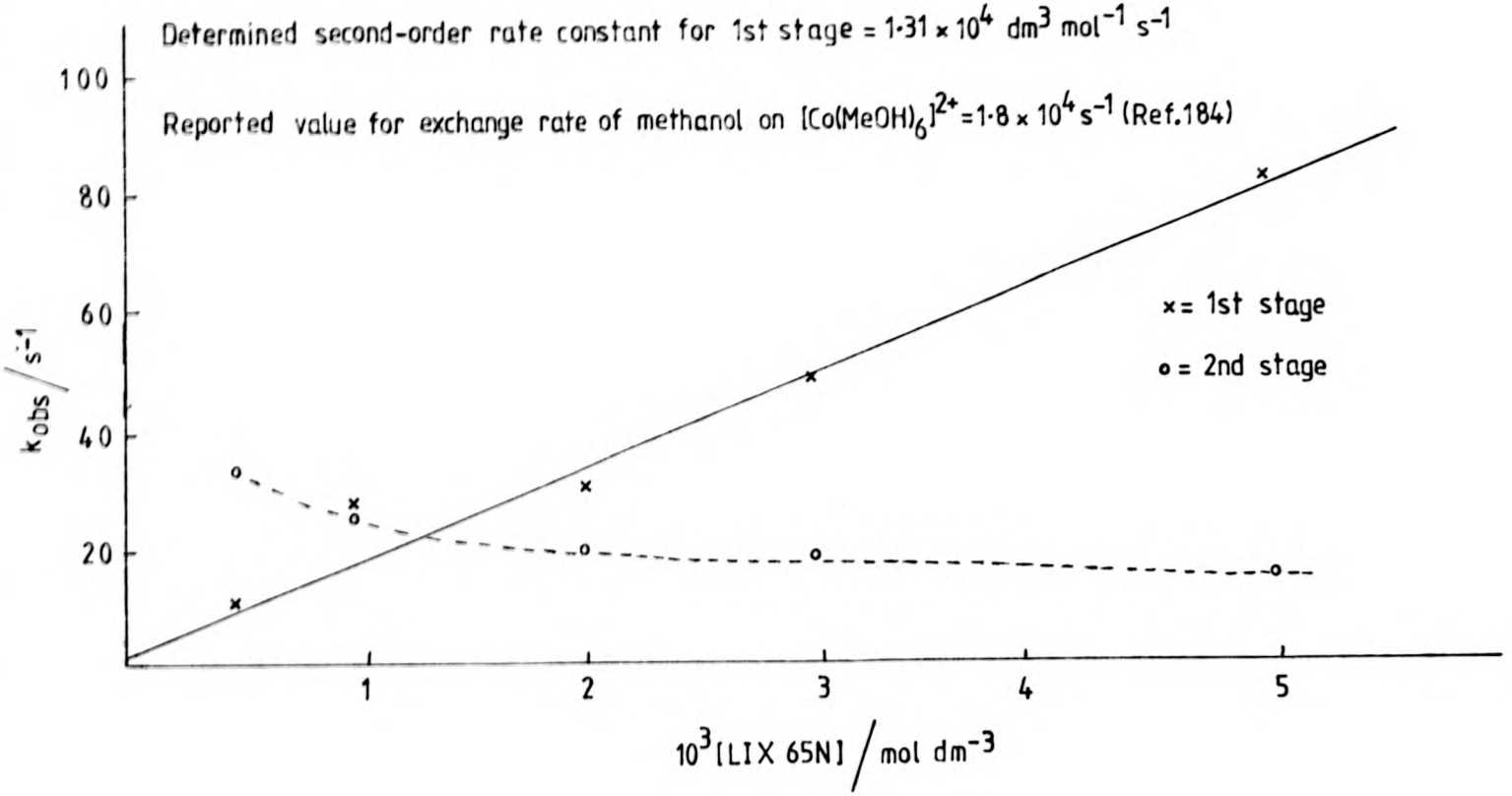

Figure 3.7. Plots of k_{obs} versus [LIX 65N] for both stages in the reaction of $[Co(MeOH)_6]^{2+}$ ion (5×10^{-5} mol dm^{-3}) with LIX 65N at 298K

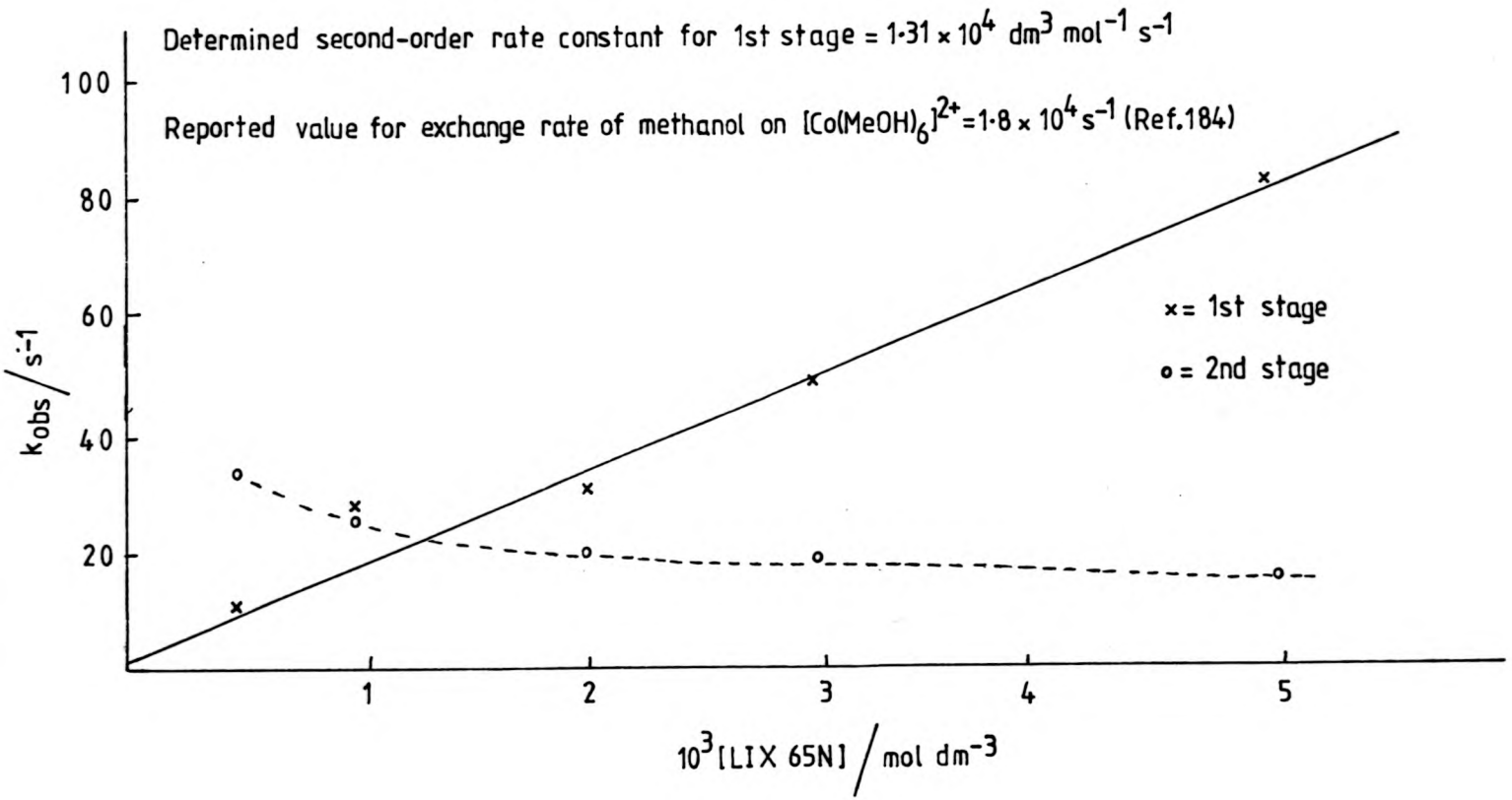

'μ-peroxo' complexes are of the structure where two molecules of the cobalt complex are bridged by a dioxygen molecule whose resultant bond length corresponds to that of a peroxide unit. The second type of complex consists of one molecule of the cobalt complex which has one molecule of dioxygen bound with a non-linear [Co-O-O] bond angle and where the O-O bond length corresponds to that of a superoxide moiety. The two types of complex are both found to be six-co-ordinate with respect to the cobalt centre, with a co-ordinating base occupying the vacant co-ordination site in a trans-position to the dioxygen molecule. Of the complexes investigated of this type the most usual base is pyridine [100] but molecules such as N,N-dimethylformamide [201] and acetonitrile [202] are also known to act in this manner. In the system studied here there are two molecules that may possibly occupy the sixth co-ordination site, namely 2,6-lutidine and methanol. Recently 2,6-lutidine [203] has been shown to act in this manner but as no co-ordination of this molecule was observed in the electronic spectral study described previously this seems unlikely. Methanol may be feasible as a co-ordinating molecule as it has been recently shown [204] that water can act as the co-ordinated base in a similar complex. It is not, however, known which of these co-ordinating molecules is involved in the oxygenated complex.

3.4. A Study of the Formation of the Copper(II) Complex of LIX 65N.

The study of the complexation reaction of copper(II) by LIX 65N was initiated in the same manner as described for the corresponding reactions of Ni(II) and Co(II). Solution electronic

spectral studies showed that the expected trans-square-planar complex was formed on the mixing of solutions of the metal ion and the ligand. It was, however, found that the previously used buffer, 2,6-lutidine, co-ordinated to the Cu^{2+} ion. When the base was added to a solution of the metal solvate a deep green colouration occurred. This enhanced co-ordinative ability over both Ni(II) and Co(II) is presumably a result of the greater stability of the copper(II) complexes (the Irving-Williams stability sequence). Trial experiments were performed with a series of other buffers but in all cases either co-ordination of the buffer occurred or the desired solubility could not be attained.

It was, therefore, decided to attempt to follow the complex formation reaction unbuffered. The reaction was monitored by the stopped-flow method at 350 nm and it was found that complexation occurred at a very rapid rate. In fact only the last stages of the complexation could be observed by this method of investigation and the half-life of the reaction was found to be less than seven milliseconds. Thus no further investigation of this system was performed since to study this reaction relaxation techniques are necessary and these were not available.

4.5. The Dissociation of $[Ni(LIX\ 65N)_2]$ in the Presence of Cu^{2+}.

Metal-metal exchange reactions are of obvious importance in metal ion liquid-liquid extraction processes, but relatively little is known about the mechanisms involved. Therefore, the dissociation of the nickel(II) complex of LIX 65N induced by the presence of the Cu^{2+} ion was investigated. Previous studies of

this type of metal exchange reaction have often allowed the observation of stepwise dissociation. For example, this approach has yielded information concerning the mechanisms of unwrapping of multidentate ligands such as EDTA [205] and ethylenediamine-diacetic acid (EDDA) [206] from metal ions.

The metal exchange reaction investigated, in which the driving force is the formation of the more stable complex of copper(II), was followed by the U.V.-visible stopped-flow spectrophotometric method. Initial mixing experiments showed when a methanolic solution of $[Ni(LIX\ 65N)_2]$ was mixed in an equimolar ratio with a methanolic solution of the $[Cu(MeOH)_6]^{2+}$ ion at a concentration of each reactant of 5×10^{-5} mol dm^{-3}, complete dissociation of the nickel(II) complex occurred. The observed electronic spectral changes indicated that the copper(II) bis-complex of LIX 65N was formed in 100% yield as determined from the known extinction coefficient of this complex (Table 2.7.). The observations described are shown in Figure 3.8.. Thus the following reaction is involved:

$$Ni(LIX\ 65N)_2 + Cu^{2+} \longrightarrow Ni^{2+} + Cu(LIX\ 65N)_2 \qquad (3.22)$$

As this reaction is purely a metal exchange reaction no proton release or capture occurs. The dissociation process can be monitored, therefore, without the use of any buffering agent, and indeed all kinetic experiments were performed in this manner.

Initial stopped-flow experiments were instigated to follow the reaction occurring when a 5×10^{-5} mol dm^{-3} methanolic

Figure 3.8. Reaction of $[Ni(LIX\ 65N)_2]$ with Cu^{2+} in methanol

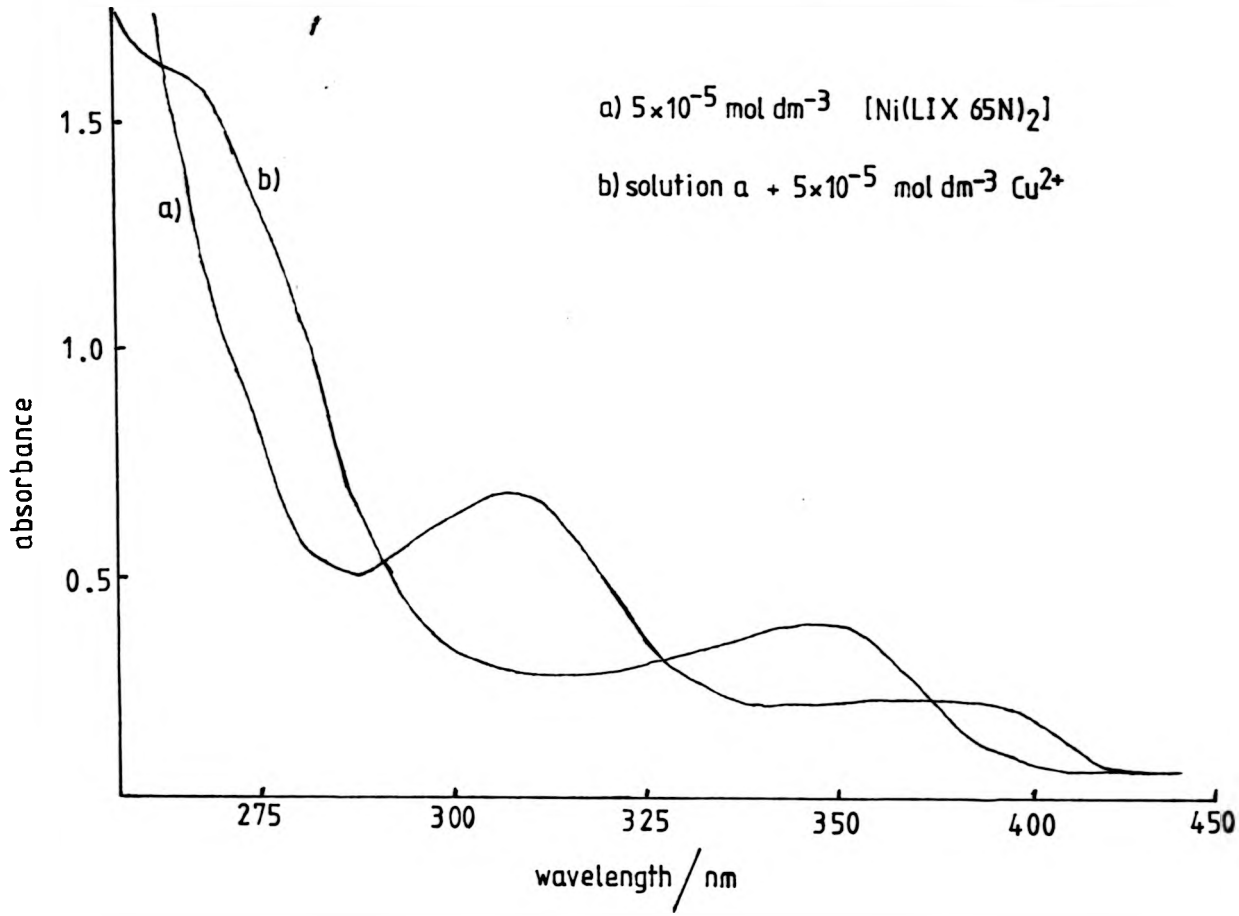

solution of the nickel(II) complex was mixed with a 5 x 10^{-5} mol dm^{-3} methanolic solution of the copper(II) solvate. Spectral changes were monitored at 350 nm where an increase in absorbance due to the formation of the $[Cu(LIX\ 65N)_2]$ was observed. It was found that the metal exchange reaction appeared to proceed by way of two distinct reaction stages. These were characterised by an initial increase in absorbance over a period of approximately two seconds followed by a slower decrease in absorbance which was complete in a period of approximately one minute (Figure 3.9.). A very slow increase in absorbance was found to occur at the completion of this latter reaction stage. This was found to correspond to the slow photodecomposition process described previously. To observe how the above absorbance changes were affected by a change in monitoring wavelength, the metal exchange reaction was subsequently investigated at 395 nm. At this wavelength a decrease in absorbance from the nickel(II) complex occurs. Under these conditions an initial rapid increase in absorbance was observed over a period of some seventy milliseconds followed by a slow decrease in absorbance over a period of approximately one minute (Figure 3.9.). Again the slow increase in absorbance resulting from the photodecomposition of the formed Cu(II) complex was observed after the exchange reaction was complete.

This apparent discrepancy in observed spectral changes at the two monitoring wavelengths is at first curious. However, these observations can be explained if the reaction is considered to occur by way of three distinct stages. When the monitoring wavelength is 350 nm the first two stages of the metal exchange reaction are both characterised by an increase in absorbance. As

Figure 3.9. Single wavelength stopped-flow traces for the reaction of $[Ni(LIX\ 65N)_2]$ (5×10^{-5} mol dm^{-3}) with Cu^{2+} (5×10^{-5} mol dm^{-3}) in methanol at 298K

1. 350 nm

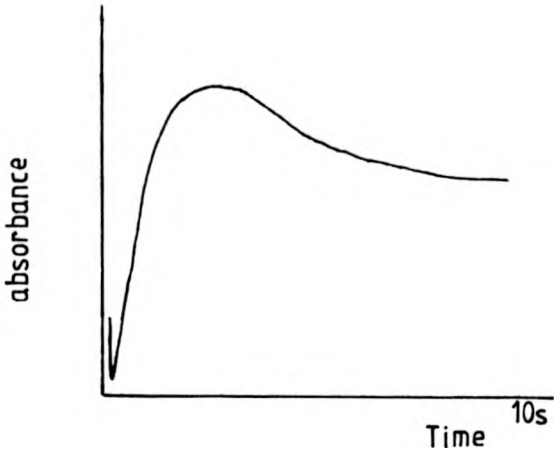

2. 395 nm

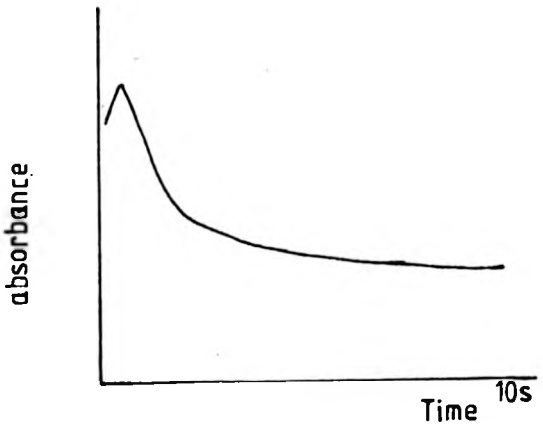

the first reaction step is much faster than the second, the two stages are not observed separately. When the monitoring wavelength is 395 nm the first reaction stage is again characterised by an increase in absorbance but the second and third stages now both occur with a decrease in absorbance and are thus not resolved as two distinct stages.

To confirm that three distinct stages were in fact involved in the metal exchange reaction it was decided to study the reaction by the technique of rapid scanning spectrometry. With our apparatus spectral changes over a range of 150nm or 300 nm can be monitored simultaneously for a single kinetic run (See Appendix A). Studies performed in this manner over the spectral range of 280-430 nm indeed confirmed the existence of these three distinct stages. Each of these reaction steps was found to give rise to distinctly different spectral changes and throughout the course of the overall exchange reaction each step was characterised by different isosbestic points. These observed spectral changes are demonstrated in Figure 3.10..

Inspection of the rapid scanning spectra shown in Figure 3.10. reveal that the first stage is characterised by an increase in absorbance in the spectral range of 325-410 nm. An isosbestic point occurs at 320-325 nm and a small decrease in absorbance is observed from 280-320 nm. Thus during this initial reaction step it appears that very little change occurs in the $\pi^* \leftarrow n$ ligand absorption band of the nickel(II) complex but a relatively large alteration occurs at the metal-to-ligand charge transfer band. This implies a very small change in the ligand environment around the nickel(II) centre with a larger change in the metal-ligand

Figure 3.10. Rapid scanning spectra for the three reaction stages found for $[Ni(LIX\ 65N)_2]$ + Cu^{2+} in methanol at 298K

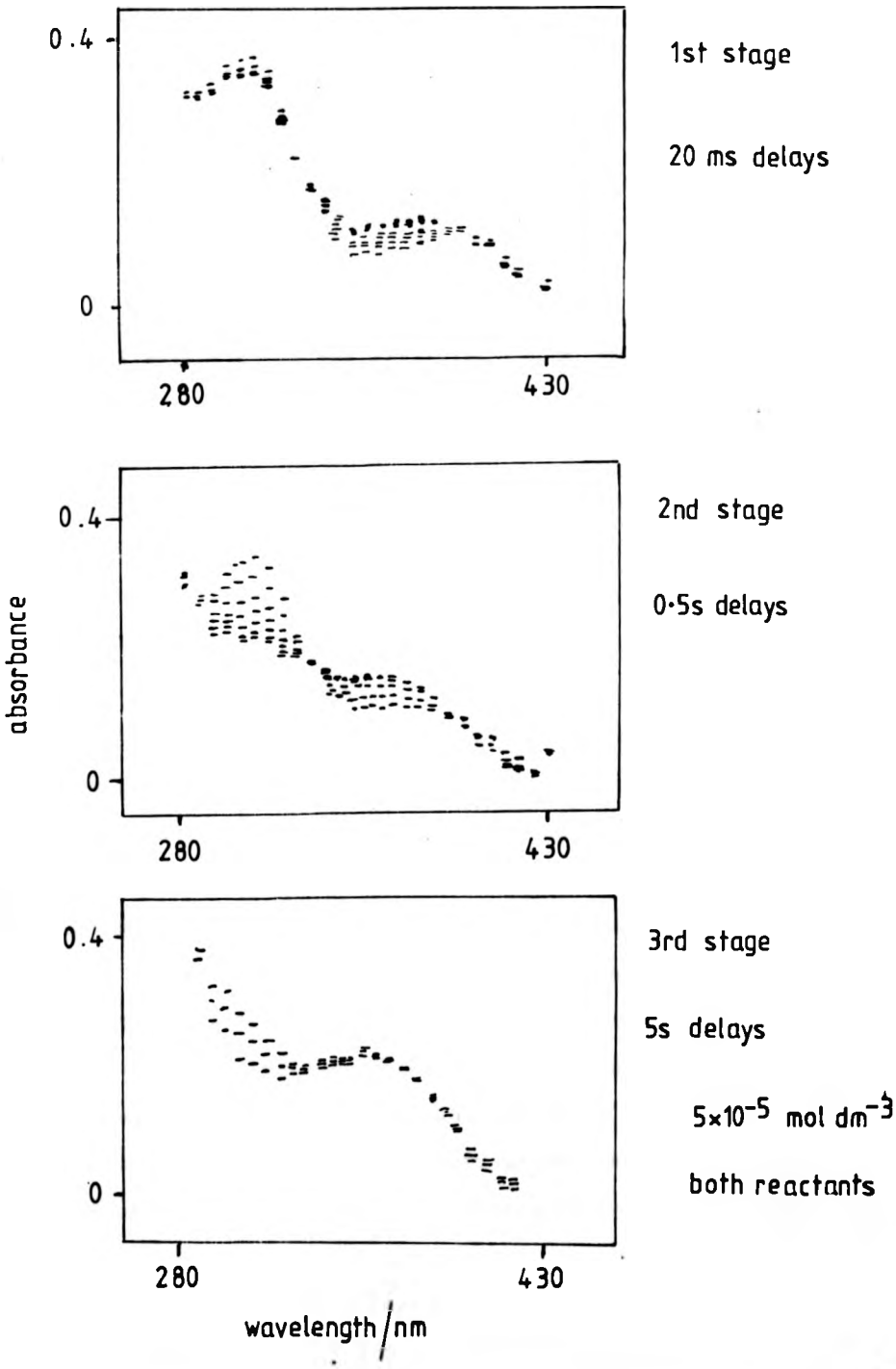

bonding system.

The second stage of the complexation reaction is found to exhibit three isosbestic points, at 285-290 nm, 325-330 nm and 380-385 nm. A small increase in absorbance is observed during the course of this reaction stage at 280-285 nm, a larger decrease in absorbance at 290-325 nm, a large increase at 335-380 nm and finally a small decrease in absorbance at 390-420 nm. These observations indicate the loss of the $\pi^* \leftarrow n$ ligand absorbance band of the nickel(II) complex, a gain in absorbance around the spectral region where the metal-to-ligand charge transfer band resulting from the copper(II) complex of LIX 65N is found and a loss of the metal-to-ligand charge transfer band resulting from the nickel(II) complex. Thus very dramatic changes occur during this second stage.

The final reaction stage is characterised by an isosbestic point at 370-375 nm. A large increase in absorbance is observed over the spectral range 280-370 nm and a small decrease is observed from 375 nm to 425 nm. The final spectrum is that of the copper(II) bis-complex and it would appear that the largest spectral change for this third stage is the growth of the band due to the $\pi^* \leftarrow n$ ligand transition of the produced copper(II) complex which has a maximum absorbance at around 260 nm (See Figure 3.8.).

With this knowledge of the electronic spectral changes, it was now possible to investigate the kinetics of the individual reaction steps. Single wavelength stopped-flow experiments were performed making use of the known isosbestic points which had been found by rapid scanning spectrometry. The first and third stages of the reaction can be investigated by performing stopped-flow

experiments while monitoring at an isosbestic point of the second stage; a montoring wavelength of 380 nm was employed. At this wavelength the first stage gives rise to an initially rapid increase in absorbance and the third stage to a much slower decrease in absorbance (at the concentrations used for rapid scanning spectral analysis the third stage is approximately 50 times slower than the first stage). The second stage of the complexation reaction was investigated at a wavelength of 340 nm where only a very small contribution to the observed absorbance is attributable to the first and third reaction stages.

Initial experiments were again performed with 5×10^{-5} mol dm^{-3} solutions of the $[Ni(LIX\ 65N)_2]$ and $[Cu(MeOH)_6]^{2+}$ ion. On mixing it was found that all three reaction stages gave rise to good first-order plots with observed rate constants of 15.5, 1.42 and 0.38 s^{-1} respectively at 298K. It was now necessary to investigate the effect of concentration of Cu^{2+} on the rates of the three different reaction stages. Using a constant concentration of $[Ni(LIX\ 65N)_2]$ (5×10^{-5} mol dm^{-3}) and increasing the concentration of copper(II) from 5×10^{-5} mol dm^{-3} to 4.75×10^{-3} mol dm^{-3} it was found that the rates of all three reaction stages were in some way dependent on the Cu^{2+} concentration.

The observed dependence of the rate of the first stage of the reaction on $[Cu^{2+}]$ is shown in Figure 3.11.. As can be seen this dependence is non-linear. It was, however, found difficult to follow this reaction stage under pseudo-first-order conditions as only small absorbance changes were observed. As the rate of the reaction increased it became increasingly difficult to obtain consistent first-order rate constants. Thus only the

Figure 3.11. Variation of k_{obs} with $[Cu^{2+}]$ for first stage of metal exchange reaction

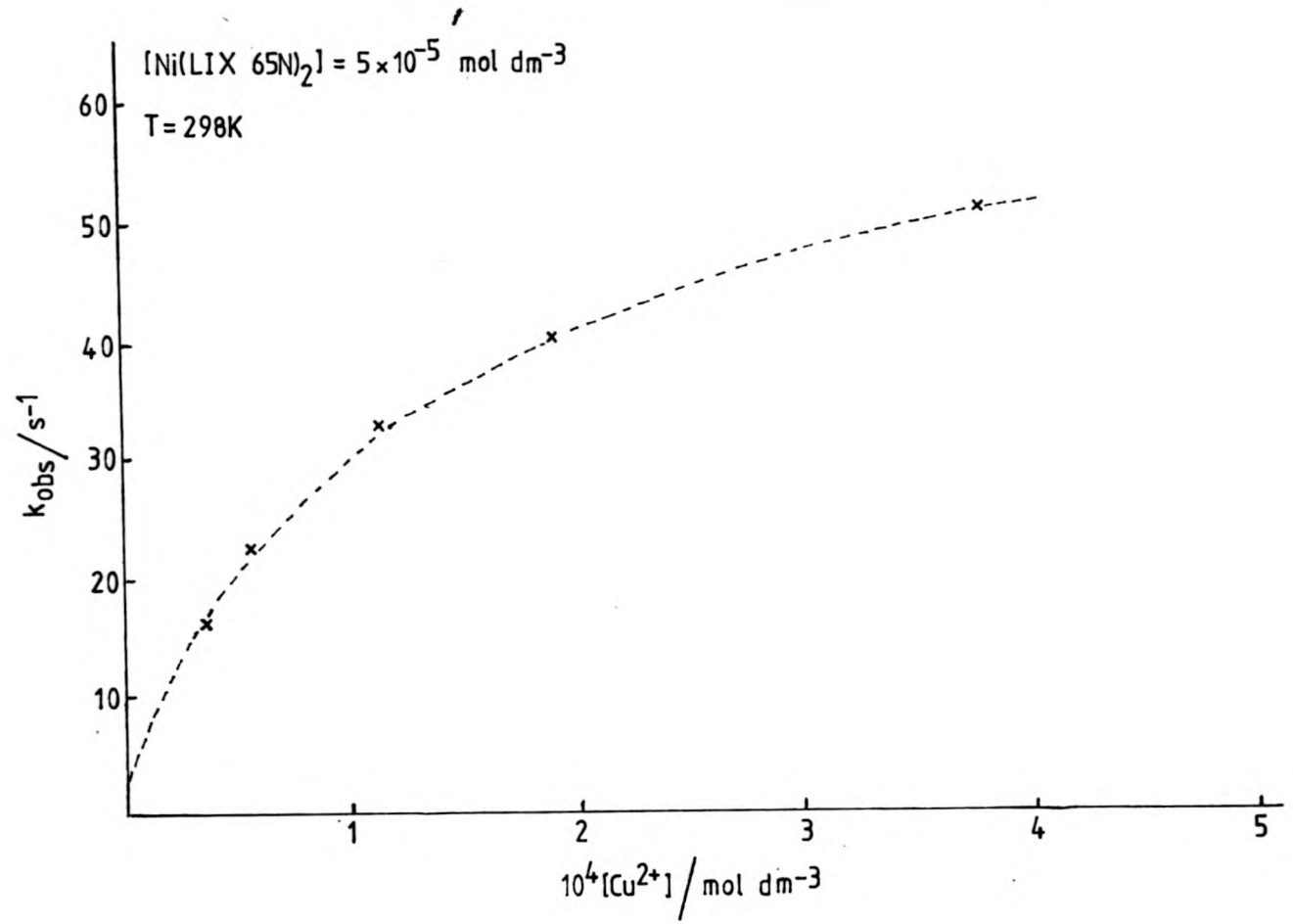

five first-order rate constants shown in Figure 3.11. could be determined accurately. The implications of this non-linear dependence on $[Cu^{2+}]$ are discussed later.

The dependence of the second stage of the reaction on $[Cu^{2+}]$ is shown in Figure 3.12.. As can be seen this reaction stage shows a linear dependence on the concentration of copper(II), under pseudo-first-order conditions. This would indicate that this step occurs by way of a normal second-order reaction.

The third stage of the metal exchange reaction again shows a dependence on copper(II) concentration but as pseudo-first-order conditions are approached the observed rate constant tends towards a limiting value. Again the small absorbance changes observed for this reaction stage did not allow accurate determinations of rate constants to be made under pseudo-first-order conditions and thus values of this parameter determined as such are not included in Figure 3.13.. However, these values did tend to support the postulation of a constant value for this rate constant. Thus in the pres ence of excess Cu^{2+} ion the third stage can be concluded to be zero-order with respect to copper(II) concentration.

Discussion.

Before discussing the observations described above it is useful to briefly summarise the results of studies that have been made for similar reactions. In investigations of the copper(II) induced decomposition of nickel(II) complexes of some tetradentate Schiff bases derived from salicylaldehyde and substituted ethylenediamines with cis-$[N_2O_2]$ donor atom sets, in DMSO solution,

Figure 3.12. Variation of k_{obs} with $[Cu^{2+}]$ for second stage of metal exchange reaction

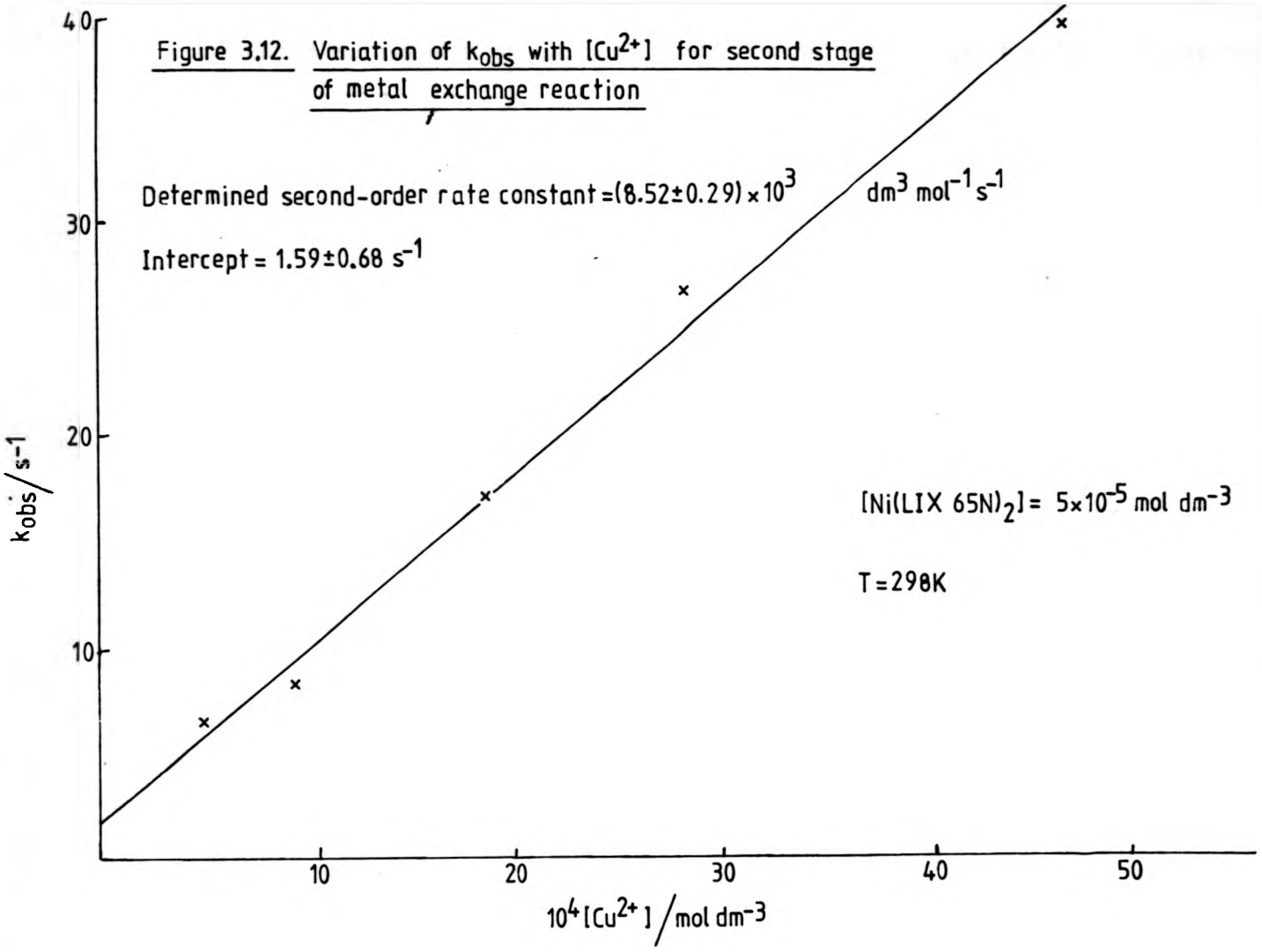

Figure 3.13. Variation of k_{obs} with $[Cu^{2+}]$ for the third stage of metal exchange reaction

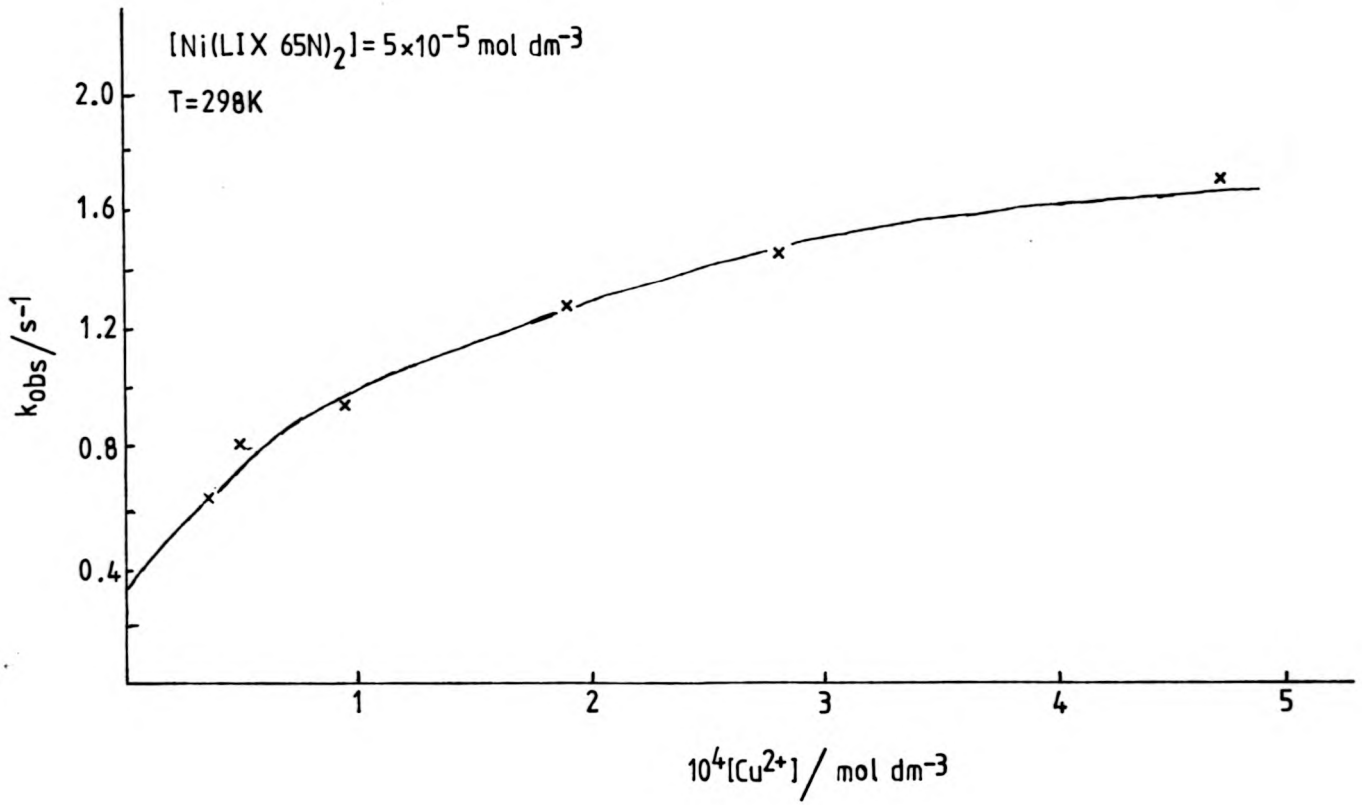

Fee et al [207,208] have observed only one reaction step. The reaction is found to be first-order with respect to both concentration of nickel(II) complex and copper(II). The mechanism which has been deduced from these observations is as follows.

$$Ni(complex) + Cu^{2+} \overset{K}{\rightleftharpoons} CuNi(complex)^{2+} \qquad (3.23)$$

$$CuNi(complex)^{2+} \xrightarrow{k_2} Cu(complex) + Ni^{2+} \qquad (3.24)$$

The rate determining step is believed to be the dissociation of the dinuclear complex. From evidence that suggests that polynuclear association occurs with these complexes, it is suggested that the dinuclear intermediate species has a structure which can be represented as such:

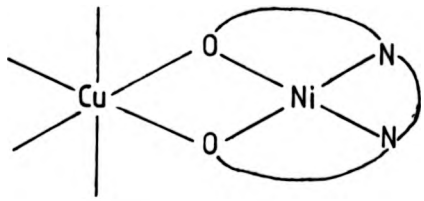

These workers have also investigated the effect of altering the substituents on the bridging alkyl chain in these complexes on the rate of the metal exchange reaction. It was found that when methyl groups are substituted on this bridging chain that a retardation of the rate of dissociation occurs. It is suggested that this substitution hinders the Ni-N bond cleavage and also the Cu-N bond formation process.

In a study of a similar reaction involving copper(II) exchange by the technique of isotopic exchange, Elias and co-workers [209,210] have found a similar mechanism to operate. Again

it is assumed that it is the metal to oxygen linkage which is ruptured initially with the formation of a dinuclear intermediate. By performing similar substitution experiments to those described above in altering the nature of the bridging alkyl chain it was again found that increased steric effects slowed the rate of copper(II) exchange. This was suggested to be evidence for a dinuclear intermediate in the sense that the increased bulkiness of the substituent hinders the rotation around the C-C bond of the ethylenediamine linkage. Again only one reaction step was found and the rate law and mechanism derived are as follows:

$$\text{Rate} = k[\text{Cu(complex)}][Cu^{2+}] \qquad (3.25)$$

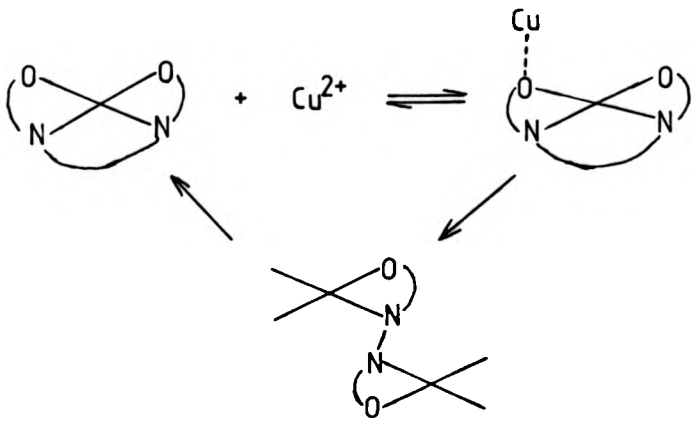

Wannowius et al [211-213] again using the technique of isotopic exchange have investigated both the metal exchange reaction and the ligand exchange reaction for a series of copper(II) complexes of salicylaldimine ligands. Again the mechanism suggested is that involving a dinuclear intermediate, with breaking of the Cu-O linkage as the first stage of the reaction. One point of

interest is that in the ligand exchange reaction [212] it is found that a rate law of the type described by equation (3.26) operates.

$$\text{Rate} = (k_s + k_{lig}[\text{ligand}])[\text{complex}] \qquad (3.26)$$

k_s is the rate constant for a solvent-assisted exchange pathway. The reaction was performed using toluene as the solvent and the rate constant for the solvent-assisted pathway was found to be dependent on the concentration of residual water in the toluene solvent. An investigation of the activation parameters for the reaction for both exchange pathways revealed that the observed trends could be explained by an associative mechanism.

Considering now the reaction that has been studied in this work it seems somewhat surprising, if mechanisms of the type described above are applicable, that three distinct reaction stages should be observed. It must be assumed, therefore, that the mechanism is in some way different to those previously observed. The first stage in the metal exchange reaction has a non-linear dependence on the concentration of copper(II) and also gives rise to first-order kinetic plots under non-pseudo-first-order conditions. These observations would indicate that for this step a mechanism is operative which involves copper(II) but in which no consumption of copper(II) occurs in the overall reaction. Referring now to the observed spectral changes in the rapid scanning spectrometric study described previously it was observed that no great change occurred at the lowest energy ligand band of the nickel(II) complex indicating that no great dissociation of the bis-complex occurs. The spectral changes observed at the

metal-to-ligand charge transfer band of the nickel(II) complex indicate that some disturbance of a metal-to-ligand bond has occurred. In view of this evidence the following mechanism for the first step of the metal exchange process can be postulated;

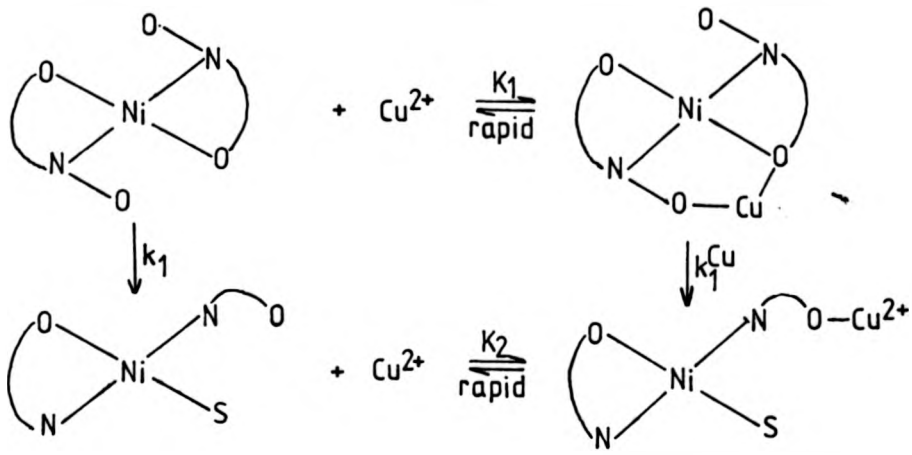

where A is the end product of the first stage. This reaction mechanism is consistent with the observations described above.

The rate of formation of A can be described by the following equation.

$$-\frac{d[A]}{dt} = -\left[\frac{d[NiL_2]}{dt} + \frac{d[I_1]}{dt}\right] = k_1[NiL_2] + k_1^{Cu}[I_1] \qquad (3.27)$$

Now

$$[I_1] = K_1[Cu^{2+}][NiL_2] \qquad (3.28)$$

Therefore

$$-\frac{d}{dt}[NiL_2]\left[1 + K_1[Cu^{2+}]\right] = (k_1 + k_1^{Cu}K_1[Cu^{2+}])[NiL_2] \qquad (3.29)$$

Hence

$$k_{obs} = \frac{k_1 + k_1^{Cu}K_1[Cu^{2+}]}{1 + K_1[Cu^{2+}]} \qquad (3.30)$$

Values of k_{obs} and $[Cu^{2+}]$ were fitted to equation (3.30) by use of the Fortran computer programme ITERAT (See Chapter 4) which allows a least squares analysis to be performed to any required function. This operation led to the derivation of values of the relevant constants shown below:

$$k_1 = (0.7 \pm 7)\ s^{-1}$$
$$K_1 = (8.0 \pm 0.4) \times 10^3\ dm^3\ mol^{-1}$$
$$k_1^{Cu}K_1 = (5.4 \pm 2.1) \times 10^5\ dm^3\ mol^{-1}\ s^{-1}$$

and subsequently the approximate value of 67 s^{-1} is derived for k_1^{Cu}.

At high concentrations of Cu^{2+} the situation will arise where $K_1[Cu^{2+}] \gg 1$ and under these conditions equation (3.30) reduces to

$$k_{obs} = k_1^{Cu} \qquad (3.31)$$

As can be seen from Figure 3.11. the value of k_{obs} in fact appears to tend towards a constant value which approximates to that determined above for k_1^{Cu}.

The value obtained for k_1 would indicate that the reaction pathway controlled by this rate constant is in fact a minor pathway and becomes relatively less important as the concentration of Cu^{2+} is increased.

The second stage of the metal exchange reaction is found to occur by way of a normal second-order rate law. The electronic spectral changes observed through the course of this reaction step show the loss of the lowest energy ligand band of the nickel(II) bis-complex as well as formation of the copper(II)-to-ligand charge transfer band. Thus ligand loss from $[Ni(LIX\ 65N)_2]$ and copper-to-ligand bond formation is occurring. The following mechanism is postulated for this reaction stage (S = MeOH):

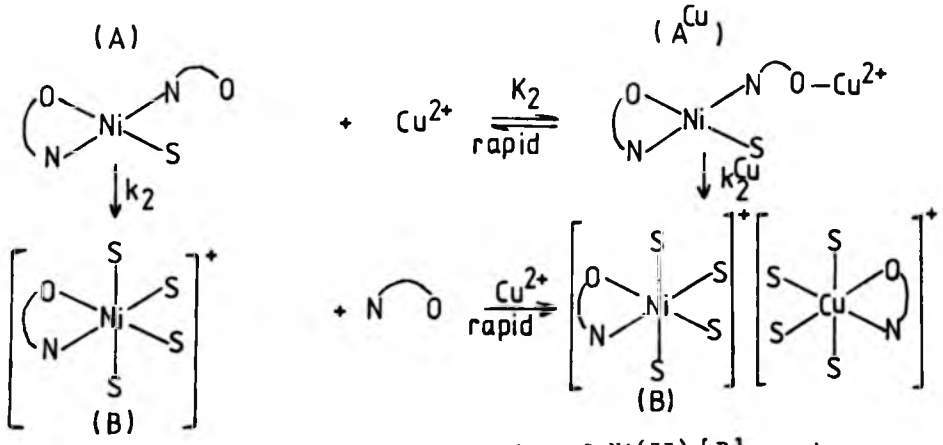

The rate of formation of the mono-complex of Ni(II), [B], can be described by the following equation.

$$\frac{d[B]}{dt} = k_2[A] + k_2^{Cu}[A^{Cu}] = \frac{-d([A] + [A^{Cu}])}{dt} \qquad (3.32)$$

Now $$K_2 = [A^{Cu}] / [A][Cu^{2+}] \quad (3.33)$$

Therefore

$$-\frac{d}{dt}[A](1 + K_2[Cu^{2+}]) = (k_2 + k_2^{Cu}K_2[Cu^{2+}])[A] \quad (3.34)$$

and

$$k_{obs} = \frac{k_2 + k_2^{Cu}K_2[Cu^{2+}]}{1 + K_2[Cu^{2+}]} \quad (3.35)$$

If the assumption is made that $K_2[Cu^{2+}] \ll 1$ at relatively low concentrations of Cu^{2+} the above equation reduces to:

$$k_{obs} = k_2 + k_2^{Cu}K_2[Cu^{2+}] \quad (3.36)$$

Thus in the plot of k_{obs} against $[Cu^{2+}]$ for this reaction stage, as shown in Figure 3.12., the value of the slope corresponds to $k_2^{Cu}K_2$ and the intercept to k_2.

As concentration of copper(II) is increased further the value of $K_2[Cu^{2+}]$ will also increase and thus a deviation from linearity of the plot in Figure 3.12. may be expected.

The observed first-order rate constants for the third stage of the metal exchange reaction again show a non-linear dependence on $[Cu^{2+}]$ and the first-order kinetic plots are again observed under non-pseudo-first-order conditions. Thus a mechanism similar to that proposed for the first reaction step is assumed to be operative. The electronic spectral changes observed for this stage indicate the formation of the final product, namely

$[Cu(LIX\ 65N)_2]$. For this third stage there are two possible copper(II) species that can react with the nickel(II) mono-complex of LIX 65N formed during the second stage of the metal exchange reaction. These are, firstly, the copper(II) mono-complex of LIX 65N which is also formed during the second stage of the reaction and, secondly, the copper(II) hexasolvate. The former copper(II) species will be important at low concentrations of Cu^{2+} and the latter will become increasingly more important as $[Cu^{2+}]$ becomes larger. A general mechanism can thus be postulated, as shown below, where the reacting Cu(II) species can be either of those described above.

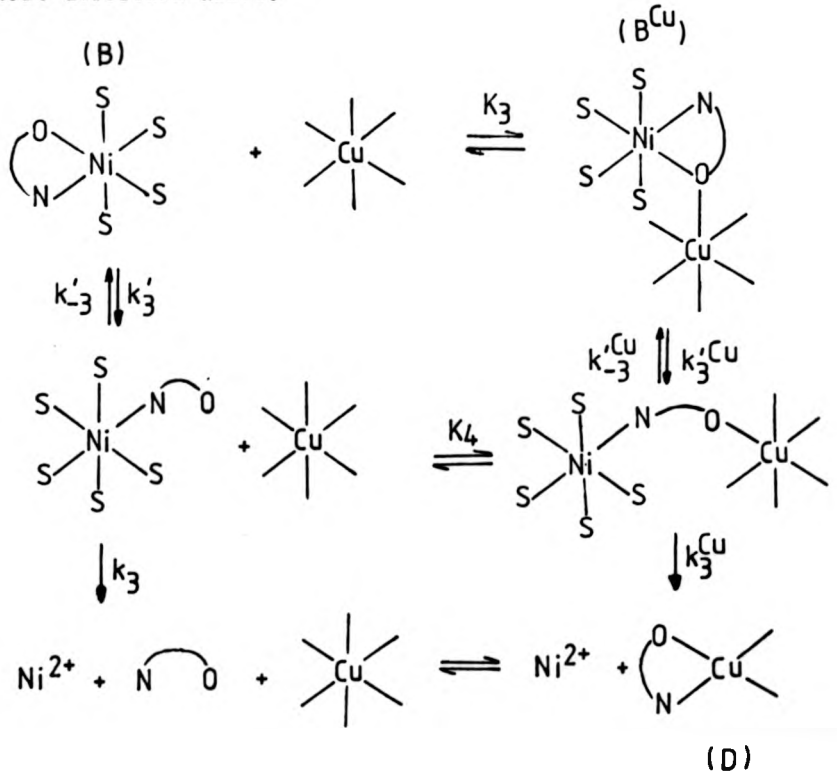

When the reacting Cu(II) species is the mono-complex of LIX 65N then the product of the above reaction scheme, labelled as D, is of course the copper(II) bis-complex. However, when the copper(II) hexasolvate is the reacting species the following two steps must be added to the above mechanism to achieve formation of the desired bis-complex.

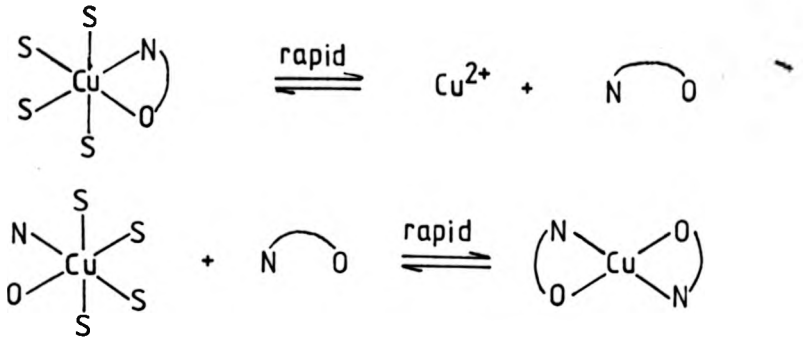

The rate law pertaining to the general mechanism is derived as follows:

$$\text{Rate} = k_3[C] + k_3^{Cu}[C^{Cu}] = (k_3 + k_3^{Cu}K_4[Cu^{2+}])[C] \qquad (3.37)$$

Applying the steady-state approximation to (C) and (C^{Cu}), which are in rapid equilibrium with each other, yields

$$(k_3' + k_3'^{Cu}K_3[Cu^{2+}])[B] = (k_3 + k_{-3}')[C] + (k_3^{Cu} + k_{-3}'^{Cu})[C^{Cu}]$$

$$= \left[(k_3 + k_{-3}') + (k_3^{Cu} + k_{-3}'^{Cu})K_4[Cu^{2+}]\right][C] \qquad (3.38)$$

Therefore from equation (3.37)

$$\text{Rate} = \frac{(k_3 + k_3^{Cu}K_4[Cu^{2+}])(k_3' + k_3'^{Cu}K_3[Cu^{2+}])[B]}{(k_3 + k_3') + (k_3^{Cu} + k_{-3}'^{Cu})K_4[Cu^{2+}]} \qquad (3.39)$$

$$= \frac{-d}{dt}([B] + [B^{Cu}]) = \frac{-d}{dt}[B](1 + K_3[Cu^{2+}]) \qquad (3.40)$$

Hence

$$k_{obs} = \frac{(k_3 + k_3^{Cu}K_4[Cu^{2+}])(k_3' + k_3'^{Cu}K_3[Cu^{2+}])}{(1 + K_3[Cu^{2+}])\left[(k_3 + k_{-3}') + (k_3^{Cu} + k_{-3}'^{Cu})K_4[Cu^{2+}]\right]} \qquad (3.41)$$

This equation reduces to the form

$$k_{obs} = \frac{a + b[Cu^{2+}] + c[Cu^{2+}]^2}{1 + d[Cu^{2+}] + e[Cu^{2+}]^2} \qquad (3.42)$$

$$a = k_3k_3'$$
$$b = (k_3k_3'^{Cu}K_3 + k_3^{Cu}k_3'K_4)$$
$$c = k_3^{Cu}k_3'^{Cu}K_3K_4$$
$$d = \left[(k_3^{Cu} + k_{-3}'^{Cu})K_4 + (k_3 + k_{-3}')K_3\right]$$
$$e = K_3K_4(k_3^{Cu} + k_{-3}'^{Cu})$$

The values of k_{obs} and $[Cu^{2+}]$ for this metal exchange reaction step were fitted to the above equation (3.42) by use of the Fortran computer programme ITERAT and it was found that the values of the constants c and e were undefined and are therefore assumed to be negligible. Thus equation (3.42) reduces to the form;

$$k_{obs} = \frac{a + b[Cu^{2+}]}{1 + d[Cu^{2+}]} \qquad (3.43)$$

On fitting the values of k_{obs} and $[Cu^{2+}]$ to this reduced form of equation (3.42) the following values of the above constants were obtained.

$$a = 0.38 \pm 0.06$$

$$b = (1.00 \pm 0.17) \times 10^4$$

$$d = (4.43 \pm 1.01) \times 10^3$$

At high concentrations of Cu^{2+} equation (3.43) will reduce to the form:

$$k_{obs} = b/d \qquad (3.44)$$

This would indicate a constant value of k_{obs} of approximately 2.25 s^{-1} at high concentrations of Cu^{2+}. This is consistent with the trends shown in Figure 3.13..

3.6. Summary and Conclusions.

The metal complex formation reaction between Ni(II) and a series of aromatic hydroxyoxime ligands has been investigated in methanol solution. All the reactions studied appear to proceed by way of the I_d mechanism which is the accepted mechanism of substitution at nickel(II). The outer-sphere complex that is formed initially in these reactions is found to be that between the metal solvate ion and the neutral ligand molecule. The rate determining step in these reactions is that of formation of the

first metal-to-ligand bond which is believed to be a metal to oximino nitrogen bond.

It has been found that the long alkyl chain substituted in the para-position to the phenolic oxygen atom in the commercial liquid-liquid extractants LIX 65N and LIX 70 has a retarding effect on the rate of nickel(II) complex formation. The complex formation rate for LIX 70 is found to be slower than that for the corresponding reaction of LIX 65N as a result of substitution of a chlorine atom in the 3-position of this molecule, which reduces its pK_a and hence the outer sphere association constant, K_o, in the I_d mechanism.

When a variation is made of the oximino carbon substituent it is found that substitution of a phenyl or methyl group for a hydrogen atom leads to an increase in the rate of complexation to approximately the same extent.

In the plots of k_{obs} versus [ligand] determined for these complexation reactions a positive intercept is found. The nature of this intercept is believed to be a measure of the rate at which the bis-complexes dissociate. The value of this rate constant, as well as being dependent on the electronic properties of the ligand, is also found to be dependent on the bulkiness of the ligands. It is found that the most bulky ligands dissociate the most rapidly even when electronic factors would suggest otherwise.

An investigation of the rate of complex formation of $[Co(LIX\ 65N)_2]$ reveals that the reaction rate is determined by the rate of methanol exchange on the cobalt(II) centre. This again suggests the I_d mechanism to be operative in this reaction. It is found that the formation reaction of this cobalt(II) complex

is followed by a slower first-order oxidation/oxygenation reaction. This reaction rate is found, as would be expected, to be independent of ligand concentration. The nature of the reaction product has not, however, been investigated.

The rate of complexation of LIX 65N by copper(II) is found to be too fast to measure by conventional stopped-flow methods.

An investigation of the dissociation of the nickel(II) bis-complex of LIX 65N induced by the prescence of copper(II) reveals three distinct reaction stages. It is suggested that in the first stage of dissociation of $[Ni(LIX\ 65N)_2]$ association of copper(II) occurs inducing a cleavage of a nickel(II) to phenolic oxygen bond after which the copper(II) is rapidly lost. The second stage of this metal exchange reaction involves association of copper(II) with the now partly dissociated $[Ni(LIX\ 65N)_2]$ complex resulting in the loss of one ligand molecule. The remaining ligand molecule is removed in the final reaction step by way of two possible pathways. At low concentrations of Cu^{2+} the reacting species is of the form $[Cu(LIX\ 65N)]^+$ whereas at higher values of $[Cu^{2+}]$ the reacting species is the copper(II) hexasolvate.

3.7. Experimental.

Chemicals and Solvents.

See Chapter 2.

Synthesis of Ligands.

See Chapter 2.

2-Hydroxy-5-methoxysalicylaldoxime.

This ligand was synthesised by reaction of 5-methoxysalicylaldehyde (Aldrich) with hydroxylamine hydrochloride (BDH). To 5-methoxysalicylaldehyde (5 g) was added sodium hydroxide (1.2 g) as a 40% solution in distilled water. On addition a yellow solid, the sodium salt of 5-methoxysalicylaldehyde, was precipitated. To this mixture was added 10 cm^3 of water containing hydroxylamine hydrochloride (2.05 g). The yellow solid dissolved and the solution was left to stir for approximately one hour. Dilute hydrochloric acid was then added in a dropwise fashion until the intense yellow colouration had disappeared. The resulting solution was stored at 0°C overnight which resulted in the precipitation of a pale yellow solid. This was isolated by filtration, dried and stored over P_2O_5 in a vacuum desiccator.

Analysis (C.H.N.) Calculated: C: 57.48%; H: 5.43%; N: 8.38%.

Found: C: 57.47%; H: 5.30%; N: 8.22%.

2-Hydroxy-5-nitrobenzophenone oxime.

This compound was prepared from the reaction of 2-hydroxy-5-nitrobenzophenone with hydroxylamine hydrochloride. The starting ketone was synthesised from the reaction of 2-hydroxybenzophenone with nitric acid in glacial acetic acid by the published method of Hrdlovic et al [214].

To 2-hydroxy-5-nitrobenzophenone (5 g) was added hydroxylamine hydrochloride (2 g) as a 75% aqueous solution. As the mixture was stirred sodium hydroxide (1.2 g) as a 40% aqueous solution was slowly added. This resulted in the formation of a yellow solution. This was left stirring overnight and then

dilute hydrochloric acid was added in a dropwise fashion until no further colour change could be observed. On standing at $0^{o}C$ for several hours a pale yellow solid was precipitated. This was recrystallised from toluene, dried and stored over P_2O_5 in a vacuum desiccator.

A ^{13}C n.m.r. spectrum (recorded under conditions as given in Section 2.5.) revealed that the resonance which is assigned (Chapter 2.) to the carbon atom in the para-position to the phenolic oxygen atom had shifted downfield and lay in the region where the bulk of the aromatic carbon atom resonances were found. This spectrum was found to correspond in all other aspects, very closely to that found for BENZOX. It was deduced that substitution of the nitro-group had been exclusively at the 5-position.

Analysis (C.H.N.) Calculated: C: 60.46%; H: 3.90%; N: 10.85%.

Found: C: 60.27%; H: 3.90%; N: 10.96%.

LIX 70.

This hydroxyoxime ligand was obtained from the commercial solvent LIX 70 (General Mills) by the method of Ashbrook [16]. The 'anti' isomer of this ligand was obtained as described for the corresponding isomer of LIX 65N (See Section 2.2.1.) as a white solid. Isomeric purity was determined by t.l.c..

Metal Complexes.

Metal salts.

Metal salts, where M = Ni(II), Co(II) and Cu(II) were prepared by reaction of the respective metal carbonate or oxide with hydrofluoroboric acid. An excess of metal carbonate or oxide

dilute hydrochloric acid was added in a dropwise fashion until no further colour change could be observed. On standing at 0°C for several hours a pale yellow solid was precipitated. This was recrystallised from toluene, dried and stored over P_2O_5 in a vacuum desiccator.

A ^{13}C n.m.r. spectrum (recorded under conditions as given in Section 2.5.) revealed that the resonance which is assigned (Chapter 2.) to the carbon atom in the para-position to the phenolic oxygen atom had shifted downfield and lay in the region where the bulk of the aromatic carbon atom resonances were found. This spectrum was found to correspond in all other aspects, very closely to that found for BENZOX. It was deduced that substitution of the nitro-group had been exclusively at the 5-position.

Analysis (C.H.N.) Calculated: C: 60.46%; H: 3.90%; N: 10.85%.

Found: C: 60.27%; H: 3.90%; N: 10.96%.

LIX 70.

This hydroxyoxime ligand was obtained from the commercial solvent LIX 70 (General Mills) by the method of Asnbrook [16]. The 'anti' isomer of this ligand was obtained as described for the corresponding isomer of LIX 65N (See Section 2.2.1.) as a white solid. Isomeric purity was determined by t.l.c..

Metal Complexes.

Metal salts.

Metal salts, where M = Ni(II), Co(II) and Cu(II) were prepared by reaction of the respective metal carbonate or oxide with hydrofluoroboric acid. An excess of metal carbonate or oxide

was used and on completion of the reaction the resulting solution was filtered and evaporayed with a rotary evaporator until precipitation commenced. On storing at $0^{o}C$ for several hours the resulting hydrated solids were isolated and pumped to dryness on a vacuum line.

Metal solvates.

All metal methanolates were prepared by the method of Van Ingen Schenau [190] using trimethyl orthoformate as the dehydrating agent for the metal fluoroborate hydrates. All solid metal solvates were found to have a co-ordination number of six by complexiometric titration and/or atomic absorption spectroscopy. All metal solvates were stored as solutions in anhydrous methanol.

Instrumentation.

For electronic spectra, ^{13}C n.m.r. spectra and microanalysis see Chapter 2.

Atomic absorption spectroscopy.

Atomic absorption spectroscopy was carried out with a Varian AA6 spectrometer. Three standard solutions were used to calibrate the instrument for each element that was estimated.

Single wavelength U.V.-visible stopped-flow spectrophotometry.

All single wavelength stopped-flow studies were performed using an apparatus that has been described previously [215]. In these studies temperature was kept at 298.2K by a thermostating bath attached to the flow apparatus, which was controlled by a Grants Instruments temperature control unit.

Kinetic plots were obtained either as a direct output on to a Servoscribe chart recorder or if a rapid reaction via a DataLab transient recorder DL905 on to the same chart recorder.

First-order rate constants were determined by use of the Algol computer programme SFTEST.

Rapid scanning spectrometry.

Rapid scanning spectrometric studies were performed using an Applied Photophysics multiplex spectrometer. Photographs were taken of traces recorded onto a Tektronix 5115 storage oscilloscope. This technique is discussed more fully in Appendix A.

CHAPTER 4.

A STUDY OF SOME DONOR SOLVENT INTERACTIONS

WITH METAL(II) IONS.

4.1. Introduction.

The four co-ordinate square-planar metal complexes of Co(II), Ni(II) and Cu(II) with salicylaldimine ligands are well known to form adducts of both five and six co-ordinate geometry in donor solvents (See Introductory Chapter). Such adducts are also well known for the nickel(II) complex of salicylaldoxime. In view of this it would be expected that the corresponding complexes of the hydroxyoxime commercial liquid-liquid extractants also form such adducts. Indeed it has been reported [216] that ammonia is co-extracted with nickel(II) by the extractant SME 529. This observation, however, has been disputed by Hosking and Rice [24] who found that no extraction of ammonia with nickel(II) by the extractants P50, LIX 65N and SME 529 occurred. It was decided therefore to investigate the ability of such complexes to form adducts and the results of this study is the main subject of this chapter.

The known behaviour of the complexes of salicylaldoxime in this respect is once again a useful reference. By far the largest number of investigations of the complexes of this ligand and their ability to form adducts has been with the complex $[Ni(SALO)_2]$ and its interaction with pyridine (py). This behaviour was first discovered by Willis and Mellor [95] and a subsequent study of this phenomenon by Csaszar [94] has revealed that the adduct is of the formulation $[Ni(SALO)_2(py)_2]$. Various other adducts of this complex have been reported [21,114,115] and all are found to be of the same stoichiometry except the corresponding adduct formed with 2-methylpyridine. This adduct has been found to exhibit different electronic spectral properties to the normal

hexa-co-ordinate bis-adducts and in view of the work of Lindoy and Mockler [126] with a similar adduct it seems most likely that a penta-co-ordinate adduct is formed in this instance.

Csaszar and Szeghalmi [21] have performed variable temperature electronic spectral studies on the behaviour of the bis-adducts of $[Ni(SALO)_2]$ and found a temperature dependent equilibrium of the type shown below to exist

$$\underset{\text{diamagnetic}}{Ni(SALO)_2} + 2B \rightleftharpoons \underset{\text{paramagnetic}}{Ni(SALO)_2(B)_2} \qquad (4.1)$$

where B is the respective nitrogen donor solvent. From these studies thermodynamic parameters for the equilibrium process have been evaluated for a number of adducts.

Only studies of the thermodynamics of this equilibrium have been performed with $[Ni(SALO)_2]$. No kinetic studies of the donor solvent exchange processes have been reported. Such kinetic studies are of interest and have been performed with related nickel(II) complexes again with a variety of donor solvents. The most commonly employed technique to investigate these kinetic phenomena has been that of ^1H n.m.r. line broadening [217-219] although ^{14}N n.m.r. [220,221] and more recently ^{13}C n.m.r. [222] techniques have also proven very useful for this type of study.

The work reported here involves the study of alkylamine exchange on the nickel(II) complex of the hydroxyoxime ligand BENZOX, which is very closely related to the commercial extractant LIX 65N, by ^{13}C n.m.r. line broadening methods. The corresponding equilibrium of the type shown above (4.1) has also been studied

and the thermodynamics of such processes investigated.

In this chapter are collected related studies of other solvent interaction processes which are continuations of previous work performed in these laboratories. These phenomena have also been investigated by n.m.r. methods. The first such study is that of the equilibrium process which exists in solutions of the nickel(II) complex of the ligand 1,4,8,11-tetramethyl-1,4,8,11-tetra-azacyclotetradecane (TMC) in the donor solvent N,N-dimethylformamide (DMF). This investigation is a continuation of previous studies [223] of the interactions of such donor solvents with metal complexes of macrocyclic ligands and is one of a series of similar studies [224] which have been performed to investigate the relative stabilities of the adducts formed with this complex in donor solvents.

The temperature dependence of the rate of methanol exchange with the $[Zn(MeOH)_6]^{2+}$ ion has also been investigated. This system has been studied previously by other workers [225]. However, the value of the activation energy has been found to vary with the concentration of the solute as a result of co-ordination of perchlorate anion at higher concentrations of zinc(II). This study has been performed employing the tetrafluoroborate as the counter anion to investigate the relative co-ordinative abilities of BF_4^- and ClO_4^-, and hopefully derive more accurate values of the activation parameters associated with methanol exchange on the hexasolvate species. These results were required for comparison with metal complex formation studies involving the $[Zn(MeOH)_6]^{2+}$ ion [226].

4.2. A Study of the Interaction of some Alkylamines with $[Ni(BENZOX)_2]$.

Initial studies of the interaction of amine ligands with $[Ni(BENZOX)_2]$ were performed using n-butylamine ($BuNH_2$). This alkylamine was chosen in preference to ammonia which is the most important amine as far as industry is concerned, for several reasons. Firstly, n-butylamine is a liquid, unlike ammonia, with a boiling point of 375.3K which renders experimental manipulation at room temperatures somewhat more practical. Secondly if ammonia is used, when n.m.r. studies of the solvent exchange process are performed, either by studying the ^{15}N or ^{1}H nucleus, only one resonance will be observed for the amine. In the case of n-butylamine, however, four resonances are observed in the ^{13}C n.m.r. spectrum. This enables possible multiple analyses to be performed on the observed spectral changes with respect to the amine ligand i.e. the four resonances can be considered separately and hence a more accurate evaluation of the parameters associated with this exchange process may also be possible.

Before commencing any kinetic studies it is essential to know the nature of the species which are involved in the exchange process i.e. the nature of the adduct formed, if indeed any formation of adduct occurred. To investigate this, the complex $[Ni(BENZOX)_2]$ was dissolved in a solution of neat amine, at which point it was noted that a distinct colour change occurred. The intense dark green colour of the square-planar bis-complex was replaced with a pale yellow colour indicating that indeed adduct formation had occurred. Evaporation of the excess amine led to the isolation of a yellow/orange powdery solid. Electronic

spectra were recorded of a solution of this adduct dissolved in n-butylamine and distinct differences were observed between the spectra of this compound and the corresponding complex $[Ni(BENZOX)_2]$ as shown in Figure 4.1.. In the electronic spectrum of the above complex no absorbance bands are observed above 800 nm and up to 1500 nm. However, in the spectrum of the adduct an absorbance band is found at 930 nm. The absorbance band which is found in the spectrum of the bis-complex at 615 nm (Table 2.7.) is lost and a new band appears as a shoulder with a λ_{max} of around 530 nm. Extinction coefficients for these absorbance bands are given in Table 4.1..

Electronic transition	λ_{max} / nm	ε_M / $dm^3\ mol^{-1}\ cm^{-1}$
$^3T_{2g} \leftarrow {}^3A_{2g}$	930	10.4
$^3T_{1g}(P) \leftarrow {}^3A_{2g}$	530 sh	15.2

Table 4.1. Electronic solution spectral data for $[Ni(BENZOX)_2(^nBuNH_2)_2]$.

The observed spectrum of the adduct is typical of that found for a pseudo-octahedral nickel(II) species [93] and thus the two bands found for the adduct can be given the assignments shown in Table 4.1.. These observations indicate that the adduct formed with $BuNH_2$ is the bis-adduct in which both vacant co-ordination sites of the complex are occupied. Microanalysis results obtained for the solid compound (Section 4.5.) tend to support this hypothesis. In view of the fact that the complex $[Ni(BENZOX)_2]$ has been found to exist in a trans-square-planar geometry it would seem most

Figure 4.1. Electronic spectra from 0.025 mol dm^{-3} solutions of $[Ni(BENZOX)_2]$ in a)$CHCl_3$ b)$BuNH_2$

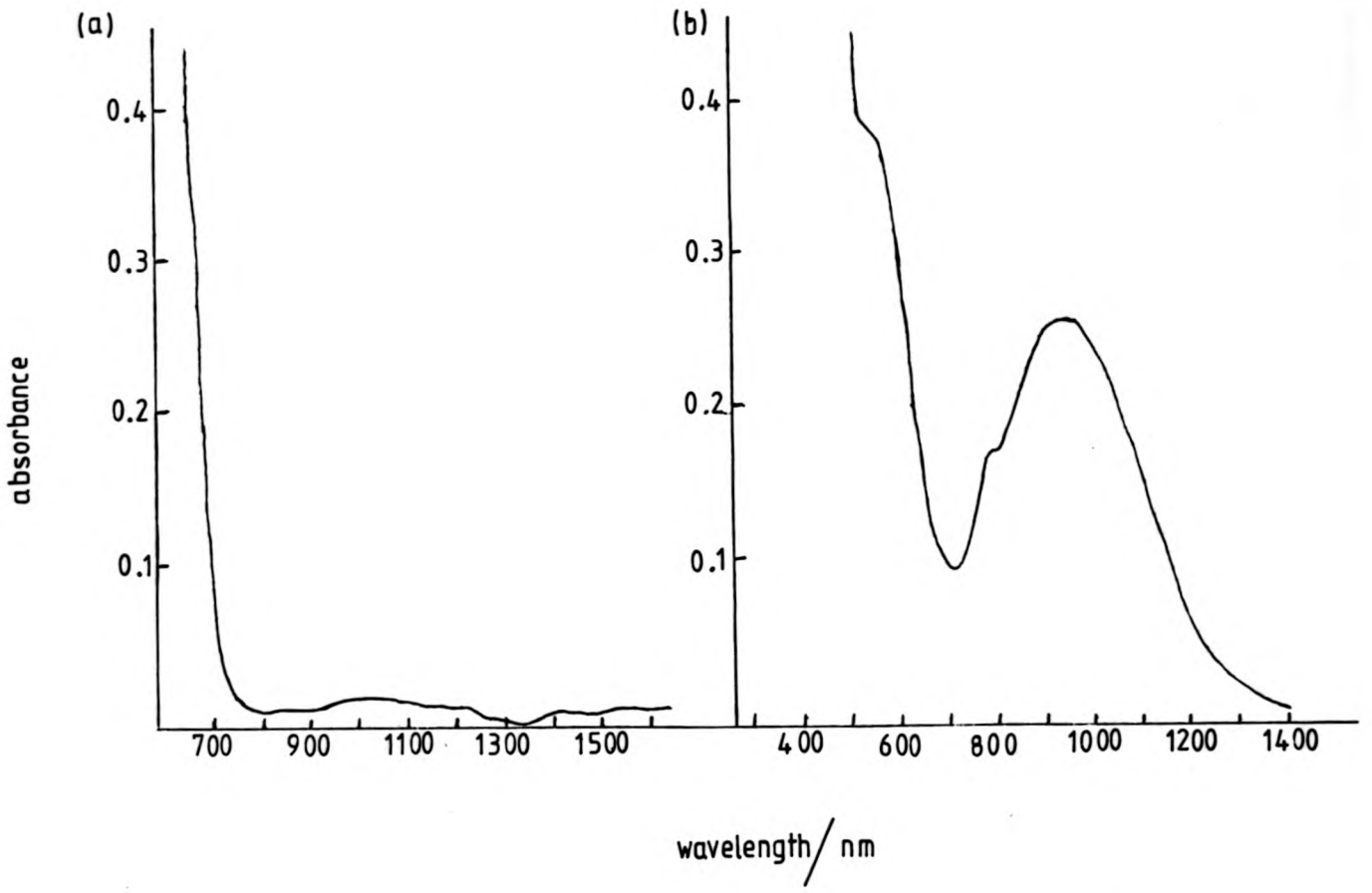

plausible that the two molecules of $BuNH_2$ will co-ordinate in a trans-fashion in the adduct. Thus any amine exchange process that occurs can be described by the scheme

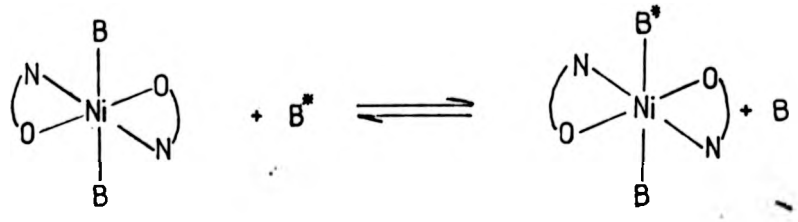

Initial investigations of this solvent exchange process were performed by monitoring the effect of temperature on the observed ^{13}C n.m.r. spectrum resulting from a solution of the above bis-adduct dissolved in excess $BuNH_2$ with ~10% $[^2H]_8$-toluene used as a lock sample. The above deuterated solvent was employed for this study as it does not compete for co-ordination to nickel(II) with the amine ligand and also allows a relatively wide temperature range to be monitored. Investigations were performed on a series of solutions containing various mole ratios of the three solution constituents and it was found that reasonable linewidth differences (1.1-73.7 Hz for β-carbon atom) could be attained by use of a solution containing a mole fraction of co-ordinated solvent, P_m, of 0.0138 (1.80 mol dm^{-3} excess amine, 1.24×10^{-2} mol dm^{-3} $[Ni(BENZOX)_2]$). The temperature dependence of the ^{13}C n.m.r. spectra resulting from such a solution is shown in Figure 4.2..

As can be seen very little broadening is observed to occur for the resonance resulting from the δ-carbon atom of $BuNH_2$

Figure 4.2. V.T. ^{13}C n.m.r. study of $BuNH_2$ on $[Ni(BENZOX)_2(BuNH_2)_2]$

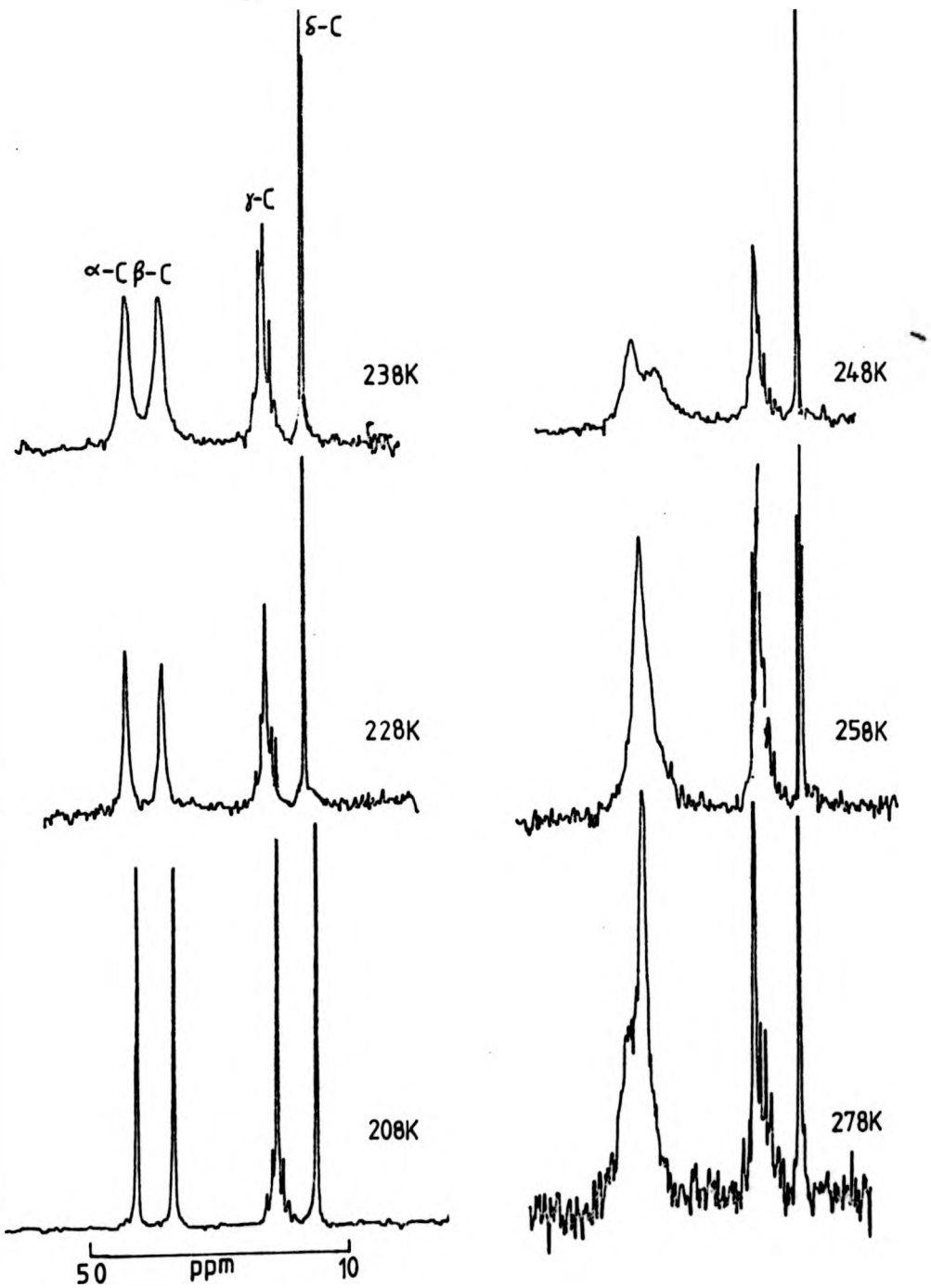

which is not surprising as this carbon atom is five atoms removed from the paramagnetic nickel(II) centre when co-ordinated. The largest linewidth changes are observed for those resonances closest to the co-ordination site i.e. the α- and β-carbons of $BuNH_2$, as would be expected.

The alkylamine n.m.r. line broadening induced by the paramagnetic nickel(II) centre can be expressed as such

$$1/T_{2p}P_m = (\Delta\nu_{obs} - \Delta\nu_{ref}) / P_m \qquad (4.3)$$

where $\Delta\nu_{obs}$ and $\Delta\nu_{ref}$ are the full linewidths at half maximum height of the alkylamine resonances and the reference solvent respectively in the presence of the paramagnetic ion. In this study values of $\Delta\nu_{ref}$ were obtained by performing a variable temperature ^{13}C n.m.r. study with a solution which contained the alkylamine and the lock solvent only in the same mole ratio as that used for obtaining values of $\Delta\nu_{obs}$ above and measuring the linewidths of all the four observed resonances at each temperature monitored. The function $(T_{2p}P_m)^{-1}$ is dependent on the solvent exchange lifetime (τ_m), the transverse relaxation time of the co-ordinated solvent nucleus (T_{2m}) and the difference in chemical shift between the free nucleus and that co-ordinated to the paramagnetic centre ($\Delta_{\omega m}$). These parameters were first related in a set of equations by Swift and Connick [168] and are given below

$$\frac{1}{T_{2p}} = \frac{1}{T_2} - \frac{1}{T_{2A}} = \frac{P_m}{\tau_m}\left[\frac{T_{2m}^{-2} + (T_{2m}\tau_m)^{-1} + \Delta_{\omega m}^{2}}{(T_{2m}^{-1} + \tau_m^{-1})^2 + \Delta_{\omega m}^{2}}\right] \qquad (4.4)$$

$$= \frac{P_m \Delta\omega_m}{(\tau_m/T_{2m} + 1)^2 + \tau_m^2 \Delta\omega_m^2} \qquad (4.5)$$

where T_2 is the observed relaxation time, T_{2A} is the relaxation time of bulk solvent and $\Delta\omega$ is the chemical shift for the free or coalesced signal relative to that of pure solvent. It has been usual practice to simplify these equations in several limiting exchange regions, including the high temperature region where exchange is faster than the n.m.r. time scale

$$1/T_{2p} = 1/T_{2m} P_m \qquad (4.6)$$

lower temperatures where the coalesced signal is exchange broadened

$$1/T_{2p} = \tau_m \Delta\omega_m^2 \qquad (4.7)$$

and at still lower temperatures where two well resolved but exchange broadened signals may be observed

$$1/T_{2p} = 1/\tau_m \qquad (4.8)$$

However it has recently been shown [182] that such approximations can lead to the determination of erroneous activation parameters, especially $\Delta S^{\ddagger}$, and that only use of the full Swift-Connick equations will give reliable values of $\Delta H^{\ddagger}$ and $\Delta S^{\ddagger}$. Thus throughout this work only the full version of these

equations has been used with computer fitting of observed line-widths and chemical shifts to equations (4.4) and (4.5).

The solvent exchange lifetime, τ_m, may be related to the pseudo-first order rate constant for exchange of a single solvent molecule, k_{ex}^I and its temperature dependence may be obtained from transition-state theory as such

$$k_{ex}^I = 1/\tau_m = \frac{k_B T}{h} \exp(\Delta S^{\ddagger}/R - \Delta H^{\ddagger}/RT) \qquad (4.9)$$

where k_B is Boltzmann's constant, h is Planck's constant and R is the universal gas constant.

To determine values of k_{ex}^I, $\Delta H^{\ddagger}$ and $\Delta S^{\ddagger}$ from the above equations the Fortran programme ITERAT has been used. This computer programme is a convential non-linear least squares programme which fits iteratively to any given function. A listing of this programme is given in Appendix C with the appropriate function for the Swift-Connick equations.

In Figures 4.3. and 4.4. are given both plots of effective chemical shift $(\Delta\omega_{obs}-\Delta\omega_{ref})$ and the function $\ln(1/T_{2p}P_m)$ versus temperature for the study of $BuNH_2$ exchange on the adduct $[Ni(BENZOX)_2(BuNH_2)_2]$ for the α- and β-carbon atom resonances of $BuNH_2$. It can be seen from these two Figures that the chemical shifts of these two carbon atoms have dependences on temperature which are of opposite sign. This results in these two resonances eventually becoming coincident at higher temperatures as demonstrated in the observed ^{13}C n.m.r. spectrum recorded at 258K and shown in Figure 4.2.. This fact renders determination of the line-widths for these two resonances very difficult at these temperatures

Figure 4.3. Dependence of linewidth and chemical shift for α-carbon of $BuNH_2$ on temperature

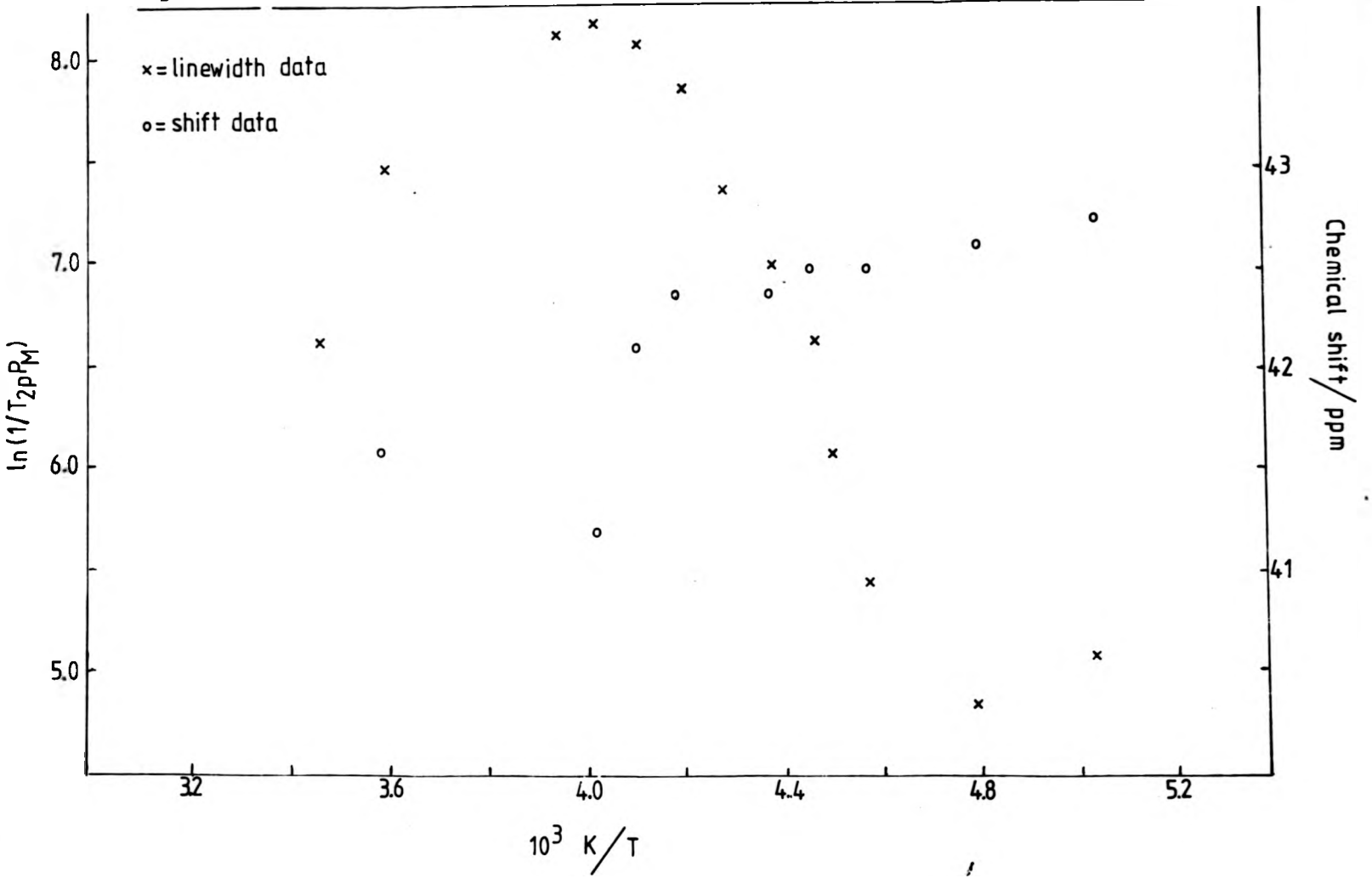

Figure 4.4. Dependence of linewidth and chemical shift for β-carbon of $BuNH_2$ on temperature

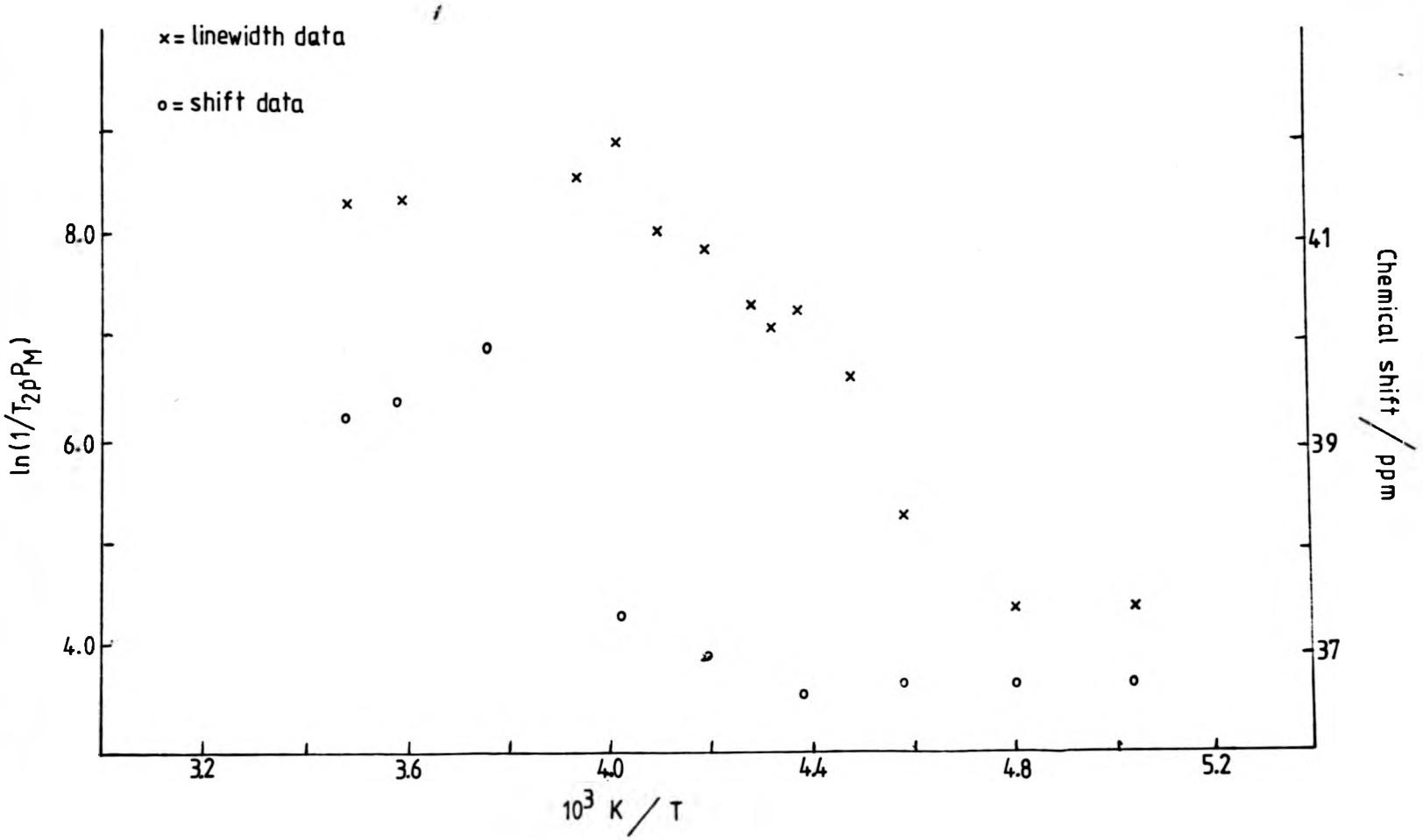

and thus only those linewidths and chemical shifts that could be determined with any accuracy are shown in Figures 4.3. and 4.4.. From Figure 4.2. it can be seen that the ^{13}C resonance resulting from the γ-carbon atom of $BuNH_2$ appears coincident with those resonances resulting from the methyl carbon atom of $[^2H]_8$-toluene. This unfortunate coincidence renders linewidth determinations for this resonance difficult. This γ-carbon atom which is four atoms removed from the metal co-ordination site displays much less dramatic linewidth and chemical shift changes than either the α- or β-carbon atoms of $BuNH_2$ and thus results in the determination of less accurate values of activation parameters. The added errors which occur as a result of the coincidence of the methyl resonances of $[^2H]_8$-toluene with this resonance render accurate determinations of the activation parameters for the solvent exchange process with data obtained for the γ-carbon resonance virtually impossible. Thus no analysis was attempted with this data relating to the γ-carbon resonance.

As might be expected the values of $\Delta H^{\ddagger}$ and $\Delta S^{\ddagger}$ obtained from a fit to the full Swift-Connick equations with these incomplete data sets are not very accurate. Indeed if both the chemical shift and linewidth data obtained are used in conjunction to determine activation parameters gross errors are found. Thus in Table 4.2. are given values of the activation parameters for the alkylamine exchange process determined from linewidth data only.

These values of $\Delta H^{\ddagger}$ and $\Delta S^{\ddagger}$, determined separately for each set of data from the two carbon atoms used in the analysis, are in reasonable agreement although possessing rather large errors.

and thus only those linewidths and chemical shifts that could be determined with any accuracy are shown in Figures 4.3. and 4.4.. From Figure 4.2. it can be seen that the ^{13}C resonance resulting from the γ-carbon atom of $BuNH_2$ appears coincident with those resonances resulting from the methyl carbon atom of $[^2H]_8$-toluene. This unfortunate coincidence renders linewidth determinations for this resonance difficult. This γ-carbon atom which is four atoms removed from the metal co-ordination site displays much less dramatic linewidth and chemical shift changes than either the α- or β-carbon atoms of $BuNH_2$ and thus results in the determination of less accurate values of activation parameters. The added errors which occur as a result of the coincidence of the methyl resonances of $[^2H]_8$-toluene with this resonance render accurate determinations of the activation parameters for the solvent exchange process with data obtained for the γ-carbon resonance virtually impossible. Thus no analysis was attempted with this data relating to the γ-carbon resonance.

As might be expected the values of $\Delta H^{\ddagger}$ and $\Delta S^{\ddagger}$ obtained from a fit to the full Swift-Connick equations with these incomplete data sets are not very accurate. Indeed if both the chemical shift and linewidth data obtained are used in conjunction to determine activation parameters gross errors are found. Thus in Table 4.2. are given values of the activation parameters for the alkylamine exchange process determined from linewidth data only.

These values of $\Delta H^{\ddagger}$ and $\Delta S^{\ddagger}$, determined separately for each set of data from the two carbon atoms used in the analysis, are in reasonable agreement although possessing rather large errors.

Linewidth data from carbon atom	$\Delta H^{\ddagger}$ / kJ mol^{-1}	$\Delta S^{\ddagger}$ / J K^{-1} mol^{-1}
α-	31.8 ± 4.2	45.4 ± 18
β-	30.3 ± 3.3	50.9 ± 17.6

Table 4.2. Activation parameters for $BuNH_2$ exchange on $[Ni(BENZOX)_2(BuNH_2)_2]$.

It was decided to repeat the above study using a different alkylamine ligand, to hopefully avoid the experimental difficulties found with the $BuNH_2$ system and improve upon the accuracy of the activation parameters thus determined. The alkylamine chosen for this second study was n-propylamine ($PrNH_2$). This ligand although having the disadvantage of a lower boiling point (336.9K) than $BuNH_2$ has the following advantages. The three resonances in the ^{13}C n.m.r. spectrum are separated by a larger chemical shift difference than the corresponding resonances of $BuNH_2$ [146]. Thus the observed coincidence of the resonances corresponding to the α- and the β-carbon atoms of $BuNH_2$ will occur at a higher temperature in the $PrNH_2$ system, if at all. Also none of the ^{13}C n.m.r. resonances of $PrNH_2$ are coincident with the methyl resonances of $[^2H]_8$-toluene and therefore the problem found in the case of $BuNH_2$ could be removed. Thus it should be possible to use the complete linewidth and chemical shift data for each of the three carbon atoms of this amine, to obtain values of the activation parameters for this solvent exchange process.

The $PrNH_2$ adduct of $[Ni(BENZOX)_2]$ was prepared in a similar manner to that described for the corresponding $BuNH_2$ adduct. Again a yellow/orange powder was isolated. The electronic

Linewidth data from carbon atom	$\Delta H^{\ddagger}$ / kJ mol^{-1}	$\Delta S^{\ddagger}$ / J K^{-1} mol^{-1}
α-	31.8 ± 4.2	45.4 ± 18
β-	30.3 ± 3.3	50.9 ± 17.6

Table 4.2. Activation parameters for $BuNH_2$ exchange on $[Ni(BENZOX)_2(BuNH_2)_2]$.

It was decided to repeat the above study using a different alkylamine ligand, to hopefully avoid the experimental difficulties found with the $BuNH_2$ system and improve upon the accuracy of the activation parameters thus determined. The alkylamine chosen for this second study was n-propylamine ($PrNH_2$). This ligand although having the disadvantage of a lower boiling point (346.9K) than $BuNH_2$ has the following advantages. The three resonances in the ^{13}C n.m.r. spectrum are separated by a larger chemical shift difference than the corresponding resonances of $BuNH_2$ [146]. Thus the observed coincidence of the resonances corresponding to the α- and the β-carbon atoms of $BuNH_2$ will occur at a higher temperature in the $PrNH_2$ system, if at all. Also none of the ^{13}C n.m.r. resonances of $PrNH_2$ are coincident with the methyl resonances of $[^2H]_8$-toluene and therefore the problem found in the case of $BuNH_2$ could be removed. Thus it should be possible to use the complete linewidth and chemical shift data for each of the three carbon atoms of this amine, to obtain values of the activation parameters for this solvent exchange process.

The $PrNH_2$ adduct of $[Ni(BENZOX)_2]$ was prepared in a similar manner to that described for the corresponding $BuNH_2$ adduct. Again a yellow/orange powder was isolated. The electronic

spectrum of this adduct recorded in neat $PrNH_2$ showed that the adduct formed was a high-spin pseudo-octahedral nickel(II) species (Table 4.3.).

Electronic transition	λ_{max} / nm	ϵ_m / $dm^3\ mol^{-1}\ cm^{-1}$
$^3T_{2g} \leftarrow {}^3A_{2g}$	930	9.6
$^3T_{1g}(F) \leftarrow {}^3A_{2g}$	530	15.0

Table 4.3. Solution electronic spectral data for $[Ni(BENZOX)_2(PrNH_2)_2]$.

This was confirmed by microanalysis of the solid adduct (Section 4.5.). Hence the species involved in the solvent exchange process was a bis-adduct of formulation $[Ni(BENZOX)_2(PrNH_2)_2]$.

Variable temperature ^{13}C n.m.r. spectra were recorded from a solution of this bis-adduct in $PrNH_2$ and $[^2H]_8$-toluene (~10%) as lock solvent. A mole fraction of bound solvent, P_m, of 0.0146 (1.79 mol dm^{-3} $[PrNH_2]$, 1.31×10^{-2} $[Ni(BENZOX)_2]$)was found to give reasonable linewidth changes (0.8 - 151.1 Hz for β-carbon atom) over the temperature range studied (195.2 - 309.2K). The observed spectral changes are shown in Figure 4.5.. As can be seen the three resonances resulting from $PrNH_2$ remain well separated up to 271K and no interference of the resonances resulting from the methyl carbon of the lock solvent occurs. Therefore, a full variable temperature study was performed with individual spectra being recorded at 5K intervals. Again a second identical experiment was performed using a solution of the free amine in the same deuterated solvent with the same mole

Figure 4.5. V.T. ^{13}C n.m.r. study of $PrNH_2$ on $[Ni(BENZOX)_2(PrNH_2)_2]$

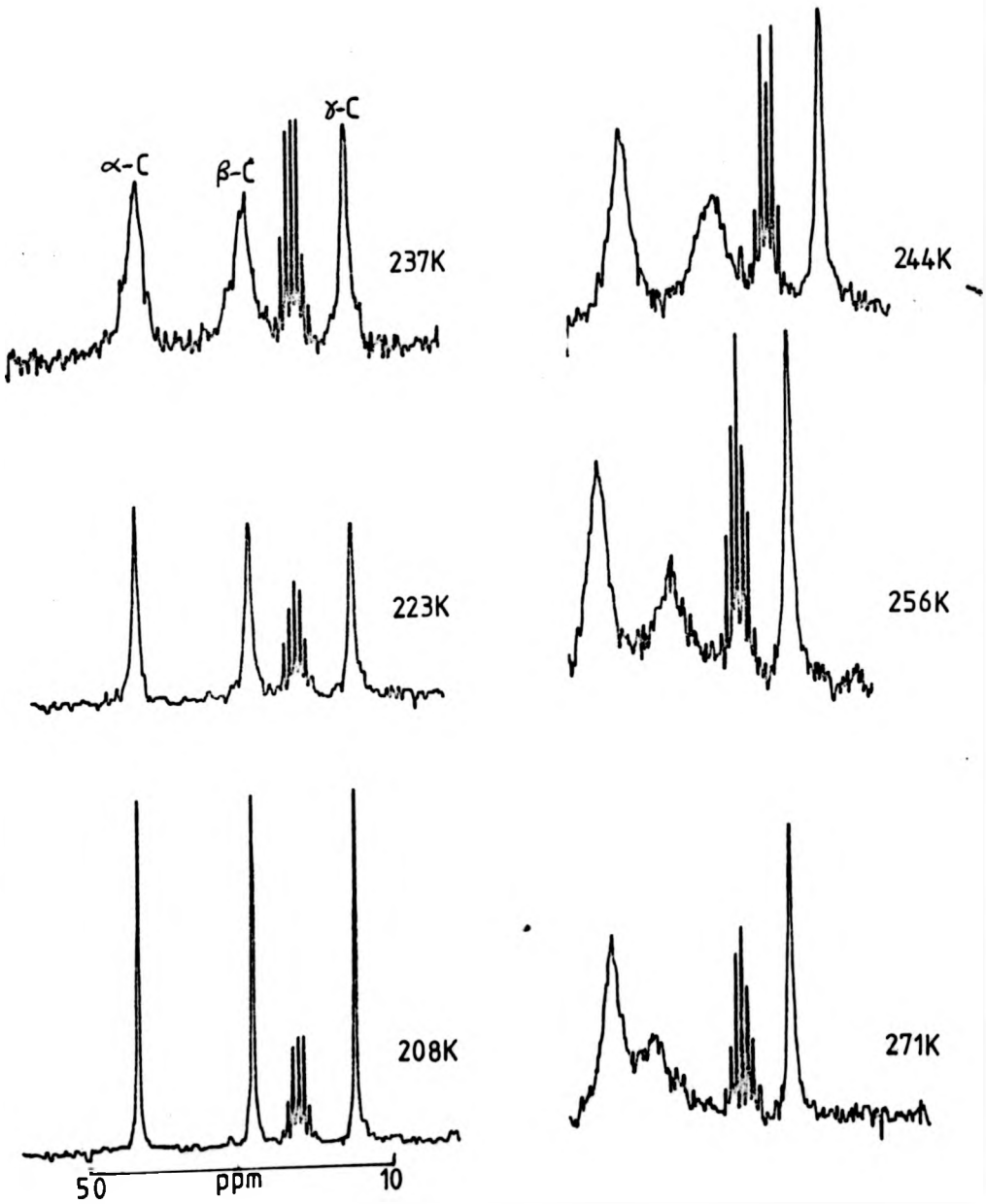

ratio as for the previous experiment with $PrNH_2$, thus enabling values of $\Delta\nu_{obs} - \Delta\nu_{ref}$ to be determined for all three $PrNH_2$ resonances. The resultant data sets are plotted as both chemical shift and $\ln(T_{2p}P_m)^{-1}$ versus reciprocal temperature in Figures 4.6. - 4.8..

Before actually determining values of the activation parameters for this solvent exchange process it was essential to investigate the nature of any equilibrium process of the type described previously (4.1) which may be expected to occur. This task was undertaken by way of a variable temperature U.V.-visible spectrophotometric study. By monitoring the concentration of six-co-ordinate species present as temperature was altered, equilibrium constants could be determined at each successive temperature. Enthalpy and entropy differences could thus be evaluated for the equilibrium process and in this way the amount of adduct present at any temperature could also be calculated. This determination is essential as any variation of P_m with temperature will alter the observed linewidths in the ^{13}C n.m.r. spectral study and thus affect the values of $\Delta H^{\ddagger}$ and $\Delta S^{\ddagger}$ to be calculated from the results of this experiment.

For this equilibrium study the most suitable absorption band to monitor is that resulting from the $^3T_{1g} \leftarrow {}^3A_{2g}$ transition at 930 nm in the electronic spectrum of the amine bis-adduct as it is well removed from any other absorption band. The monitoring of absorbance changes in this region of the spectrum is also advantageous as in this reportedly[119,120] stepwise type of equilibrium process any five-co-ordinate adduct formed will be characterised by the presence of a series of absorbance bands in

Figure 4.6. Dependence of linewidth and chemical shift for α-carbon of $PrNH_2$ on temperature

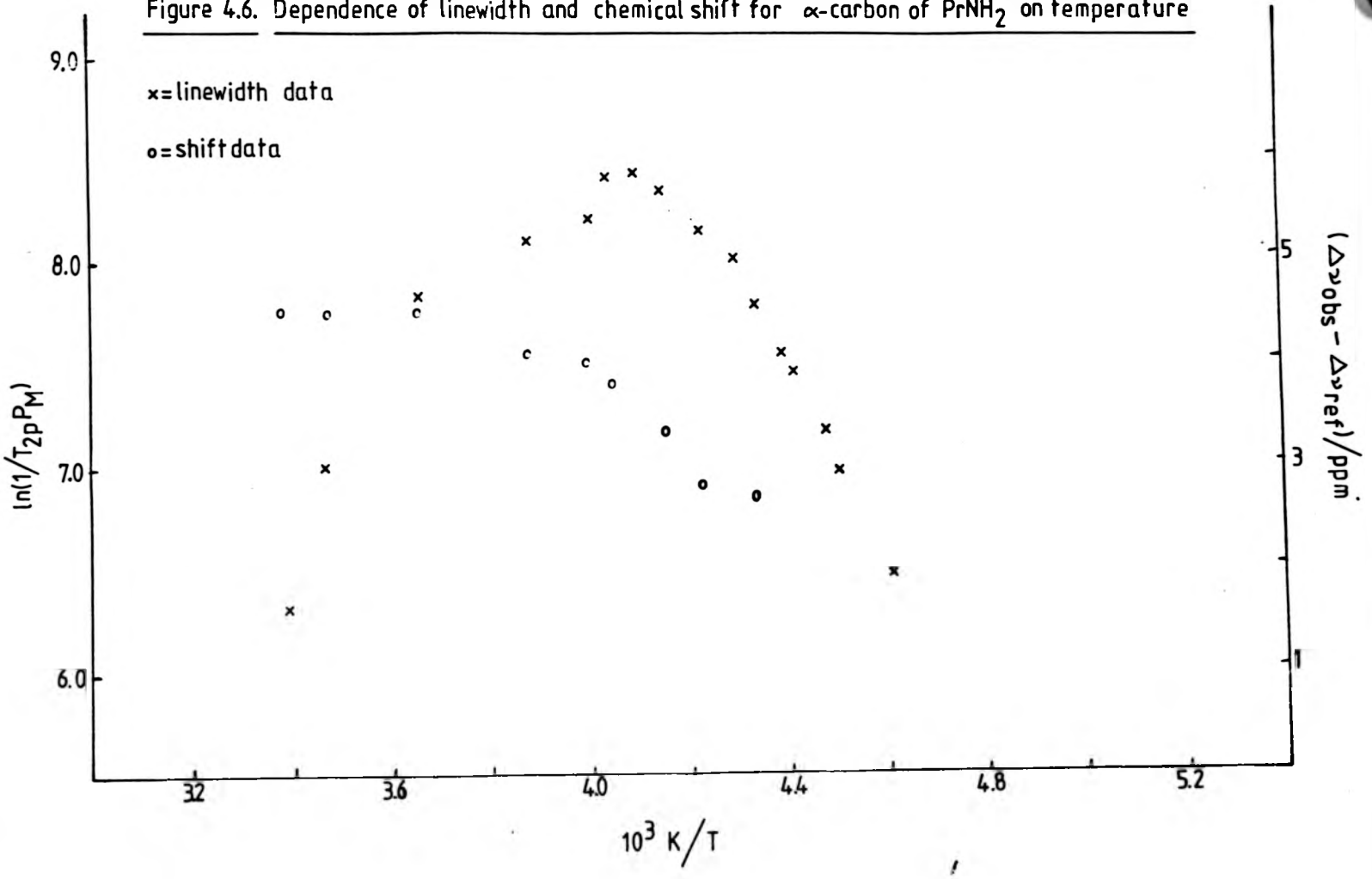

Figure 4.7. Dependence of linewidth and chemical shift for β-carbon of $PrNH_2$ on temperature

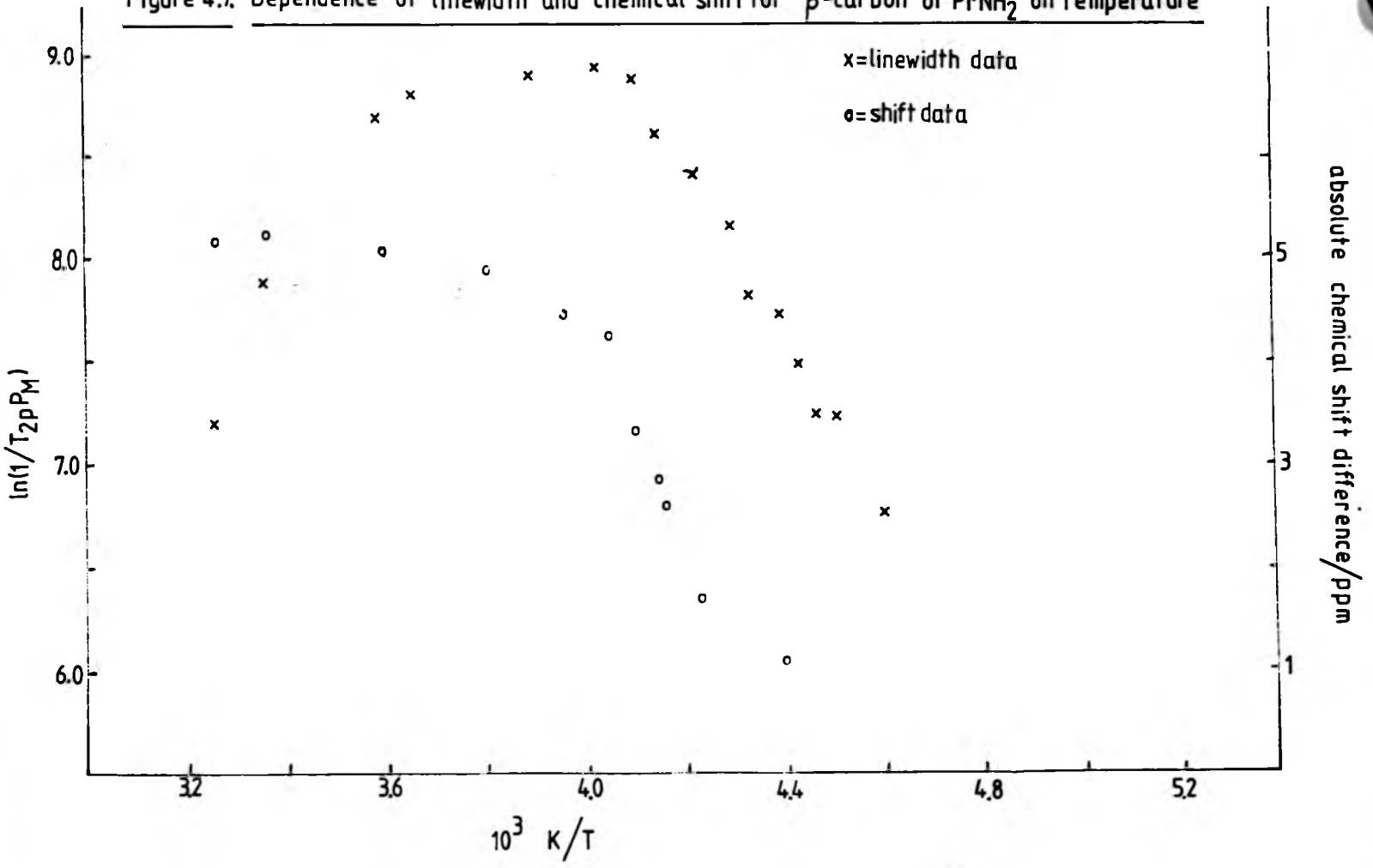

Figure 4.8. Dependence of linewidth and chemical shift for γ-carbon of $PrNH_2$ on temperature

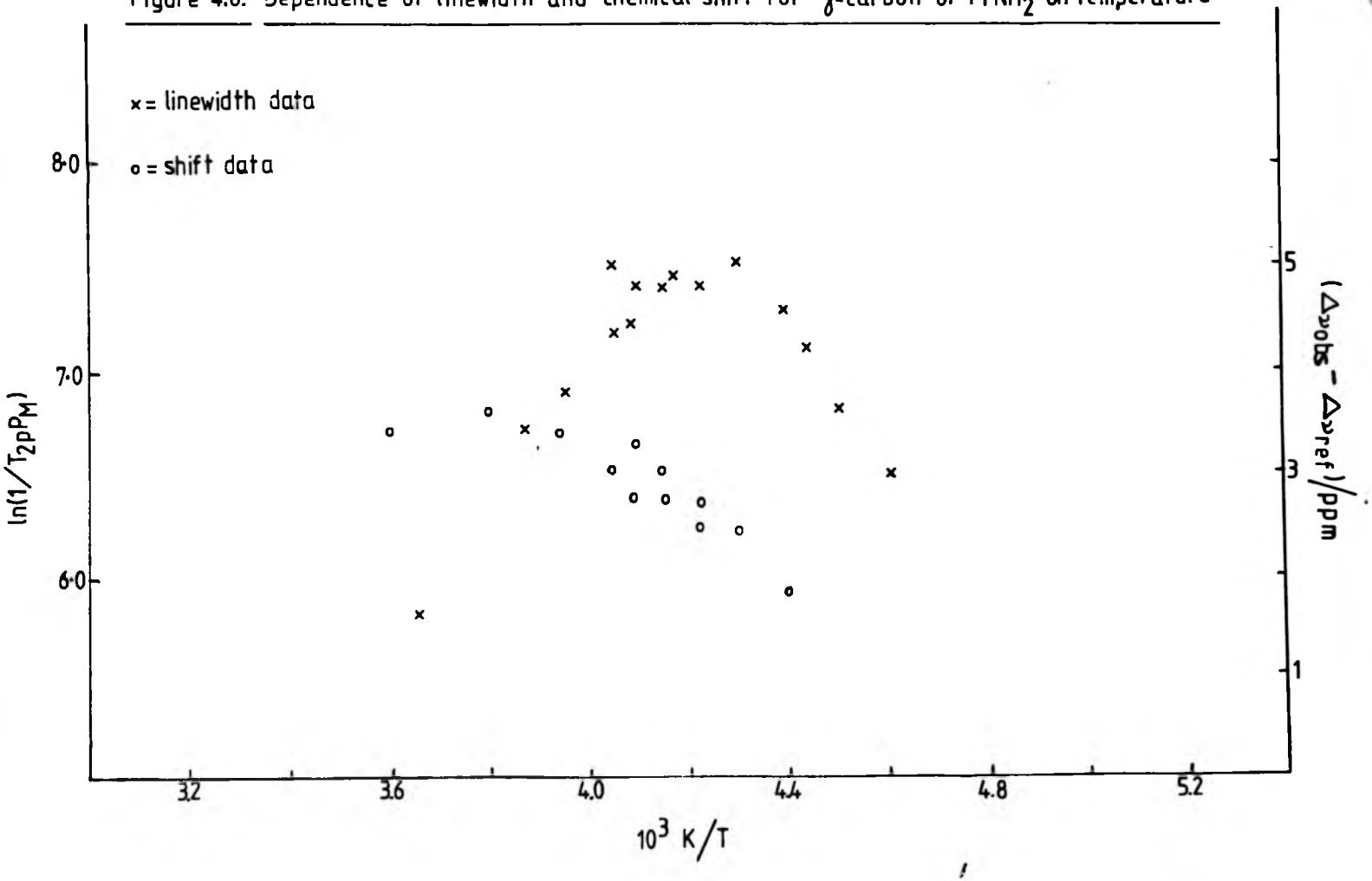

this near-infra-red region of the electronic spectrum. Before commencing this variable temperature study it was necessary to have an accurate value of the extinction coefficient of the absorbance band that was to be monitored. To determine this parameter variable temperature electronic spectra were recorded of a solution of the $PrNH_2$ bis-adduct in neat $PrNH_2$ i.e. to maximise the concentration of free amine and thus force the position of equilibrium as far to the side of bis-adduct formation as possible. In this manner it was found that as temperature was lowered the absorbance at 930 nm increased until a temperature of 296K was reached. At this point any further decrease in temperature caused no observable change in the electronic spectrum to occur. It could be assumed therefore that below this temperature the equilibrium position was that of total bis-adduct in solution and hence the extinction coefficient at this wavelength could be determined.

With this information it was possible to investigate the equilibrium process. A solution containing exactly the same mole ratio of co-ordinated to bulk amine as in the variable temperature ^{13}C n.m.r. experiment was thus subjected to a variable temperature electronic spectral study. Spectra were recorded over a temperature range of 286 - 333K at approximately 10K intervals and the results of this study are shown in Figure 4.9.. As can be seen from these spectra there is no evidence of a five-co-ordinate species and thus the concentrations of any such species can be assumed to be very small.

The overall formation reaction for the bis-adduct can be described as follows

Figure 4.9. V.T. electronic spectral study of the equilibrium

$[Ni(BENZOX)_2] + 2PrNH_2 \rightleftharpoons [Ni(BENZOX)_2(PrNH_2)_2]$

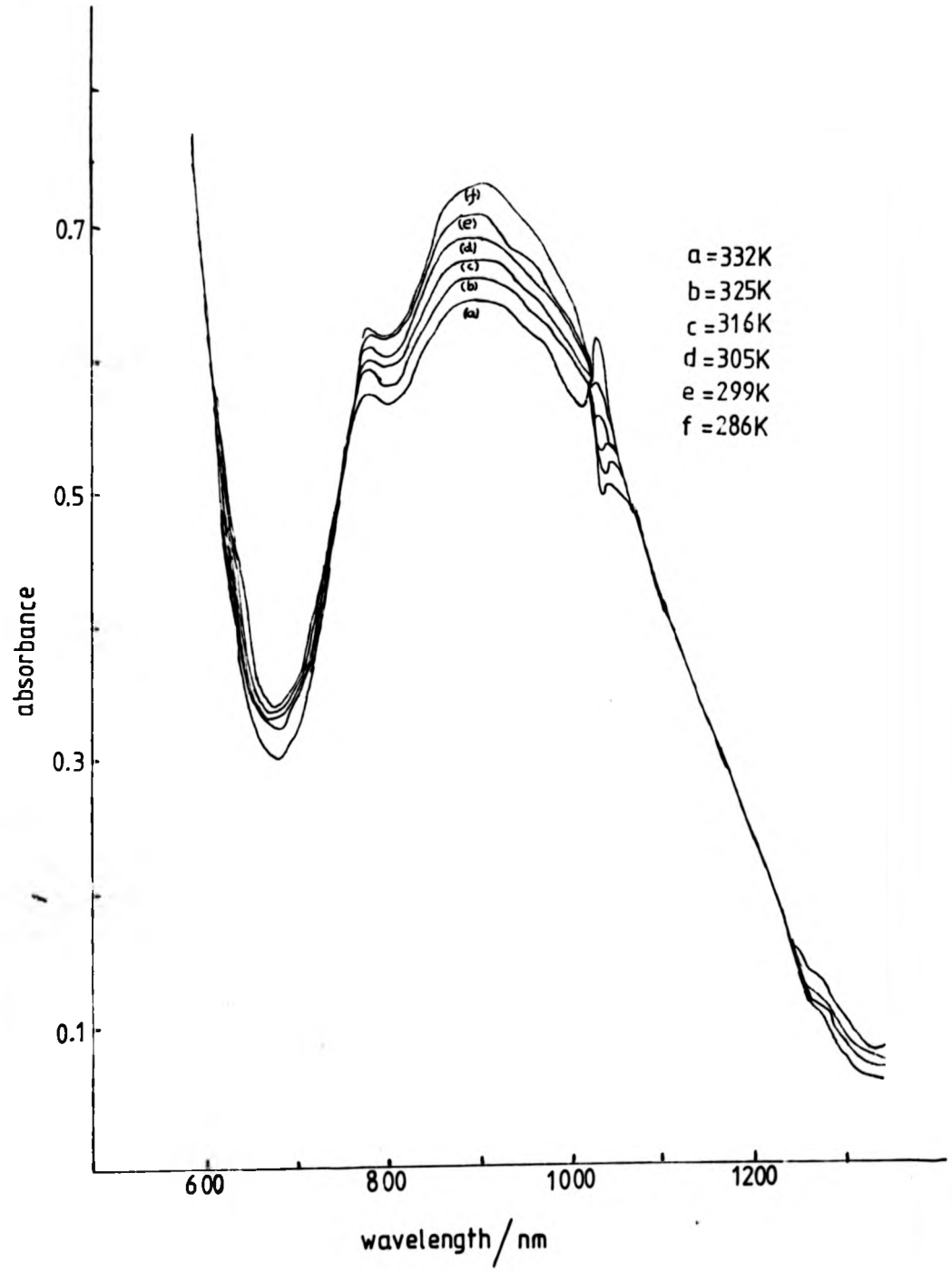

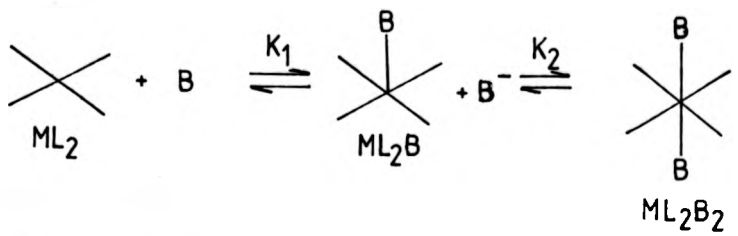

(4.10)

where K_1 and K_2 are the equilibrium constants for formation of the five-co-ordinate species and the six-co-ordinate species respectively where

$$K_1 = \frac{[ML_2B]}{[ML_2][B]} \qquad K_2 = \frac{[ML_2B_2]}{[ML_2B][B]} \tag{4.11}$$

Thus the overall formation equilibrium constant is given by

$$\beta_2 = K_1K_2 = \frac{[ML_2B_2]}{[ML_2][B]^2} \tag{4.12}$$

As no five-co-ordinate species is observed it is expected that the situation exists where $K_2 \gg K_1$.

At any specific temperature the concentration of bis-adduct can be determined as such

$$[ML_2B_2] = b(A_T/A_o) \tag{4.13}$$

b is the total concentration of solute, A_m is the absorbance observed at temperature T and A_o is the calculated absorbance for total adduct formation. Thus

$$\beta_2 = \frac{[bA_m/A_o]}{[b-bA_m/A_o][c-2bA_m/A_o]} \tag{4.14}$$

The relevant values of β_2 are given in Table 4.4..

The enthalpy and entropy changes for this equilibrium process are related to β_2 by the well known equation

$$-RT\ln\beta_2 = \Delta H^\circ - T\Delta S^\circ \qquad (4.15)$$

Thus a plot of $\ln\beta_2$ versus reciprocal temperature will have a slope of $-\Delta H^\circ/R$ and intercept $+\Delta S^\circ/R$. In Figure 4.10. is shown such a plot determined for the data given in Table 4.3.. As well as yielding values of ΔH° and ΔS° this plot allows evaluation of β_2 at any temperature and also the mole fraction of bound solvent can be calculated at any temperature.

The values of ΔH°, ΔS° and β_2 at 298K obtained from Figure 4.10. by a linear least squares analysis are given in Table 4.5.. These can be compared to the corresponding values reported [21] for the equilibrium process between the complex $[Ni(SALO)_2]$ and n-butylamine which are also given in the same Table. It is observed that the values of ΔH° for the two systems are very similar which would indicate metal-amine bond formations of similar strengths. However, for the $[Ni(BENZOX)_2(PrNH_2)_2]$ system the value of ΔS° is more negative and thus, as the enthalpy changes are similar for the two systems, β_2 is smaller than for the corresponding equilibrium process of $[Ni(SALO)_2(BuNH_2)_2]$. This more negative entropy for the $[Ni(BENZOX)_2]$ system can be explained by the observation that the two benzene rings in BENZOX are not co-planar and thus this non-planar molecule can cause more steric repulsion of the amine than the planar SALO molecule.

From this variable temperature electronic spectral study

Figure 4.10. Plot of $\ln \beta_2$ versus $1/T$ for equilbrium

$[Ni(BENZOX)_2] + 2PrNH_2 \rightleftharpoons [Ni(BENZOX)_2(PrNH_2)_2]$

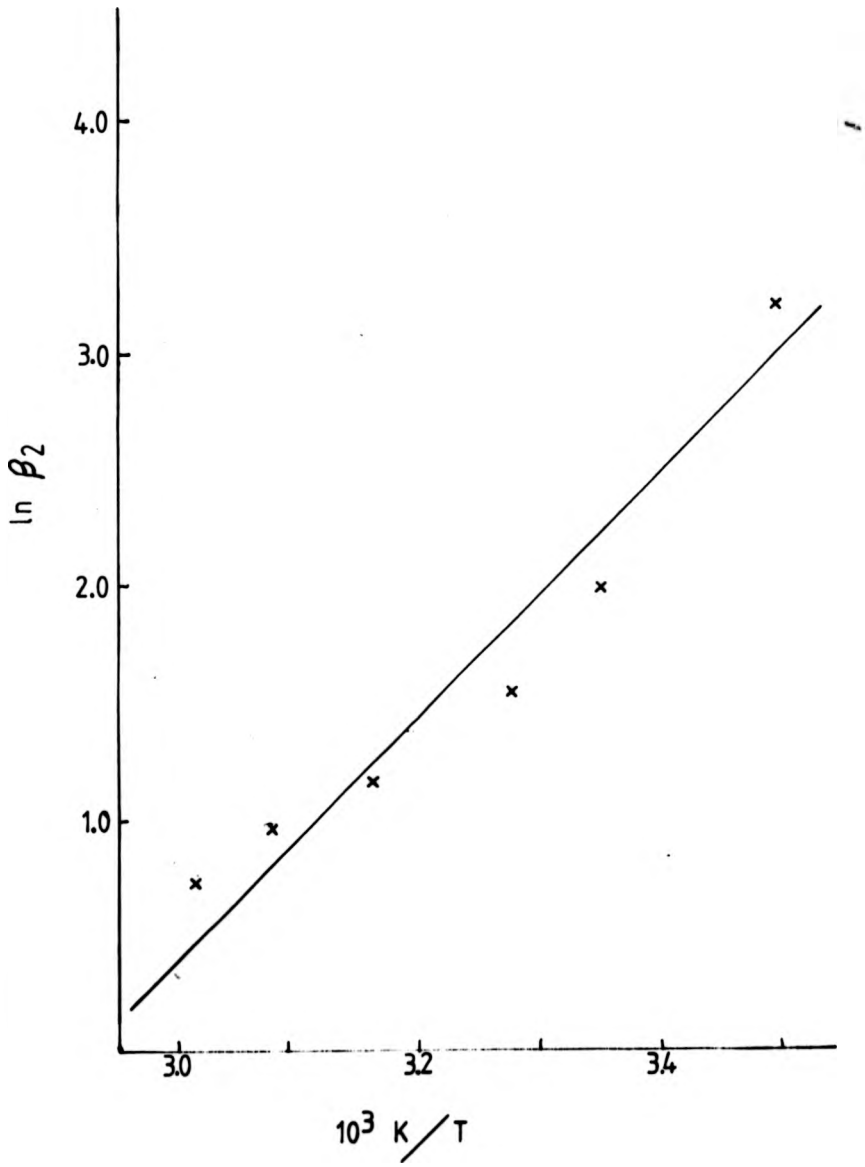

Table 4.4. Temperature dependence of β_2 for the equilibrium

$[Ni(BENZOX)_2] + 2PrNH_2 \rightleftharpoons [Ni(BENZOX)_2(PrNH_2)_2]$.

$10^3 K/T$	3.4965	3.3500	3.2786	3.1695	3.0816	3.0156
$\ln_{e}\ \beta_2$	3.20	2.00	1.54	1.16	0.96	0.73

Table 4.5. Thermodynamic data at 298K for the equilibrium

$[NiL_2] + 2B \rightleftharpoons [NiL_2B_2]$.

L	B	ΔH^o / kJ mol^{-1}	ΔS^o / J K^{-1} mol^{-1}	β_2 / dm^3 mol^{-1}
BENZOX	$PrNH_2$	-40.7 ± 6.3	-118 ± 20	2.14
SALO*	$BuNH_2$	-34.6	-64.2	15.2

* Taken from Reference 21.

Table 4.4. Temperature dependence of β_2 for the equilibrium

$[Ni(BENZOX)_2] + 2PrNH_2 \rightleftharpoons [Ni(BENZOX)_2(PrNH_2)_2]$.

$10^3 K/T$	3.4965	3.3500	3.2786	3.1695	3.0816	3.0156
$\ln \beta_2$	3.20	2.00	1.54	1.16	0.96	0.73

Table 4.5. Thermodynamic data at 298K for the equilibrium

$[NiL_2] + 2B \rightleftharpoons [NiL_2B_2]$.

L	B	ΔH° / kJ mol^{-1}	ΔS° / J K^{-1} mol^{-1}	β_2 / dm^3 mol^{-1}
BENZOX	$PrNH_2$	-40.7 ± 6.3	-118 ± 20	2.14
SALO*	$BuNH_2$	-34.6	-64.2	15.2

* Taken from Reference 21.

it was thus possible to evaluate P_m at any temperature and thus make the appropriate corrections to the values of $\ln(T_{2p}P_m)^{-1}$ and indeed in Figures 4.6. - 4.8. these corrections have been made. The now corrected data obtained from the ^{13}C n.m.r. variable temperature study was thus subjected to analysis by a fit to the full Swift-Connick equations. Values of the activation parameters and the rate constant for exchange of one amine molecule were determined with the linewidth data only and then with the chemical shift data as well, separately for all three carbon atom resonances, and the results of these analyses are given in Table 4.6..

Considering firstly those values of the activation parameters and the solvent exchange rate constant obtained from the linewidth data alone it can be seen that there is an excellent agreement between the values determined from the data observed for the α- and β-carbon atom resonances. The values obtained from the data from the γ-carbon atom resonance does not agree so well with the above values. This is not surprising as the linewidth changes observed for the γ-carbon resonance of $PrNH_2$ are much smaller (1-28 Hz) than the corresponding linewidth changes observed for the α- and β-carbon atom resonances (1-67 Hz and 1-100 Hz respectively) and thus the values obtained from analysis of this data would be expected to be less accurate. Even so the agreement is fairly good.

Considering now the values of $\Delta H^{\ddagger}$, $\Delta S^{\ddagger}$ and k_{ex}^{I} for the amine exchange process obtained from the fit to both linewidth and chemical shift data it can be seen that there is a fair agreement between the values of $\Delta H^{\ddagger}$ and indeed a reasonable agreement between these values and those obtained from linewidth

Table 4.6. Activation parameters for exchange of $PrMH_2$ on $[Ni(BENZOX)_2(PrMH_2)_2]$.

Linewidth data only.

Carbon atom	$\Delta H^{\ddagger}$ / kJ mol^{-1}	$\Delta S^{\ddagger}$ / J K^{-1} mol^{-1}	$10^7 k_{ex}$ / s^{-1}
α	36.7 ± 0.9	26.1 ± 3.9	4.0 ± 0.6
β	37.1 ± 1.1	28.4 ± 4.8	4.49 ± 0.7
γ	35.3 ± 2.3	18.3 ± 10.1	2.76 ± 1.3

Linewidth and chemical shift data.

Carbon atom	$\Delta H^{\ddagger}$ / kJ mol^{-1}	$\Delta S^{\ddagger}$ / J K^{-1} mol^{-1}	$10^7 k_{ex}$ / s^{-1}
α	31.8 ± 1.3	-30.6 ± 5.5	0.032 ± 0.007
β	35.9 ± 1.4	-12.1 ± 6.0	0.056 ± 0.009
γ	36.2 ± 2.4	-5.3 ± 10.4	0.050 ± 0.015

Mean values from data from α- and β-carbon atoms of linewidths only

$$\Delta H^{\ddagger} = 36.9 \pm 0.5 \text{ kJ mol}^{-1}$$

$$\Delta S^{\ddagger} = 27.3 \pm 2.2 \text{ J K}^{-1} \text{ mol}^{-1}$$

$$10^7 k_{ex} = 4.25 \pm 0.3 \text{ s}^{-1}$$

Table 4.6. Activation parameters for exchange of $PrNH_2$ on $[Ni(BENZOX)_2(PrNH_2)_2]$.

Linewidth data only.

Carbon atom	$\Delta H^{\ddagger}$ / kJ mol^{-1}	$\Delta S^{\ddagger}$ / J K^{-1} mol^{-1}	$10^7 k_{ex}$ / s^{-1}
α	36.7 ± 0.9	26.1 ± 3.9	4.0 ± 0.6
β	37.1 ± 1.1	28.4 ± 4.8	4.49 ± 0.7
γ	35.3 ± 2.3	18.3 ± 10.1	2.76 ± 1.3

Linewidth and chemical shift data.

Carbon atom	$\Delta H^{\ddagger}$ / kJ mol^{-1}	$\Delta S^{\ddagger}$ / J K^{-1} mol^{-1}	$10^7 k_{ex}$ / s^{-1}
α	31.8 ± 1.3	-30.6 ± 5.5	0.032 ± 0.007
β	35.9 ± 1.4	-12.1 ± 6.0	0.056 ± 0.009
γ	38.2 ± 2.4	-5.3 ± 10.4	0.050 ± 0.015

Mean values from data from α- and β-carbon atoms of linewidths only

$$\Delta H^{\ddagger} = 36.9 \pm 0.5 \text{ kJ mol}^{-1}$$

$$\Delta S^{\ddagger} = 27.3 \pm 2.2 \text{ J K}^{-1} \text{ mol}^{-1}$$

$$10^7 k_{ex} = 4.25 \pm 0.3 \text{ s}^{-1}$$

data only. However, the values of $\Delta S^{\ddagger}$ are not in agreement and are of opposite sign to those derived from the linewidth data. The values of k_{ex}^{I} do not agree with those obtained from the linewidth data either and indeed are a factor of 10^2 smaller. A negative value of $\Delta S^{\ddagger}$ implies an associative type of exchange mechanism which has never been postulated for such reactions of nickel(II). The values of k_{ex}^{I} from these analyses are more typical of solvent exchange of a hexa-amine of nickel(II) (e.g. k_{ex}^{I} for $[Ni(NH_3)_6]^{2+}$ is observed [227,228] to be 1.0×10^5 s^{-1}) than exchange of an amine on a complex of this type where the rate of exchange would be expected to be somewhat greater. It would seem, therefore, that the values of $\Delta S^{\ddagger}$ and k_{ex}^{I} obtained from linewidth and chemical shift data together are somewhat erroneous. These errors can be explained by consideration of the fact that the larger the observed linewidth of a resonance the more difficult it is to ascertain precisely the chemical shift of this resonance. Thus the largest errors are found with the data from the α- and β-carbon atom resonances which give rise to the largest linewidths. The values of $\Delta S^{\ddagger}$ obtained from the data from the changes observed at the β-carbon atom has a lower negative value than the corresponding value obtained from the α-carbon data. From Figures 4.6. and 4.7. it can be seen that much larger chemical shifts are found for the β-carbon atom resonance than for that of the α-carbon atom and thus a more accurate value of $\Delta S^{\ddagger}$ would be expected. The value of $\Delta S^{\ddagger}$ obtained from the data from the γ-carbon atom resonance is even less negative than that obtained for the β-carbon atom data. This can be explained as a result of the much smaller linewidths associated with the

γ-carbon atom resonance which enables a more accurate evaluation of absolute chemical shift. However, the fact that smaller chemical shifts are also associated with this resonance result in errors in determining the variation of this parameter with temperature and thus as demonstrated by Figure 4.8. a large scatter is observed in the chemical shift data. In conclusion it would seem therefore that the activation parameters and solvent exchange rate constant values obtained from the linewidth data alone are the most reliable as is mirrored in the excellent agreement found between the values of these parameters evaluated from the data for the α- and β-carbon resonances.

Before discussing the values of these parameters a mention should be made of the fact that both linewidths and chemical shifts for the three carbon atom resonances of $PrNH_2$ increase in absolute value with temperature in the order $\beta > \alpha > \gamma$. This observation is somewhat surprising as it would be expected that the values of these two parameters would decrease with distance of the respective carbon atom from the paramagnetic centre. The effects produced by the paramagnetic centre are directional in the sense that they are produced by σ electron density distributions along the bonds in the molecule. It would thus seem that in this case more σ electron density of the unpaired electron of the nickel(II) is on the β-carbon atom than the α-carbon atom of $PrNH_2$ (an alternant effect).

The values of the activation parameters for the exchange of $PrNH_2$ on $[Ni(BENZOX)_2(PrNH_2)_2]$ cannot be compared directly with any other systems as no studies of amine exchange with directly related complexes have been performed. However, several

studies have been made of the exchange rates of other nitrogen donor solvents which form bis-adducts with square planar nickel(II) complexes of ligands which are also nitrogen donating. Although these studies are slightly removed from the investigations reported here they are the most comparable studies available. Rusnack and Jordan [217] have reported the activation parameters for the exchange of DMF on the nickel(II) complex of the ligand shown below

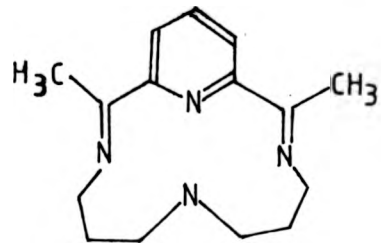

and found values of $\Delta H^{\ddagger}$, $\Delta S^{\ddagger}$ and k_{ex}^{I} of 39.71 kJ mol^{-1}, -9.2 J K^{-1} mol^{-1} and 1.9 x 10^{6} s^{-1} respectively. As can be seen the value of $\Delta H^{\ddagger}$ is very comparable to that reported here for the exchange of $PrNH_2$ on $[Ni(BENZOX)_2]$. In the study described above the authors have not applied a full Swift-Connick analysis to their data and thus error will be expected mostly in the reported value of $\Delta S^{\ddagger}$. The negative value of $\Delta S^{\ddagger}$ is not expected for this type of exchange reaction where a dissociative interchange mechanism is believed to operate. If this negative value of $\Delta S^{\ddagger}$ is indeed erroneous and should be positive then it can be seen that the value of k_{ex}^{I} will increase more towards the order of magnitude of that reported here for $PrNH_2$ exchange.

In an investigation of the solvent exchange of aceto-nitrile on the nickel(II) complex of the isomer of the macrocyclic

ligand TMC shown below

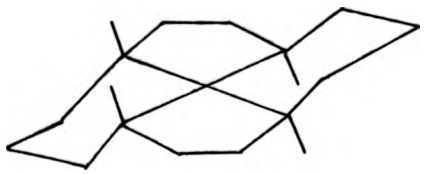

Herron and Moore [222] have obtained values of the activation parameters and k_{ex}^{I} for this process by way of a fit to the full Swift-Connick equations. The values reported ($\Delta H^{\ddagger}$=41.5±1.1 kJ mol^{-1}, $\Delta S^{\ddagger}$=+32±5 J K^{-1} mol^{-1}, k_{ex}^{I}=1.47 x 10^{7} s^{-1}) are indeed of the magnitude found in this study. Thus it can be concluded that the values of $\Delta H^{\ddagger}$, $\Delta S^{\ddagger}$, k_{ex}^{I} found for the exchange of $PrNH_2$ on $[Ni(BENZOX)_2(PrNH_2)_2]$ are typical for the exchange of a nitrogen donor ligand on a square planar nickel(II) complex of a ligand with strong nitrogen donor characteristics.

Summary and Conclusions.

It has been found that, as in the case of $[Ni(SALO)_2]$, the nickel(II) complex of BENZOX forms octahedral bis-adducts with both n-butylamine and n-propylamine. As this ligand is the non-alkylated model compound for the liquid-liquid extractant LIX 65N it would seem feasible that its nickel(II) complex should also form adducts, with amine ligands, in a similar manner.

An investigation of the exchange of amine molecules on these adducts by ^{13}C n.m.r. paramagnetic line broadening methods has been performed. In the case of the $BuNH_2$ adduct of $[Ni(BENZOX)_2]$ experimental difficulties have led to only approximate values of

the parameters associated with this exchange process being determined. In the case of the corresponding bis-adduct with $PrNH_2$ evaluation of the rate and activation parameters has been achieved by separate analysis of linewidth data for all three carbon atom resonances of the amine ligand. These independent analyses have produced values of $\Delta H^{\ddagger}$, $\Delta S^{\ddagger}$ and k_{ex}^{I} which are in good agreement and have thus allowed more accurate values of these parameters to be determined. The values determined are found to be typical for this type of exchange process.

An equilibrium has been found to exist between $[Ni(BENZOX)_2]$ and its $PrNH_2$ bis-adduct. A value of the adduct formation equilibrium constant at 298.2K of 2.14 has been determined. The enthalpy and entropy changes associated with this equilibrium process have been evaluated by means of a variable temperature electronic spectral study. The values of these parameters have been compared to reported values for a similar equilibrium process with $[Ni(SALO)_2]$ and its $BuNH_2$ adduct. The lower value of β_2 and more negative value of ΔS^{o} have been attributed to the non-planar nature of BENZOX which results in more steric repulsion between the incoming amine ligands and the complexed hydroxyoxime molecules.

4.3. A Study of the Interaction of DMF with (1,4,8,11-tetramethyl-1,4,8,11-tetra-azacyclotetradecane)nickel(II) perchlorate.

The work reported in this section is analogous to that described in the previous section, and is a continuation of previous studies in these laboratories of the interaction of metal

complexes of macrocyclic ligands with donor solvents. In a recent article Vigee et al [229] have reported a study of the equilibria established between the complex (1,4,8,11-tetra-azacyclotetradecane)nickel(II) perchlorate ($[Ni(cyclam)](ClO_4)_2$) and its octahedral bis-adducts formed in several donor solvents. The results from these studies indicate that the stabilities of these adducts decrease with donor solvent in the order $DMF > CH_3CN > (CH_3)_2SO > H_2O$. which is somewhat unusual. As part of a similar series of studies[224] with the complex $[Ni(TMC)](ClO_4)_2$ the investigations described here were initiated.

Both the nickel(II) complexes described above can exist in two isomeric forms. These isomers of $[Ni(TMC)]^{2+}$, which are labelled as trans-I and trans-III using the nomenclature of Bosnich et al [230], unlike those of the $[Ni(cyclam)]^{2+}$ ion are non-interconvertible by virtue of the methyl substituents on the four donor nitrogen atoms as shown below

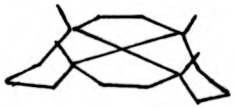

trans-I

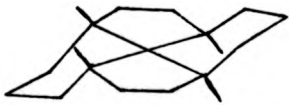

trans-III

The trans-I isomer is known to readily form mono-adducts [231,232] with donor solvents whereas the trans-III isomer forms octahedral bis-adducts and it is this species that is the subject of this study.

The trans-III complex was prepared by published methods[233] and isolated as orange/red crystals. When this complex is

dissolved in DMF a mauve solution results. The electronic spectrum of the adduct formed shows absorbance maxima at 625 nm and 505 nm. These observations can be compared to the λ_{max} values reported [233] for the bis-DMF adduct of $[Ni(cyclam)]^{2+}$ of 630 nm and 500 nm. Thus it is concluded that the corresponding adduct formed with $[Ni(TMC)]^{2+}$ is also a bis-adduct and of a pseudo-octahedral configuration. On heating a DMF solution of the adduct to a temperature of approximately 350K it was found that the mauve colour changes to an orange/red colour. Thus an equilibrium of the type described below exists,

$$[Ni(TMC)(DMF)_2]^{2+} \overset{K}{\rightleftharpoons} [Ni(TMC)]^{2+} + 2DMF \qquad (4.16)$$

where the equilibrium position is forced to the right with increasing temperature.

To investigate the temperature dependence of this equilibrium, paramagnetic ^1H n.m.r. methods were employed. Values of the enthalpy and entropy changes associated with this equilibrium were determined by monitoring the temperature dependence of the paramagnetic chemical shifts of the macrocycle protons. In the absence of any appreciable shift in the equilibrium position with temperature, the observed chemical shifts of the paramagnetic nickel(II) species are expected to follow a Curie Law dependence (i.e. a linear dependence with reciprocal temperature). However, if the equilibrium (4.16) shifts appreciably either to the right or left then deviations will occur from this linear dependence as the concentration of the paramagnetic species either decreases or increases. The magnitude of these deviations from linearity

in Curie-type plots thus yield information concerning the value of the equilibrium constant, K, and the manner in which this parameter varies with temperature, which leads to evaluation of ΔH° and ΔS° for the process.

If the assumption is made that the donor solvent molecules are in fast exchange, which is reasonable in view of the work reported in the previous section, then only one resonance will be observed for each proton of the macrocyclic ligand (which is in very slow chemical exchange). The magnitude of the chemical shift of each resonance is a weighted average of contributions from the diamagnetic species and from the paramagnetic species. Thus the observed chemical shift for a particular resonance can be described by the following equation

$$\omega_{obs} = (1-\alpha)\omega_{dia} + \alpha\omega_{para} \qquad (4.17)$$

where ω_{obs}, ω_{dia} and ω_{para} are the chemical shifts observed, for the pure diamagnetic species and the pure paramagnetic species respectively and α is the mole fraction of paramagnetic species formed. The quantity ω_{para} is dependent on temperature and can thus be related to a Curie-type constant, C.

$$\omega_{para} - \omega_{dia} = C/T \qquad (4.18)$$

Variable temperature ^{1}H n.m.r. spectra of a solution of the trans-III isomer of $[Ni(TMC)]^{2+}$ were recorded in $[^{2}H]_{7}$-DMF to avoid the problem of large solvent resonances in the spectra which might obscure the resonances relevant to the study, and

at the same time to provide a lock signal. Spectra were recorded over the temperature range 284-367K at approximately 10K intervals and the observations are demonstrated in Figure 4.11. (N.B. spectra are reversed i.e. high field is to the left of each spectrum). The trans-III isomer of $[Ni(TMC)]^{2+}$ has seven sets of magnetically equivalent protons which are labelled as a-g below.

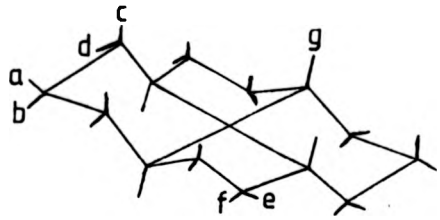

where a, d and e are equatorial, b, c and f are axial protons and g are the methyl protons of the N-Me groups.

In a recent publication Doi [234] has assigned the paramagnetic chemical shifts observed in the ^1H n.m.r. spectrum of a $[Ni(cyclam)]^{2+}$ species, and these assignments are used to label the resonances observed in the above spectra shown in Figure 4.11.. It is observed that as temperature is increased the upfield resonances shift in a downfield direction and the observed downfield resonance shifts towards an upfield position i.e. as more of the diamagnetic species is formed the observed chemical shifts tend towards their diamagnetic values.

The largest chemical shift changes with temperature are found for those resonances which are shifted most downfield and thus the information obtained from these yield the most accurate values of ΔH° and ΔS°. Therefore only the three resonances most downfield have been considered in this study. The temperature

Figure 4.11. V.T. ^1H n.m.r. study of the equilibrium processes for $[Ni(TMC)]^{2+} + 2DMF \rightleftharpoons [Ni(TMC)(DMF)_2]^{2+}$

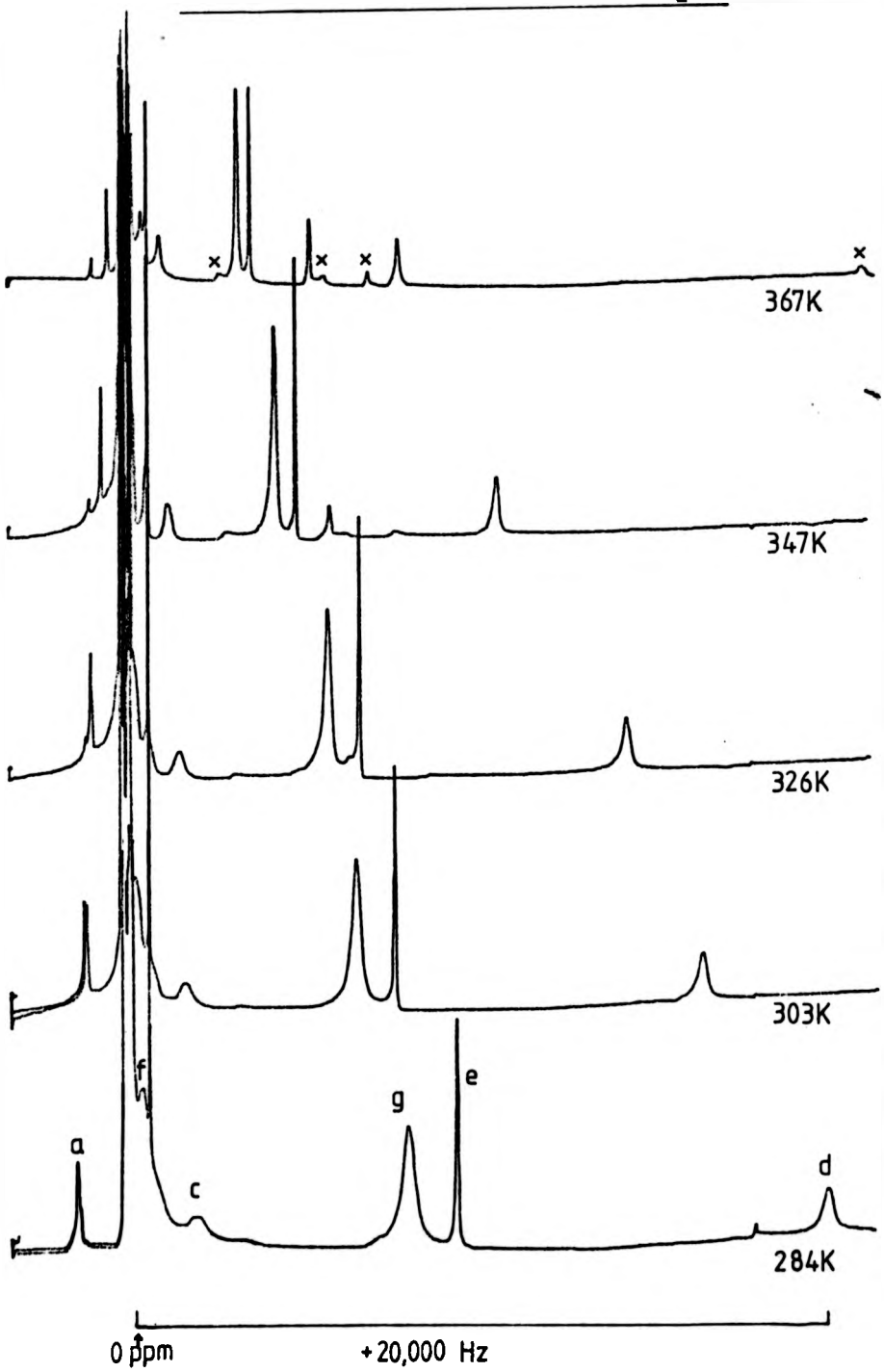

dependence of the observed chemical shifts for these three resonances are shown in Table 4.7..

The data in Table 4.7. were fitted to the equations described previously using the Fortran programme ITERAT (Appendix C) with the new subroutine FUNC (Appendix C). Values of ΔH°, ΔS°, K, the diamagnetic chemical shifts (ω_{dia}) of the three sets of protons and values of the Curie constants C_{1-3} for the three resonances were determined in this way. These are given in Table 4.7.. The plots of reciprocal temperature versus observed chemical shift are shown in Figure 4.12. where the deviations expected from the Curie Law are easily demonstrated.

Close inspection of the ^{1}H n.m.r. spectra shown in Figure 4.11. reveals the presence of some small extra resonances which also have temperature dependent chemical shifts (these are labelled as X). These resonances are also observed to increase in size as the temperature is increased. A ^{1}H n.m.r. spectrum of the resultant solution recorded after completion of the variable temperature experiment, revealed these other resonances to be present in the same intensity as observed in the highest temperature ^{1}H n.m.r. spectrum. This observation would indicate that the increase in concentration of the species responsible for this second set of resonances was an irreversible process. On further heating of the sample it was observed that a colour change occurred. The initially mauve solution of the DMF adduct now appeared as a green solution at room temperature which reverted to the red colour of the square planar trans-III $[Ni(TMC)]^{2+}$ species at higher temperatures. This observation and the fact that the grouping of the resonances in the ^{1}H n.m.r. spectrum of

Figure 4.12. Plot of chemical shift versus 1/T for <u>trans</u>-$[Ni(TMC)(DMF)_2]^{2+}$

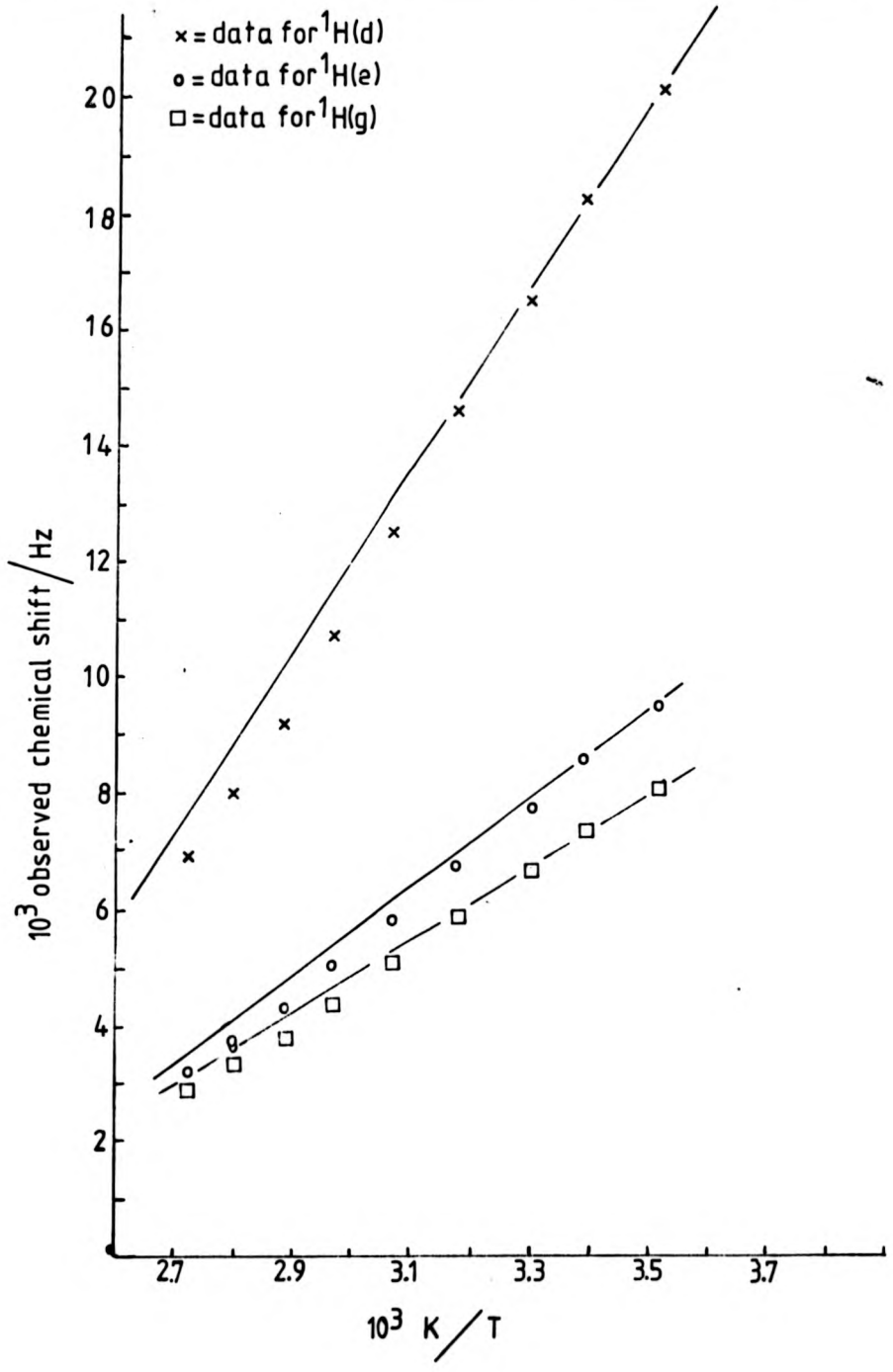

this secondary species were very similar to that of the main resonances from $[Ni(TMC)(DMF)_2]^{2+}$ indicated that the unknown was in fact another form of adduct species. A ^1H n.m.r. spectrum recorded of this now green solution indicated that the concentration of the secondary species had indeed increased.

To investigate the nature of the second species a variable temperature electronic spectral study was initiated. Spectra were recorded over the ranges 350-750 nm and 295-346K at roughly 10K intervals and the results are shown in Figure 4.12.. As can be seen no isosbestic points are observed in this variable temperature study indicating that more than one chemical process is produced. The spectral changes observed are a shift of the band at 625 nm of the major DMF adduct to around 640 nm and the absorbance band at 505 nm appears to gain intensity at shorter and longer wavelengths. The fact that the spectral changes are so slight is further evidence for a species closely related to the major adduct form. The two species can be attributed to the cis- and trans-forms of the DMF bis-adduct as shown below.

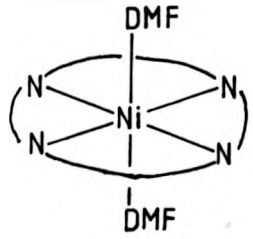

trans-

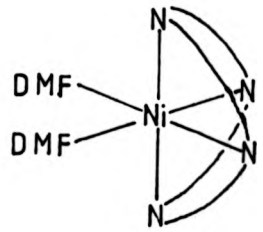

cis-

As temperature is increased it is expected that loss of the trans-bis-adduct occurs in conjunction with an increase in concentration of the square-planar complex. This would be characterised by a loss in absorbance of the bands at 625 and 505 nm and

Table 4.7. Temperature dependence of the paramagnetic ^{1}H n.m.r. chemical shifts of trans-III $[Ni(TMC)(DCF)_2]^{2+}$.

T / K	Resonance d	Resonance e	Resonance f
	ν_{obs} / Hz	ν_{obs} / Hz	ν_{obs} / Hz
284.1	20214.8	9527.6	8160.4
295.3	18347.2	8624.3	7409.7
303.5	16619.9	7800.5	6732.2
315.5	14581.5	6811.5	5908.2
325.9	12567.1	5859.4	5114.7
336.7	10797.1	5023.2	4412.8
346.9	9253.0	4290.8	3808.6
357.0	8013.9	3735.3	3350.8
366.9	6921.4	3186.0	2880.9

$\Delta H^o = -28.12 \pm 1.31$ kJ mol^{-1}

$\Delta S^o = -84.17 \pm 4.22$ J K^{-1} mol^{-1}

$K = 5.39 \pm 0.12$ dm^3 mol^{-1}

$^1\nu_{dia} = 2230 \pm 432$ Hz

$CC_1 = (5.97 \pm 0.19) \times 10^6$ Hz

$^2\nu_{dia} = 955 \pm 209$ Hz

$CC_2 = (2.84 \pm 0.09) \times 10^6$ Hz

$^3\nu_{dia} = 1052 \pm 175$ Hz

$CC_3 = (2.36 \pm 0.08) \times 10^6$ Hz

this secondary species were very similar to that of the main resonances from $[Ni(TMC)(DMF)_2]^{2+}$ indicated that the unknown was in fact another form of adduct species. A ^1H n.m.r. spectrum recorded of this now green solution indicated that the concentration of the secondary species had indeed increased.

To investigate the nature of the second species a variable temperature electronic spectral study was initiated. Spectra were recorded over the ranges 350-750 nm and 295-346K at roughly 10K intervals and the results are shown in Figure 4.12.. As can be seen no isosbestic points are observed in this variable temperature study indicating that more than one chemical process is produced. The spectral changes observed are a shift of the band at 625 nm of the major DMF adduct to around 640 nm and the absorbance band at 505 nm appears to gain intensity at shorter and longer wavelengths. The fact that the spectral changes are so slight is further evidence for a species closely related to the major adduct form. The two species can be attributed to the cis- and trans-forms of the DMF bis-adduct as shown below.

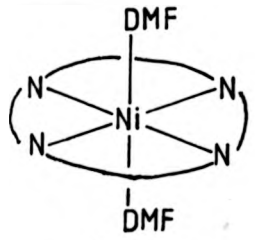

trans-

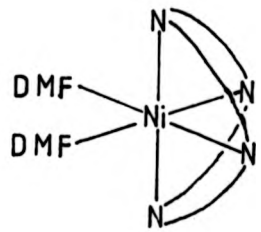

cis-

As temperature is increased it is expected that loss of the trans-bis-adduct occurs in conjunction with an increase in concentration of the square-planar complex. This would be characterised by a loss in absorbance of the bands at 625 and 505 nm and

Figure 4.13. V.T. electronic spectral study of $[Ni(TMC)(DMF)_2]^{2+}$

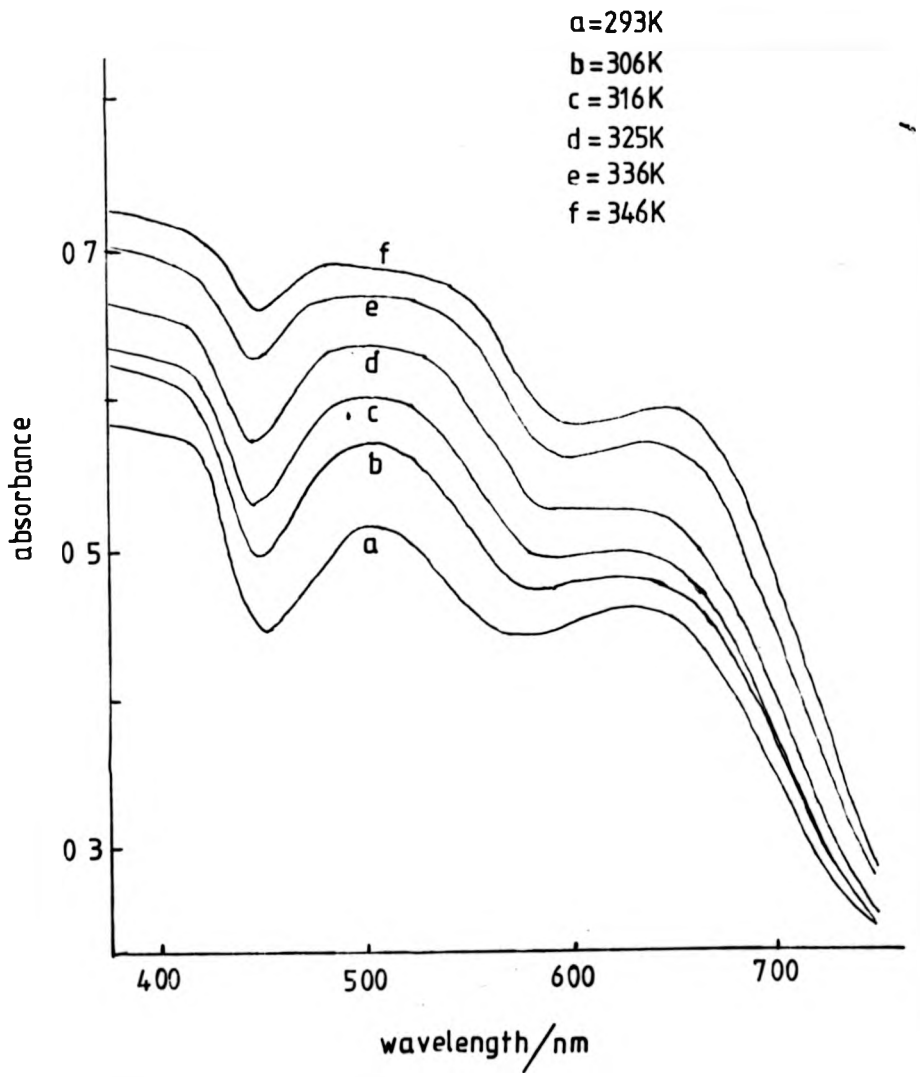

an increase in absorbance at around 494 nm (reported [232] value for trans-III $[Ni(TMC)]^{2+}$). Indeed as shown in Figure 4.13. this is the case. The observation of an increase in absorbance at the low energy sides of the two main absorbance bands indicates that the increase in temperature promotes the conversion of the trans-adduct to the cis-adduct.

The above assignment of the secondary species to the cis-adduct of DMF is further evidenced by the observations of Cook and Mckenzie [235,236] in studies of the interaction of dimethylsulphoxide with nickel(II) complexes of some open chain multidentate amine ligands. These authors have observed that the trans-adduct of the complex $[Ni(2,3,2\text{-tet})(DMSO)_2]$ (2,3,2-tet = $NH_2CH_2CH_2NH(CH_2)_3NHCH_2CH_2NH_2$) isomerises very slowly ($t_{\frac{1}{2}} \sim 14$ hrs) to form the cis-adduct in an equilibrium process. The reason given for the occurrence of this slow equilibrium is that it is a consequence of the 'uniquely ordered solvent shell' which exists in DMSO solution.

A similar type of computer analysis, to that described for the trans-adduct, was performed to evaluate the enthalpy and entropy changes for this second equilibrium process with the chemical shift data obtained from the variable temperature ^{13}C n.m.r. experiment described previously. Data were analysed only from the most downfield shifted proton resonance as at several temperatures other resonances were found to be obscured by the resonances resulting from the trans-adduct. A plot of observed chemical shift for this resonance versus reciprocal temperature is shown in Figure 4.14. and these values are listed in Table 4.8. along with the determined values of the parameters

Figure 4.14. Plot of chemical shift versus 1/T for cis-isomer of $[Ni(TMC)(DMF)_2]^{2+}$

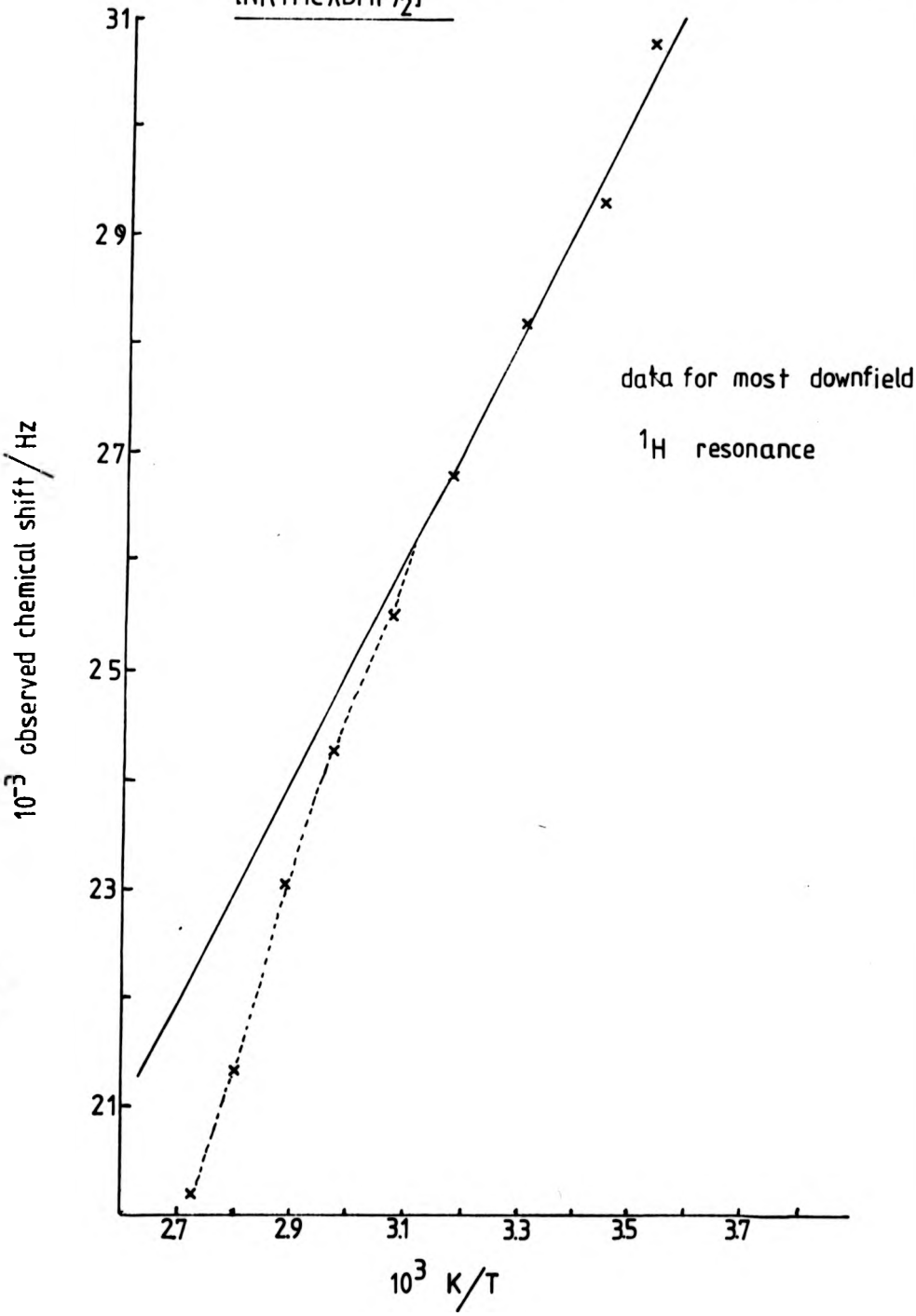

Table 4.8. Temperature dependence of the paramagnetic ^1H n.m.r. chemical shifts of trans-III cis-$[Ni(TMC)(DMF)_2]^{2+}$.

T / K	ν^1_{obs} / Hz
284.1	30786.2
295.3	29515.2
303.5	28204.3
315.5	26800.5
325.9	25518.8
336.7	24285.8
346.9	23040.9
357.0	21551.3
366.9	20172.1

$\Delta H^o = -27.75 \pm 3.22$ kJ mol^{-1}

$\Delta S^o = -62.74 \pm 8.63$ J K^{-1} mol^{-1}

$K = 29.5 \pm 7.4$ dm^3 mol^{-1}

$CC_1 = (8.64 \pm 0.07) \times 10^6$ Hz

associated with the equilibrium process.

As can be seen these values possess larger errors than the corresponding parameters for the equilibrium process for the trans-adduct. This is a direct consequence of using the chemical shift data for only one resonance. A comparison of the thermodynamic parameters for the two exchange processes (Tables 4.7. and 4.8.) indicates that the assignment of the second species to a cis-structure is reasonable. Values of ΔH° for the two processes are found to be virtually identical as expected if the two species are the cis- and trans-adducts. However, the value of ΔS° is more negative for the equilibrium involving formation of the trans-isomer than for that of the cis-isomer. In the case of the trans-adduct steric repulsion occurs between the co-ordinated DMF molecules and the six-membered chelate rings of the macrocyclic ligand as well as the N-methyl groups. In the case of the cis-adduct this steric repulsion is expected to be lessened since the macrocyclic ligand is now folded away from the co-ordination sites of the solvent molecules. This increases the stability of the cis-adduct by increasing ΔS°.

The values of ΔH°, ΔS° and K for the equilibrium process involving formation of the trans-adduct of $[Ni(TMC)]^{2+}$ of DMF can now be compared to the corresponding values obtained by Vigee et al [229] for solvent interactions with the complex $[Ni(cyclam)]^{2+}$. The results obtained by these authors indicate that DMF is more strongly bound to the above complex than acetonitrile. The thermodynamic parameters reported here for the trans-adduct are more in keeping with the corresponding values for the acetonitrile equilibrium with $[Ni(cyclam)]^{2+}$ than for the DMF equilibrium.

Previous work in these laboratories [232] has indicated that, as would be expected, acetonitrile in fact co-ordinates more strongly than DMF to the trans-III isomer of $[Ni(TMC)]^{2+}$ and thus this investigation would tend to support this conclusion.

Summary and Conclusions.

In the above study the interaction of DMF with the trans-III isomer of $[Ni(TMC)]^{2+}$ has been investigated by paramagnetic ^1H n.m.r. methods. It is found that initially a bis-adduct species forms on dissolution of the complex in DMF, of a trans-configuration. This adduct is in equilibrium with the parent complex and the thermodynamic parameters for this process have been evaluated. This trans-adduct slowly equilibrates with its cis-isomer which in turn is also in equilibrium with the parent square planar complex. Thermodynamic parameters have been evaluated for the formation of the cis-species.

4.4. A Study of the Exchange of Methanol on the Cation $[Zn(MeOH)_6]^{2+}$.

The investigations described in this section were initiated to try to ascertain more accurate activation parameters for the exchange of methanol molecules with the $[Zn(MeOH)_6]^{2+}$ ion than those which have previously been reported [225]. In the ^1H n.m.r. study reported by Al-Baldawi and Gough [225] a concentration dependence of the activation energy associated with the exchange process has been observed. This is believed to be a result of co-ordination of ClO_4^- to the zinc(II) centre, and in this study investigations have been performed employing $[Zn(MeOH)_6](BF_4)_2$

instead.

The tetrafluoroborate counterion was chosen for use as it is relatively unco-ordinating and has the advantage over the perchlorate anion that its metal complexes are non-explosive (unlike the perchlorate salts) and thus more practical to work with. Therefore the above hexasolvate was prepared, by published methods [190], and isolated as white needle-shaped microcrystals.

The complex was dissolved in a mixture of protio-methanol and ~10% $[^2H]_4$-methanol, as lock sample. Initial ^1H n.m.r. spectra recorded at ambient temperature showed the pres ence of two resonances, corresponding to the methyl protons and the hydroxyl protons of all methanol species. A further ^1H n.m.r. spectrum of the above sample recorded at 180K showed the pres ence of another resonance. This is at low field to the main hydroxyl resonance and is attributed to the hydroxyl protons of the methanol molecules co-ordinated to Zn(II). Thus at this temperature the exchange rate of methanol molecules is in the slow exchange limit giving rise to hydroxyl resonances from both bulk and co-ordinated solvent.

For a diamagnetic metal ion, when exchange between bulk and co-ordinated solvent is comparable or greater than the frequency separation (in Hertz) of the co-ordinated and bulk resonances, only one resonance is observed in the n.m.r. spectrum. This single resonance is an average resonance in the sense that the observed chemical shift of such a resonance is dependent upon the concentrations of bulk and co-ordinated solvent. As temperature is lowered the rate of exchange of solvent molecules will decrease until it is less than the frequency separation of the

resonances arising from the bulk and co-ordinated solvent molecules, and thus as described above two resonances will be observed.

In the limit of slow exchange

$$\tau \simeq (\pi \Delta\nu)^{-1} \tag{4.19}$$

where τ is the average time spent by a solvent molecule at one particular co-ordination site and $\Delta\nu$ is the excess linewidth observed for the bound solvent resonance (i.e. the difference in full linewidth at half maximum height between the exchange broadened resonance and one not affected by chemical exchange).

Another way of writing equation (4.19) is as follows;

$$1/T_2 = 1/T_{2o} + 1/\tau \tag{4.20}$$

where T_2 is the transverse relaxation time in the presence of chemical exchange ($= 1/\pi\omega$ where ω is the full linewidth in Hertz at half maximum height) and T_{2o} is the transverse relaxation time in the absence of chemical exchange ($= 1/\pi\omega_o$).

As temperature is increased exchange broadening reaches a maximum when the exchange rate is comparable to the chemical shift separation between the resonances for bulk and co-ordinated solvent. As the temperature is further increased the now single averaged resonance decreases in width with increasing solvent exchange rate. To obtain kinetic information from spectra of this type a full lineshape analysis was carried out. The observed lineshape in the fast exchange regions at one specific temperature is determined by such factors as the rate of solvent exchange,

resonances arising from the bulk and co-ordinated solvent molecules, and thus as described above two resonances will be observed.

In the limit of slow exchange

$$\tau \simeq (\pi \Delta\nu)^{-1} \qquad (4.19)$$

where τ is the average time spent by a solvent molecule at one particular co-ordination site and $\Delta\nu$ is the excess linewidth observed for the bound solvent resonance (i.e. the difference in full linewidth at half maximum height between the exchange broadened resonance and one not affected by chemical exchange).

Another way of writing equation (4.19) is as follows;

$$1/T_2 = 1/T_{2o} + 1/\tau \qquad (4.20)$$

where T_2 is the transverse relaxation time in the presence of chemical exchange ($= 1/\pi\omega$ where ω is the full linewidth in Hertz at half maximum height) and T_{2o} is the transverse relaxation time in the absence of chemical exchange ($= 1/\pi\omega_o$).

As temperature is increased exchange broadening reaches a maximum when the exchange rate is comparable to the chemical shift separation between the resonances for bulk and co-ordinated solvent. As the temperature is further increased the now single averaged resonance decreases in width with increasing solvent exchange rate. To obtain kinetic information from spectra of this type a full lineshape analysis was carried out. The observed lineshape in the fast exchange regions at one specific temperature is determined by such factors as the rate of solvent exchange,

the chemical shift separation of bulk and co-ordinated resonances at this temperature, the relative concentrations of bulk and co-ordinated solvent molecules (the population of each resonance, p_A and p_B respectively) and the values of ω_o (the full linewidth in Hertz at half maximum height at this temperature in the absence of chemical exchange; the natural linewidth) for the two resonances. The relationship between these parameters in the faster exchange regions has been discussed sufficiently elsewhere [238]. Thus in the manner described above by recording spectra at selected temperatures and submitting these to full lineshape analysis and having knowledge of the various parameters that affect the shape of the observed resonance(s) values for the rates of solvent exchange can be determined.

Before commencing any such kinetic study it is of importance to have knowledge of the co-ordination number of the zinc(II) species involved in the exchange process (this factor determines the value of p_B the population of the resonance resulting from the co-ordinated solvent molecules). The co-ordination number of zinc(II) solvate species is usually six but it has often been found that the anions associated with the solvate complexes can co-ordinate to form species of the type $[Zn(S)_{6-n}X_n]^{(2-n)+}$ where n has the value of 1-4. For example, zinc(II) solvate complexes of dimethylsulphoxide [239], water [240] and methanol [225] have all been shown to bind the usually non-co-ordinating perchlorate anion. The nitrate anion has been found to co-ordinate with zinc(II) solvates of both methanol [241] and ethane-1,2-diol [242] and halide ions have also been found to co-ordinate with the Zn(II) solvates of water [243,244]. In the cases of

$[Zn(MeOH)_{6-n}X_n]^{(2-n)+}$ where X = nitrate and perchlorate, the number of co-ordinated methanol molecules, n, has been found to be concentration dep endent in the sense that as the concentration of the zinc(II) salt is increased the value of n is found to decrease from six to four. Thus in this study it is necessary to repeat a similar concentration dependency investigation to ascertain if such a co-ordination alteration occurs for the tetrafluoroborate anion.

As indicated previously a ^1H n.m.r. spectrum of the zinc(II)-methanol solvate recorded at 180K gave rise to two hydroxyl resonances associated with bulk and co-ordinated methanol molecules. Thus with a knowledge of the concentration of the zinc(II) salt values of the co-ordination number can be obtained from the relative areas of the two hydroxyl resonances. In this manner ^1H n.m.r. spectra were recorded at 180K of methanolic solutions of the zinc(II) solvate, with 10-20% $[^2H]_4$-methanol added as a lock signal, at concentrations ranging from 0.325-0.88 mol kg^{-1} of the solvate. Molality units are used throughout this study as they are temperature independent.

Calculations of n, were performed in the following manner. The ratios of concentrations of bulk and co-ordinated methanol can be related by the following equation.

$$\frac{[OH_c]}{[OH_b]} = \frac{[OD_c]}{[OD_b]} = R \qquad (4.21)$$

where R is the ratio of peak areas of co-ordinated to bulk solvent determined directly from the n.m.r. spectra. The molalities of

protio-methanol and $[^2H]_4$-methanol are described by [OH] and [OD] where the subscripts c and b are co-ordinated and bulk methanol species respectively.

The total molalities of methanol species, $[OH_{tot}]$ and $[OD_{tot}]$, are described as

$$[OH_{tot}] = [OH_c] + [OH_b] \qquad (4.22)$$

$$[OD_{tot}] = [OD_c] + [OD_b] \qquad (4.23)$$

Therefore

$$\frac{[OH_c]}{[OH_{tot}] - [OH_c]} = \frac{[OD_c]}{[OD_{tot}] - [OD_c]} = R \qquad (4.24)$$

As the values of R, $[OH_{tot}]$ and $[OD_{tot}]$ are known the values of $[OD_c]$ and $[OH_c]$ can be calculated.

The number of co-ordinated methanol molecules, $\underline{n}$, can be defined as follows

$$\underline{n} = \frac{[OH_c] + [OD_c]}{[Zn^{2+}]} \qquad (4.25)$$

The values of $\underline{n}$ determined in this way are shown in Table 4.9.. As can be seen, within experimental error, $\underline{n}$ does not fluctuate from the value of six across the total concentration range investigated. These results can be compared to the corresponding studies performed employing perchlorate [225] and nitrate [241] anions.

Table 4.3. The dependence of the number of methanol molecules co-ordinated to Zn(II) on the concentration of Zn(II).

[Zn] / mol kg^{-1}	N
0.325	6.05
0.390	5.81
0.520	6.01
0.540	5.97
0.625	6.01
0.750	6.40
0.880	5.92

Mean value = 6.02

In both these cases, investigated over a slightly larger concentration range, the value of n was found to vary from six to four. It would seem that the tetrafluoroborate anion has a weaker affinity for zinc(II) than either the perchlorate or nitrate anions. The reasons for this may be a result of a higher affinity of zinc(II) for oxygen donors rather than fluorine donors. It is also feasible that hydrogen bonding considerations may account for the lack of co-ordination of BF_4^-. In the case of the perchlorate and nitrate anions hydrogen bonding of an intramolecular nature may assist co-ordination more readily than in the case of the BF_4^- donor anion. Indeed in a crystallographic structural determination Ferrari et al [245] have shown that with $[Zn(H_2O)_6](NO_3)_2$ the nitrate anions are held together by a network of hydrogen bonds with each water molecule forming two such bonds with the oxygen atoms of the nitrato groups. This would tend to support the importance of hydrogen bonding with these zinc(II) solvates.

Having confirmed that the number of co-ordinated methanol molecules for $[Zn(MeOH)_6](BF_4)_2$ was six, and remained so over a fairly wide concentration range, it was now possible to investigate the kinetics of the methanol exchange process. The ^1H n.m.r. spectrum of pure methanol in the absence of any proton exchange processes consists of two main resonances which appear as a quartet, for the hydroxyl proton, and a doublet for the methyl resonance as a result of proton-proton spin coupling which occurs between the two sets of protons. Thus in the ^1H n.m.r. spectra of methanolic solutions of $[Zn(MeOH)_6]^{2+}$ contributions to the overall lineshape(s) will be made from these coupling phenomena.

To avoid these complications all ^1H n.m.r. spectra recorded were those in which proton-proton spin couplings had been removed by homonuclear decoupling of the methyl resonance. This act removes the signal arising from the relaxation process of the methyl protons by saturation and hence removes the coupling from these protons to both the bulk and co-ordinated hydroxyl resonances.

It was necessary to chose a suitable lock solvent for use in these experiments. The most obvious choice is $[^2H]_4$-methanol which in low concentration should not effect the solvent exchange rate sufficiently. However, the decoupled ^1H n.m.r. spectrum of a solution containing this deuterated solvent revealed that the chemical shift of the bulk hydroxyl resonances resulting from residual protons in the $[^2H]_4$-methanol was sufficiently isotopically shifted to be observed as slightly separated from the bulk hydroxyl resonance resulting from the protio-methanol. This separation of the two types of hydroxyl resonances was not sufficient for the two to be non-overlapping and thus this would provide complications in determining lineshape analyses.

A different choice of lock solvent was thus necessary. The properties of such a solvent would need to be that of a low freezing point (to allow slow exchange limit spectra to be recorded), inertness and non-co-ordination to zinc(II). The most readily available and suitable deuterated solvent was found to be $[^2H]_6$-acetone. It was found, however, that when a solution of $[Zn(MeOH)_6]^{2+}$ containing this lock solvent were subjected to low temperature ^1H n.m.r. investigation that at least two hydroxyl exchange processes were occurring. This phenomenon was not investigated further but the observations may indicate the presence

of species with only five or four co-ordinated methanol molecules with acetone occupying the remaining co-ordination sites.

As $[^2H]_6$-acetone was the only really suitable internal lock solvent it was decided to employ a system which had an external lock sample. To achieve this an arrangement of two n.m.r. tubes was used as shown below.

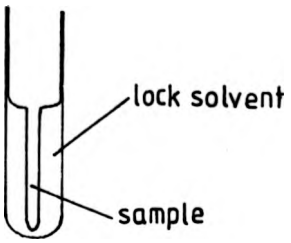

In this manner the lock solvent could be excluded from contact with the sample to be studied. It was found that the best results could be achieved when the lock solvent was in the outer compartment of the two tube system and the solution of $[Zn(MeOH)_6]^{2+}$ in the capillary tubing.

As described previously an important factor in determination of kinetic information by n.m.r. line broadening techniques is the linewidths of the resonances under study in the absence of chemical exchange at each temperature at which the exchange phenomenon is investigated. To determine this parameter a second n.m.r. sample was prepared containing methanol, the lock solvent and anhydrous sodium tetrafluoroborate at exactly the same molality as the sample containing the zinc(II) methanolate. In this manner any extra line broadening caused by viscosity effects at low temperature in the zinc(II) sample could be compensated for by the presence of the sodium tetrafluoroborate in the

of species with only five or four co-ordinated methanol molecules with acetone occupying the remaining co-ordination sites.

As $[^2H]_6$-acetone was the only really suitable internal lock solvent it was decided to employ a system which had an external lock sample. To achieve this an arrangement of two n.m.r. tubes was used as shown below.

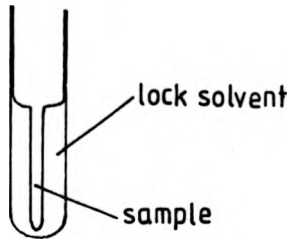

In this manner the lock solvent could be excluded from contact with the sample to be studied. It was found that the best results could be achieved when the lock solvent was in the outer compartment of the two tube system and the solution of $[Zn(MeOH)_6]^{2+}$ in the capillary tubing.

As described previously an important factor in determination of kinetic information by n.m.r. line broadening techniques is the linewidths of the resonances under study in the absence of chemical exchange at each temperature at which the exchange phenomenon is investigated. To determine this parameter a second n.m.r. sample was prepared containing methanol, the lock solvent and anhydrous sodium tetrafluoroborate at exactly the same molality as the sample containing the zinc(II) methanolate. In this manner any extra line broadening caused by viscosity effects at low temperature in the zinc(II) sample could be compensated for by the presence of the sodium tetrafluoroborate in the

sample used for natural linewidth determination.

Subsequently ^{1}H n.m.r. spectra were recorded of a sample containing 0.492 mol dm^{-3} of $[Zn(MeOH)_6](BF_4)_2$ in anhydrous methanol with $[^{2}H]_6$-acetone as the external lock solvent and a sample containing 0.492 mol dm^{-3} of anhydrous sodium tetrafluoroborate in anhydrous methanol with $[^{2}H]_6$-acetone as the internal lock sample. Successive spectra were recorded for both samples, with ^{1}H-decoupling of the methyl resonances, over the temperature range 185-222K at 5K intervals, and the results are shown in Figure 4.15..

Before subjecting the observed spectra to a full lineshape analysis it is important to ascertain the temperature dependence of the chemical shifts of the bulk hydroxyl resonance and the co-ordinated hydroxyl resonance [237]. As temperature is increased there are changes in the chemical shifts of both hydroxyl resonances which arise from two distinct causes. Firstly, there is a chemical shift change due to the coalescence of the two resonances as the solvent exchange rate increases and secondly chemical shift changes occur as the hydrogen bonding characteristics of the system change with temperature. It is the alteration of the chemical shift separation between the two hydroxyl resonances with temperature due to this second reason which must be determined. To achieve this the procedure of Nakamura and Meiboom [237] was adopted.

For a set of chemical shift separations ($\Delta\omega$) between the two hydroxyl resonances ^{1}H n.m.r. spectra were simulated, by use of the computer programme LSHAPE 3 [246], for a series of given values of τ. Linewidths of these spectra at half maximum height

Figure 4.15. V.T. ^1H n.m.r. study of methanol exchange on $[Zn(MeOH)_6]^{2+}$

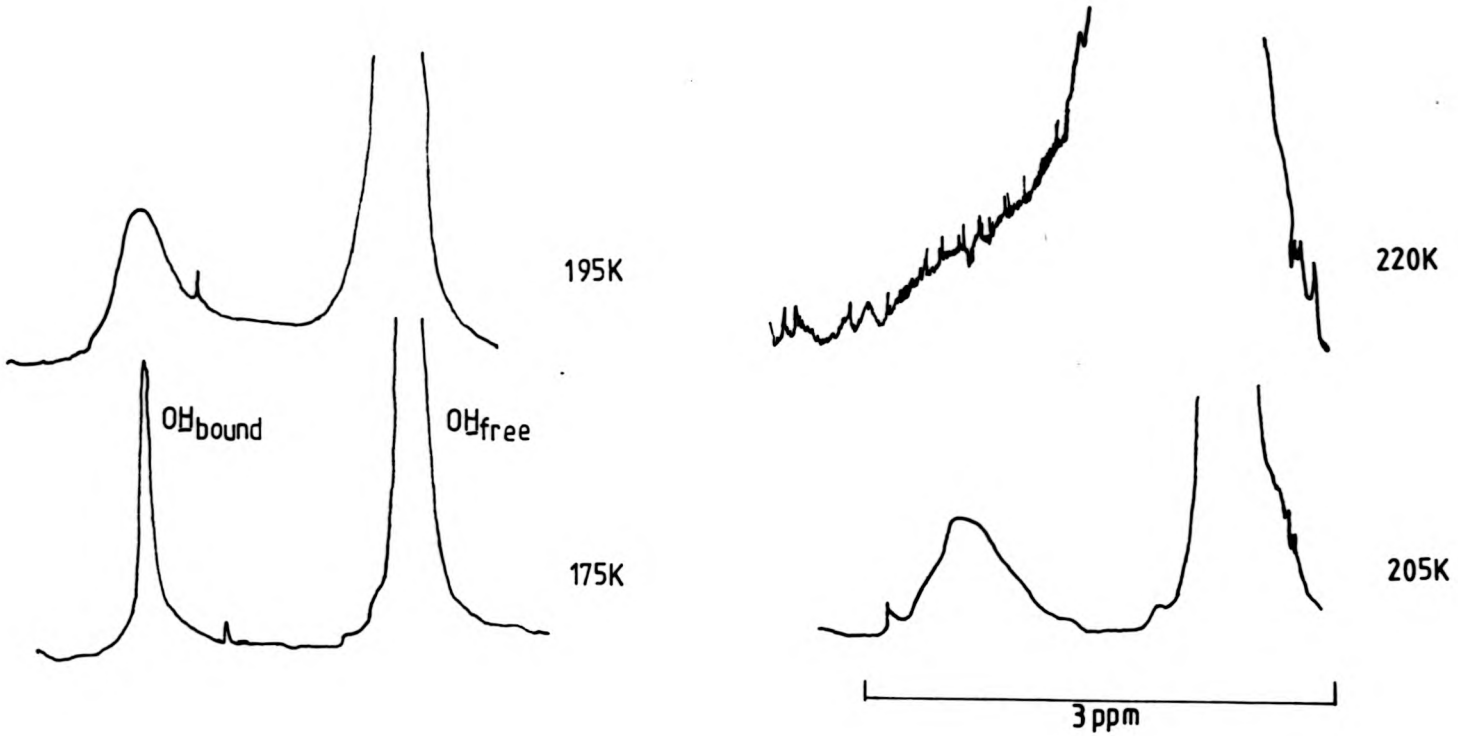

were measured from the simulated spectra for each successive value of τ, and from these values a plot of the linewidths versus $1/\tau$ was made. A typical plot is shown in Figure 4.16., and from this an estimation of the maximum linewidth that is observed for this particular value of $\Delta\omega$ can be ascertained. The whole process was repeated for a series of values of $\Delta\omega$, and from these experiments it is possible to plot a graph of the observed maximum linewidths versus $\Delta\omega$. A linear relationship between these two parameters, as shown in Figure 4.17., exists.

From the temperature dependence of the observed linewidth for the bulk hydroxyl resonance which was determined experimentally, it is possible to plot a graph of the observed linewidth versus reciprocal temperature. Such a graph is shown in Figure 4.18. for these experimentally determined linewidths. As can be seen a value of maximum linewidth can also be determined from this plot which corresponds to a specific temperature. This value of maximum linewidth is also associated with a specific value of $\Delta\omega$ which can be determined from Figure 4.17.. Therefore, in this manner a value of $\Delta\omega$ has been evaluated at a relatively high temperature when the two hydroxyl resonances are coalesced. Values of $\Delta\omega$ can be obtained directly from the observed ^1H n.m.r. spectra in the limit of slow exchange and these can be extrapolated to the high temperature point using a plot of $\Delta\omega$ versus temperature. In this way values of $\Delta\omega$ can be more accurately determined up to the temperature at which maximum linewidth occurs. This interpolation is shown in Figure 4.19..

With a knowledge of $\Delta\omega$ at any temperature it is possible to subject the recorded variable temperature spectra to a full

Figure 4.16. Effect of variation of k on oberved linewidth at fixed $\Delta\omega$.

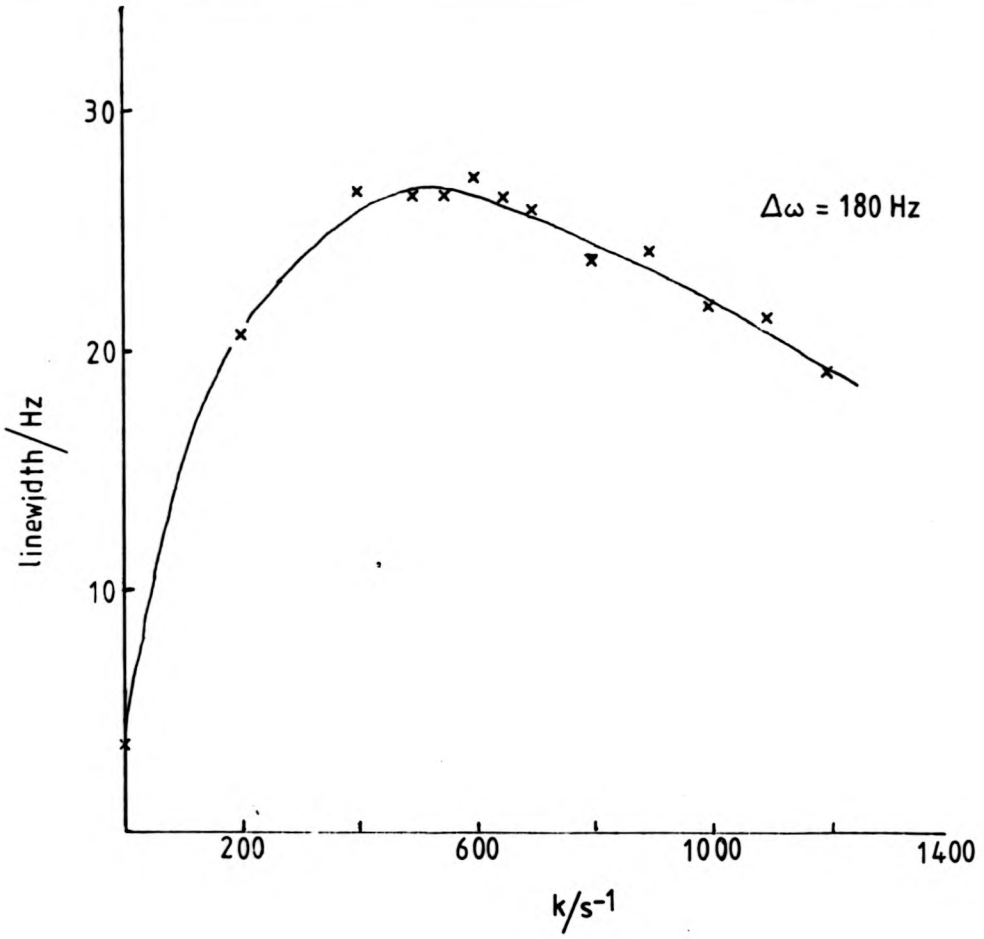

Figure 4.17. Plot of $\Delta\omega$ versus maximum linewidth

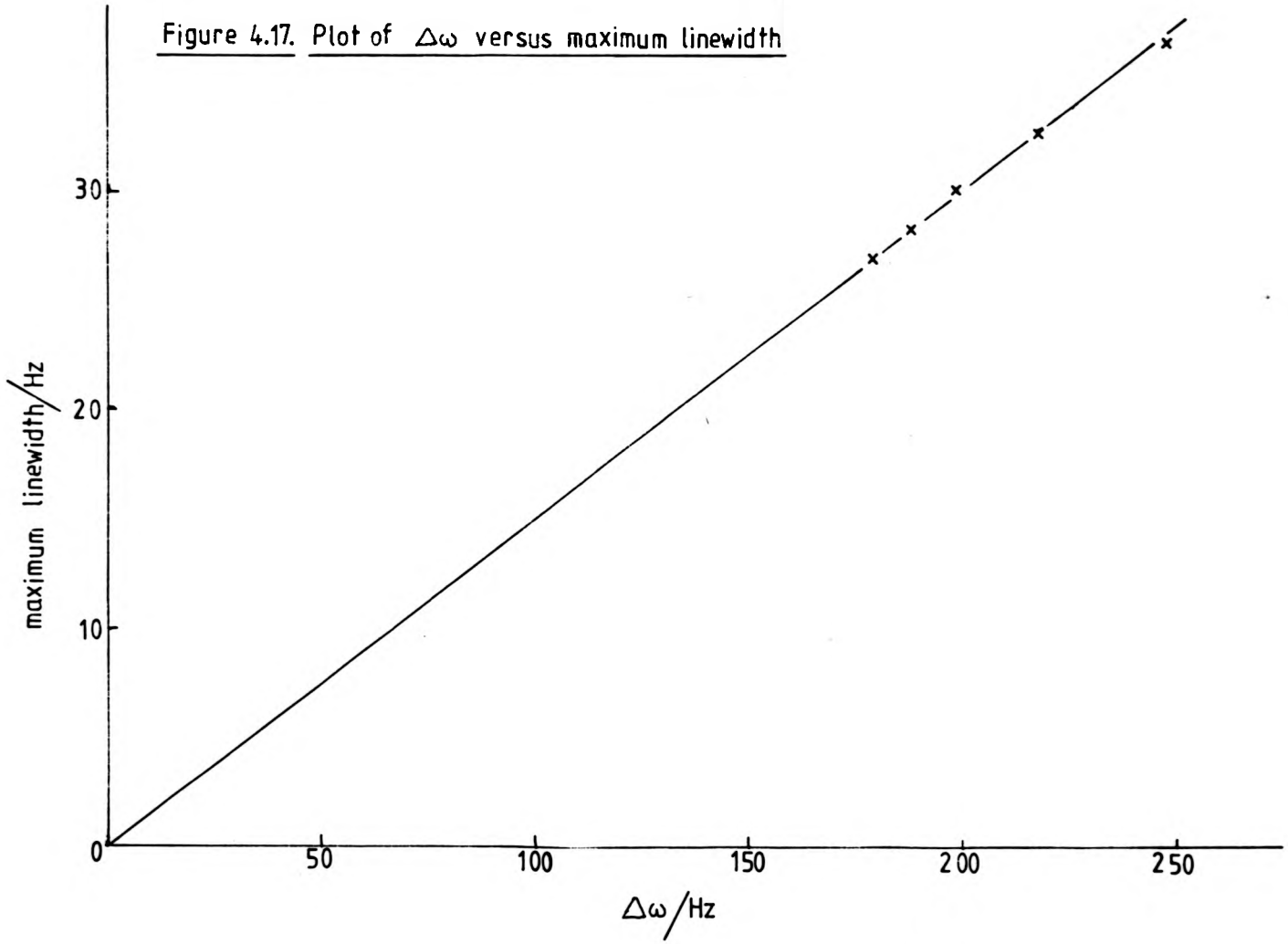

Figure 4.18. Observed linewidth versus 1/T for methanol exchange on $[Zn(MeOH)_6]^{2+}$

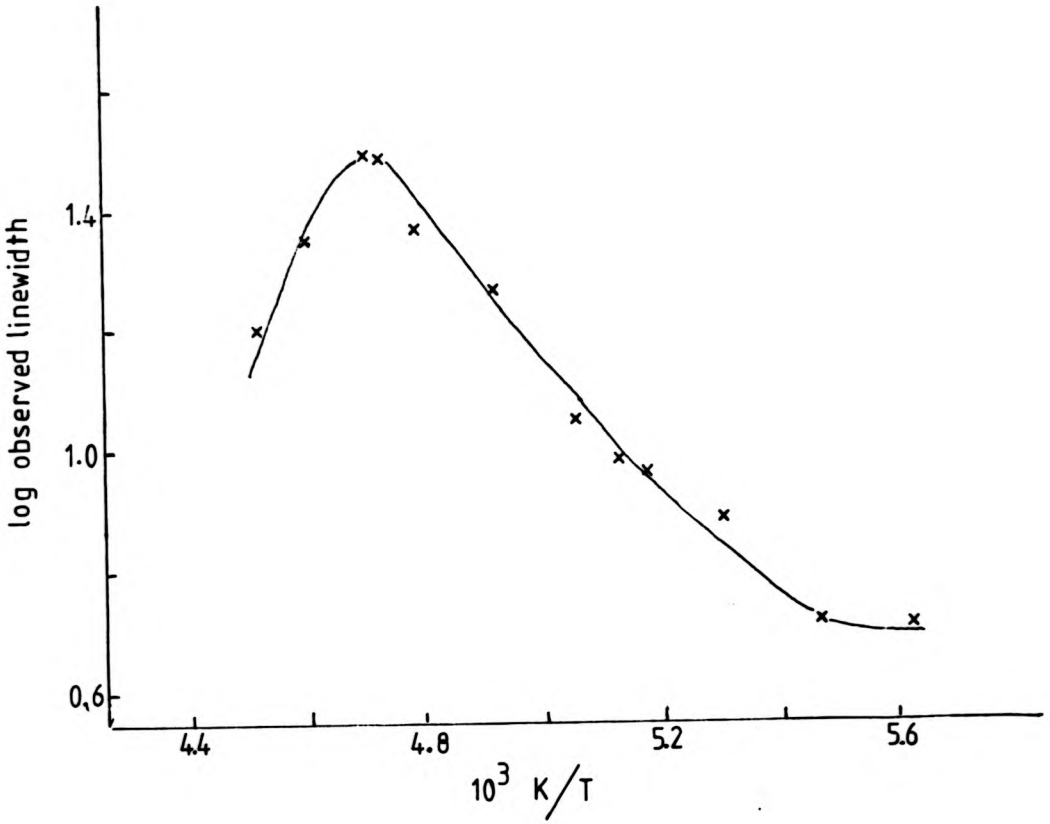

Figure 4.19. Plot of $\Delta\omega$ versus temperature for methanol exchange on $[Zn(MeOH)_6]^{2+}$

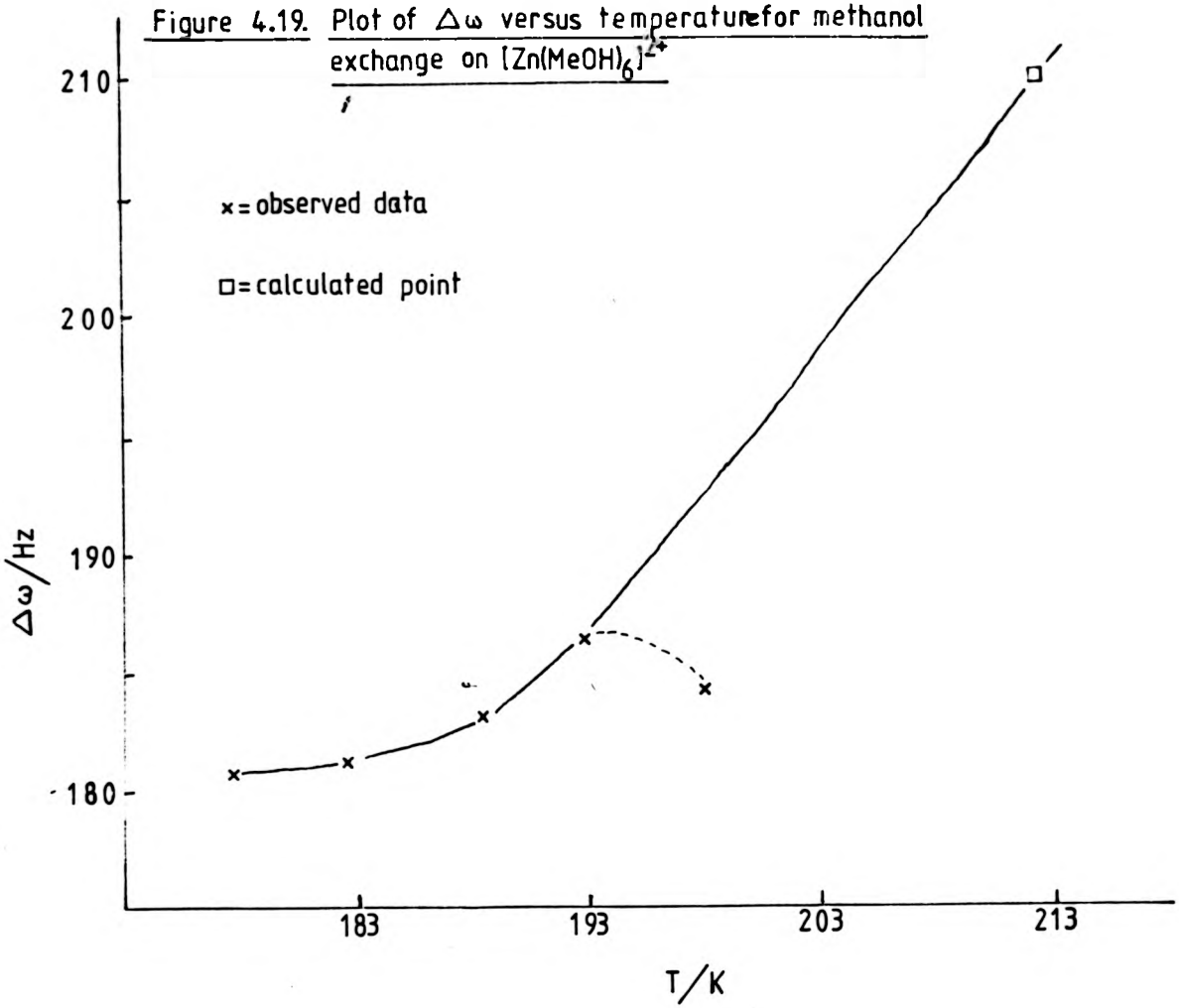

lineshape analysis as all parameters necessary to determine the rate constant for methanol exchange are known. These analyses were performed by use of the Algol computer programme [247] NMRLSA which is a version of the previously described LSHAPE 3. Up to seven parameters were fitted iteratively by non-linear least squares to obtain the best line fit to the observed n.m.r. spectra. The values of τ obtained in this way are related to the exchange rate constant by the equation

$$k_{ex}^{I} = p_A/\tau \qquad (4.22)$$

where p_A is the fractional population of the bulk solvent.

The values of k_{ex}^{I} derived in this manner are given in Table 4.9.. From these values of k_{ex}^{I} can be obtained estimates of the activation parameters associated with the solvent exchange process as well as the value of k_{ex}^{I} at 298.2K. These parameters were evaluated by use of the Algol computer programme ACTPAR which by way of a linear least squares analysis fits to equation (4.9). The determined values of these three parameters are also given in Table 4.10..

It can be seen that the values of activation parameters for the methanol exchange process have relatively large errors associated with them. These errors are believed to be caused by two factors. The first is that natural linewidth determinations were obtained from an external source in the sense that these values were not derived from the same sample used to obtain the kinetic parameters. Secondly the fact that the $[Zn(MeOH)_6]^{2+}$ solution in a capillary tube causes difficulties in obtaining

Table 4.19. Activation parameters for exchange of MeOH on $[Zn(MeOH)_6]^{2+}$.

T / K	k_{ex} / s^{-1}
182.9	20.14 ± 1.4
188.7	34.5 ± 0.8
193.5	130.3 ± 1.2
198.2	167.1 ± 1.4
203.8	385.5 ± 2.8
209.5	502.3 ± 3.6
221.8	4118 ± 34

$\Delta H^{\ddagger}$ = 43.2 ± 2.9 kJ mol^{-1}

$\Delta S^{\ddagger}$ = 19.6 ± 14.5 J K^{-1} mol^{-1}

k_{ex} at 298.2K = 1.74 x 10^{6} s^{-1}

reliable ^{1}H n.m.r. spectra. Only a small amount of the sample is present and thus very weak signals arise. It is difficult to optimise homogeneity of the magnetic field across such a small sample which causes a certain amount of inaccuracy in the observed lineshapes.

The values obtained for the solvent exchange rate constant associated with this exchange process can be compared to that derived from the work of Al-Baldawi and Gough [225] of approximately 1.7×10^{4} s^{-1} at 0.25 mol dm^{-3} solute. The value of k_{ex}^{I} obtained from this work is somewhat greater than the above but in this case it is known that six methanol molecules constitute the inner co-ordination sphere of zinc(II) whereas in the previously reported instance the number of co-ordinated methanol molecules is uncertain. The value of k_{ex}^{I} obtained is more consistent with the corresponding value associated with exchange of water [248] on $[Zn(H_2O)_6]^{2+}$ of 3×10^{7} s^{-1} and the more recently [249] reported value of 9.2×10^{6} s^{-1} for exchange of tetramethylthiourea (tmu) on $[Zn(tmu)_4]^{2+}$. The values of $\Delta H^{\ddagger}$ and $\Delta S^{\ddagger}$ are consistent with a dissociative interchange mechanism for methanol exchange as would be expected for octahedral zinc(II).

Summary and Conclusions.

In the previous section is described an investigation of the solvent exchange process involved with the species $[Zn(MeOH)_6]^{2+}$. The independence of the co-ordination number (6.0 ± 0.1) of the zinc(II) with metal ion concentration (0.525 to 0.88 mol kg^{-1}) was established for the tetrafluoroborate salt. This is in contrast to previous studies of ClO_4^- and NO_3^- salts

where it has been found that the number of methanol molecules bound to the metal centre can vary from six to four as solute concentration is increased. This is believed to be a result of anion co-ordination. In this manner it is concluded that zinc(II) has a lower affinity for BF_4^- than ClO_4^- which is probably a result of the differences in hydrogen bonding existing in the prescence of the two anions.

A ^1H n.m.r. investigation of the temperature dependence of the rate of exchange of methanol on $[Zn(MeOH)_6]^{2+}$ has allowed evaluation of the activation parameters associated with this exchange process. The value of k_{ex}^I evaluated at 298.2K is considered more reliable than that which has been previously reported as in this earlier study the nature of this species under investigation was not exclusively the hexasolvate.

4.5. Experimental.

Chemicals and Solvents.

All chemicals and solvents used were as described in Chapter 2 except as follows. Both n-butylamine and n-propylamine were purified by distillation from KOH pellets under a dry nitrogen atmosphere. All deuterated solvents were purchased and used without any further purification.

Synthesis of Metal Complexes.

The complex $[Ni(BENZOX)_2]$ was prepared as described in Chapter 2. The trans-III isomer of $[Ni(TEC)]^{2+}$ was prepared following the published method of Wagner and Barefield [253]. The complex

$[Zn(MeOH)_6](BF_4)_2$ was prepared by the method of Van Ingen Schenau[190] and stored as an anhydrous methanol solution.

Preparation of Adducts.

Both the $BuNH_2$ and $PrNH_2$ bis-adducts of $[Ni(BENZOX)_2]$ were prepared in similar fashions. The above complex (0.5 g) was dissolved in excess alkylamine to form the appropriate adduct. This solution was then evaporated to dryness on a rotary evaporator and the resulting yellow solid isolated.

Analyses (B.M.A.C.)

Calculated for ($C_{54}H_{42}N_4NiO_4$): C: 64.88%; H: 6.72%; N: 8.90%.

Found: C: 61.74%; H: 7.12%; N: 9.04%.

Calculated for ($C_{52}H_{38}N_4NiO_4$): C: 65.91%; H: 6.57%; N: 9.32%.

Found: C: 65.85%; H: 6.54%; N: 9.34%.

Instrumentation.

All instrumentation was as described in Chapter 2 unless given below.

^1H n.m.r. spectra.

All ^1H n.m.r. spectra were recorded with a Bruker WH90 pulse Fourier transform n.m.r. spectrometer at 90.01 MHz in 5 mm diameter tubes unless described differently in the text.

Variable temperature studies.

For variable temperature n.m.r. and U.V.-visible spectrometric experiments the sample temperature was measured using a calibrated Comark thermocouple and was held constant ± 0.5K with

a standard Bruker temperature control unit or a Churchill temperature control unit respectively.

CHAPTER 5.

CONCLUSIONS AND EXTENSIONS.

The results described in the previous chapters of this thesis have led to the following conclusions and suggestions for future extensions of this work.

The nickel(II) and copper(II) complexes of the commercial hydroxyoxime liquid-liquid extractant LIX 65N both exist in the square-planar trans-configuration in non-donor and weakly donating solvents. As in the case of the corresponding complex of salicylaldoxime the cobalt(II) bis-complex of this extractant is very oxygen sensitive. There is some doubt as to the preferred configuration of the cobalt(II) complex and it would therefore be of interest to ascertain this. The most conclusive way of performing this task would be by way of a structural determination. However, the possibility of growing crystals is slight for the above complex as a consequence of the presence of the long alkyl chains on the LIX 65N ligand. These chains are of varying lengths and degrees of branching which render attempts to grow crystals difficult if not impossible. It may be more fruitful, therefore, to attempt crystal growth of the cobalt(II) complex of the non-alkylated model compound BENZOX.

Another point of interest with this cobalt(II) complex of LIX 65N is the manner in which it interacts with dioxygen. It is not known whether oxidation alone occurs or whether oxygenation also occurs. If indeed the latter phenomenon occurs the mode of bonding associated with this dioxygen uptake, whether it be of a 'μ-peroxo' or 'superoxide' nature, is also unknown and could be investigated.

It would be of interest to investigate the behaviour of

these commercial liquid-liquid extractants towards complexation with other metal(II) species, but the two most relevant metals to be investigated, manganese(II) and iron(II), are both expected to be oxidation/oxygenation sensitive as is the cobalt(II) species and thus difficulties in experimentation will arise.

In investigations of the rates of complex formation of a series of aromatic hydroxyoxime ligands by nickel(II) it is found that the I_d mechanism operates and the rate determining step in these reactions is the formation of the first metal to ligand bond. It is found that the long alkyl chains of the hydroxyoxime extractants have a retarding effect on the rate of complex formation which is by a factor of approximately 1.5. It would be of interest therefore to investigate the complexation, by nickel(II), of a series of hydroxyoxime ligands which possess alkyl chains of various lengths and degrees of branching to determine how these factors effect the rates of complexation. However, it must be borne in mind that any such alteration to the extractant ligand that improves the kinetics of complexation must not result in too great a loss of solubility of both the ligand and the resulting metal complex to be of use commercially.

Further evidence for the operation of the I_d mechanism for metal complex formation in these systems could be obtained from kinetic studies of the type described in Chapter 3 using different solvent media. In this manner the observed rates of complex formation should be determined by the particular solvent exchange rate.

A series of experiments of great interest that can be

these commercial liquid-liquid extractants towards complexation with other metal(II) species, but the two most relevant metals to be investigated, manganese(II) and iron(II), are both expected to be oxidation/oxygenation sensitive as is the cobalt(II) species and thus difficulties in experimentation will arise.

In investigations of the rates of complex formation of a series of aromatic hydroxyoxime ligands by nickel(II) it is found that the I_d mechanism operates and the rate determining step in these reactions is the formation of the first metal to ligand bond. It is found that the long alkyl chains of the hydroxyoxime extractants have a retarding effect on the rate of complex formation which is by a factor of approximately 1.5. It would be of interest therefore to investigate the complexation, by nickel(II), of a series of hydroxyoxime ligands which possess alkyl chains of various lengths and degrees of branching to determine how these factors effect the rates of complexation. However, it must be borne in mind that any such alteration to the extractant ligand that improves the kinetics of complexation must not result in too great a loss of solubility of both the ligand and the resulting metal complex to be of use commercially.

Further evidence for the operation of the I_d mechanism for metal complex formation in these systems could be obtained from kinetic studies of the type described in Chapter 3 using different solvent media. In this manner the observed rates of complex formation should be determined by the particular solvent exchange rate.

A series of experiments of great interest that can be

performed now that an understanding of metal complex formation has been achieved are those that would determine the effect of the prescence of the aliphatic hydroxyoxime LIX 63 on the rate of metal complex formation. In this way it may be possible to determine the nature of the observed catalytic effect induced by this molecule on such reactions.

As postulated in Chapter 3 the observed intercepts in the plots of pseudo-first-order rate constant versus concentration of ligand may correspond to the rate constant for dissociation of the formed bis-complexes. To confirm this suggestion a series of experiments involving ligand exchange studies of the bis-complexes could be undertaken. If the nature of the intercepts is as described above then the rate determining step in these reactions should be that involving loss of the first ligand molecule i.e. this rate will be determined by the value of the observed intercepts.

As an extension of the metal exchange reaction studies reported in Chapter 3 a very useful series of experiments to perform would be those involving variable temperature studies of the three reaction stages observed. Information concerning these reactions determined in this manner will yield thermodynamic data for the three separate stages. In this way confirmatory evidence could be obtained for the postulated mechanisms of metal exchange. These mechanistic studies can, of course, be extended to different systems i.e. other ligands and other metals, to determine whether the suggested reaction pathways are of a more general nature.

The studies of the interactions of donor solvents with the nickel(II) complexes of the model compounds of the commercial extractants are also worthy of further study. It would be of interest to investigate these interactions with a series of such ligands both from a kinetic and a thermodynamic viewpoint to ascertain how the nature of the donor solvent affects the behaviour of these hydroxyoxime complexes towards adduct formation. One obvious study would be of the interaction of the nickel(II) complex of one of the available extractants or its model compound with the nitrogen base 2-methylpyridine. This donor ligand may well induce the formation of a five co-ordinate adduct and it would be of interest to determine how such adduct formation affects the configuration of the parent complex.

APPENDICES.

APPENDIX A. Rapid Scanning Spectrometry.

Single wavelength stopped-flow spectrophotometry while being well established is not very effective in the study of transient intermediates. Full electronic spectra of such species have to be constructed by performing individual stopped-flow experiments at many wavelengths in the spectral range of interest i.e. on a point-to-point basis. Spectra constructed in this manner are susceptible to a degree of experimental error which becomes unacceptable when overlapping spectra of successive intermediates or of the product occurs.

The development of the technique of rapid scanning spectrometry has allowed successive electronic spectra to be accumulated over short periods of time enabling full spectra to be recorded of transient intermediates. The apparatus that was employed to study the reactions described in Chapter 3 was a model 601 Multiplex spectrometer supplied by Applied Photophysics Ltd., London. A schematic diagram of the above apparatus is shown overleaf.

Radiation from a power-stabilised 150-W xenon-arc lamp is channelled through the reaction cell of a stopped-flow spectrophotometer featuring an all glass inlet system, from which it is focused on the entrance slit of a modified F/4 Czerny-Turner grating monochromator. This monochromator produces a spectrum in the plane of a row of quartz optical fibres which are arranged in thirty groups. Each one of these groups is taken to a separate model IP28 photomultiplier in the detector unit. The signal outputs from these are coupled to precision amplifiers and following controlled analogue signal 'multiplexing', the outputs

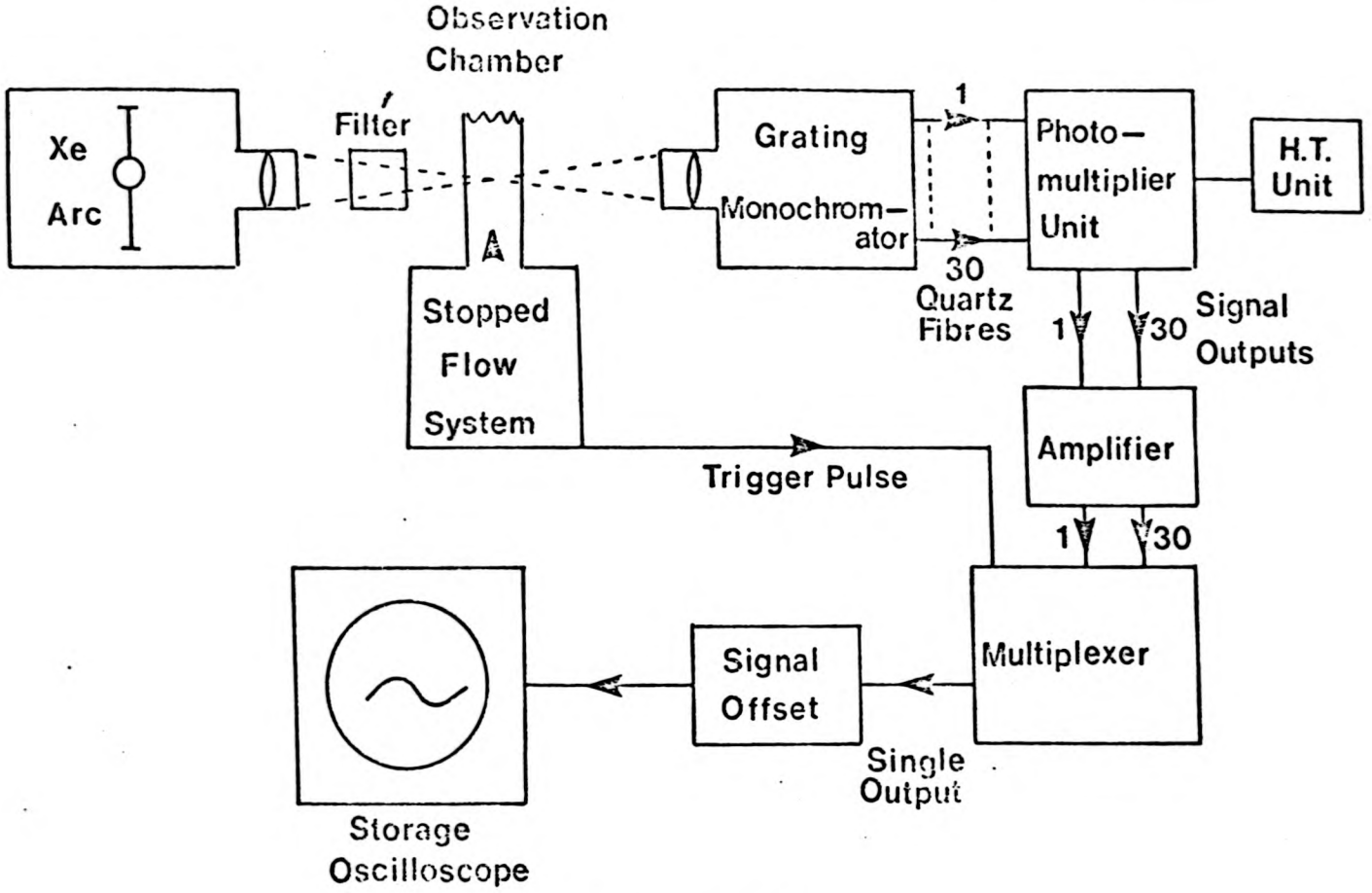

Schematic Diagram of R.S.S

are 'multiplexed' on a single output line. Individual gain controls are available for each channel to correct for the wavelength dependences of both the photomultiplier gain and the lamp output. Up to 900 separate scans can be recorded with delays of between 0.5 ms and 5 s between successive scans. The electronic spectra may be observed over a range of either 150 or 300 nm, depending upon the diffraction grating used. The signal is displayed on a Tektronix model 5115 storage oscillascope as a stepped function with thirty horizontal lines corresponding to 5 or 10 nm of the overall spectrum. In addition to the observation of time resolved spectra curves of transmittance against time can be obtained at one or more wavelengths simultaneously enabling the comparison of reaction rates at different monitoring wavelengths.

APPENDIX B. Kinetic Data for Reactions Discussed in Chapter 3.

a) Complexation reactions of Ni^{2+}.

Ligand	10^3 Ligand / mol dm^{-3}	10^2 k_{obs} / s^{-1}
SALO	0.50	3.60 ± 0.02
	1.00	5.75 ± 0.06
	2.00	9.75 ± 0.08
	3.00	15.50 ± 0.06
ACETOX	0.50	3.35 ± 0.05
	1.00	8.40 ± 0.03
	2.01	14.60 ± 0.13
	3.01	20.50 ± 0.06
BENZOX	0.50	5.10 ± 0.02
	1.00	8.10 ± 0.07
	2.00	13.90 ± 0.01
	3.00	20.90 ± 0.02
LIX 65N	0.52	3.80 ± 0.02
	1.03	6.40 ± 0.08
	2.06	10.50 ± 0.11
	3.09	14.60 ± 0.06
	5.15	22.40 ± 0.06
LIX 70	0.50	4.02 ± 0.10
	0.74	4.49 ± 0.08
	1.03	5.22 ± 0.02
	2.06	7.99 ± 0.03
	3.09	14.70 ± 0.07
MeOSALO	0.50	3.13 ± 0.02
	1.00	5.00 ± 0.02
	2.00	10.20 ± 0.03
	3.00	15.80 ± 0.09
	5.00	25.30 ± 0.08

b) Metal exchange reaction (equation (4.22)).

Reaction Stage	10^4 Cu^{2+} / mol dm^{-3}	k_{obs} / s^{-1}
1	0.38	15.4 ± 0.2
	0.57	23.4 ± 0.7
	1.14	32.7 ± 0.6
	1.9	40.6 ± 0.4
	3.8	51.9 ± 1.0
2	4.75	4.74 ± 0.07
	9.5	8.48 ± 0.2
	19	16.2 ± 0.7
	28.5	26.7 ± 0.6
	47.5	38.9 ± 1.2
3	0.38	0.62 ± 0.03
	0.48	0.82 ± 0.03
	0.95	0.92 ± 0.02
	1.9	1.26 ± 0.05
	2.85	1.40 ± 0.02
	4.75	1.67 ± 0.07

APPENDIX C. Listing of Fortran Computer Programme ITERAT.

a) Main programme.

```
      PROGRAM ITERAT
      IMPLICIT REAL*8
      DIMENSION X(1125),X2(1125),Y(1125),YOLD(1125),W(1125)
      DIMENSION COEF(43,3),C(43,43),B(43,43),DIAG(43),RHS(43)
      DIMENSION GUESS(43),ANSWER(43),ARRAY(43,43)
      DIMENSION TITLE1(13),TITLE2(13)
      CALL INPUT
      READ(1,99) TITLE1
      READ(1,99) TITLE2
      CALL READIN(1236)
      WRITE(1,947) TITLE1
      WRITE(2,947) TITLE1
      WRITE(2,114)
      WRITE(1,947) TITLE2
      WRITE(2,947) TITLE2
      WRITE(2,114)
  947 FORMAT(1X,13A6)
      WRITE(1,133) NUMBER
      READ(1,7)(GUESS(I),I=1,NUMBER)
      WRITE(1,132) NOINT
      DO 333 I=1,NOINT
      READ(1,7)(X(I),X2(I),Y(I),W(I))
  333 CONTINUE
      WRITE(1,1234.6)
      WRITE(2,334)
      WRITE(2,334)
  334 FORMAT(23X,19HSOLUTION VECTOR,7X,8HVALUES)
      WRITE(1,335)(I,GUESS(I),I=1,NUMBER)
      WRITE(2,335)(I,GUESS(I),I=1,NUMBER)
  335 FORMAT(27X,I1,7X,E15.8)
      WRITE(2,114)
      WRITE(2,114)
      NOIT=3
      IPRINT=1
      ICX=33
      IDX=1
  999 CONTINUE
      CALL ITER(
      WRITE(2,9116)
 9116 FORMAT(8X,"X",14X,"Y",13X,"Y(SOLVED)",13X,"Y(ERROR)",8X,
     1"WEIGHT")
```

APPENDIX C. Listing of Fortran Computer Programme ITERAT.

a) Main programme.

```
[illegible]
[illegible]
[illegible]
[illegible]
[illegible]
[illegible]
[illegible]
[illegible]
[illegible]
      DIMENSION X(1125),X2(1125),Y(1125),YCALC(1125),V(1125)
      DIMENSION C(40,1),C(40,40),B(40,40),DELS(40),RHS(40)
      DIMENSION GUESS(40),VECTOR(40),ARRAY(40,40)
      DIMENSION TITLE1(12),TITLE2(12)
[illegible]
[illegible]
[illegible]
[illegible]
[illegible]
[illegible]
[illegible]
[illegible]
[illegible]
```

```
C
C
C
```

```
11433      93 IF(ICOUNT.LT.1)FACTOR=3.1/2
11533         IF(ICOUNT/4)*4.EQ.ICOUNT)FACTOR=FACTOR*2
11633         IF(FACTOR.GT.1.)FACTOR=1.
11733         IF(ICOUNT/4)*4.EQ.ICOUNT)WRITE(1,111)FACTOR
11833         IF(ICOUNT/4)*4.EQ.ICOUNT)WRITE(2,111)FACTOR
11933      111 FORMAT(/" DAMPING FACTOR =",F9.3/)
12033       94 CONTINUE
12133          DO 91 I=1,NUMBER
12233       91 GUESS(I)=GUESS(I)+CORR(I,1)*FACTOR
12333          GO TO 5
12433       40 CONTINUE
12533          WRITE(1,114)
12633      114 FORMAT(/)
12733          ESD=SQRT(ERR/(NDATA-NUMBER-1))
12833          ESD=SQRT(ESD)
12933          WRITE(1,113)ESD
13033          WRITE(2,113)ESD
13133      113 FORMAT(4X," ESTIMATED STANDARD DEVIATION OF OBSERVATIONS =E
           9.2E3.4)
13233          WRITE(1,114)
13333          WRITE(2,114)
13433          WRITE(1,139)
13533          WRITE(2,139)
13633      139 FORMAT(3X,13H PARAMETER,7X,5H VALUE,3X,23H EST.STANDARD
           DEVIATION)
13733          DO 99 I=1,NUMBER
13833          ESD=SQRT(DIAG(I)*SQRT(ERR/(NDATA-NUMBER-1))
13933          WRITE(1,138)I,GUESS(I),ESD
14033          WRITE(2,138)I,GUESS(I),ESD
14133       99 CONTINUE
14233          DO 9999
14333          WRITE(1,114)
14433          WRITE(1,81)
14533       81 FORMAT(" 1) PLOT RESULTS TYPE 1 (RETURN)")
14633          WRITE(1,114)
14733          READ(1,133)IPT
14833          IF(IPT.LT.1)GO TO 9999
14933      9999 CONTINUE
15033          CALL CURVE(NDATA,X,X2,Y,NUMBER,GUESS)
15133       11 FORMAT(/5X,11,7X,E15.8,E15.8)
15233       13 FORMAT(11)
15333       12 FORMAT(I)
15433       14 FORMAT(4E15.8)
15533      9999 CONTINUE
15633      9999 CONTINUE
15733          STOP
15833       99 WRITE(2,511)ICOUNT
15933          WRITE(1,511)ICOUNT
16033      511 FORMAT(I9," ) CONVERGENCE IN ,I2,4H BUT CURRENT PARAMETER
           VALUES
16133         1CAUSE DIVERGED.)
16233          GO TO 41
16333          END
16433          SUBROUTINE SETUP(NUMBER,GUESS,ARRAY,VECTOR,NDATA,X,X2,Y,
16533         1YCALC,RES,IPRINT,W)
16633          DIMENSION GUESS(NUMBER),ARRAY(NUMBER,NUMBER),VECTOR(NUMBER)
```

```
11400      93 IF(IC.INT.LT.1)FACTOR=3.1525
11500         IF((IC.INT/4)*4.EQ.IC.AND.IC.INT.GT.4)FACTOR=FACTOR*2
11600         IF(FACTOR.GT.1.)FACTOR=1.
11700         IF((IC.INT/4)*4.EQ.IC.AND.IC.INT.GT.4)WRITE(1,111)FACTOR
11800         IF((IC.INT/4)*4.EQ.IC.AND.IC.INT.GT.4)WRITE(2,111)FACTOR
11900    111 FORMAT(//" DAMPING FACTOR =",F9.3/)
12000      94 CONTINUE
12100         DO 33 I=1,NUMBER
12200      33 GUESS(I)=GUESS(I)+CORR(I,1)*FACTOR
12300         IC=IC+1
12400      40 CONTINUE
12500         WRITE(1,114)
12600         WRITE(2,114)
12700    114 FORMAT(//)
12800         ESO=SQRT(SO/(NDATA-NUMBER-1))
12900         SO=SQRT(SO)
13000         WRITE(1,113)ESO
13100         WRITE(2,113)ESO
13200    113 FORMAT(47H ESTIMATED STANDARD DEVIATION OF OBSERVATIONS =E
           1,E14.4)
13300         WRITE(1,114)
13400         WRITE(2,114)
13500         WRITE(1,139)
13600         WRITE(2,139)
13700    139 FORMAT(3X,13H PARAMETER,7X,6H VALUE,3X,23H EST.STANDE
           1,DEVIATION)
13800         DO 38 I=1,NUMBER
13900         EST=SQRT(DIAG(I)*SO)/ERR2(NDATA-NUMBER-1))
14000         WRITE(1,138)I,GUESS(I),EST
14100         WRITE(2,138)I,GUESS(I),EST
14200      38 CONTINUE
14300         GO TO 9997
14400         WRITE(1,114)
14500         WRITE(1,81)
14600     81 FORMAT(" TO PLOT RESULTS TYPE 1 (RETURN)")
14700         WRITE(1,114)
14800         READ(5,133)IPT
14900         IF(IPT.LT.1)GO TO 9998
15000 9997 CONTINUE
15100         CALL CURVE(NDATA,X,X2,Y,NUMBER,GUESS)
15200    133 FORMAT(7X,I1,7X,E15.8,E15.8)
15300    131 FORMAT(I1)
15400    132 FORMAT(I2)
15500    135 FORMAT(4E15.8)
15600 9998 CONTINUE
15700 9999 CONTINUE
15800         STOP
15900      99 WRITE(2,511)ICOUNT
16000         WRITE(1,511)ICOUNT
16100     511 FORMAT(19H NO CONVERGENCE IN ,I2,41H BUT CURRENT PARAMETER
           1 VALUES
16200        1CAUSED,E15.8)
16300         ICOUNT=4
16400         END
16500         SUBROUTINE SETUP(NUMBER,GUESS,ARRAY,VECTOR,NDATA,X,X2,Y,
16600        1ICOUNT,ESS,IPRINT,W)
16700         DIMENSION GUESS(NUMBER),ARRAY(NUMBER,NUMBER),VECTOR(NUMBER)
```

```
      DIMENSION RHS(NUMBER),X(NDATA),X2(NDATA),Y(NDATA),YCALC(
     1NDATA)
      DIMENSION V(NDATA)
      DO 11 I=1,NUMBER
      RHS(I)=0.0
      DO 22 I=1,NUMBER
      ARRAY(I,I)=0.0
   22 CONTINUE
   11 CONTINUE
      DO 33 I=1,NDATA
      XTEMP=X(I)
      XTEMP2=X2(I)
      DO 44 I=1,NUMBER
      CALL DIFF2(NUMBER,GUESS,XTEMP,XTEMP2,I,ANSWER)
   44 VECTOR(I)=ANSWER
      IF(IPRINT.NE.1)GO TO 45
      WRITE(2,1)(VECTOR(I),I=1,NUMBER)
    1 FORMAT(14H DIFFERENTIALS,1P5E15.6)
   45 CONTINUE
      DO 55 I=1,NUMBER
      RHS(I)=RHS(I)+(Y(I)-YCALC(I))*VECTOR(I)*V(I)
      DO 61 K=1,NUMBER
      ARRAY(I,K)=ARRAY(I,K)+VECTOR(I)*VECTOR(K)*V(I)
   61 CONTINUE
   55 CONTINUE
   33 CONTINUE
      IF(IPRINT.NE.1)GO TO 99
      WRITE(2,2)(RHS(I),I=1,NUMBER)
    2 FORMAT(14H RIGHT HAND S ,1P5E15.6)
      DO 77 I=1,NUMBER
      WRITE(2,3)(ARRAY(I,J),J=1,NUMBER)
    3 FORMAT(14H ARRAY VALUES ,1P5E15.6)
   99 CONTINUE
   55 CONTINUE
      RETURN
      END
      SUBROUTINE DIFF2(NUMBER,GUESS,XTEMP,XTEMP2,I,ANSWER)
      DIMENSION GUESS(NUMBER)
      REAL DIFFDL
      DIFFDL=1.0E-4
      CALL FUNC(NUMBER,GUESS,XTEMP,XTEMP2,CALC)
      IF(GUESS(I).EQ.0.0)DEL=DIFFDL
      IF(GUESS(I).NE.0.0)DEL=GUESS(I)*DIFFDL
      GUESS1=GUESS(I)
      GUESS(I)=GUESS(I)+DEL
      CALL FUNC(NUMBER,GUESS,XTEMP,XTEMP2,CALNEW)
      ANSWER=CALNEW/DEL-CALC/DEL
      GUESS(I)=GUESS1
      RETURN
      END
      SUBROUTINE MATMPY(A,B,C,I,J,K)
      DOUBLE PRECISION DDUM
      DIMENSION A(I,J),B(J,K),C(I,K)
      DO 33 N=1,I
      DO 33 M=1,K
```

```
      DOUBR=0.0
      DO 21 L=1,J
      DOUBR=A(N,L)*B(L,M)+DOUBR
   21 CONTINUE
      C(N,M)=DOUBR
   31 CONTINUE
      RETURN
      END
      SUBROUTINE MATINV(A,N,DIAG)
      DIMENSION A(N,N),LL(40),DIAG(N)
      DET=1.0
      DO 5 K=1,N
      PIVOT=0.0
      DO 1 J=K,N
      D=ABS(A(J,K))
      IF(D.LT.PIVOT) GO TO 1
      PIVOT=D
      M=J
    1 CONTINUE
      IF(PIVOT.NE.0.0) GO TO 2
      DET=0.0
      RETURN
    2 PIVOT=A(M,K)
      DET=DET*PIVOT
      LL(K)=M
      A(K,K)=A(K,K)
      A(K,K)=1.0
      DO 3 I=1,N
      A(I,K)=A(I,K)/PIVOT
    3 CONTINUE
      DO 5 J=1,N
      IF(K.EQ.J) GO TO 5
      D=A(K,J)
      A(K,J)=A(K,J)
      A(K,J)=0.0
      IF(D.EQ.0.0) GO TO 5
      DO 4 I=1,N
      A(I,J)=A(I,J)-D*A(I,K)
    4 CONTINUE
    5 CONTINUE
      I=N
    6 IF(I.EQ.LL(I)) GO TO 8
      K=LL(I)
      DO 7 K=1,N
      D=A(K,M)
      A(K,M)=A(K,I)
      A(K,I)=D
    7 CONTINUE
    8 IF(I.EQ.1) GO TO 17
      I=I-1
      GO TO 6
   17 DO 18 II=1,N
   18 DIAG(II)=A(II,II)
      RETURN
      END
```

```
      FUNCTION MENT(X)
      X2=3.5
      IF(X.LT.3.)X2=-3.5
      Y=X+X2
      Y=Y
      RETURN
      END
      SUBROUTINE CURVE(NDATA,XDATA,X2DATA,YDATA,XJESS,IJESS)
      DIMENSION NDATA(1),XDATA(NDATA),X2DATA(NDATA),YDATA(NDATA)
      DIMENSION IJESS(XJESS+2)
      DIMENSION XX(33),CC(33),YY(33)
      PI=4.141592654
      CALL PAPER(1)
      CALL PSPACE(3.,3.,419.,3.,3.,419)
      CALL WIND(3.,7.25,3.,7.25)
      CALL CTRANS(1.,1)
      CALL PLANE(3.75,3.75)
      CALL TYPECS(CC,33)
      CALL PLANE(3.15,3.25)
      CALL TYPECS(XX,33)
      CALL PLANE(3.15,4.75)
      CALL TYPECS(DD,33)
      CALL PSPACE(3.1364,3.8431,3.1364,3.8439)
      CALL RESET
      YY=YDATA(1)
      XX=XDATA(1)
      Y=YDATA(1)
      X=XDATA(1)
      DO 111 I=1,NDATA
      IF(YDATA(I).LT.YY)YY=YDATA(I)
      IF(YDATA(I).GT.YX)YX=YDATA(I)
      IF(XDATA(I).LT.XX)XX=XDATA(I)
      IF(XDATA(I).GT.XX)XX=XDATA(I)
111   CONTINUE
      CALL WIND(XX-(XX-XM)/13.,X+(XX-XM)/13.,YY-(YX-YM)/13.,YX+(YX
     1-YM)/13.)
      CALL AXES
      CALL CTRANS(1.,1)
      CALL PLOT(XDATA,YDATA,1,NDATA,43)
      CALL FUNC(MENT,IJESS,XTEMP,1.,CALC)
      YYY=CALC
      CALL PLINE(XX,YYY)
      DO 222 I=2,1111
      XTEMP=XX+(I-1)*(XX-XM)/1111
      CALL FUNC(MENT,IJESS,XTEMP,1.,YCALC)
      YTEMP=YCALC
      IF(I.LE.1)WRITE(1,111)I,YTEMP
111   FORMAT(2X,I1,2X,E13.6)
      CALL PLINE(XTEMP,YTEMP)
222   CONTINUE
      CALL RESET
      RETURN
      END
```

b) Function used for fits to Swift-Connick equations used in Section 4.2..

```
SUBROUTINE FUNC(N,A,X,X2,Y)
DIMENSION A(N)
PM=0.01458
BC=1.380662E-23
PC=6.626176E-34
R=8.31441
PI=3.141592654
T=1000.0/X
DH=A(1)
DS=A(2)
B1=A(3)
CORR=0.0
DELOMM=2.0*PI*B1/T
RECTAU=(BC*T/PC)*EXP(DS/R-DH/R/T)
AM=0
EM=4000.0
RECT2M=AM*EXP(EM/R/T)
AOS=0.0
EOS=4000.0
RT2OS=AOS*EXP(EOS/R/T)
DELOMR=DELOMM/((RECT2M/RECTAU+1)**2+(DELOMM/RECTAU)**2)
DELOM=DELOMR*PM
RECT2R=RECT2M*RECT2M+RECT2M*RECTAU+DELOMM*DELOMM
RECT2R=RECT2R*RECTAU/((RECT2M+RECTAU)**2+DELOMM)
RECT2R=RECT2R+RT2OS
Y=RECT2R*PM
Y=ALOG(Y)
SHIFT=(DELOM/2.0/PI)+CORR
SCALE=20.0
SHIFT=SHIFT/SCALE
Y=Y*X2+SHIFT*(1.0-X2)
RETURN
END
```

c) Function used for analysis of paramagnetic ^{1}H n.m.r. shifts in Section 4.3.

```
      SUBROUTINE FUNC(N,A,X,X2,Y)
      DIMENSION A(N)
      R=8.31441
      CT=0.6774
      DH=A(1)
      DS=A(2)
      FD1=A(3)
      CC1=A(4)
      FD2=A(5)
      CC2=A(6)
      FD3=A(7)
      CC3=A(8)
      T=1000.0/X
      EC=EXP(DS/R-DH/R/T)
      CP=CT/(1.0+1.0/EC)
      CD=CT-CP
      FP1=CC1/T
      FP2=CC2/T
      FP3=CC3/T
      YO=FD1*CD/CT+FP1*CP/CT
      Y1=FD2*CD/CT+FP2*CP/CT
      Y2=FD3*CD/CT+FP3*CP/CT
      IF(X2.LT.0.1)Y=YO
      IF(X2.LT.0.1)GO TO 1010
      IF(X2-1.0.LT.0.1)Y=Y1
      IF(X2-1.0.LT.0.1)GO TO 1010
      IF(X2-2.0.LT.0.1)Y=Y2
1010  CONTINUE
      RETURN
      END
```

REFERENCES.

1. P. J. Bailes, C. Hanson and M. A. Hughes, Chem. Eng., 1976, 83, 86.

2. A. W. Ashbrook and G. M. Ritcey, Canad. Mining J., 1972, 93, 70.

3. S. Goszczynski and J. Szymanowski, Mater. Sci., 1977, 3, 115.

4. R. R. Swanson, U. S. P. 3,224,873/1965.

5. R. R. Swanson, U. S. P. 3,248,449/1969.

6. E. R. DeMent and C. R. Merigold, AIME meeting, Denver, February, 1970.

7. C. R. Merigold, AIME meeting, New York, February, 1971.

8. D. W. Agers and E. R. DeMent, AIME meeting, San Francisco, February, 1972.

9. J. A. Hartlage and A. D. Cronberg, Canad. Inst. Mining Bulletin, 1975, 68, 99.

10. D. W. Agers, J. E. House, R. R. Swanson and J. L. Drobnicki, 'Copper Recovery from Acid Solutions using Liquid Ion Exchange', General Mills Chemicals Inc.

11. I. Dahl, Analyt. Chim. Acta, 1968, 41, 9.

12. J. R. Parrish, J. S. African Chem. Inst., 1970, 23, 129.

13. A. R. Burkin and J. S. Preston, J. Inorg. Nuclear Chem., 1975, 37, 2187.

14. R. F. Rekker and J. U. Veenland, Rec. Trav. Chim., 1959, 78, 739.

15. D. Hadzi and L. Premru, Spectrochim. Acta, 1967, 23A, 35.

16. A. W. Ashbrook, J. Chromatography, 1975, 105, 141.

17. R. L. Atwood and J. D. Miller, Trans. Soc. Min. Eng. AIME, 1973, 254, 319.

18. A. W. Ashbrook, Hydrometallurgy, 1975, 1, 5.

19. W. Sowa, B. H. Licht and I. J. Itzkovitch, J. Chromatography, 1976, 116, 197.

20. K. Burger, F. Ruff, I. Ruff and I. Egyed, Acta Chim. Acad. Sci. Hung., 1965, 46, 1.

21. J. Csaszar and J. Szeghalmi, Acta Univ. Szegid. Acta Phys. et Chem., 1966, 12, 117.

22. K. K. Ramaswarmy, C. I. Jose and D. N. Sen, Indian J. Chem., 1967, 5, 156.

23. R. Neelameggham, Ph.D. Thesis, University of Utah, 1972.

24. J. W. Hosking and N. M. Rice, Hydrometallurgy, 1978, 3, 217.

25. C. A. Fleming, National Institute for Metallurgy Report, No. 1793, Johannesburg, South Africa, 1976.

26. L. Hummelsteldt, T. Tammi, E. Paatero, H. Andresen and J. Karjaluoto, Fourth International Congress in Scandanavia on Chemical Engineering, Copenhagen, 1977, Metallurgical Processes p. 123.

27. B. N. Laskorin, V. V. Yaskin, V. S. Ul'yanov and A. Mirokhin, Proceeding of International Solvent Extraction Conference, 1974, Society of Chemical Industry, London, p. 1775.

28. R. J. Whewell, M. A. Hughes and C. Hanson, Proceeding of International Solvent Extraction Conference, 1977, Canadian Institute of Mining and Metallurgy.

29. R. Price and J. A. Tumulty, "Hydrometallurgy", Inst. Chem. Eng. Symp. Ser., No. 42, Paper No. 18, 1975.

30. D. S. Flett, Accounts Chem. Res., 1977, 10, 99.

31. R. F. Dalton, F. Hauxwell and J. A. Tumulty, Chem. Ind. (London), 1976, 181.

32. J. Meisenheimer and O. Beisswenger, Ann., 1932, 495, 262.

J. G. Pritchard, G. F. Field, K. Koch, G. Raymond, L. H. Sternbach, V. Toome and S. Traimare, Applied Spect., 1966, 20, 363.

33. T. W. J. Taylor and E. K. Ewbank, J. Chem. Soc., 1926,2818.

34. A. H. Blatt, J. Amer. Chem. Soc., 1938, 61, 214.

35. K. J. Dignam and A. F. Hegarty, J. C. S. Chem. Commun., 1976, 862.

36. W. B. Jennings, S. Al-Showiman, D. R. Boyd and R. M. Campbell, J. C. S. Perkin (II), 1976, 1501.

37. J. S. Preston and R. J. Whewell, J. Inorg. Nuclear Chem., 1977, 39, 1675.

38. K. E. Japalpurwala, K. A. Venkatachalam and M. B. Kabadi, J. Inorg. Nuclear Chem., 1964, 26, 1011.

39. R. P. Patel and R. D. Patel, J. Inorg. Nuclear Chem., 1970, 32, 2591.

40. C. F. Coleman, K. B. Brown, J. G. Moore and D. J. Crouse, Ind. and Eng. Chem., 1958, 50, 1756.

41. W. J. McDowell and C. F. Coleman, J. Inorg. Nuclear Chem., 1967, 29, 1325.

42. J. W. Roddy, C. F. Coleman and S. Arai, J. Inorg. Nuclear Chem., 1971, 33, 1099.

43. I. P. Alimarin, Yu, A. Zolotov and V. A. Bodnya, Pure Appl. Chem., 1971, 25, 667.

44. R. W. Cattrall and S. J. E. Slater, Co-ordination Chem. Rev., 1973, 11, 227.

45. J. Rydberg, Acta Chem. Scand., 1969, 23, 647.

46. C. Anderson, S. O. Anderson, J. O. Liljensen, H. Reinhardt and J. Rydberg, Acta Chem. Scand., 1969, 23, 2781.

47. H. Johansson and J. Rydberg, Acta Chem. Scand., 1969, 23, 2797.

48. H. Reinhardt and J. Rydberg, Chem. Ind., 1970, 50, 448.

49. W. Nitsch, Dechema Monograph, 1965, 55.

50. F. Baumgartner and L. Finsterwalder, J. Phys. Chem., 1970, 74, 108.

51. R. J. Whewell, M. A. Hughes and C. Hanson, J. Inorg. Nuclear Chem., 1975, 37, 2303.

52. S. J. Kirchner and Q. Ferdinando, Analyt. Chem., 1977, 49, 1636.

53. A. W. Ashbrook, Analyt. Chim. Acta, 1972, 58, 115.

54. A. W. Ashbrook, Co-ordination Chem. Rev., 1975, 16, 285.

55. D. S. Flett, D. N. Okuhura and D. R. Spink, J. Inorg. Nuclear Chem., 1973, 35, 2471.

56. T. A. B. Al-Diwan, M. A. Hughes and R. J. Whewell, J. Inorg. Nuclear Chem., 1977, 39, 1419.

57. M. A. Hughes, E. Mistry and R. J. Whewell, J. Inorg. Nuclear Chem., 1978, 40, 1696.

58. J. D. Miller and R. L. Atwood, J. Inorg. Nuclear Chem., 1975, 37, 2539.

59. D. S. Flett, J. Melling and D. R. Spink, J. Inorg. Nuclear Chem., 1977, 39, 701.

60. R. L. Atwood, D. N. Thatcher and J. D. Miller, Metallurgical Trans. B, AIME, 1975, 6B, 465.

61. J. S. Preston, J. Inorg. Nuclear Chem., 1975, 37, 1235.

62. R. J. Whewell, M. A. Hughes and C. Hanson, J. Inorg. Nuclear Chem., 1976, 38, 2071.

63. J. Preston and R. J. Whewell, J. Inorg. Nuclear Chem., 1977, 39, 1675.

64. D. S. Flett, M. Cox and J. D. Heels, J. Inorg. Nuclear Chem., 1975, 37, 2533.

65. C. Hanson, M. A. Hughes, J. S. Preston and R. J. Whewell, J. Inorg. Nuclear Chem., 1976, 38, 2306.

66. V. I. Lakshmanan, G. J. Lawson and J. L. Tomliens, J. Inorg. Nuclear Chem., 1975, 37, 2181.

67. S. Dobson and A. J. Van der Zeeuw, Chem. Ind., 1976, 175.

68. M. A. Hughes, P. D. Middlebrook and R. J. Whewell, J. Inorg. Nuclear Chem., 1977, 39, 1679.

69. A. Chakravorty, Co-ordination Chem. Rev., 1974, 13, 1.

70. E. G. Cox and K. C. Webster, J. Chem. Soc., 1935, 731.

71. M. A. Jarski and E. C. Lingafelter, Acta Cryst., 1964, 17, 1109.

72. P. Orioli, E. C. Lingafelter and B. W. Brown, Acta Cryst., 1964, 17, 1113.

73. L. L. Merritt Jnr., C. Guare and A. E. Lessor, Acta Cryst., 1956, 9, 253.

74. R. C. Srivastava, E. C. Lingafelter and P. C. Jain, Acta Cryst., 1967, 22, 922.

75. C. E. Pfluger, R. L. Harlow and S. H. Simonsen, Acta Cryst, Sect. B, 1970, 26, 1631.

76. V. K. Syal and P. C. Jain, Indian J. Chem., 1973, 11, 494.

77. E. C. Lingafelter, Co-ordination Chem. Rev., 1966, 1, 151.

78. S. Yamada, Co-ordination Chem. Rev., 1966, 1, 415.

79. R. H. Holm, G. W. Everett Jnr. and A. Chakravorty, Progress Inorg. Chem., 1966, 7, 83.

80. R. H. Holm and M. J. O'Connor, Progress Inorg. Chem., 1971, 14, 241.

81. H. S. Maslen and T. N. Waters, Co-ordination Chem. Rev., 1975, 17, 137.

82. E. N. Baker, D. Hall and T. N. Waters, J. Chem. Soc.,A. 1966, 680.

83. E. R. Boyco, D. Hall, M. E. Kinloch and T. N. Waters, Acta Cryst., 1966, 21, 614.

84. G. Bombieri, C. Panattoni, E. Fursellini and R. Graziani, Acta Cryst. Sect. B., 1969, 25, 1208.

85. D. Hall, R. H. Sumner and T. N. Waters, J. Chem. Soc., A, 1969, 420.

86. L. Wei, R. M. Stogsdill and E. C. Lingafelter, Acta Cryst., 1964, 17, 1058.

87. L. M. Shkol'nikova, A. N. Knyazeva and V. A. Voblikova, J. Struct. Chem., 1967, 8, 77.

88. R. L. Braun and E. C. Lingafelter, Acta Cryst., 1966, 21, 546.

89. R. L. Braun and E. C. Lingafelter, Acta Cryst., 1967, 22, 787.

90. V. W. Day, M. D. Glick and J. L. Hoard, J. Amer. Chem. Soc., 1968, 90, 4803.

91. L. Sacconi, Co-ordination Chem. Rev., 1966, 1, 126.

92. R. H. Holm, Accounts Chem. Res., 1969, 2, 307.

93. A. P. B. Lever, "Inorganic Electronic Spectroscopy", Elsevier, Amsterdam, 1968.

94. J. Csaszar, Acta Chim. Acad. Sci. Hung., 1962, 32, 343.

95. J. B. Willis and D. P. Mellor, J. Amer. Chem. Soc., 1947, 69, 1237.

96. J. Ferguson, Spectrochim. Acta, 1961, 17, 316.

97. R. Holm, J. Amer. Chem. Soc., 1961, 83, 4683.

98. H. Nishikawa and S. Yamada, Bull. Chem. Soc. Japan, 1964, 37, 1164.

99. R. H. Bailes and M. Calvin, J. Amer. Chem. Soc., 1947, 69, 1886.

100. M. R. Paris and D. Aymes, Bull. Soc. Chim. France, 1976, 1431.

101. H. Weigold and B. O. West, J. Chem. Soc., A, 1967, 1310.

102. M. Hariharan and P. L. Urbach, Inorg. Chem., 1969, 8, 556.

103. R. H. Holm, J. Amer. Chem. Soc., 1960, 82, 5632.

104. R. C. Elder and M. C. Hill, Inorg. Chem., 1979, 18, 729.

105. H. Nishikawa and S. Yamada, Bull. Chem. Soc. Japan, 1964, 37, 8.

106. L. Sacconi, M. Ciampolini, F. Maggio and F. P. Cavasino, J. Inorg. Nuclear Chem., 1961, 19, 73.

107. S. J. Cline, J. R. Wasson, W. E. Hatfield and D. J. Hodgson, J. C. S., Dalton, 1978, 1051.

108. L. Sacconi and M. Ciampolini, J. Chem. Soc., 1964, 276.

109. T. P. Cheeseman, D. Hall and T. N. Waters, J. Chem. Soc., A, 1966, 694.

110. S. Yamada, E. Ohno, Y. Kuge, A. Takeuchi, K. Yamanouchi and K. Iwasaki, Co-ordination Chem. Rev., 1968, 3, 247.

111. S. Yamada, H. Nishikawa and E. Yoshida, Bull. Chem. Soc. Japan, 1966, 39, 994.

112. S. Yamada and H. Nishikawa, Bull. Chem. Soc. Japan, 1965, 38, 683.

113. J. Csaszar and J. Szeghalmi, Acta Univ. Szegid., Acta Phys. Chim., 1966, 12, 117.

114. V. Romano, F. Maggio and T. Pizzino, J. Inorg. Nuclear Chem., 1971, 33, 2611.

115. F. Maggio, V. Romano, T. Pizzino and L. Pellerito, Ann. Chim. (Italy), 1968, 58, 725.

116. F. Basolo and W. Matoush, J. Amer. Chem. Soc., 1953, 75, 5663.

117. T. S. Kannan and A. Chakravorty, Inorg. Chem., 1970, 9, 1153.

118. G. M. Mockler, G. W. Chaffey, E. Sinn and H. Wong, Inorg. Chem., 1972, 11, 1308.

119. D. R. Dakternieks and D. P. Graddon, Australian J. Chem., 1973, 26, 2379.

120. D. R. Dakternieks, D. P. Graddon, L. F. Lindoy and G. M. Mockler, Inorg. Chim. Acta, 1973, 7, 467.

121. L.-T. Ang and D. P. Graddon, Australian J. Chem., 1976, 29, 565.

122. R. B. Jordan and L. L. Rusnak, Inorg. Chem., 1976, 15, 709.

123. A. Ewert, K. J. Wannowius and H. Elias, Inorg. Chem., 1978, 17, 1691.

124. D. N. Bone, E. D. Mackenzie and K. Rowan, J. C. S. Chem. Commun., 1970, 420.

125. G. N. La Mar, Inorg. Chim. Acta, 1969, 3, 183.

126. L. F. Lindoy and G. M. Mockler, J. Co-ord. Chem., 1973, 3, 169.

127. G. Kiss-Imreh, Z. Szekely and R. Ripan, Rev. Roum. Chem., 1966, 11, 47.

128. M. S. Kachhawaha and A. K. Bhattacharya, Z. Anorg. Allgem. Chemie, 1963, 325, 321.

129. P. B. S. Reddy and S. B. Rao, Curr. Sci., 1978, 47, 4.

130. K. R. Manalov, Zh. Neorg. Khim., 1967, 12, 2715.

131. S. Mandal and A. K. Dey, J. Inorg. Nuclear Chem., 1968, 30, 1221.

132. R. Ugo, E. La Monica, S. Cenini and F. Bonati, J. Organo-metallic Chem., 1968, 11, 159.

133. P. V. Takalkor and V. R. Rao, J. Inorg. Nuclear Chem., 1975, 37, 2103.

134. N. S. Biradar, V. H. Kulkarni and B. R. Havinale, J. Karnatak Univ. Sci., 1976, 21, 150.

135. V. I. Shlenskaya, A. A. Biryukov, T. I. Tikhvinskaya and L. N. Voronina, Zh. Neorg. Khim., 1969, 14, 3331.

136. T. B. Sing and A. K. Dey, Rev. Chim. Miner., 1970, 7, 463.

137. H. Nakamura, Y. Shimura and R. Tsuchida, Bull. Chem. Soc. Japan, 1963, 36, 296.

138. K. Burger and A. Buvari, Inorg. Chim. Acta, 1974, 11, 25.

139. A. Nakamura, A. Konishi and S. Otsuka, J. C. S. Dalton, 1979, 488.

140. A. Nakamura, A. Konishi, Y. Tatsuno and S. Otsuka, J. Amer. Chem. Soc., 1978, 100, 3443.

141. C. N. R. Rao, "Ultra-violet and Visible Spectroscopy - Chemical Applications", Butterworths, London, 1967.

142. W. F. Forbes and A. R. Knight, Canadian J. Chem., 1959, 37, 334.

143. J. Fabian, M. Legrand and P. Poirier, Bull. Soc. Chim. France, 1956, 1499.

144. L. J. Bellamy, "The Infra-red Spectra of Complex Molecules", Methuen, London, 1958.

145. G. C. Levy and G. L. Nelson, "Carbon-13 Nuclear Magnetic Resonance for Organic Chemists", Wiley, New York, 1972.

146. J. B. St others, "Carbon-13 NMR Spectroscopy - Organic Chemistry", Academic Press, New York, 1972.

147. G. E. Maciel and R. V. James, J. Amer. Chem. Soc., 1964, 86, 3893.

148. E. G. Cox, F. W. Pinkard, W. Wardlaw and K. C. Webster, J. Chem. Soc., 1935, 459.

149. R. C. Aggarwal, N. K. Singh and R. P. Singh, Inorg. Chim. Acta, 1979, 32, L87.

150. N. S. Biradar, M. D. Patil, S. D. Angadi and N. B. Mallur, Rev. Roum. Chem., 1979, 24, 1315.

151. E. P. Dudek and G. Dudek, Inorg. Nuclear Chem. Letts., 1967, 3, 241.

152. G. C. Percy and D. A. Thornton, J. Inorg. Nuclear Chem., 1973, 35, 2319.

153. P. Gluvchinsky, G. M. Mockler and E. Sinn, Spectrochim. Acta, 1977, 33A, 1073.

154. J. E. Kovacic, Spectrochim. Acta, 1967, 23A, 183.

155. H. Kato and T. Sakamoto, J. Amer. Chem. Soc., 1974, 93, 4131.

156. B. Bosnich, J. Amer. Chem. Soc., 1968, 90, 627.

157. H. Lund and J. Bjerrum, Ber. 1931, 64, 210.

158. E. P. Kohler and W. F. Bruce, J. Amer. Chem. Soc., 1931, 53, 1569.

159. A. Schweiger and H. H. Guenthard, Chem. Phys., 1978, 32, 35.

160. K. Sone, J. Amer. Chem. Soc., 1953, 75, 5207.

161. A. Fratiello, Prog. Inorg. Chem., 1972, 17, 57.

162. S. F. Lincoln, Co-ordination Chem Rev., 1971, 6, 309.

163. S. F. Lincoln, Progr. React. Kinet., 1977, 9.

164. R. G. Wilkins, "The Study of Kinetics and Mechanism of Reactions of Transition Metal Complexes", Allyn and Bacon, Boston, 1974.

165. K. Kustin and J. Swinehart, Progr. Inorg. Chem., 1970, 13, 107.

166. R. E. Connick and D. Fiat, J. Chem. Phys., 1966, 44, 4103.

167. A. G. Desai, H. W. Dodgen and J. P. Hunt, J. Amer. Chem. Soc., 1969, 91, 5001.

168. T. J. Swift and R. E. Connick, J. Chem. Phys., 1962, 37, 307.

169. D. Rablen and G. Gordon, Inorg. Chem., 1969, 8, 395.

170. D. B. Bechtold, G. Liu, H. W. Dodgen and J. P. Hunt, J. Phys. Chem., 1978, 82, 333.

171. F. W. Breivogel Jnr., J. Phys. Chem., 1969, 73, 4205.

172. S. Thomas and W. L. Reynolds, J. Chem. Phys., 1967, 46, 4164.

173. S. Blackstaffe and R. A. Dwek, Mol. Phys., 1968, 15, 279.

174. N. S. Angerman and R. B. Jordan, Inorg. Chem., 1969, 8, 2579.

175. G. S. Vigee and P. Ng, J. Inorg. Nuclear Chem., 1971, 33, 2477.

176. J. C. Boubel and J. J. Delpuech, Mol. Phys., 1974, 27, 113.

177. P. J. Nichols and M. W. Grant, Aust. J. Chem., 1978, 31, 2581.

178. D. K. Ravage, T. R. Stengle and C. H. Langford, Inorg. Chem., 1967, 6, 1952.

179. N. A. Matwiyoff and S. V. Hooker, Inorg. Chem., 1967, 6, 1127.

180. J. F. O'Brien and W. L. Reynolds, Inorg. Chem., 1967, 6, 2110.

181. V. K. Kapur, J. Phys. Chem., 1973, 77, 634.

182. K. E. Newman, F. K. Meyer and A. E. Merbach, J. Amer. Chem. Soc., 1979, 101, 1470.

183. Z. Luz and S. Meiboom, J. Chem. Phys., 1964, 40, 1066.

184. Z. Luz and S. Meiboom, J. Chem. Phys., 1964, 40, 2686.

185. T. E. Rogers, J. H. Swinehart and H. Taube, J. Phys. Chem., 1965, 69, 134.

186. A. M. Chmelnick and D. Fiat, J. Chem. Phys., 1968, 49, 2101.

187. W. L. Earl, F. K. Meyer and A. E. Merbach, Inorg. Chim. Acta, 1977, 25, L91.

188. D. J. Hewkin and R. H. Prince, Co-ordination Chem. Rev., 1970, 5, 45.

189. R. G. Pearson and P. Ellgen, Inorg. Chem., 1967, 6, 1379.

190. A. D. Van Ingen Schenau, W. L. Groeneveld and J. Reedijk, Rec. Trav. Chim., 1972, 91, 88.

191. A. I. Vogel, "A Textbook of Quantitative Inorganic Analysis", Longmans, London, 1968.

192. W. A. Johnson and R. G. Wilkins, Inorg. Chem., 1970, 9, 1917.

193. D. W. Margerum, G. R. Cayley, D. C. Weatherburn and G. K. Pagenkopf, 'Co-ordination Chemistry; Volume 2', Ed. A.E. Martell, A.C.S. Monograph 174, 1978.

194. J. C. Williams and S. Petrucci, J. Amer. Chem. Soc., 1973, 95, 7619.

195. Y. Eini, B. Perlmutter-Hayman and M. A. Wolff, J. Co-ord. Chem., 1977, 7, 27.

196. C. D. Hubbard and A. D. Pacheco, J. Inorg. Nuclear Chem., 1977, 39, 1373.

197. R. G. Wilkins, Accounts Chem. Res., 1970, 3, 408.

198. C. D. Hubbard, J. Inorg. Nuclear Chem., 1974, 36, 1177.

199. K. Burger and I. Egyed, J. Inorg. Nuclear Chem., 1965, 27, 2361.

200. J. Schwarzenbach, "Complexiometric Titrations", Methuen and Co., London, 1960, p. 78.

201. E. Cesarotti, M. Gullotti, A. Pasini and R. Ugo, J. C. S. Dalton. 1977, 757.

202. G. B. Jameson, W. T. Robinson and C. A. Rodley, J. C. S. Dalton. 1978, 191.

203. R. L. Lancashire, T. D. Smith and J. R. Pilbrow, J. C. S. Dalton. 1979, 66.

204. B. T. Huie, R. M. Leyden and W. P. Schafer, Inorg. Chem., 1979, 18, 125.

205. D. W. Margerum, D. L. Janes and H. M. Rosen, J. Amer. Chem. Soc., 1965, 87, 4463.

206. R. K. Steinhaus and R. L. Swann, Inorg. Chem., 1973, 12, 1855.

207. W. W. Fee, J. D. Pulsford and P. D. Vowles, Aust. J. Chem., 1973, 26, 1459.

226. D. W. Buck, P. J. Benson and P. Moore, unpublished data.

227. W. L. Rice and B. B. Wayland, Inorg. Chem., 1968, 7, 1040.

228. A. L. Van Geet, Inorg. Chem., 1968, 7, 2026.

229. G. S. Vigee, C. L. Watkins and H. F. Bowen, Inorg. Chim. Acta, 1979, 35, 255.

230. B. Bosnich, C. K. Poon and M. L. Tobe, Inorg. Chem., 1965, 4, 1106.

231. E. K. Barefield and F. Wagner, Inorg. Chem., 1973, 12, 2435.

232. N. Herron and P. Moore, Inorg. Chim. Acta, 1979, 36, 89.

233. F. Wagner and E. K. Barefield, Inorg. Chem., 1976, 15, 408.

234. A. Dei, Inorg. Chem., 1979, 18, 891.

235. D. F. Cook and E. D. Mckenzie, Inorg. Chim. Acta, 1978, 29, 193.

236. D. F. Cook and E. D. Mckenzie, Inorg. Chim. Acta, 1978, 31, 59.

237. S. Nakamura and S. Meiboom, J. Amer. Chem. Soc., 1967, 89, 1765.

238. J. A. Pople, W. G. Schneider and H. J. Bernstein, "High Resolution Nuclear Magnetic Resonance", McGraw-Hill, New York, 1959, Ch. 10.

239. S. Ahrland and N. O. Bjork, Acta Chem. Scand., 1974, 28, 823.

240. J. Celada and V. Jedinakova, Coll. Czech. Chem. Commun., 1967, 32, 271.

241. S. A. Al-Baldawi, M. H. Brooker, T. E. Gough and D. E. Irish, Canadian J. Chem., 1970, 48, 1202.

242. D. Knetsh and W. L. Groeneveld, Rec. Trav. Chim., 1973, 92, 855.

243. V. Jedinakova and J. Celada, Coll. Czech. Chem. Commun., 1968, 30, 555.

244. G. E. Maciel, L. Simeral and J. J. H. Ackerman, J. Phys. Chem., 1977, 81, 263.

245. A. Ferrari, A. Braibanti, A. M. M. Lanfredi and A. Tiripicchio, Acta Cryst., 1967, 22, 240.

246. D. A. Couch, LSHAPE version 3, Nicolet Users Society.

247. P. Moore, J. C. S. Faraday I, 1976, 826.

248. F. Fittipaldi and S. Petrucci, J. Phys. Chem., 1967, 71, 3414.

249. M. N. Tkaczuk and S. F. Lincoln, Aust. J. Chem., 1979, 32, 1915.